SYNTHESIS, CHARACTERISATION AND BIOLOGICAL ACTIVITY STUDIES OF ORGANO-BRIDGED METAL SCHIFF BASE COMPLEXES WITH QUINOXALINE DERIVATIVE

by

MOHLALA REAGAN LEHLOGONOLO

RESEARCH DISSERTATION

Submitted in fulfilment of the requirements for the degree of

MASTER OF SCIENCE

in

CHEMISTRY

in the

FACULTY OF SCIENCE AND AGRICULTURE

(School of Physical and Mineral Sciences)

at the

UNIVERSITY OF LIMPOPO (Turfloop campus)

SUPERVISOR: **Dr. R.M. Mampa**

CO-SUPERVISORS: **Dr. W. Nxumalo**

Dr. M.S. Thomas

2016

DECLARATION

I declare that “Synthesis, characterisation and biological activity studies of organo-bridged metal Schiff base complexes with quinoxaline derivative” is my own, unaided work submitted for the degree of Master Science at Limpopo. It has not been submitted for any degree or examination in any other University, and all sources I have used or quoted have been indicated and acknowledged by means of complete references.

Name: Mohlala Reagan Lehlogonolo (Mr.)

Date……..2016

Signature:.....

DEDICATIONS

To my parents, Andrew and Monica, and my siblings

ABSTRACT

Imidazolyl-salicylaldemine Schiff base ligands were prepared by the condensation of different substituted salicylaldehydes with histamine dihydrochloride: 2,4-di-tert-butyl-6-{[2-(1H-imidazol-4-yl)-ethylimino]-methyl}-phenol **L1**; 4-methoxy-6-{[2-(1H-imidazol-4-yl)-ethylimino]-methyl}-phenol **L2**; 2-ethoxy-6-{[2-(1H-imidazol-4-yl)-ethylimino]-methyl]-phenol **L3**; 2-methyl-6-{[2-(1H-imidazol-4-yl)-ethylimino]-methyl}-phenol **L4**; 3-methyl-6-{[2-(1H-imidazol-4-yl)-ethylimino]-methyl}-phenol **L5**; 4-methyl-6-{[2-(1H-imidazol-4-yl)-ethylimino]-methyl}-phenol **L6**; 5-methyl-6-{[2-(1H-imidazol-4-yl)-ethylimino]-methyl}-phenol **L7**; 2-tert-butyl-6-{[2-(1H-imidazol-4-yl)-ethylimino]-methyl}-phenol **L8**; 3-methoxy-6-{[2-(1H-imidazol-4-yl)-ethylimino]-methyl}-phenol **L9**; 4-tert-butyl-6-{[2-(1H-imidazol-4-yl)-ethylimino]-methyl}-phenol **L10**. The ligands were characterised by ^{1}H, ^{13}C and ^{15}N NMR, FT-IR, UV-vis spectroscopic methods, mass spectroscopy and elemental analysis where possible. Reactions of **L1**-**L9** with $MnCl_2$ and $CuCl_2$ yielded complexes **C1**–**C18** all in a ratio of (1:1). **C1** – **C18** here, i.e. **C18** 2-methyl-6-{[2-(1H-imidazol-4-yl)-ethylimino]-methyl}-phenol Cu(II) chloride. The complexes that are paramagnetic were mainly characterised by FT-IR spectroscopy, UV-vis spectroscopy, mass spectroscopy and elemental analysis. Reaction of **L9** with $ZnCl_2$ yielded 2-methyl-6-{[2-(1H-imidazol-4-yl)-ethylimino]-methyl}-phenol Zn(II) chloride, **C19** which is diamagnetic and was characterised by ^{1}H, ^{13}C NMR spectroscopy Mass spectroscopy and Elemental analysis. Condensation of *o*-phenylenediamine and glyoxylic acid yielded 2-quinoxalinone **Q1**, reaction of 2-quinoxalinone and benzenesulfonyl chloride yielded 2-benzenesulfonyloxyquinoxaline **Q2**, and the reaction of 2-benzenesulfonyloxyquinoxaline with ethynyltrimethylsilane yielded 2-ethynyltrimethylsilanequinoxaline **Q3**. Quinoxaline and its preceding starting compounds were characterised by ^{1}H, ^{13}C NMR spectroscopy. Attempts to cross couple Schiff base complex **C19** and **Q3** via Sonogashira cross coupling mechanism method was not successful after two attempts from following two different reaction routes and conditions. The trans-metalation route yielded quinoxaline derivative **QA** in good yield after the reaction of **Q3** with $ZnCl_2$ and, **C19** in the presence of Et_2NH which were characterised by NMR (^{1}H, ^{13}C and HMBC), Mass spectroscopy (HRMS) and Elemental analysis.

These reactions showed hydroamination instead of coordination in yield of (90%) using $ZnCl_2$ as catalyst and 60% using **C19** as catalyst.

Biological activity studies were done by quantitative antibacterial activity by assay of minimum inhibition concentration (MIC). Bacterial cells used as pathogenic microorganisms were gram negative: *Escherichia coli* and *Pseudomonas aeruginosa*, gram positive: *Staphylococcus aureus* and *Enterococcus faecalis*. Compound used for testing : **L9**, **C19**, **C18**, **C9**, **Q3** and **QA**. All compounds were found to be active against bacterial cells of *E. coli and E. faecalis* with a minimum inhibition concentration of 0.004 mg/ml average and total activity of 500 mg/ml average. For all compounds used for testing bacterial activity against cells of *P. aeruginosa* and *S. aureus*, the lowest concentration was 0.063 mg/ml average and total activity of 266 mg/ml average for **C18**. *P. aeruginosa* and *S. aureus* were found to be less active compared to bioactive standards used for *E. coli and E. faecalis*.

TABLE OF CONTENTS

LIST OF FIGURES

LIST OF SCHEMES

LIST OF TABLES

LIST OF ABBREVIATIONS

δ	chemical shift
d	doublet
DCM	dichloromethane
DMAP	4-dimethylamino pyridine
DMF	dimethylformamide
DMSO	dimethylsulfoxide
DNA	deoxyribonucleic acid
DNA-SH	deoxyribonucleic acid sulphur hydride
EtOH	ethanol
Et_2NH	diethylamine
Et_3N	triethylamine
FT-IR	Fourier Transforms Infrared
H	hour
HCl	hydrochloric acid
HRMS	High resolution Mass Spectroscopy
Hz	hertz
INT	*p*-Iodonitrotetrazolium
J	constant coupling
KI	potassium iodide
KOH	potassium hydroxide
M	concentration
m	meta
m	multiplet
MeOH	methanol
MIC	minimum inhibitory concentration
µl	microliter
mg/ml	milligram per millilitre
ml	millilitre
mmol	millimole

M.p	melting point
NMR	nuclear magnetic resonance
o	ortho
p	para
%	percentage
π	pi
ppm	parts per million
q	quartet
rt	room temperature
s	singlet
THF	tetrahydrofuran
TLC	thin layer chromatography
TMS	trimethylsilane
t	triplet
UV-vis	ultraviolet visible

ACKNOWLEDGEMENTS

Above all I would like to thank God ‘Lord of mercy’ for the life he gave to me. I would like to extend my sincere gratitude and appreciation to my supervisor Dr. R.M. Mampa for: guidance, support, mentorship, good personality, open advising discussion and time he had for this study with patience.

I would also like to appreciate the support and mentorship of my co-supervisors: Dr. W. Nxumalo and Dr M.S Thomas.

The following Institutions are acknowledged based on their contributions

University of Stellenbosch: for Mass spectra analysis

Rhodes University: for Elemental analysis

This study received financial support from Sasol Inzalo Foundation and National Research Foundation which are gratefully acknowledged.

The department of Chemistry in the University of Limpopo is highly acknowledged for giving me privilege to enroll this study.

The following people are acknowledged according to their contribution:

- Dr. K.D. Modibane: for his help in photophysical studies.
- Prof P. Masoko: for helping in biological studies.
- Dr. V. Mbazima: for UV analyses.
- Prof J. Darkwa: for fruitful advices of part of the study.

I would also like to thank my research group members, friends and my internal league team at the University of Limpopo Turfloop campus (Torros) which have been my second family. To my family I would say I was blessed to have all your support and courage through hard and nice times. Finally but not least I would like to express my deepest appreciation of love and care from Morongwa Sabina Nkgoeng and Tswelopele Jesse Nkgoeng in my life.

SCIENTIFIC CONTRIBUTIONS

Conferences attended:

Faculty of Sciences and Agriculture, University of Limpopo Research day Limpopo South Africa 2014

Title: Synthesis characterisation of imidazolyl-salicylaldimine Schiff base ligands derivatives for their potential applications

Bi-national Organic Chemistry Conference 2014 Stellenbosch-South Africa

Title: Synthesis, characterisation and biological activity studies of organo-bridged metal Schiff base complexes with quinoxaline derivative

SACI Convention 2015 Durban-South Africa

Title: Synthesis, spectroscopic and photophysical properties correlation of imidazolyl-salicylaldimine Schiff bases derivatives

CHAPTER ONE

REVIEW OF SCHIFF BASES, SCHIFF BASE COMPLEXES, QUINOXALINES, SCHIFF BASED-QUINOXALINE COMPOUNDS AND THEIR COMPLEXES.

1.1 Introduction

Transitional metal complexes consist of a central metal surrounded by array of bounded ligands and organometallic complex with at-least one carbon-metal bond [1; 2]. Metal complexes were known for their good industrial contribution for various catalytic applications [1; 2; 3]. Metal-based compounds demonstrate many physico-chemical properties such as metal-ligands exchange and geometrical arrangements in both homogenous and heterogonous catalysis based on their geometrical arrangement and oxidation state [4; 5]. In addition metal complexes also demonstrate various applications in medicinal field. The study of complexes for medicinal purpose emerged surprisingly after cisplatin and its derivatives were discovered and applied as wonder drugs for cancer treatment [6]. Factors such as redox states, geometrical arrangements, coordination modes and possibility of ligand exchange enhances their medicinal properties [6]. Generally, introduction of transition metals to organic compounds changes the pharmacological properties of organic compounds by enhancing its biological strength [3]. The interest of studying metal complexes towards medicinal application is growing because of their good results in toxicity towards harmful pathogens.

Schiff base complexes exhibit wide spectrum of biological activities which (covered in the next section) and are generally characterised by nitrogen-carbon double bond with nitrogen atom coordinated to the metal centre, therefore becoming possible potential analogs of cisplatin, which favours them to exhibit biological properties. Quinoxalines on the other hand are heterocyclic compounds which contain a phenyl ring fused to a pyrazine ring and more importantly exhibit biological activities [7; 8]. The literature scope of Schiff bases, Schiff base complexes and quinoxalines in medicinal chemistry is extremely large and is reviewed in the next sections. The next section **1.2** covers the backgrounds chemistry and applications of Schiff base ligand.

1.2 Schiff base ligands

1.2.1 Historical background of Schiff base ligands

Schiff base ligands also known as imines or azomethine were discovered by Hugo Schiff, a German scientist after condensing primary amines with carbonyl compounds in 1864 [9; 10]. The Schiff base ligands are compounds that contain carbon-nitrogen double bond backbone $R_3R_2C=NR_1$ [10]. The substituents R_1, R_2 and R_3 may be alkyl, aryl, heteroaryl or hydrogen. These organic compounds occur in various derivatives and can be found in nature like many organic compounds which exist naturally. Schiff base compound were found to be useful as ligands for preparation of metal complexes and as bioactive agents in medicinal fields [1]. To date the contribution and chemistry of Schiff base compounds is growing with interesting findings since their discovery which is covered in the next section.

1.2.2 The chemistry of Schiff base ligands

Schiff base ligands can be obtained as products after condensation of primary amines with aldehydes or ketones. These reactions generally occur under reflux in the presence of acid or base as the catalyst and drying agents such as sodium sulphate, molecular sieves or magnesium sulphate for water removal which is produced as a by-product [10; 11]. **Scheme 1.1** shows the detailed mechanism for the condensation reaction where acid/base reaction protonate the carbonyl group to be active and more susceptible to attack by a neutral nucleophilic nitrogen of the primary amine. The attack from the nitrogen nucleophile to the electrophilic carbonyl carbon group is followed by *pi* electrons going to the oxygen which becomes positively charged. The removal of the proton neutralises the positve charge on the nitrogen and forms the carbinolamine intermediate. Then protonation followed to generate water molecule which is a good leaving group (dehydration process). The electrophilic of the nitrogen helps to push out the leaving group (water molecule) forming an iminium ion. Deprotonation of the iminium nitrogen generate imine product and regenerates the acid catalyst [12]. The mechanism details the formation

of imine. Schiff base ligands have the ability to coordinate as mono-dentate to multi-dentate such as tetra-dentate, tri-dentate, bi-dentate and chelation abilities in the presence of donor sites [11]. They normally coordinate to the metal center through nitrogen or phosphate lone pair of electrons and oxidatively through the deprotonated hydroxyl group. Some of the Schiff base ligands are stable, solid and can be carefully purified with minimum loss of the desired product [12; 13]. The variation of substituents on the Schiff base ligands are often used to induce substrate chirality and enhancing the solubility and stability of the resultant complexes [14]. The derivative, imidazole containing substituent on Schiff base ligand behave as monodentates ligand at lower pH and as a bridging ligand at higher pH in accordance with the flexibility of the compound [14]. The properties of Schiff base ligand varies based on substituents bonded to the imine functional group.

The mechanism on **Scheme 1.1** demonstrates condensation of primary amines with aldehydes to form Schiff base compounds under acidic conditions.

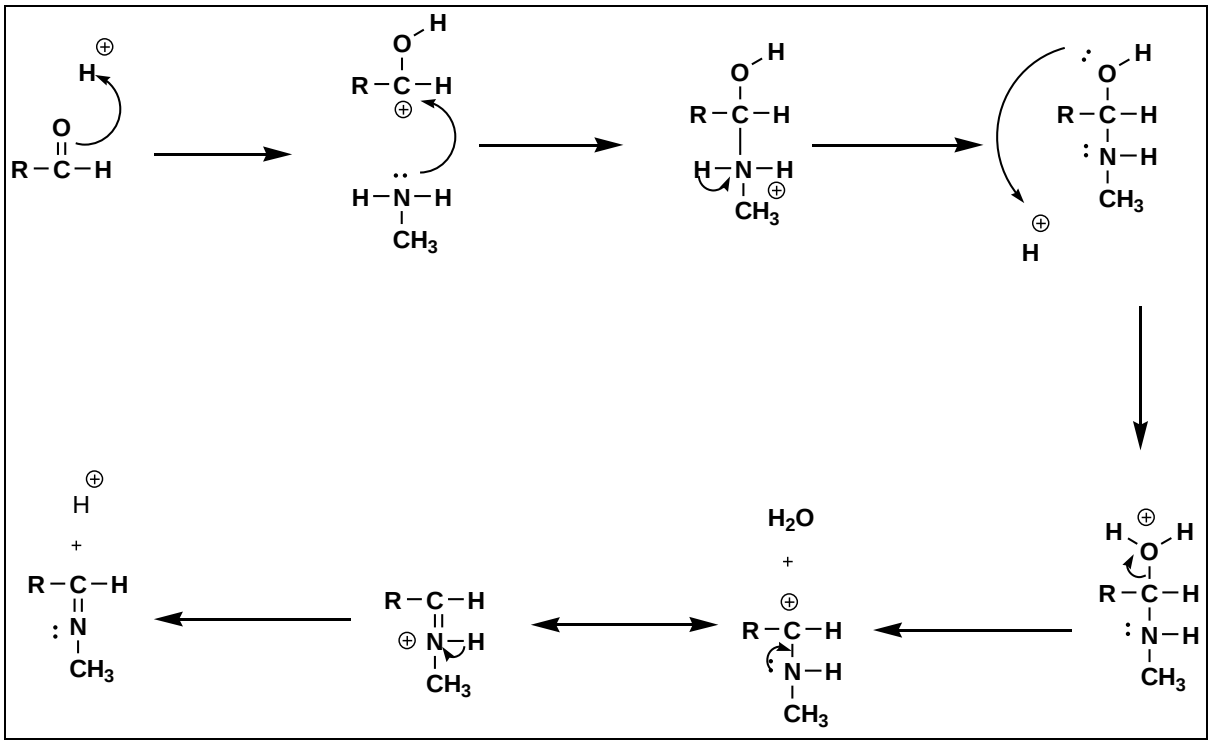

Scheme 1.1: Mechanism for condensation of primary amine with an aldehyde to form Schiff base compound [12]

Schiff base ligands can be synthesised using various routes where the commonly known method is condensation of aldehydes or ketones with primary amines. Some

of these routes are illustrated and discussed below. Aldehydes and ketones are derived from corresponding alcohol via oxidative processes. The intermediate to Schiff bases formation from ketones or aldehyde involves alcohol group formation step. **Scheme 1.2** demonstrates aerobic oxidative synthesis for preparation of Schiff bases using alcohol and primary amine.

The **Schemes 1.2-1.5** describe the formation of imine (N=C) using different substrates and reaction conditions. The example of a detailed mechanism discussed on **Scheme 1.1** summarise the formation of imine group.

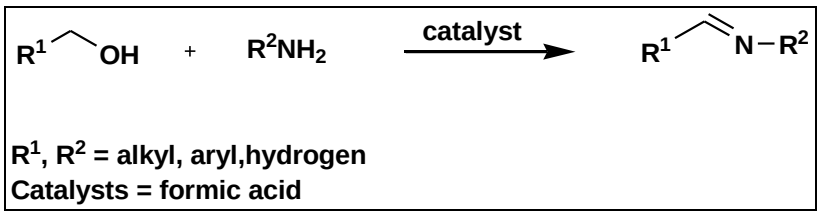

Scheme 1.2: Aerobic oxidative preparation of Schiff bases from alcohol and primary amines [10]

Oxidative preparation of imines from primary amines is demonstrated below.

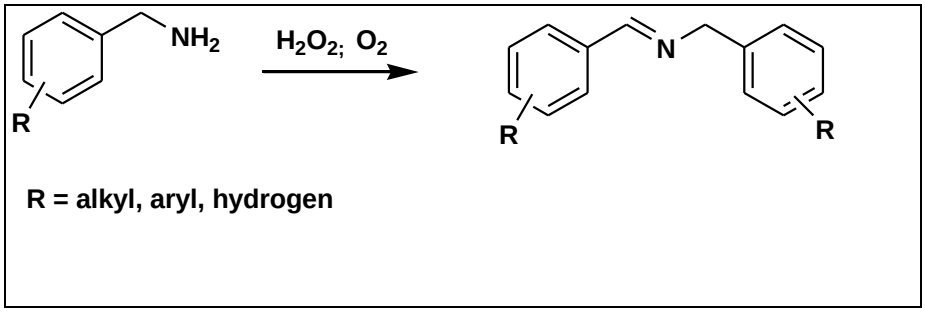

Scheme 1.3: Aerobic oxidative preparation of Schiff bases from primary amine derivatives [15]

Preparation of ketimines from phenol and nitriles demonstrates another route to Schiff base formation in the presence of hydrochloric acid.

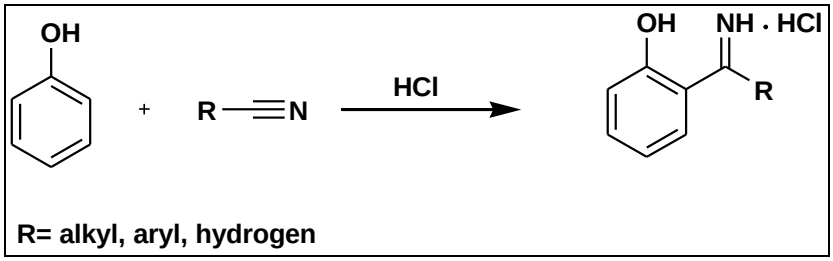

Scheme 1.4: Preparations of ketimines [16]

Aliphatic aldehydes are used to prepare imines by a competitive reaction due to condensation product from aldol reactions forming a reversible intermediate.

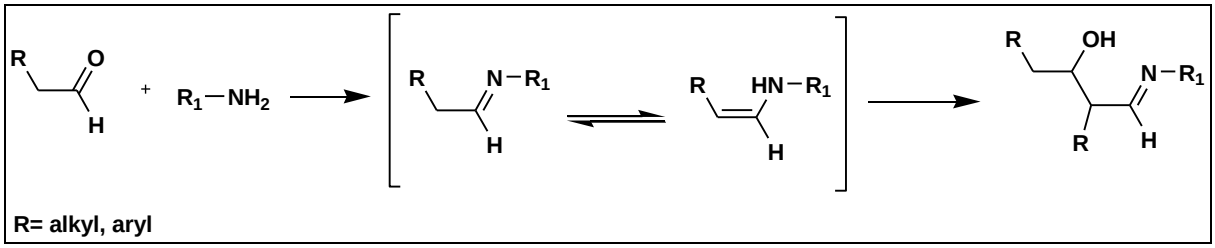

Scheme 1.5: Aldol condensation of aliphatic aldehydes [17]

Schiff base ligands have various flexible coordination modes depending on functional groups which makes them good candidate for coordination chemistry. The **Figure 1.1** illustrate coordination flexibility of some common Schiff base compounds, both tri, and tetra-dentate coordination modes. Ligands showing tri-dentate coordination possibility are **2**, **3**, **4**, **5** and **6** in **Figure 1.1.** Only ligand **1** in **Figure 1.1** has possibilities for tetra-dentate coordination.

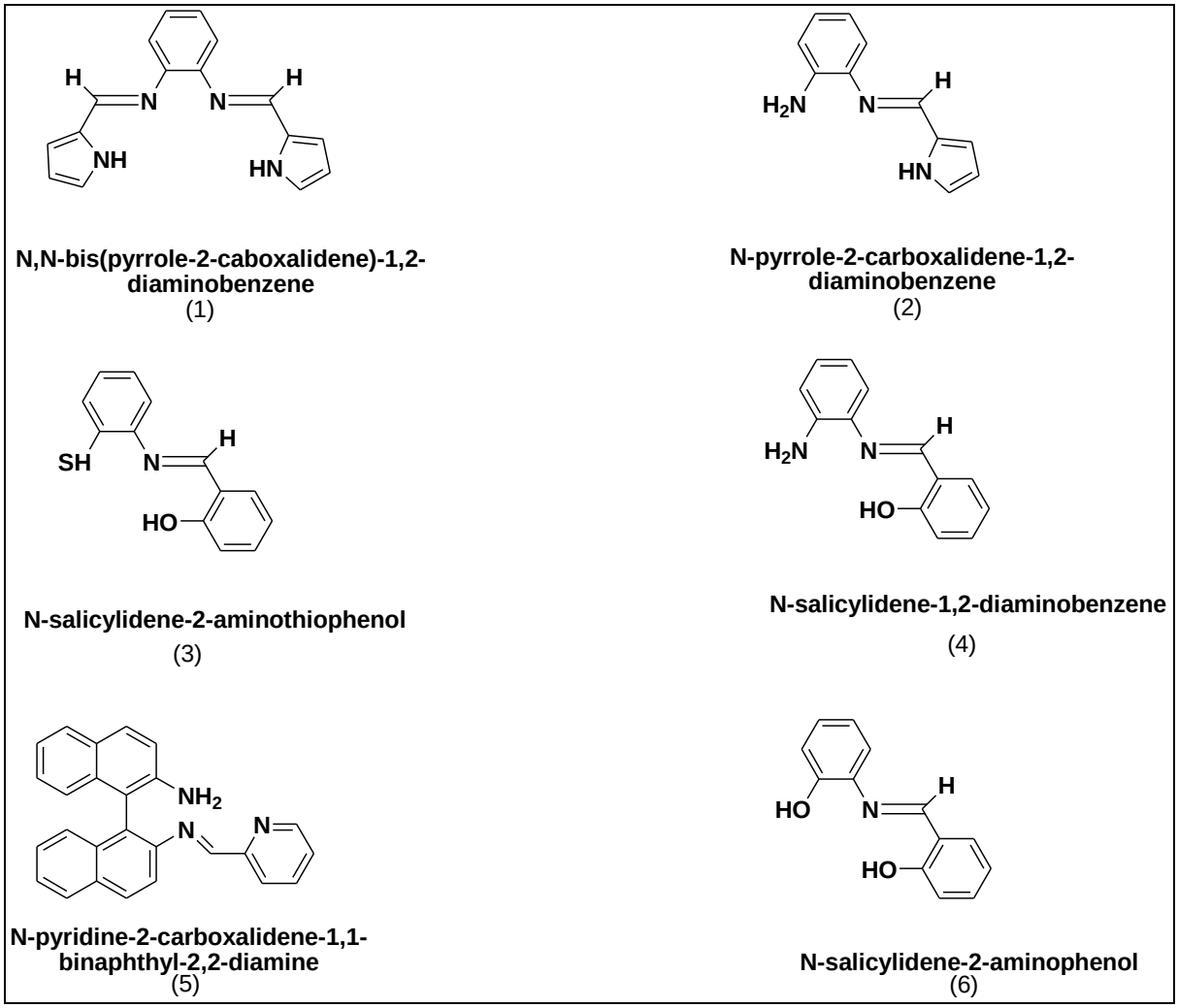

Figure 1.1: Tri-dentate and tetra-dentate Schiff base compounds [18; 19]

Salen Schiff base compounds are obtained by condensing salicylaldehyde derivatives with diamine derivatives giving two nitrogen and hydroxyl group compounds [18; 19]. These types of compound are classified as Salen ligands because they form tetradentate coordination modes as shown below.

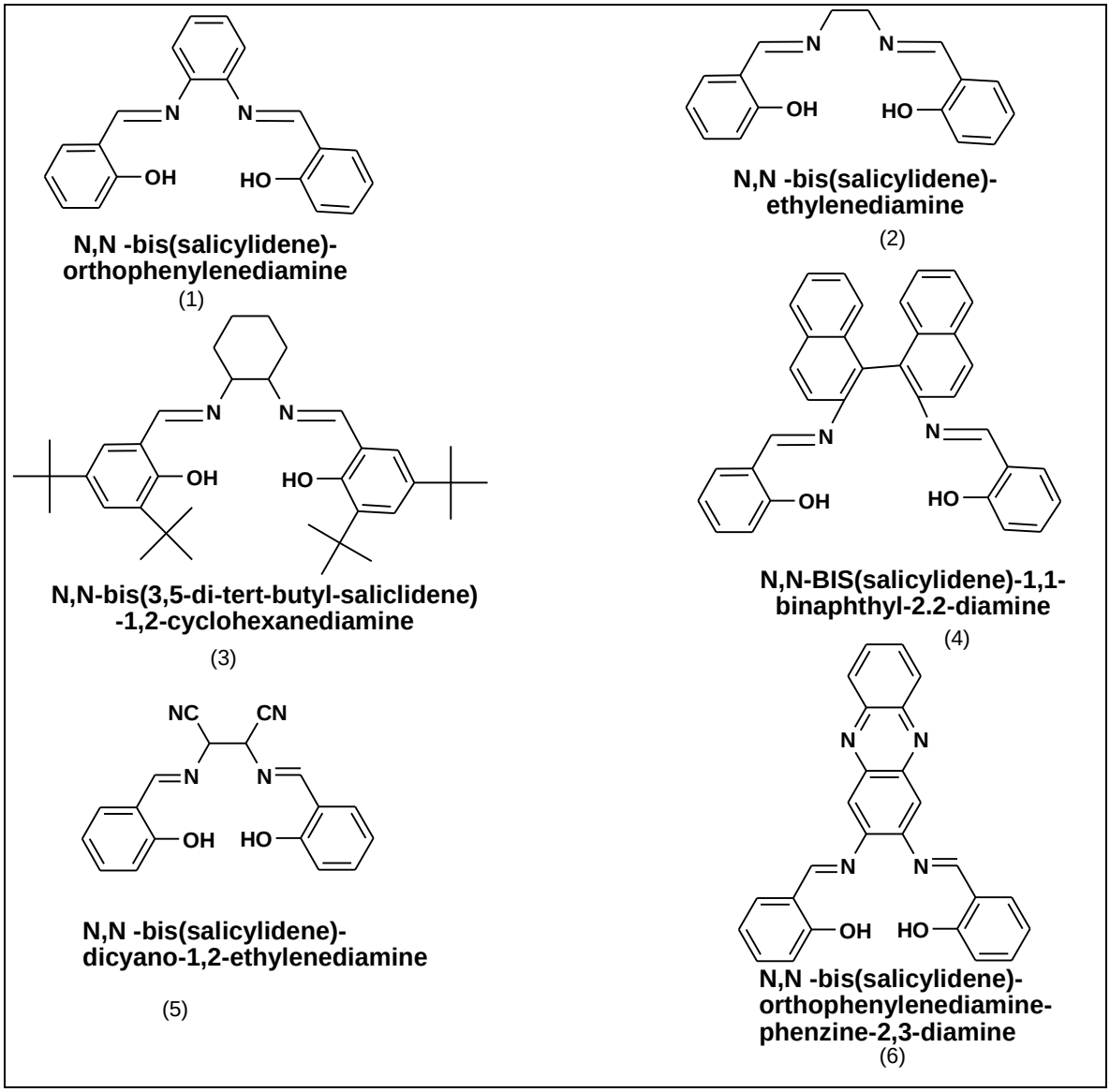

Figure 1.2: Salen Schiff base compounds [18; 20]

Furthermore, there is a group of macrocyclic Schiff base compounds shown in **Figure 1.3** which differs from Salen Schiff bases by cyclic arrangements. These can be prepared by the self-condensation reaction of ketone and primary amines precursors [20; 21]. Macrocyclic compounds mainly comprises of oxygen, sulphur and nitrogen as donor atoms [22]. Macrocyclic compounds with more donor atoms are flexible and better host for metal coordination [21]. Macrocyclic Schiff bases containing nitrogen donor atom has mixed hard–soft donor character, flexible coordination mode, shows good biochemical properties including biological activities such as antibacterial and anticancer [23].

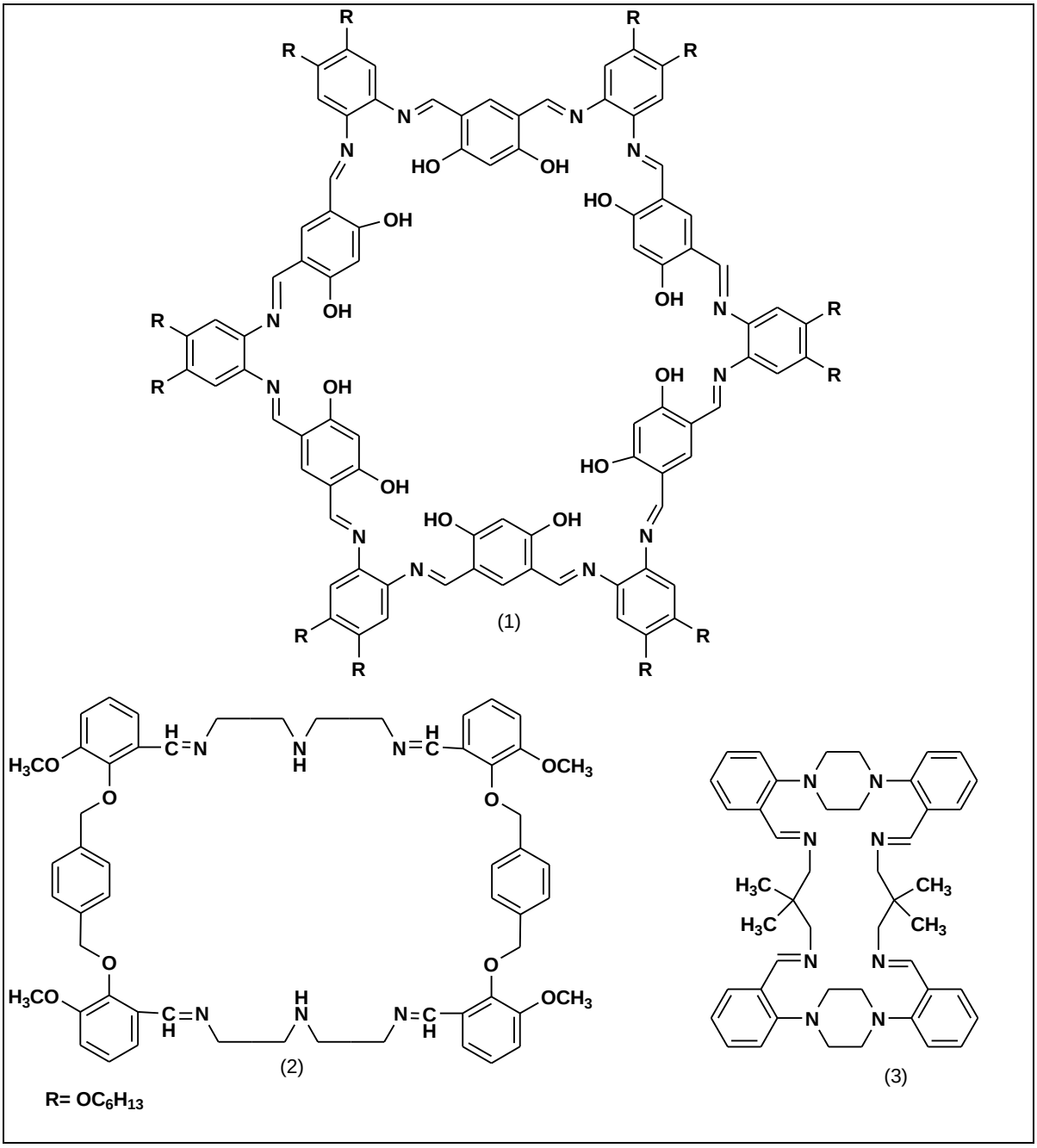

Figure 1.3: Macrocyclic Schiff base compounds (2) [21]; (1) [22]; (3) [23]

There are many types of Schiff base ligands including Salen and macrocyclic groups which covers a wider area in different research fields and are thus regarded as important compounds in both industrial and medicinal fields.

1.2.3 Applications of Schiff base ligands

Schiff base ligands can be considered as supportive ligands during the synthesis of metal complexes and organic products demonstrated on **Scheme 1.6** [24; 25]. Schiff base ligands coordinate to the metal centre to form desired metal complexes [26; 27]. Schiff base ligands have various biological abilities which seem to improve with coordination to the metal center [3].

Generally, Schiff base compounds containing functional groups such as thiosemicarbazones, imidazole's, indole, pyrazole, furylglyoxal, azomethine, *p*-toluidene, thiazole, benzothiazole, isatin, azo compounds, pyridoxal, hydrazones and other fussed heterocyclic compounds have shown different desired properties in pharmacological studies such as antibacterial, anticancer, antifungal, antimicrobial, antiviral [11-25]. The Schiff base ligand properties make them to be good candidates for use in industries for oxygenation, hydrolysis, electro-reduction and decomposition; in agricultural sectors for plant regulation as insecticides [28]; and are medicinally used as antiviral [29], antibacterial [30] and antitumor agents [31].

The following **Scheme 1.6** shows the use of Schiff base as intermediates in organic and inorganic synthesis.

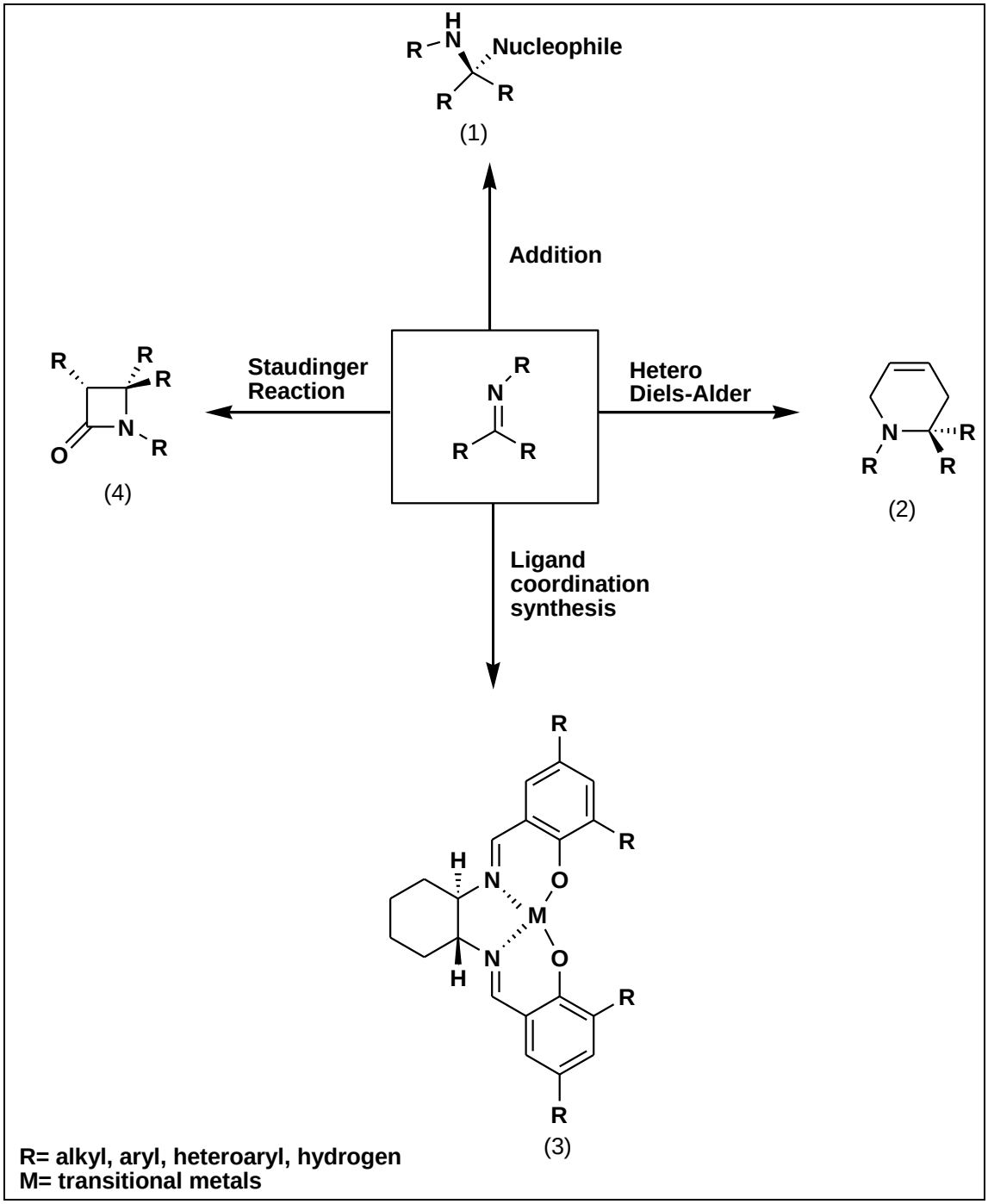

Scheme 1.6: Schiff bases as intermediate during synthesis [10].

The next section **1.3** covers the scope of Schiff bases coordination chemistry and various applications.

1.3 Schiff base complexes

1.3.1 Historical background of Schiff base complexes

The discovery of Schiff base compounds paved the way for the synthesis of Schiff base complexes. Schiff base complexes were explored in the 19th century for their various use, though they were discovered in the early 18th century [14]. Schiff base complexes are known for their contribution in coordination chemistry because of their good physico-chemical properties. The physico-chemical properties possessed by Schiff base complexes vary from type of metal and functional groups on Schiff bases used which is reviewed in the next section.

1.3.2 The chemical structure of Schiff base complexes

The Schiff base complexes derived from transition metals are widely considered and preferably studied because of their interesting chemical and physical properties [1]. The physico-chemical properties of Schiff base complexes such as geometrical arrangements, redox properties, multiple coordination modes and the high possibilities of ligands exchange makes them valuable ligands [8].

The structural diversity of metal complexes in relation to pure organic compounds is different from each other. The contrast in stereochemistry of the metal-based compound and pure organic compounds are interesting; i.e. an organic carbon bonded to four different bonds can demonstrate two different enantiomers [6] whereas a metal complexes containing six different groups in an octahedral arrangement coordinated to one metal center will have fifteen different geometric isomers where each isomer has a mirror image, i.e. each existing as a pair of enantiomers to make a total of thirty stereoisomers [6]. The structural diversity of transition metal complexes will extremely exceed that of pure organic compounds in a three-dimensional orientation template where the central atom is carbon as compared to transition metal. The stereo-chemical stability of the metal-based compounds limits the possibility of racemic products as compared to pure organic molecules due to ligands contribution. These factors may differ from one metal-based compound to another because of structural conformation, stability and oxidation states [6]. The geometrical properties of pure organic compounds and that

of metal-based compounds both contribute to the functioning ability of the final desired compounds.

Redox properties of Schiff base complexes cover the scope of oxidation state, electron transfer, and the half-reactions; where oxidation involves loss of electrons whereas reduction involves gain of electrons. Oxidation in this case helps to measure the extent of reduction of metal-based compounds, [6] where most metal-based compounds and transitional metals readily undergo electron transfer. These often occur to metal-based compounds consisting of transitional metal due to the fact that they are electron rich and can easily donate electrons [6]. However, the mechanism involves the ligand to donate a pair of electron to the metal centre, which possibly induces *pi* (π) back bond donation to occur. The redox properties of metal-based compounds play a major role in both applications and reaction mechanisms. The next section deals with the preparation of Schiff base complexes.

Schiff base complexes can be synthesised in variety of ways as illustrated in the **Scheme 1.7**.

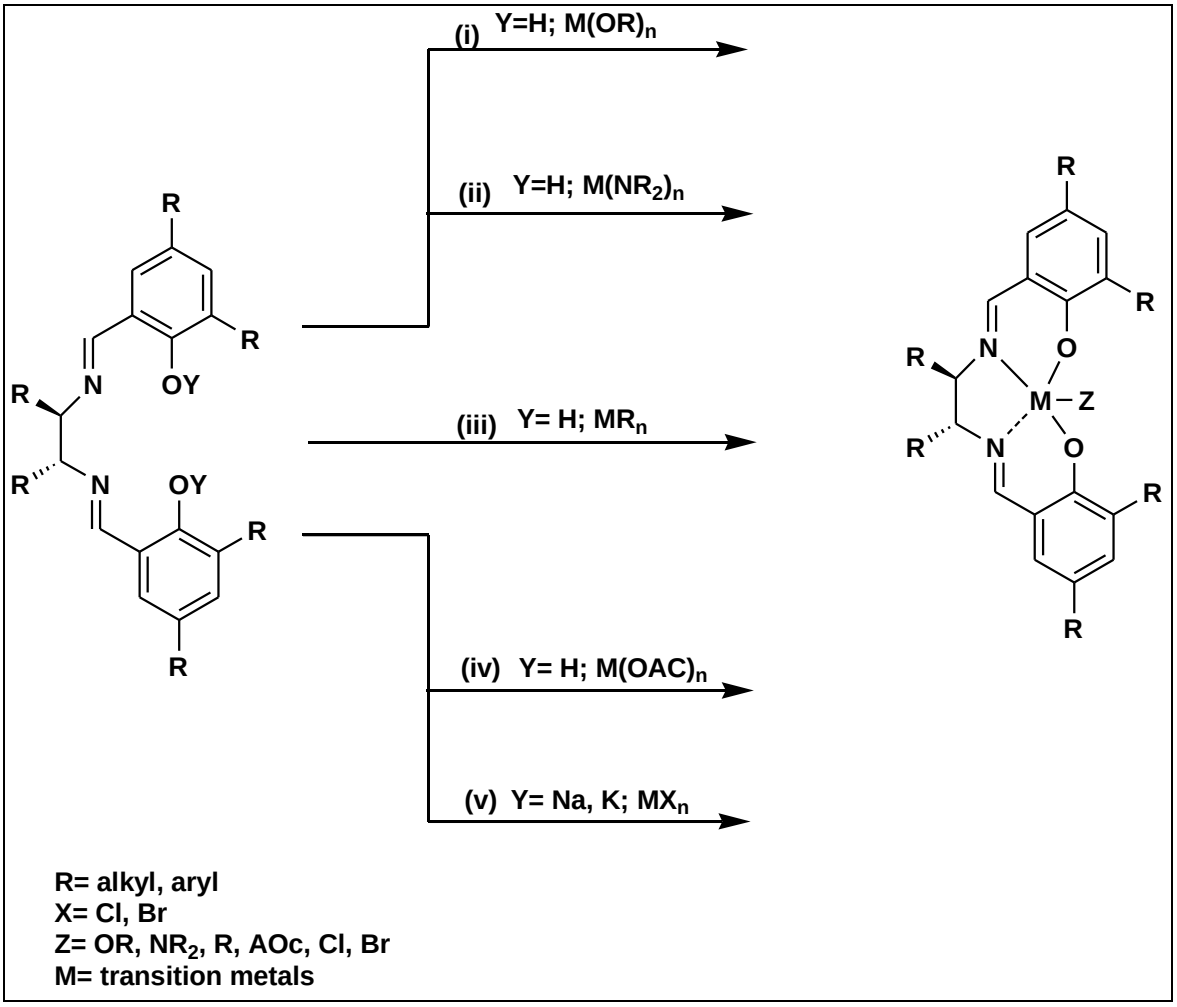

Scheme 1.7: Different routes for synthesise of Schiff base complexes [18]

The first route (i) involves transition metal alkoxide complexes which are air-sensitive, similar to the second route (ii) transition metal Nitrogen-alkyl complexes [18]. These complexes are commercially available and capable of forming Schiff base complexes. The third (iii) and fourth (iv) routes involve metal alkyl and metal acetates respectively which when treated with Schiff bases under reflux yields Schiff base complexes. The fifth (v) route involves metal halides reacting with Schiff base compounds in a two steps mechanism where the first step involves the deprotonation of Schiff base compounds using strong base followed by direct coordination to the metal center. However this reaction can also proceed without any strong base treatment, i.e. just stirring at room temperature for longer time.

The following complexes demonstrate flexible coordination capability such as bi-dentate and tri-dentate coordination modes of Schiff base complexes which can be

synthesised by route (v) of the previous reaction **Scheme 1.7**. The complexes shown below have active centre through the metal-halide bond which plays a major role during catalysis and ligand exchange application.

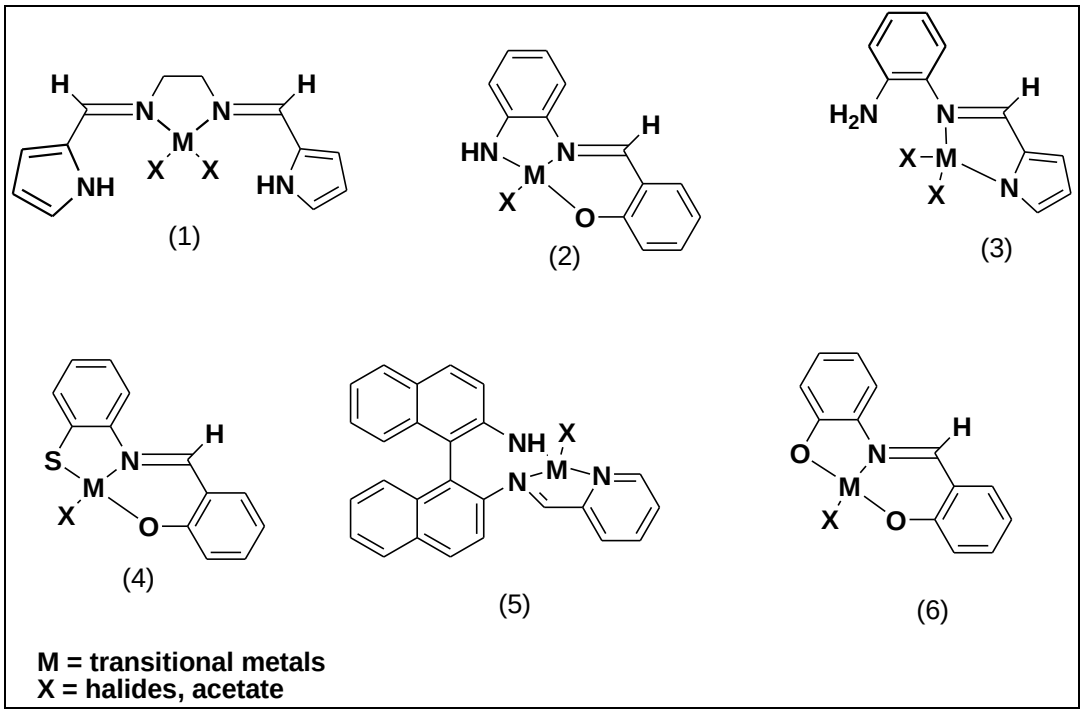

Figure 1.4: Coordination of bi and tri-dentate ligand to transition metal in low oxidation states [19]

Another type of Schiff base complexes are derived from Salen Schiff base ligands which coordinate as tetradentate as demonstrated on **Figure 1.5**. The Salen Schiff base compounds can be prepared as demonstrated before in **Scheme 1.1** using ketone and primary amine condensation. These types of complexes can be synthesised by route (iv) in **Scheme 1.7**. Their oxidation state can be controlled because of the Salen geometrical arrangement. The metal centre activity site is reduced due to lack of highly active metal-halide bond. The Salen Schiff bases contain two covalent and two coordinate covalent sites in a planar array to coordinate to metal centre. Section 1.3.3 looks at the extensive application of Schiff base complexes.

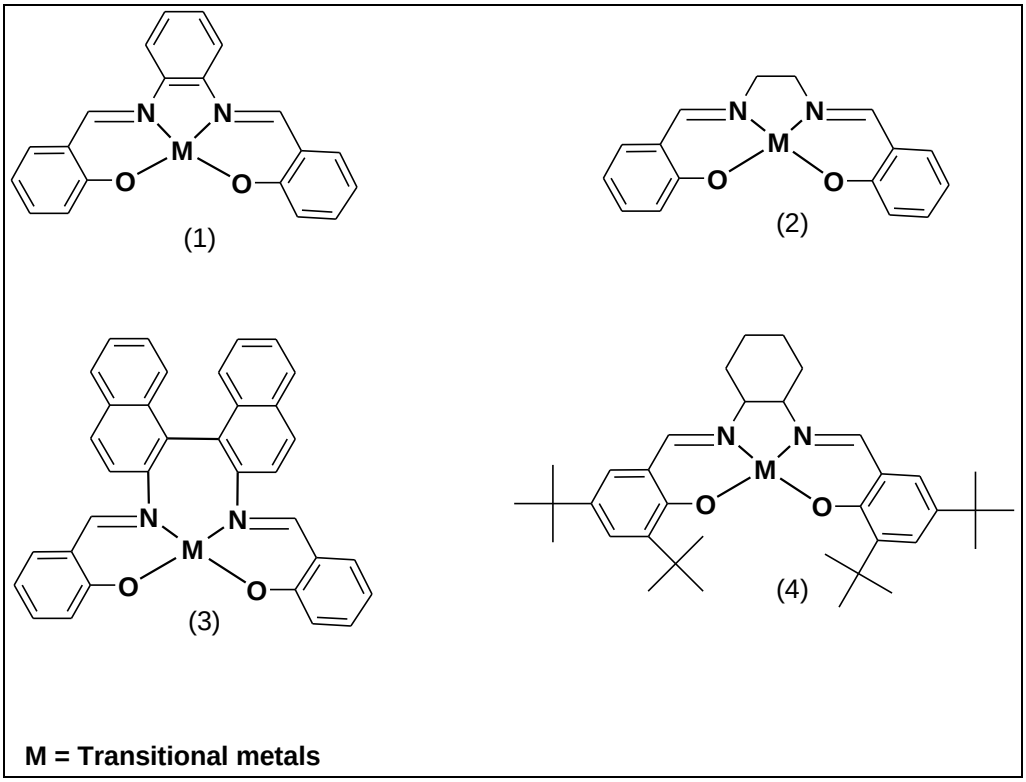

Figure 1.5: Tetra-dentate Schiff base complexes [21]

1.3.3 Chemical applications of Schiff base complexes

Schiff base transition metal complexes exhibit various biological activities and have since developed a huge interest in pharmaceutical and agricultural sectors [1; 2]. The use of metal complexes in medicinal fields was further revitalised by the discovery of cisplatin and its analogues for clinical application as anticancer drug [32; 33]. The biological activities of Schiff base ligands have also been proven to increase by introduction of transition metal to form complexes [32]. There are a number of drugs which shows increased activity when administered as complexes than as purely organic molecules [32].

According to Hambley and co-workers: pharmaceutical metal-based compounds in applications can be classically arranged into seven categories depending on the type of transition metal and ligand functions [4]: (i) in an inert condition the metal complex is active, (ii) in a reactive condition where there is possible metal-ligand exchange the metal complex is active, (iii) the active site of the metal complex is mainly one fragment, (iv) the whole compound consist of a radioactive metal centred site, (v) the final metal complex is reactive, (vi) the ligand as an organic moiety is biologically active, and (vii) the radiation of the compound is enhanced by the metal centre. The above mentioned probable conditions rely on the type and properties of compounds chosen for reaction. Many complexes which are derived from Schiff base ligands such as imidazole, pyrazole, indole, thiosemicarbazones, hydrazones, salicylaldehyde, sulfane thiadizole, thiosemicarbazones, furylglyoxal, azomethine, *p*-toluidene, thiazole, benzothiazole, isatin, azo compounds, pyridoxal, and other heterocyclic ligands show biological activities such as, enzyme inhibition [33], antiviral [34] antimicrobial [34], antifungal [34], antitumour [34 ;35], antiinflammatory [35].

Transition metals such as Co(II), Mn(II), Pd(II), V(III), Fe(III), Zn(II), Cu(II) and others coordinated to Schiff base ligands have been used as catalysts for oxidation, epoxidation, hydrolysis, disproportionation, decomposition, polymerisation, electro-reduction, ring opening of polymerisation and epoxides [32-44]. The ability of Schiff base transition metal complexes to reversibly bind to oxygen plays a major role in industries for both homogeneous and heterogeneous catalysis [44].

Interesting properties such as ligand exchange occurs during applications and synthesis of metal-based compounds. This property has also been observed when metal-based compounds undergo ligand exchange during medicinal applications [6]. The cisplatin compound serves as one examples of the generally known compound which has ligand exchange mechanism that takes place during administration [4]. The ligand exchange capabilities in coordination chemistry bring diversity in medicinal applications especially in the generation of chemotherapeutic drugs derived from metal-based compounds. Metal-based compounds rely mainly on ligand exchange possibilities to improve their biological activities and performance for medicinal applications. The ligand exchange mechanism becomes simpler in the presence of halogens and ligands with good abilities to exchange with other groups coordinated to the metal center. **Scheme 1.8** illustrates water (H_2O) exchanging with chlorine (Cl) and DNA exchanging with H_2O. **Scheme 1.9** illustrates the ligand exchange during medicinal applications were chlorine molecule is replaced by water molecule and protein-S

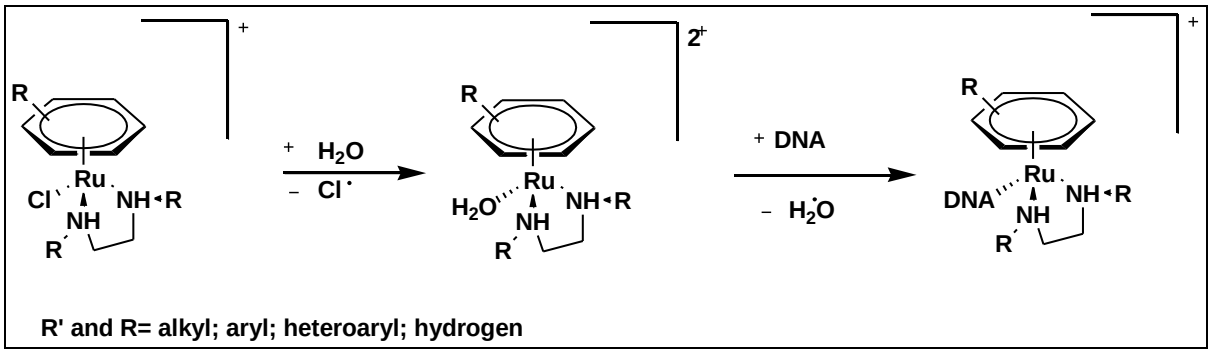

Scheme 1.8: Ruthenium derivatives demonstrating Cl, H_2O and DNA ligands exchange [6]

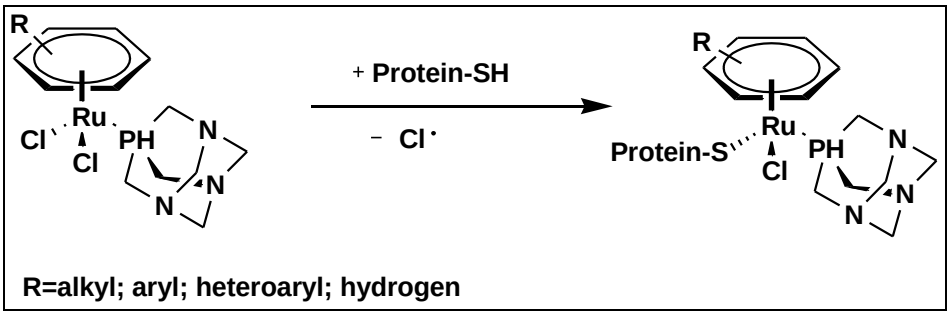

Scheme 1.9: Ruthenium derivatives demonstrating Cl and DNA-SH ligands exchange [6]

The next section **1.4** entails the scope of quinoxalines molecules as the second organic group that will be used for coordination which covers the backgrounds chemistry and application of quinoxaline derivatives. In line with the title of the project, we aim to introduce an organic moiety into the metal complex hopefully to enhance, bioactivity of Schiff base complexes. The chemistry, current medicinal application and the synthesis of quinoxalines derivatives is discussed in the next section **1.4**.

1.4 Quinoxalines

1.4.1 Historical background of quinoxalines

Quinoxalines are classified as heterocyclic compounds which contains benzene ring fused to pyrazine ring [45]. Quinoxalines are widely spread as natural products isolate and produce very good intermediates which can be useful in medicinal chemistry [45]. Quinoxalines are naturally occurring products and there are several methods reported for their synthesis [45].

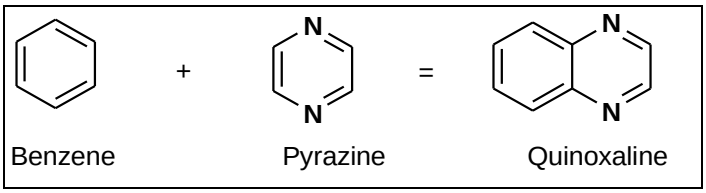

Figure 1.6: Quinoxaline and its building blocks

1.4.2 The chemistry of quinoxalines and Sonogashira-type coupling strategy

Quinoxalines are prepared by condensation of aromatic diamines and alpha-dicarbonyl compounds. There are many reported methods for synthesis of quinoxaline derivatives, however the commonly used method involves condensation of 1,2 di-ketones and primary di-amines using ethanol, methanol or acetic acids as solvent. There are other methods involved as demonstrated in the **Schemes 1.10 - 1.13** [45-47]. The **Scheme 1.10** below demonstrate Beirut reaction using an unsymmetrical mono-substituted or a di-substituted benzofuroxan, carrying different groups to synthesise quinoxaline derivatives. This reaction can form two regio-isomers as a result of a mixture of products. Tautomerisation of benzofuroxan forms two isomers which provide possibility for mixture of products. Tautomerisation stability depends on the nature of substituents as electron withdrawing or electron donating used for quinoxaline derivative synthesis [46].

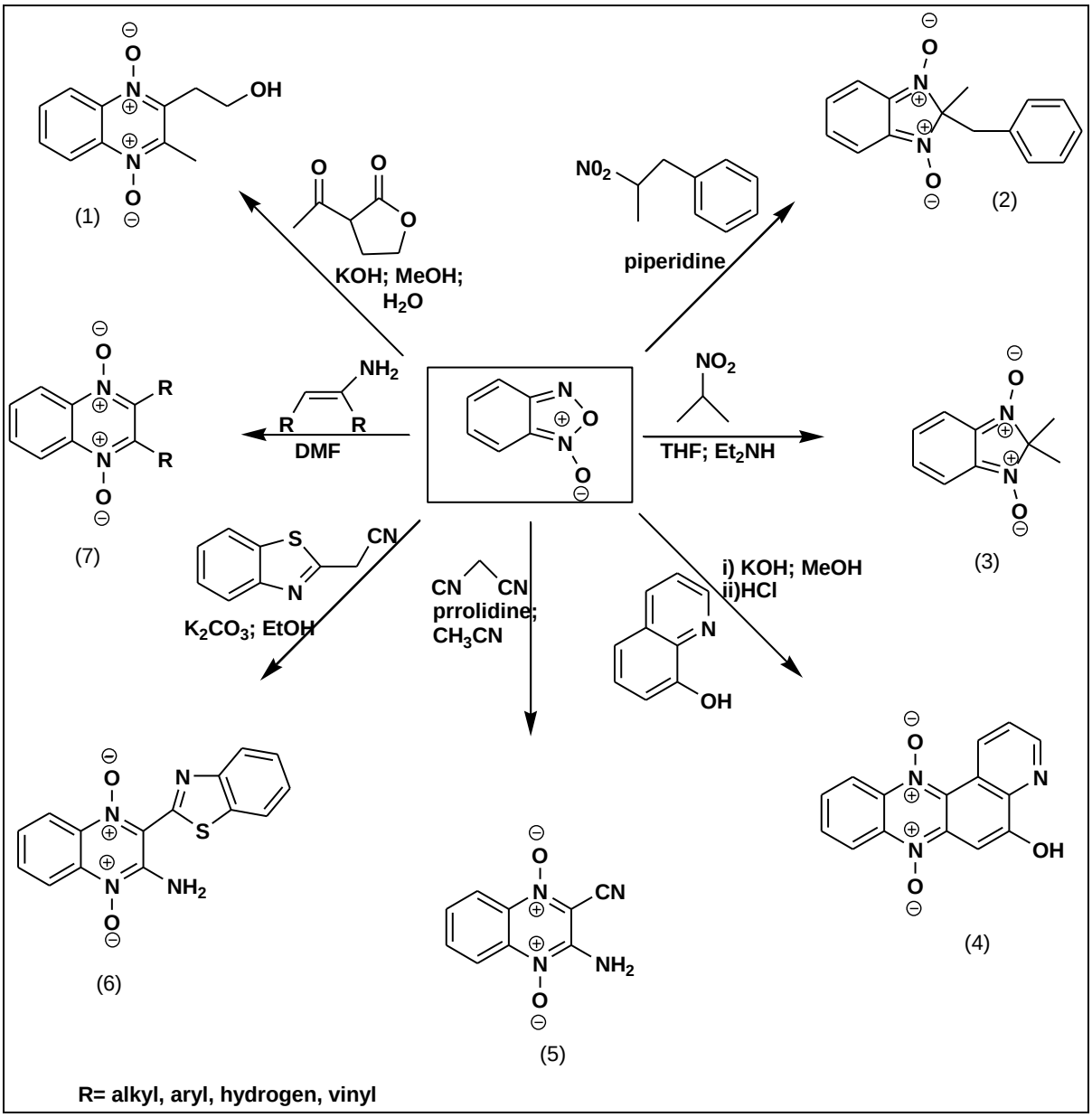

Scheme 1.10: Different routes for synthesis of quinoxaline derivatives [46]

Scheme 1.11 demonstrates the reaction mechanism using 1-keto and di-amine derivative for quinoxaline synthesis. The tautomer formed by the benzofuroxan depends on the nature of substituents used for the synthesis. First step involves nucleophilic attack to the acid hydrogen, followed by electron movement to form negative charge on the oxygen. The next step shows attack on the benzofuroxan followed by tautomerisation and base loss.

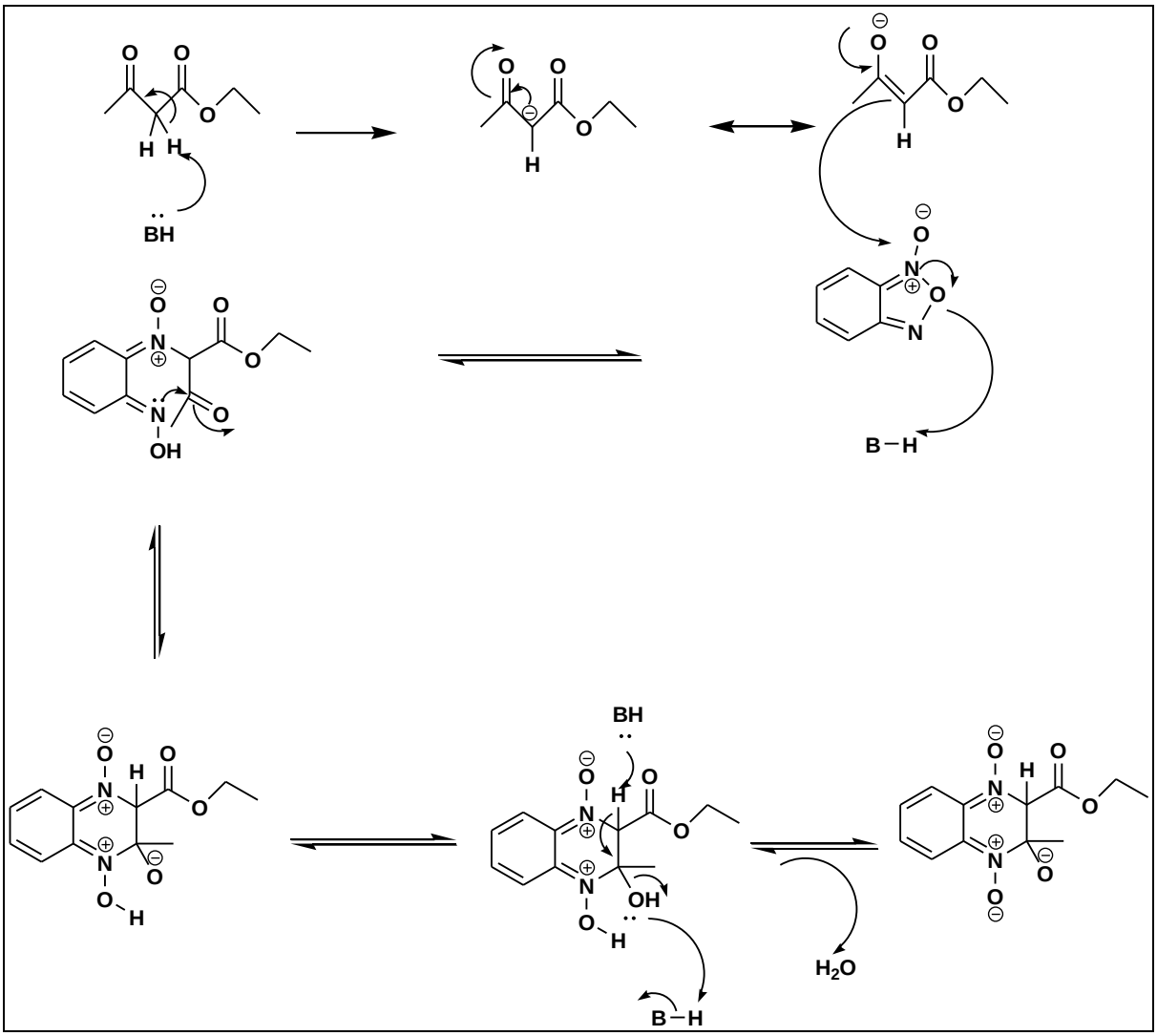

Scheme 1.11: Reaction mechanism of quinoxaline using benzofuran oxide and di-ketone derivatives [46]

Scheme 1.12 demonstrates the commonly used method for quinoxaline derivatives synthesis, where primary diamine and di-ketone condenses at various temperatures. The temperature which is the other parameter which contributes for tautomerisation control i.e. high temperatures favours tautomerism from alcohols to ketones plays a vital role to the desired target molecule.

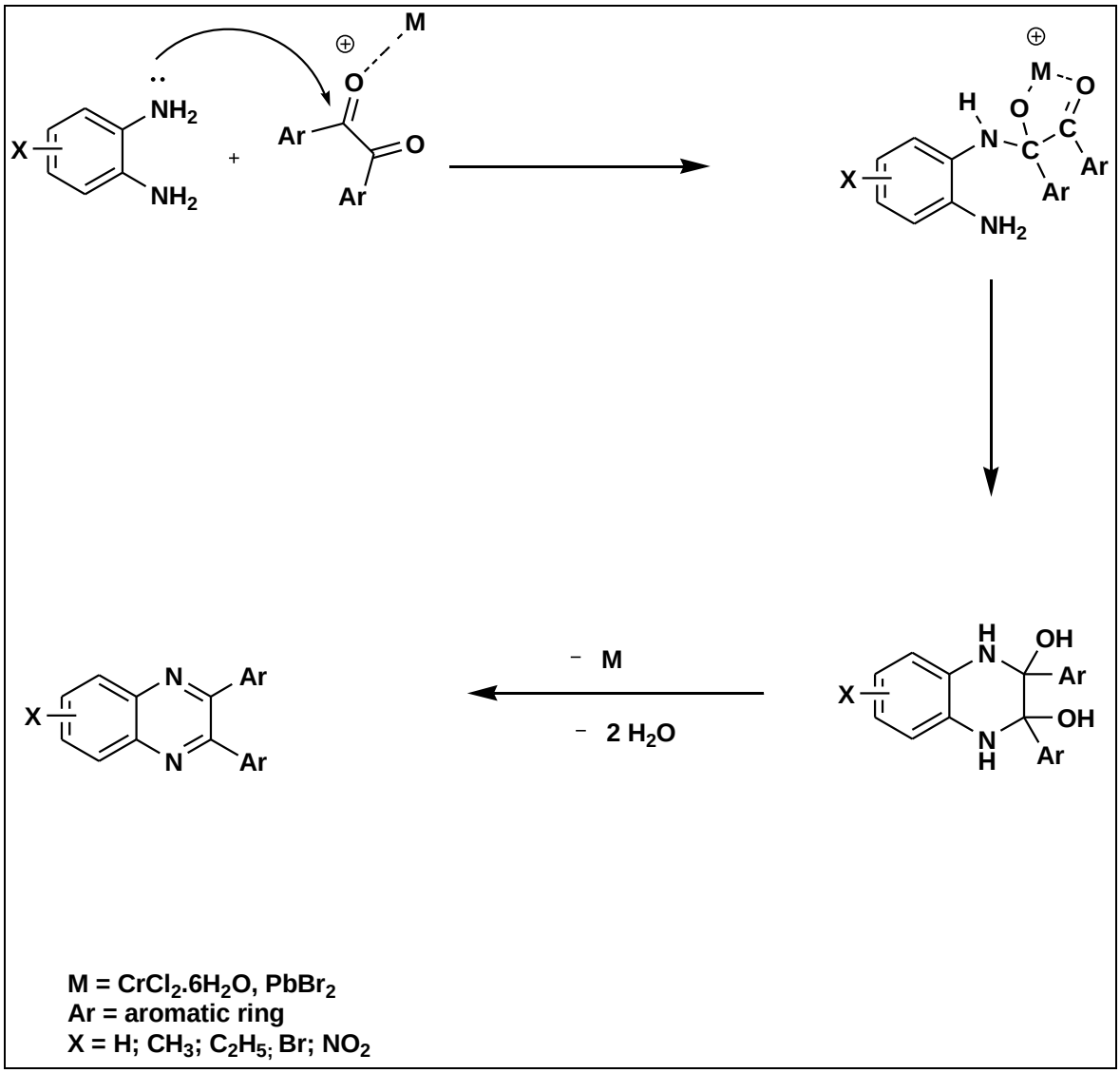

Scheme 1.12: Reaction mechanism for the synthesis of quinoxaline using di-amine and di-ketone derivatives [47]

Scheme 1.13 involves pyridine as a catalyst for quinoxaline derivatives synthesis. The first step as outlined in the mechanism pyridine attacks methylene carbon to form a pyridine bromonium salt, followed by the nucleophilic attack by the amine from *o*-phenylene substrate on the methylene carbon to weaken the pyridine bond. The remaining steps, nucleophilic attack of amine group from *o*-phenylene substrate on carbonyl carbon followed by water elimination and oxidation to produce the desired product.

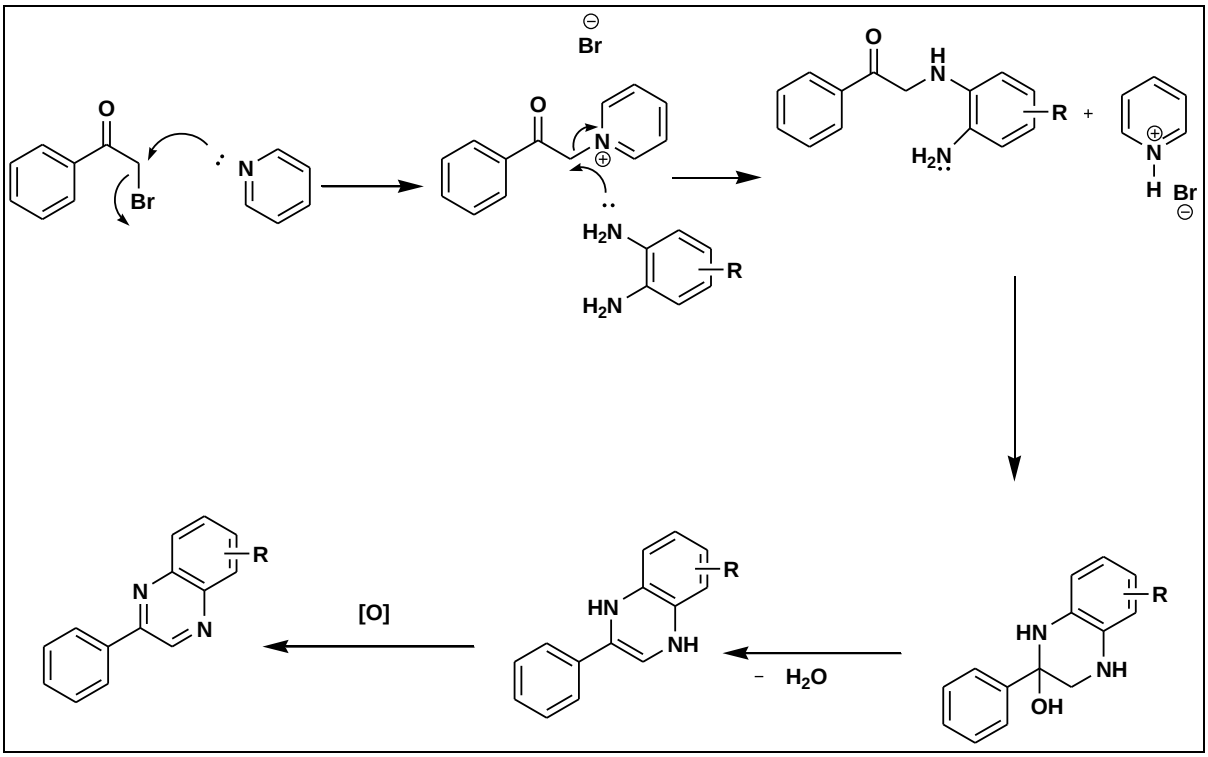

Scheme 1.13: Reaction mechanism for synthesis of quinoxaline derivatives using pyridine as a catalyst [45]

The Sonogashira cross-coupling method was discovered and first reported by Cassar [47] and Heck [48] groups in 1975. Sonogashira cross-coupling involves the coupling of terminal alkynes with aryl halides or vinyl using palladium catalysts [49]. The palladium catalyst group have been the most reliable catalysts in the construction of carbon-carbon bond to form new organic compounds [49]. Later after the discovery; Sonogashira and co-workers discovered that using copper iodide as co-catalyst accelerates the cross-coupling reaction [50; 51]. The Sonogashira reaction procedure can be viewed as alkyne version of Heck reaction and Stephen-Castro reaction using palladium as a catalyst where aryl halides couples with stoichiometrically copper(I) acetylides [52-54]. Recently the utility of copper(I) as co-catalysts in Sonogashira procedure has been applied successfully by many researchers [55]. The reaction scheme below demonstrates a simplified reaction of Sonogashira cross-coupling using palladium catalysts.

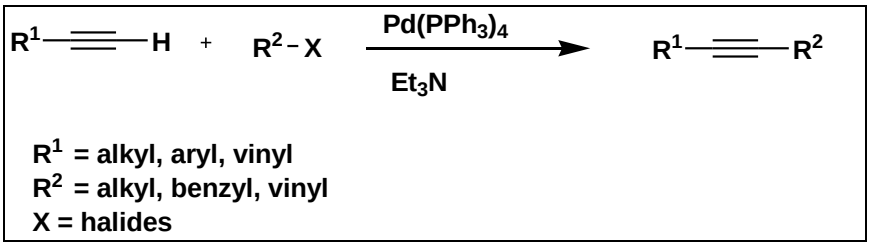

Scheme 1.14: Reaction scheme demonstrating Sonogashira cross-coupling [49]

The reaction mechanism in **Scheme 1.15** demonstrates Sonogashira cross-coupling method using palladium catalyst, copper bromine as co-catalysts and tri-ethylamine as base. Sonogashira coupling mechanism demonstrated in **Figure 1.15** shows four steps involved. The first step involves oxidative addition of alkyl and halide coordination to the palladium catalyst. Coordinating by both bromine and alkyl group to form palladium(II) from palladium(0). The second step involves triethylamine deprotonating the alkyne followed by nucleophilic attack of the alkynyl to copper. Alkynyl substrate substitutes the bromine to maintain palladium(II). The third step involves ligands rearrangement. The fourth step involves oxidative elimination and termination to produce the product followed by the catalyst regenerative cycle [50].

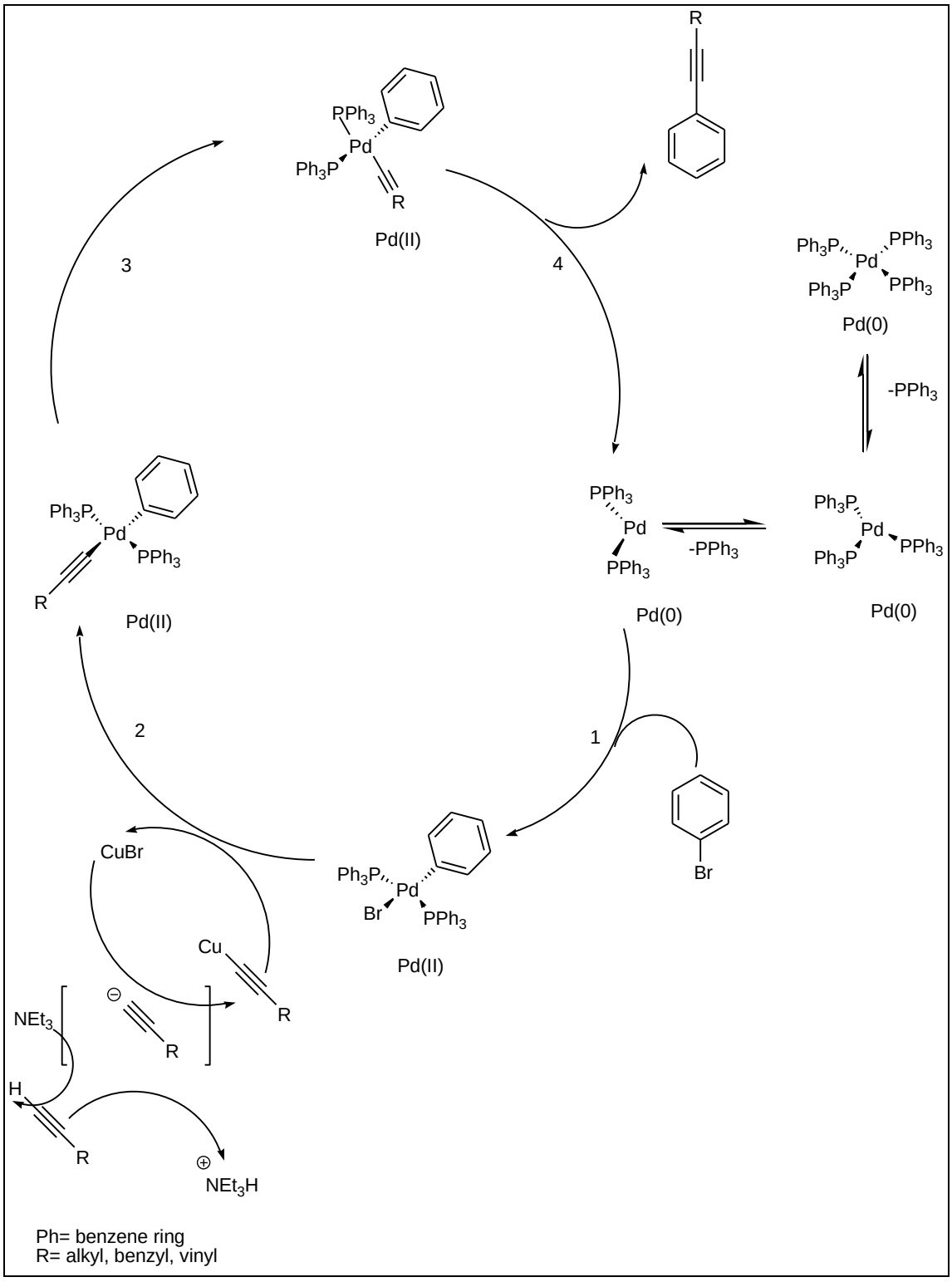

Scheme 1.15: Catalytic reaction mechanism showing Sonogashira cross-coupling [50; 51]

1.4.3 Applications of quinoxalines

Quinoxalines are attractive because of their rich biological and chemical properties. Many quinoxalines derivatives have been used and continue to be applied in medicinal fields as bioactive agents for treatment of various diseases. They generally show high biological activities such as antibacterial [55], antiviral [56], antiproliferative [57] antihelminthic [58], antitransplantable tumour [59] and antimycobacteriumactivity [60].. Below are types of current quinoxaline derivatives which are active against malaria and pathogenic microbes in **Figure 1.7**.

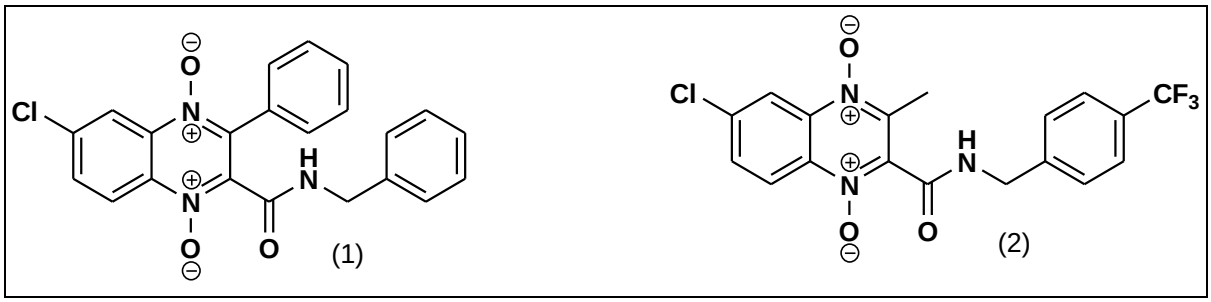

Figure 1.7: Examples of antimicrobial quinoxaline derivatives [47]

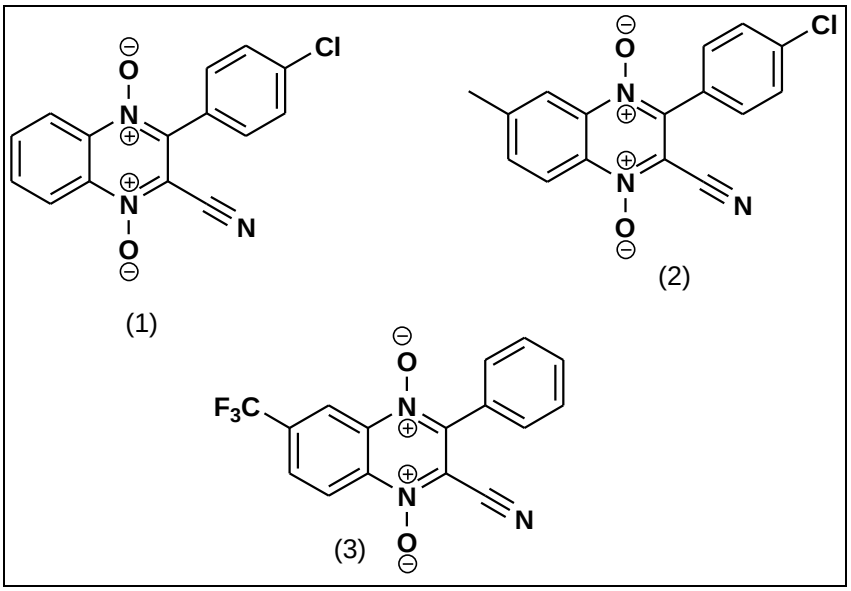

Figure 1.8: Examples of antimalarial quinoxaline derivatives [47]

The following section **1.5** discusses their combined effect i.e. Schiff base compounds/complexes containing quinoxalines with respect to their chemistry and applications.

1.5 Schiff base compounds/complexes containing quinoxaline

1.5.1 The chemistry of Schiff base-quinoxaline compounds and Schiff bases-quinoxaline complexes

The Schiff based-quinoxalines compounds are organic ligands which are derived from quinoxaline and imine backbone [61]. This class of heterocyclic compound are known for their contribution in both industries and pharmaceutical sectors. These compounds are also used as intermediates in coordination chemistry to develop complexes. **Figure 1.9** shows types of Schiff based-quinoxaline compounds which are used as supportive ligands for complex formation [61].

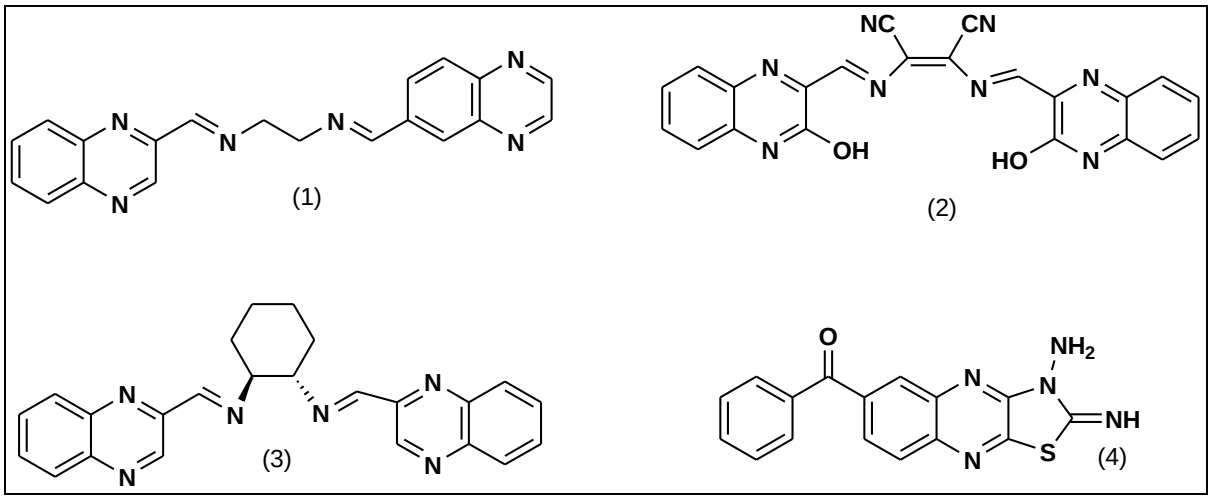

Figure 1.9: Examples of Schiff based-quinoxaline ligands derivatives [61]

The synthesis of Schiff based-quinoxaline compounds can be achieved by different condensation methods for the desired target molecule. One of the routes is shown

below which demonstrates condensation reaction to achieve Schiff based-quinoxaline ligands and their complexes [62].

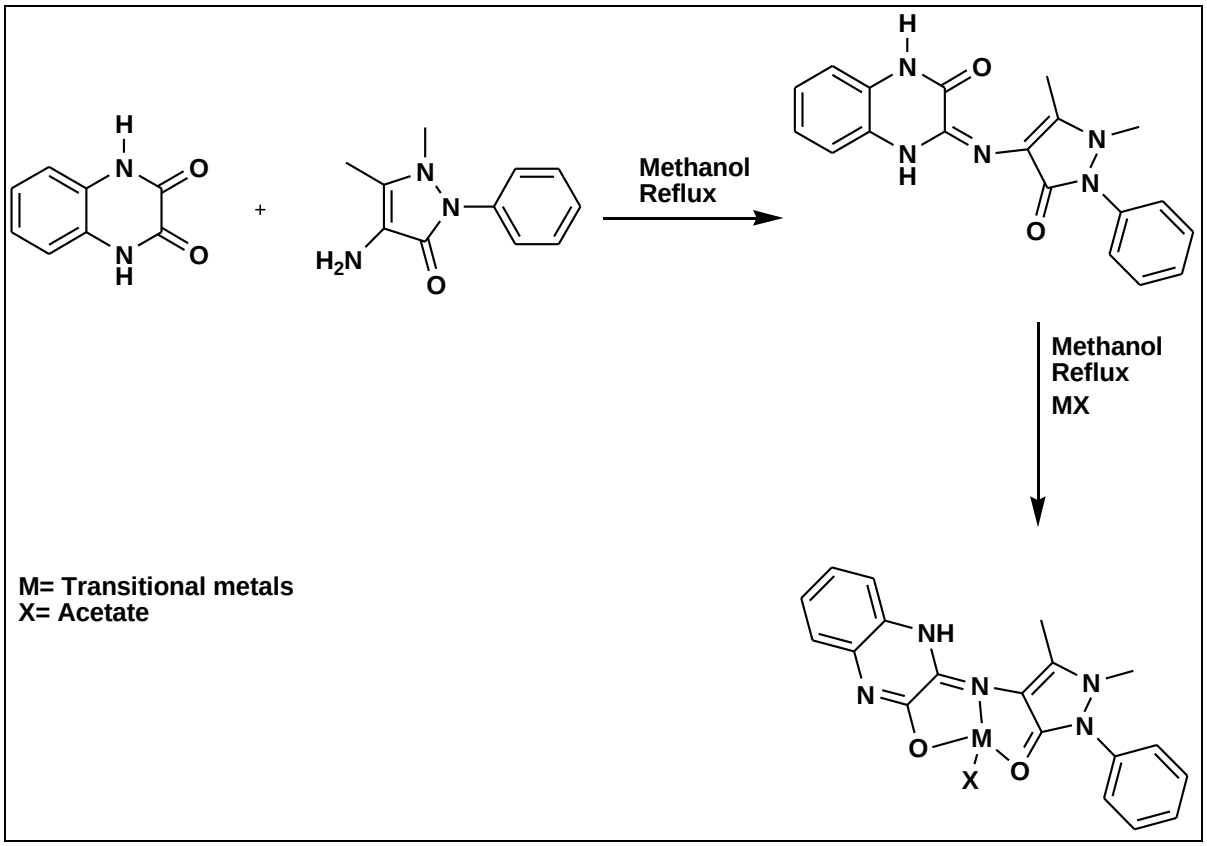

Scheme: 1.16 Example of a Schiff based-quinoxaline ligand and its complex [61]

Literature search reveals that there are few Schiff base ligands derived from quinoxaline derivatives [63]. Majority of reported cases are instances where quinoxalines derivative or Schiff base ligands are individually coordinated to the metal centre and very rare cases where both groups are simultaneously coordinated to the metal centre

Figure 1.10 shows some of quinoxaline-based Schiff base complexes reported by Chellalian *et al***.** [61]. The following complexes in **Figure 1.10** comprise of heterocyclic multi-dentate ligands containing triazine and quinoxaline were synthesised by template method in which the ligand coordinates to metal as a dibasic tridentate ligand [61].

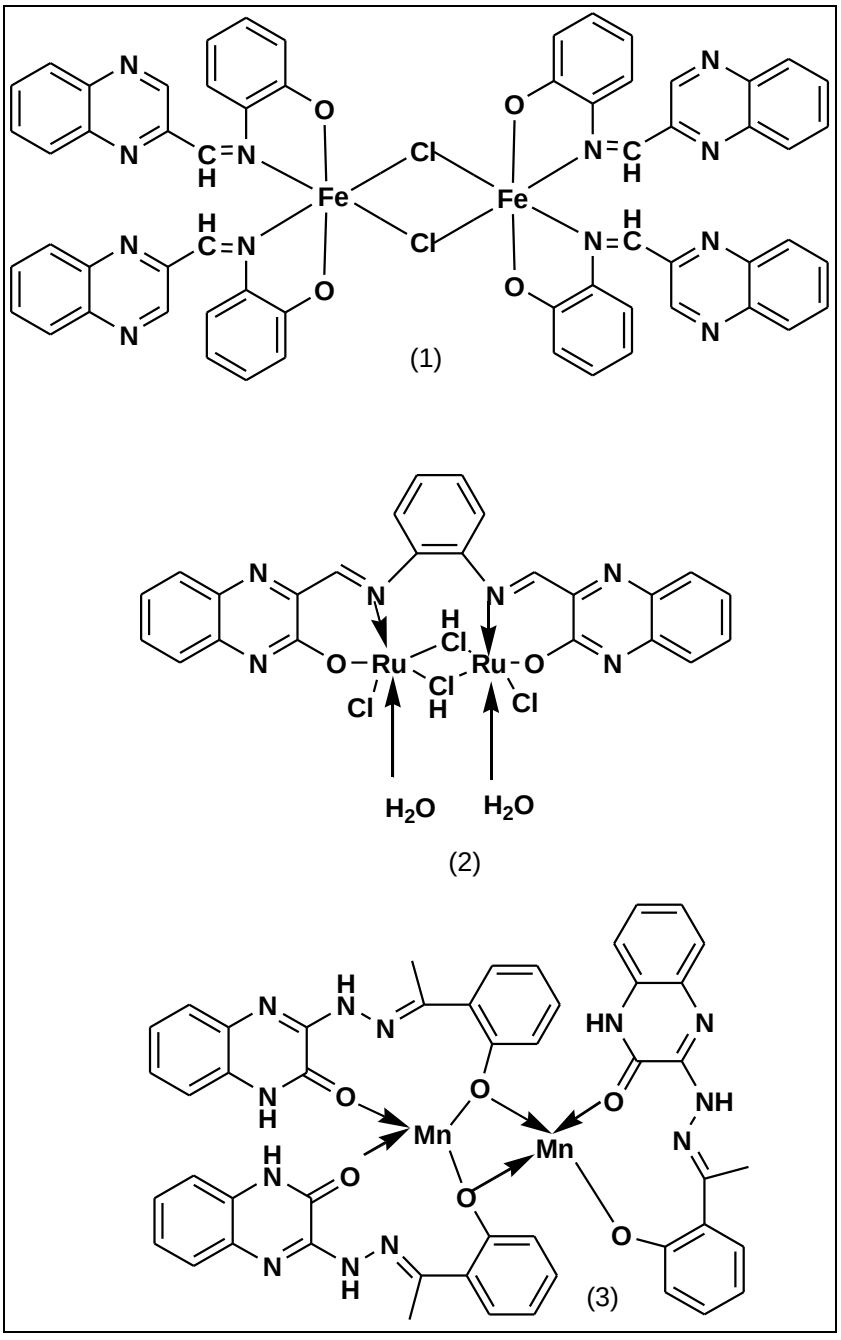

Figure 1.10: Examples of Schiff based-quinoxalines complexes [61]

1.5.2 Applications of Schiff base-quinoxalines complexes

Except for coordination modes, quinoxalines coupled Schiff base ligands were reported for their wide spectrum of application in pharmaceutical sectors [61]. They have shown biological activities such as antibacterial [62, 67], antimicrobial [61; 64] anticancer [65], antidiabetic [61], antifungal [61; 64] and DNA photo-cleavage [66; 67]. There are reported complexes derived from quinoxaline and Schiff base ligands which demonstrate enhanced biological activities after coordinating to the metal centre [62; 64]. Schiff based-quinoxalines complexes have also shown activity as catalyst for cross-coupling reactions and oxidation of alcohol [68; 69]**.** The following section **1.6** involves metal-based complexes in medicinal chemistry applications.

1.6. Metal-based complexes in medicinal chemistry

In the main metal-based complexes dominate the industrial sectors as catalyst and other products. These metal-based complexes were also found to exhibit medicinal properties. Cisplatin became a wonder drug for cancer treatment against transplantable tumours after showing good clinical stages results [70]. These findings about cisplatin paved the way to the application of metal-based complexes for medicinal use. The complexes in **Figure 1.11** are almost at the end of their clinical stages after showing various activities against harmful bacterial agents, tumours and viruses [6; 61; 65]. On **Figure 1.11** compound (1) has interesting antimalarial activity [6], compound (2) has good anticancer activity [62], compound (3) shows some interesting antitumour activity [6], compound (4) has some DNA cleavage and protein kinase activities [6], compound (5) has antibacterial activities for both gram positive bacteria *Klebsiella pneumoniae* and gram negative bacteria *Escherichia coli* and *Pseudomonas aeruginosa* [61].

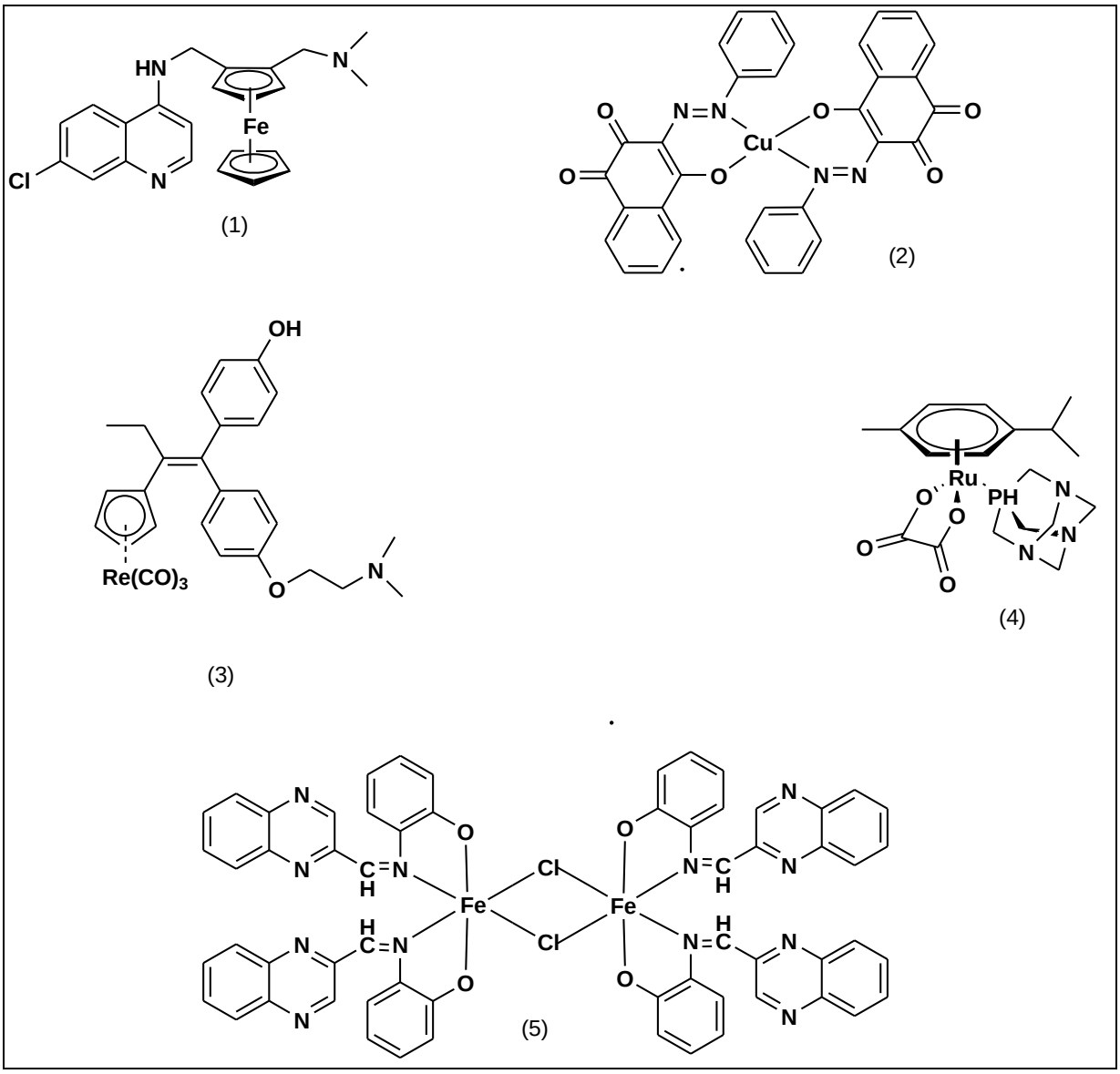

Figure 1.11: Biologically active Metal-based complexes [6; 61; 65]

1.7 Aim and objectives

The aim of this study was to synthesise complexes derived from a series of Schiff base ligands and quinoxaline derivative, and evaluate the newly synthesised compounds for biological studies against pathogenic species (quantitative antibacterial activity by assay of minimum inhibition concentration).

The objectives of this study were to:

i. Synthesise Schiff base ligand and their complexes,
ii. Synthesise quinoxalines derivatives,
iii. Coordinate Schiff base complexes to quinoxaline derivative,
iv. Characterise where possible synthesised compounds and complexes by: Solution Nuclear Magnetic Resonance (NMR), Ultra-violet spectroscopy (UV-Vis) and Infra-red spectroscopy (FT-IR), Mass Spectroscopy (MS), Elemental analysis (EA).
v. Test for biological activities using quantitative antibacterial activity by assay of minimum inhibition concentration.

1.8 References

[1] S. Kumar, D.N. Dhar, P.N. Saxena; Applications of metal complexes of Schiff base-A review, *Journal of Scientific & Industrial Research*, 68 (2009) 181-187.

[2] S. Demir, T.K. Yazicilar, M. Tas*;* Two novel analogous Ni(II) and Cd(II) complexes of an imidazole based Schiff base obtained from imidazole-4-carbaldehyde and 2-aminophenol, *Inorganica Chimica Acta,* 409 (2014) 399-406.

[3] M. Nath, P.K Saini, A. Kumar; New di- and triorganotin(IV) complexes of tripodal Schiff base ligand containing three imidazole arms: Synthesis, structural characterization, anti-inflammatory activity and thermal studies, *Journal of Organometallic Chemistry*, 695 (2010) 1353-1362.

[4] N. Graf, S.J. Lippard; Redox activation of metal-based pro-drugs as a strategy for drug delivery*, Advanced Drug Delivery Reviews,* 64 (2012) 993-1004.

[5] A. Vessières; Metal carbonyl tracers and the ferrocifen family; Two facets of bioorganometallic chemistry*, Journal of Organometallic Chemistry,* 734 (2013) 3-16.

[6] G. Gasser, N. Metzler-Nolte; The potential of organometallic complexes in medicinal chemistry, *Current Opinion in Chemical Biology,* 16 (2012) 84-91.

[7] V.K. Tandon, D.B. Yadav, H.K. Maurya, A.K. Chaturvedi, P.K. Shuklab; Design, synthesis, and biological evaluation of 1,2,3-trisubstituted-1,4-dihydrobenzo[g]quinoxaline-5,10-diones and related compounds as antifungal and antibacterial agents*, Bioorganic & Medicinal Chemistry ,* 14 (2006) 6120-6126.

[8] H. Xu, L. Fan; Synthesis and antifungal activities of novel 5,6-dihydro-indolo[1,2-a]quinoxaline derivatives*, European Journal of Medicinal Chemistry, 46* (2011) 1919-1925.

[9] G. Plesch, V. Kettmann, J. Si', O. Svajleno, C. Friebel; Coordination geometries and cooperative ordering effects in copper(ll) complexes with tridentate Schiff base dianions (Vl) Structure and EPR spectra of (imidazole) (N-salicylidene-beta-alaninato)copper (II), *Polyhedron*, 17 (1998) 539-545.

[10] W. Qin, S. Long, M. Panunzio, S. Biondi; Schiff Bases; A Short Survey on an Evergreen Chemistry Tool, *Molecules,* 18 (2013) 12264-12289.

[11] A. Xavier, N. Srividhya; Synthesis and Study of Schiff base Ligands, *IOSR Journal of Applied Chemistry (IOSR-JAC),* 7 (2014) 06-15.

[12] M. Zarei, A. Jarrahpour; Green and efficient synthesis of azo Schiff bases, *Iranian Journal of Science & Technology,* 3 (2011) 235-242.

[13] R.V. Savalia, A.P. Patel, P.T. Trivedi, H.R. Gohel, D.B. Khetani; Rapid and Economic Synthesis of Schiff Base of Salicylaldehyde by Microwave Irradiation, *Research Journal of Chemical Sciences,* 3 (2013) 97-99.

[14] A. Golcu, M. Tumer, H. Demirelli, R.A. Wheatley; Cd(II) and Cu(II) complexes of polydentate Schiff base ligands: synthesis, characterization, properties and biological activity, *Inorganica Chimica Acta*, 385 (2005) 1785-1797.

[15] B. Huang, H. Tian, S. Lin, M. Xie, X. Yu, Q. Xu; Cu(I)/TEMPO-catalyzed aerobic oxidative synthesis of imines directly from primary and secondary amines under ambient and neat conditions, *Tetrahedron Letters.* 54 (2013) 2861-2864.

[16] E.C. Britton, M. Mich, F. Bryner; Method of making imides of ketones, *U.S. Patent* 1,938,890.9 April (1932).

[17] G. Reddelien, Über Selbstkondensation bei Anilen. (Studien über Zinkchlorid als Kondensationsmittel III) (in German). *Berichte der deutschen chemischen Gesellschaft* 46 (1913) 2172–2178.

[18] I. Anis, M. Aslam, N. Afza, L. Iqbal, Z. Noreen, A. Hussain, M. Safder; A review (part c) – a overview of biological activities of Schiff base transition metals complexes, *International Journal of Current Pharmaceutical Research,* 5 (2013) 0975-7066.

[19] S.G. Telfer, T. Sato, T. Harada, R. Kuroda, J. Lefebvre, D.B. Leznoff; Mono- and Dinuclear Complexes of Chiral Tri- and Tetradentate Schiff-Base Ligands Derived from 1,1-Binaphthyl-2,2-diamine, *Inorganic Chemistry,* 43 (2004) 6168-6176.

[20] J. Cheng, K. Wei, X. Ma, X. Zhou, H. Xiang; Synthesis and Photophysical Properties of Colorful Salen-Type Schiff Bases, *Journal of Physical Chemistry,* 117 (2013) 16552-16563.

[21] H. Keypour, P. Arzhang, N. Rahpeyma, M. Rezaeivala, Y. Elerman, O. Büyükgüngör, L. Valencia, H.R. Khavasi; Synthesis and characterization of Ni(II), Cu(II) and Zn(II) complexes with new macrocyclic Schiff base ligands containing piperazine moiety, *Journal of Molecular Structure*, 977 (2010) 6-11.

[22] S. Akine, S. Sunaga, T. Taniguchi, H. Miyazaki, T. Nabeshima; Core-Shell Oligometallic Template Synthesis of Macrocyclic Hexaoxime, *Inorganic Chemistry Communication*, 46 (2007) 2959-2961.

[23] S. Kedy, N. Almhna, F. Kandil; Synthesis and characterization of new Macrocyclic schiff bases by the reaction of: 1,7-Bis (6-methoxy- 2-formylphenyl)-1,7-dioxaheptane and their use in solvent extraction of metals, *Arabian Journal of Chemistry,* 8 (2015) 93-99.

[24] W. Zhang, J. L. Loebach, S.R. Wilson, E.N. Jacobsen; Enantioselective Epoxidation of Unfunctionalized Olefins Catalyzed by (Sa1en) manganese Complexes, *American Chemical Society,* 112 (1990) 2801-2803.

[25] N. Raman, A. Kulandaisamy, A. Shunmugasundaram; Synthesis, spectral, redox and antimicrobial activities of Schiff€ base complexes derived from 1-phenyl-2,3-dimethyl-4-aminopyrazol-5-one and acetoacetanilide, *Transition Metal Chemistry,* 26 (2001) 131-135.

[26] R.N. Patel, N. Singh, V.L.N. Gundla*;* Synthesis, structure and properties of ternary copper(II) complexes of ONO donor Schiff base, imidazole, 2,20-bipyridine and 1,10-phenanthroline*, Polyhedron*, 25 (2006) 3312-3318.

[27] P. Mittal, V.Uma; Synthesis, spectroscopic and cytotoxic studies of biologically active new Co (II), Ni (II), Cu (II) and Mn (II) complexes of Schiff base hydrazones*, Der Chemica Sinica* , 3 (2010) 124-137.

[28] K.S. Siddiqi, R.I. Kureshy, N.H. Khan, S. Tabassum, S. Zaidi; Schiff base derived from sulfane thoxazole and salicylaldehyde, *Inorganica chemical Acta*, 108 (1988) 95-100.

[29] A.B. Mirzabdullaeu, D.K. Aslanova, F.I. Ershov; Prep. Induktory Interferona, *Imst Biological Organic Khim*, 99 (1984) 129-344.

[30] R.J. Young, G.W. Cooper; Dissociation of intermolecular linkages of the sperm head and tail by, primary amines, aldehydes, sulfhydryl reagents and deterngents, *Journal Reprod Fertil*, 69 (1983) 1-10.

[31] Y. Gaowen, X. Xiaping, T. Huan, Z. Cheunxue; Synthesis antitumor activity of Schiff base coordination compounds; *Yingyoung Hauxue*, 12 (1995) 13-15.

[32] D. Nartop, N. Sarı, H. Öğütçü; Pt(IV) Complexes with Polystrene-bound Schiff Bases as Antimicrobial Agent: Synthesis and Characterization, *World Academy of Science, Engineering and Technology,* 78 (2013) 06-25.

[33] C.M. Che, F.M. Siu; Metal complexes in medicine with a focus on enzyme inhibition, *Current Opinion of Chemical Biology,* 14 (2010) 255-261.

[34] A. Garoufis, S.K. Hadjikakou, N. Hadjiliadis; Palladium coordination compounds as anti-viral, anti-fungal, anti-microbial and anti-tumor agents, *Coordination Chemistry Reviews*, 253 (2009) 1384-1397.

[35] F. Shabani, L.A. Saghatforoush, S. Ghammamy; Synthesis, characterization and anti-tumour activity of iron(III) Schiff base complexes with unsymmetric tetradentate ligands, *Chemical Society of Ethiopia,* 24 (2010) 193-199.

[36] R.G. Cavell, K. Aparna, R.P. Kamalesh Babu, Q.Wang, 4-Methyl-2-[(E)-phen-yl(1,2,3,4-tetrahydro-1-naphthylimino)methyl]phenol, *Journal of Molecular Catalysis Chemica.* 189 (2002) 137.

[37] D.E. De Vos, P.P. Knops-Gerrits, D.L. Vanoppen, P.A. Jacobs, Epoxidation with managanese N,N′-bis(2-pyridinecarboxamide) complexes encapsulated in zeolite Y, *Supramolecular Chemistry*, 108 (1997) 445–452.

[38] M.R. Mason, A.M. Perkins, Alkylaluminophospshonate-catalyzed ring-opening homopolymerization of epichlohydrin and propylene oxide, *Journal of Organic Chemistry*, 599 (2000) 200-2007.

[39] M. Nath, P.K. Saini, A. Kumar; New di- and triorganotin(IV) complexes of tripodal Schiff base ligand containing three imidazole arms: Synthesis, structural characterization, anti-inflammatory activity and thermal studies, *Journal of Organometallic Chemistry*, 695 (2010) 1353-1362.

[40] A.A. Abou-Hussein, W. Linert; Molecular and Biomolecular Spectroscopy, Spectrochim*. Acta Part A:* 117 (2014) 763-771.

[41] S. Jie, S. Zhanga, K. Wedekinga, W. Zhanga, H. Maa, X. Lub, Y. Dengb, W.H. Suna; Cobalt(II) complexes bearing 2-imino-1,10-phenanthroline ligands: synthesis, characterization and ethylene oligomerisation, *C. R. Chimie ,* 9 (2006) 1500-1509.

[42] O. Pouralimardan, A. Chamayou, C. Janiak, H. Hosseini-Monfared, Hydrazone; Schiff base-manganese(II) complexes: Synthesis, crystal structure and catalytic reactivity, *Inorganica Chimica Acta ,* 360 (2007) 1599-1608.

[43] A.R. Stefankiewicz, M.W. sa-Chorab, H.B. Szczes´niak, V. Patroniak, M. Kubicki, Z. Hnatejko, J. Harrowfield; Grid-corner analogues: Synthesis, characterisation and spectroscopic properties of meridional complexes of tridentate NNO Schiff-base ligands, *Polyhedron*, 29 (2010) 178-187.

[44] A.A. Khandar, K. Nejati, Z. Rezvani; Syntheses, Characterization and Study of the Use of Cobalt (II) Schiff–Base Complexes as Catalysts for the Oxidation of Styrene by Molecular Oxygen, *Molecules*, 10 (2005) 302-311.

[45] S.B. Wadavrao, R.S. Ghogare, A.V Narsaia; A Simple and efficient protocol for the synthesis of quinoxalines catalyzed by pyridine*, Organic Communication*, 6:1 (2013) 23-30.

[46] L.M Lima, D.N. do Amaral; Beirut Reaction and its Application in the Synthesis of Quinoxaline-N,N'-Dioxides Bioactive Compounds, *Revista Virtual Quimica*, 5 (2013) 1075-1100.

[47] R. Soleymani, N. Niakan, S. Tayeb, S. Hakimi; Synthesis of Novel Aryl Quinoxaline Derivatives by New Catalytic Methods, *Oriental Journal of Chemistry*, 28 (2012) 687-701.

[48] L. Cassar; Palladium catalyzed synthesis of aryl, heterocyclic and vinylic acetylene derivatives, *Journal Organometallic Chemistry,* (1975) *93* 253-259.

[49] H.A. Dieck, F.R. Heck; Palladium catalyzed synthesis of aryl, heterocyclic and vinylic acetylene derivatives, *Journal Organometallic Chemistry*, 93 (1975) 259-263.

[50] M. Bakherad; Recent progress and current applications of Sonogashira coupling reaction in water, *Applied Organometallic Chemistry*, 27 (2013) 125-140.

[51] K. Sonogashira, Y. Tohda, N. Hagihara; A convenient synthesis of acetylenes: catalytic substitution of acetylynic wiyh hydrogen bromoalkanes, idoarenes and bromopyridines, *Tetrahedron Letters*, 50 (1975) 4467-4470.

[52] K. Sonogashira; Development of Pd–Cu catalyzed cross-coupling of terminal acetylenes with sp2-carbon halides, *Journal of Organometallic Chemistry*, 653 (2002) 46-49.

[53] R. D. Stephens, C.E. Castro; The Substitution of Aryl Iodides with Cuprous Acetylides. A Synthesis of Tolanes and Heterocyclics, *Journal of Organometallic Chemistry*, 28 (1963) 3313-3315.

[54] M. Mehrdad; Advance organic synthesis, *Journal of Advanced Chemistry Synthesis,* 103 (1981) 1-25.

[55] S.A. Khan, K. Saleem, Z. Khan; Synthesis, characterization and in vitro antibacterial activity of new steroidal thiazolo quinoxalines, *European Journal of Medicinal Chemistry*, 42 (2007) 103-108.

[56] M.O. Shibinskaya, A.S. Karpenko, S.A. Lyakhov, A. Andronati, N.M. Zholobak, N.Y Spivak, N.A. Samochina, L.M. Shafran, M.J. Zubritsky, V.F. Galat; Synthesis and biological activity of 7H-benzo[4,5]indolo[2,3-b]-quinoxaline Derivatives, *European Journal of Medicinal Chemistry*, 46 (2011) 794-798.

[57]] L. Gavara, E. Saugues , G. Alves, E. Debiton, F. Anizon, P. Moreau*;* Synthesis and biological activities of pyrazolo[3,4-g]quinoxaline derivatives, *European Journal of Medicinal Chemistry*, 45 (2010) 5520-5526.

[58] C. Barea, A. Pabón, D. Castillo, M. Zimic, M. Quiliano, S. Galiano, S. Pérez-Silanes, A. Monge, E. Deharo, I. Aldana; New salicylamide and sulfonamide derivatives of quinoxaline 1,4-di-N-oxide with antileishmanial and antimalarial activities, *Biology and Medical Chemistry Letters,* 21 (2011) 4498-4502.

[59] M.N. Noolvi, H.M. Patel, V. Bhardwaj, A. Chauhan; Synthesis and in vitro antitumor activity of substituted quinazoline and quinoxaline derivatives: Search for anticancer agent, *European Journal of Medicinal Chemistry*, 46 (2011) 2327-2346.

[60] A. Jaso, B. Zarranz, I. Aldana, A. Monge; Synthesis of new 2-acetyl and 2-benzoyl quinoxaline 1,4-di-N-oxide derivatives as anti-Mycobacterium tuberculosis agents, *European Journal of Medicinal Chemistry*, 38 (2003) 791-800.

[61] C.J. Dhanaraj, J. Johnson, J. Joseph, R.S. Joseyphus; Quinoxaline-based Schiff base transition metal complexes: review, *Journal of Coordination Chemistry*, 66 (2013) 1416–1450.

[62] C.J. Dhanaraj, J. Johnson; Synthesis, characterization, electrochemical and biological studies on some metal(II) Schiff base complexes containing quinoxaline

moiety, *Spectrochimica Acta Part A: Molecular and Biomolecular Spectroscopy* 118 (2014) 624-631.

[63] M. Sebastian, V. Arun, P.P. Robinson, P. Leeju, D. Varghese, G. Varsha, K.K. Yusuff; Synthesis, characterization, and structure of a new cobalt(II) Schiff-base complex with quinoxaline-2-carboxalidine-2-amino-5-methylphenol, *Journal of Coordination Chemistry*, 63 (2009) 307-314.

[64] N. Raman, S. Sobha, M. Selvaganapathy; Probing the DNA binding mode of transinal metal basedbiologically active compounds: validation by spectroscopic methods, *International Journal of Pharma and Bio Sciences,* 3 (2012) 240-268.

[65] C. Santini, M. Pellei, V. Gandin, M. Porchia, F. Tisato, C. Marzano; Advances in Copper Complexes as Anticancer Agents, *Chemical Reviews*, 114 (2014) 815−862.

[66] C. Urquiola, M. Vieites, M.H. Torre, M. Cabrera, M.L. Lavaggi, H. Cerecetto, M. González, A.L. de Cerain, A. Monge, P. Smircich, B. Garat, D. Gambino; Cytotoxic palladium complexes of bioreductive quinoxaline N1,N4-dioxide prodrugs, *Bioorganic & Medicinal Chemistry* 17 (2009) 1623-1629.

[67] R. Aggarwal, G. Sumran, V. Kumar, A. Mittal; Copper(II) chloride mediated synthesis and DNA photocleavage activity of 1-aryl/heteroaryl-4-substituted-1,2,4-triazolo[4,3-a]quinoxalines, *European Journal of Medicinal Chemistry,* 46 (2011) 6083-6088.

[68] F. Saleem, G.K. Rao, P. Singh, A.K. Singh; Chalcogen-Dependent Palladation at the Benzyl Carbon of 2,3-Bis[(phenylchalcogeno)methyl]quinoxaline: Palladium Complexes Catalyzing Suzuki−Miyaura Coupling via Palladium−Chalcogen Nanoparticles, *Organometallics* 32 (2013) 387-395.

[69] S. Mayadevi, P.G. Prasad, K.K. Mohammed Yusuff; *Synthesis and Reactivity in Inorganic and Metal-Organic Chemistry*, 33 (2003) 481-496.

[70] B. Rosenberg, L. Van Camp, T. Krigas; Affinity Biosensor for Antitumoral Drugs Determination, *Nature*, 205 (1965) 698-705.

CHAPTER TWO

SYNTHESIS AND CHARACTERISATION OF IMIDAZOLYL-SALICYLALDEMINE SCHIFF BASES AND THEIR COMPLEXES, QUINOXALINE DERIVATIVES AND SCHIFF BASE COMPLEXES COUPLED TO QUINOXALINE DERIVATIVE.

2.2. Experimental procedure

2.2.1 Materials and instrumentation

All inorganic synthesis was performed under inert conditions using standard Schenk technique in the presence of high pure nitrogen (N_2) gas. All the solvents used were of analytical grade, dried and distilled. Methanol, absolute ethanol, dimethylformamide (DMF), formic acid (HCOOH), ethyl acetate (EtOAc), potassium iodide (KI), potassium hydroxide (KOH), diethylamine (Et_2NH) and triethylamine (Et_3N) were obtained from Rochelle Chemicals and used as received. Tertrahydrofuran (THF) and hexane obtained from Rochelle Chemicals were dried and distilled over sodium metal lumps with benzophenone and stored over activated molecular sieves. Dichloromethane (DCM) obtained from Rochelle Chemicals was distilled over diphosphorous pentoxide (P_2O_5) and stored over activated molecular sieves. The following starting materials, 3,5-ditert-butyl-2-hydroxybenzaldehyde, 3-ethoxysalicylaldehyde, 2-hydroxy-5-methoxybenzaldehyde, 3-tert-butyl-2-hydroxybenzaldehyde, 5-tert-butyl-2-hydroxybenzaldehyde, 2-hydroxy-4-methoxy-methylbenzaldehyde, 2-hydroxy-3-methylbenzaldehyde, 2-hydroxy-5-methylbenzaldehyde, salicylaldehyde, 2-hydroxy-4-methylbenzaldehyde, sodium hydrogen carbonate ($NaHCO_3$), magnesium sulphate anhydrous ($MgSO_4$), histamine dihydrochloride, manganese chloride ($MnCl_2$), copper chloride ($CuCl_2$), zinc chloride ($ZnCl_2$), *o*-Phenyledinediamine, glyoxylic acid, glacial acetic acid, benzene sulfonyl chloride, 4-dimethylamino pyridine (DMAP), tetrakis(triphenylphosphine)palladium(0) ($Pd(PPh_3)_4$, copper iodide (CuI), anhydrous

calcium chloride and sodium sulphate (Na_2SO_4) were obtained from Sigma Aldrich and used as received. The ligands, complexes and quinoxaline derivatives were synthesised using the respective methods from the literature which were optimised [1; 2, 3].

The NMR spectra were recorded on a Bruker 400 MHz Avans NMR spectrometer operating at 400.00 MHz (^{1}H), 75.40 MHz (^{13}C) and 40.70 (^{15}N) at room temperature. The chemical shifts are reported in δ (ppm) with reference to their residual proton (^{1}H) and carbon (^{13}C) in different solvents (7.26 ppm (^{1}H) and 77.16 ppm (^{13}C) for $CDCl_3$), (2.54 ppm (^{1}H) and 40.45 ppm (^{13}C) in $(CD_3)_2SO$) and (3.31 ppm (^{1}H) and 49.00 ppm (^{13}C) for CD_3OD). The (^{15}N) chemical shift is reported with respect to nitromethane signal at 0.00 ppm. The Mass spectra were recorded on a Waters API Quattro Micro Spectrophotometer at University of Stellenbosch, South Africa. Elemental analyses were performed at the Department of Chemistry, Rhodes University on a Vario Elementar III microcube CHNS analyser. The FT-IR spectra were recorded on the Agilent Technologies Carry 660 FT-IR Spectrophotometer at the University of Limpopo South Africa. The melting points were recorded from Stuart melting point SMP10 at the University of Limpopo South Africa. The ultra violet visible studies were recorded from BECKMAN COULTER DU 730 spectrophotometer at the Biotechnology, Biochemistry and Microbiology department at University of Limpopo South Africa.

The preparation of ligands for electronic studies by Ultra-violet visible spectroscopy was done by dissolving an appropriate amount ligand in 100 ml of solvent (methanol, ethanol, dimethylsulfoxide and acetonitrile) at standardized concentration of 3.05×10^{-5} M. The preparation of complexes for electronic studies by Ultra-violet visible spectroscopy was done by dissolving an appropriate amount Schiff base complexes in 100 ml of solvent (methanol and ethanol) at standardized concentration of 2.4×10^{-5} M.

2.2.2 Synthesis of Schiff base ligands

The following reaction procedure was followed for the synthesis of Schiff base [3].

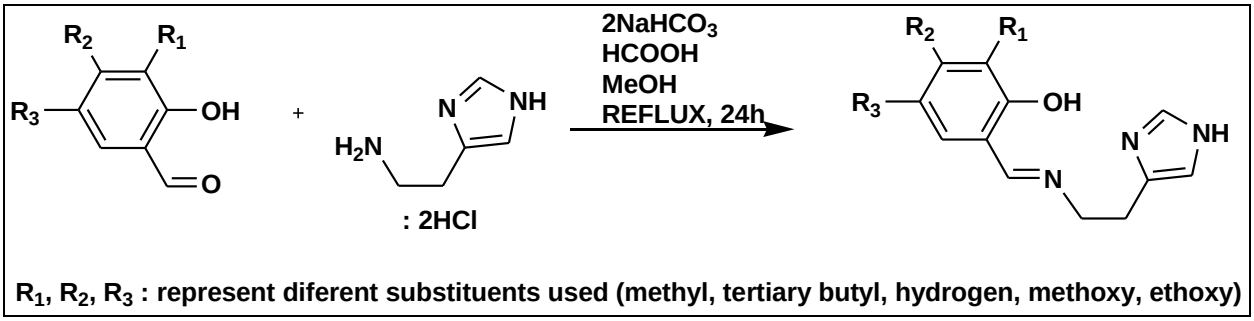

Scheme 2.1 Synthesis of Schiff base ligands [3]

2.2.2.1 Synthesis of 2,4-di-tert-butyl-6-{[2-(1H-imidazol-4-yl)-ethylimino]-methyl}-phenol [L1]

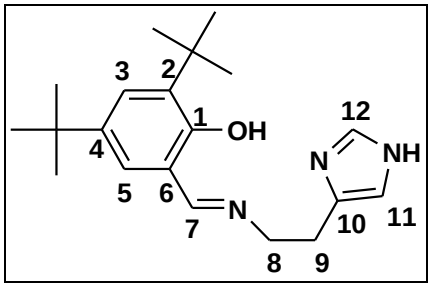

All ligands were prepared following the method reported by S. Boltina *et al*. [3]. The aldehyde, in this case 3,5-ditert-butyl-2-hydroxybenzaldehyde (1.27 g, 5.43 mmol), histamine dihydrochloride (1.00 g, 5.43 mmol), sodium hydrogen carbonate (0.91 g, 0.01 mol) and catalytic amount of formic acid (six, 6 drops) as a catalyst were added to methanol (50.00 ml) in a round bottomed flask. The solution was allowed to reflux at boiling point of methanol 64.7 °C for twenty four hours. The solution turned yellowish after two hours and the reaction was continuously stirred. After twenty four hours, the solution was cooled and anhydrous magnesium sulphate (0.10 g) was added to the solution as a drying agent. The solution was filtered to remove magnesium sulphate and

sodium hydrogen carbonate. The solvent and formic acid were removed under reduced pressure to obtain a bright yellow solid product which was re-dissolved in chloroform and filtered to remove insoluble impurities. The chloroform was removed under reduced pressure to give a solid product with a yield of (91%) and m.p (95 – 97 °C) which is consistence with the literature report [3]. ^{1}H NMR ($CDCl_3$, δ (ppm), *J* (Hz)): δ 1.29 (s, 9H, C_6H_2-5-C-($C\underline{H}_3)_3$); δ 1.44 (s, 9H, C_6H_2-3-C-($C\underline{H}_3)_3$); δ 2.98 (t, 2H, J = 6.8, $C\underline{H}_2$-C-CNH); δ 3.88 (t, 2H, J = 6.8, CH=N-$C\underline{H}_2$); 6.81 (s,1H, HN-C<u>H</u>=C); δ 7.01 (d, 1H, J = 2.4, *m*-C_6H_2-OH); 7.37 (d, 1H, J = 2.4, *m*-C_6H_2-OH); 7.57 (s, 1H, N-C<u>H</u>-N); 8.28 (s, 1H, C<u>H</u>=N). ^{13}C ($CDCl_3$): δ 29.65 (C_6H_2-3-C ($CH_3)_3$); δ 29.68 (C_6H_2-3-C-($CH_3)_3$); δ 31.42 (C_6H_2-5-C ($CH_3)_3$)); δ 34.04 (C_6H_2-5-C ($CH_3)_3$);δ 34.94 (im-N-C-CH_2); δ 59.09 (-CH=NCH_2-); δ 117.11 (HN-CH-); δ 117.11; δ 125.81; δ 126.84; δ 134.61; δ 135.08 (CH-C_6H_5); δ 136.57 (im-N-C-); δ 139.93 (-N-CH-N-); δ 158.08 (C_6H_4-OH); δ 166.53 (-CH=N-). ^{15}N ($CDCl_3$): (CH=<u>N</u>) 293.40. FT-IR cm^{-1}: 3461 υ(OH); 3356 υ(NH); 2956 υ(C-H); 2871 υ(O-H---N); 1633 υ(C=N: imine); 1570 υ(C=N imidazole), UV-vis transitions 281nm (imidazole), 327nm (phenol), 425nm (imine). Analytical calculations for $C_{20}H_{29}N_3O$ (%): C, 73.36; H, 8.88; N, 12.83. Found (%): 0.55 CH_3OH, C, 74.72; H, 9.18; N, 11.49. HRMS (ESI): calculated for $[M+H]^+$ 328.2311, found m/z 328.2383.

2.2.2.2 Synthesis of 4-methoxy-6-{[2-(1H-imidazol-4-yl)-ethylimino]-methyl}-phenol [L2]

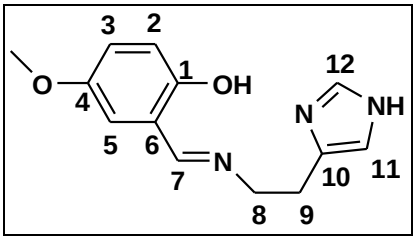

Preparation of **L2** followed the same synthesis procedure as for **L1**. The aldehyde, 2-hydroxy-5-methoxybenzaldehyde (2.50 g, 0.02 mol), histamine dihydrochloride (3.00 g, 0.02 mol), sodium hydrogen carbonate (2.74 g, 0.03 mol) and catalytic amount of formic acid (six, 6 drops) were added to 50 ml methanol. The clear solution turned yellow after one hour, and then turned to brown after three hours. The solution was filtered to

remove sodium hydrogen carbonate. The solution was purified by column chromatography using an eluent of 90% hexane and 10% ethyl acetate. The solvents and formic acid were removed under reduced pressure to give a brown solid product with a yield of (73%) and M.p (88 – 91°C). ^{1}H NMR ($CDCl_3$, δ (ppm), *J* (Hz)) : δ 2.97 (t, 2H, J = 6.8, C<u>H</u>$_2$-C-CNH); δ 3.84 (t, 2H, J = 6.8, CH=N-C<u>H</u>$_2$), δ 3.74 (s, 3H, C<u>H</u>$_3$-O) 6.69 (s, 1H, HN-C<u>H</u>=C), δ 6.79 (d, 1H, J = 2.8, *m*-C_6H-3-OH), δ 6.85 (d, 1H, J = 7.2, *m*-C_6H-5-OH), δ 6.88 (d, 1H, J = 7.2, *o*-C_6H-2-OH), δ 7.53 (s,1H, N-C<u>H</u>-N); δ 8.13 (s, 1H, C<u>H</u>=N). ^{13}C NMR ($CDCl_3$): δ 28.82 (im-N-C-CH_2); δ 55.69 (CH_3O); δ 59.07 (-CH=NCH_2-); δ 113.91 (HN-CH-); δ 114.76; δ 117.72; δ 125.30; δ 119.31 (CH-C_6H_5); δ 134.68, δ 135.88 (im-N-C-); δ 151.93 (-N-CH-N-); δ 155.36 (C_6H_4-OH); δ 165.04 (-CH=N-). ^{15}N ($CDCl_3$): (CH=<u>N</u>) 297.00. FT-IR cm^{-1}: 3416 υ(OH); 3325 υ(NH); 2919 υ(C-H); 2804 υ(O-H---N); 1591 υ(C=N: imine); 1576 υ(C=N imidazole). UV-vis transitions 277nm (imidazole), 300nm (phenol), 400nm (imine). Analytical calculations for $C_{13}H_{16}N_3O$ (%): C, 63.66; H, 6.52; N, 17.13. Found (%): 0.5 CH_3OH, C, 64.44; H, 6.07; N, 15.95. HRMS (ESI): calculated for $[M+H]^+$ 246.1164, found m/z 246.1246.

2.2.2.3 Synthesis of 2-ethoxy-6-{[2-(1H-imidazol-4-yl)-ethylimino]-methyl}-phenol [L3]

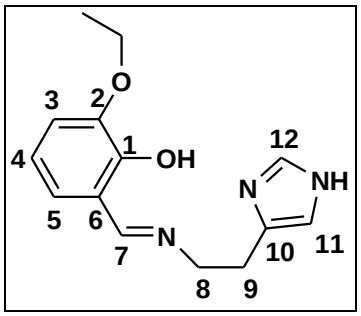

Preparation of **L3** followed the same procedure as **L1**. The aldehyde, 2-hydroxy-3-ethoxybenzaldehyde (0.90 g, 5.43 mmol), histamine dihydrochloride (1.00 g, 5.43 mmol), sodium hydrogen carbonate (0.912 g, 0.01 mol) and catalytic amount of formic acid (six, 6 drops) were added to 50 ml methanol. The clear solution turned yellow after two hours and the reaction was continuously stirred as yellowish solution. The solution

was filtered to remove sodium hydrogen carbonate. The solution was purified by column chromatography using an eluent of 90% diethyl ether and 10% ethyl acetate. The solvents and formic acid were removed under reduced pressure to give a yellow solid product with a yield of (74%) and M.p (90 – 93 °C). ^{1}H NMR ($CDCl_3$, δ (ppm), *J* (Hz)): δ 1.43 (t, 3H, J = 6.8, C<u>H</u>$_3$-C<u>H</u>$_2$-O), δ 2.98 (t, 2H, J = 6.4, C<u>H</u>$_2$-C-CNH); δ 3.88 (t, 2H, J = 6.4, CH=N-C<u>H</u>$_2$), δ 4.09 (q, 2H, J = 7.2, O-C<u>H</u>$_2$-CH$_3$), 6.69 (s, 1H, HN-C<u>H</u>=C), δ 6.80 (d, 1H, J = 9.2, *m*-C_6H-3-OH) δ 6.89 (t, 1H, j = 8, *p*-C_6H-4-OH) , δ 6.88 (d, 1H, J = 7.6, m-C_6H-5-OH) δ 7.52 (s, 1H, N-CH-N); δ 8.19 (s, 1H, C<u>H</u>=N). ^{13}C NMR: ($CDCl_3$): δ 14.85 (CH_2), δ 28.86 (im-N-C-CH_2); δ 57.81 (-CH=NCH_2-); δ 64.37 (CH_2O); δ 115.16 (HN-CH-); δ 117.33; δ 118.08; δ 122.35; δ 123.04; δ 134.92 (CH-C_6H_5); δ 134.92 (im-N-C-); δ 148.06 (-N-CH-N-); δ 153.96 (C_6H_4-OH); δ 165.31 (-CH=N-). ^{15}N ($CDCl_3$): (CH=<u>N</u>) 274.70. FT-IR cm^{-1}: 3514 υ(OH); 3399 υ(NH); 2984 υ(C-H); 2888 υ(O-H---N); 1638 υ(C=N: imine); 1578 υ(C=N imidazole). UV-vis transitions 277nm (imidazole), 300nm (phenol), 400nm (imine). Analytical calculations for $C_{14}H_{18}N_3O_2$ (%): C, 64.85; H, 6.56; N, 16.21. Found (%): 0.73 CH_3OH, C, 65.22; H, 6.20; N, 17.02. HRMS (ESI): calculated for $[M+H]^+$ 260.1321, found m/z 260.1398.

2.2.2.4 Synthesis of salicylaldehyde-2-{[2-(1H-imidazol-4-yl)-ethylimino]-methyl}-phenol [L4]

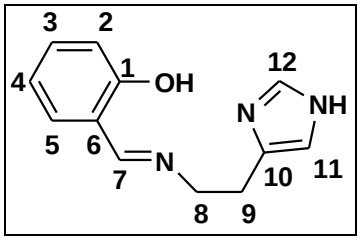

Preparation of **L4** followed the same synthesis procedure as for **L1**. Salicylaldehyde (0.66 g, 5.43 mmol), histamine dihydrochloride (1.00 g, 5.43 mmol), sodium hydrogen carbonate (0.912 g, 0.01 mol) and catalytic amount of formic acid (six, 6) drops were added to 50 ml methanol. The clear solution turned yellow after thirty minutes and the brown after two hours, the reaction was continuously stirred as brown solution. The solution was filtered to remove sodium hydrogen carbonate. The solvent and formic acid

were removed under reduced pressure to give a brown product with a yield of (82%) and M.p (80 – 82 °C). ^{1}H NMR ($CDCl_3$, δ (ppm), *J* (Hz)): δ 2.96 (t, 2H, J = 6.4, C<u>H</u>$_2$-C-CNH); δ 3.81 (t, 2H, J = 6.4, CH=N-C<u>H</u>$_2$), δ 6.76 (s, 1H, HN-C<u>H</u>=C), δ 6.80 (m, 1H, *o*-C_6H-2-OH), δ 6.85 (m, 1H, *m*-C_6H-3-OH), δ 6.89 (m, 1H, *p*-C_6H-$_6$-OH), δ 7.14 (m, 1H, *m*-C_6H-5-OH) δ 7.70 (s, 1H, N-C<u>H</u>-N); δ 8.20 (s, 1H, C<u>H</u>=N). ^{13}C NMR: ($CDCl_3$): δ 27.90 (im-N-C-CH_2); δ 59.19 (-CH=NCH_2-); δ 117.11 (HN-CH-); δ 118.50; δ 119.89; δ 131.52; δ 132.60; δ 133.69 (CH-C_6H_5); δ 134.15 (im-N-C-); δ 137.02 (-N-CH-N-); δ 161.68 (C_6H_6-OH); δ 165.67 (-CH=N-). ^{15}N ($CDCl_3$): (CH=<u>N</u>) 292.80. FT-IR cm^{-1}: 3520 υ(OH); 3326 υ(NH); 2990 υ(C-H); 2849 υ(O-H---N); 1636 υ(C=N: imine); 1580 υ(C=N imidazole). UV-vis transitions 280nm (imidazole), 319nm (phenol), 410nm (imine). Analytical calculations for $C_{12}H_{13}N_3O$ (%): C, 66.96; H, 6.04; N, 19.52. Found (%): 0.42 CH_3OH, C, 65.33; H, 6.06; N, 18.20. HRMS (ESI): calculated for $[M+H]^+$ 216.1059, found m/z 216.1302.

2.2.2.5 Synthesis of 4-methyl-6-{[2-(1H-imidazol-4-yl)-ethylimino]-methyl}-phenol [L5]

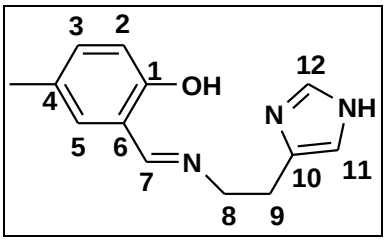

Preparation of **L5** followed the same synthesis procedure as for **L1**. The aldehyde 2-hydroxy-5-methylbenzaldehyde (1.50 g, 0.01 mol), histamine dihydrochloride (2.00 g, 0.01 mol), sodium hydrogen carbonate (1.83 g, 0.02 mol) and catalytic amount of formic acid (six, 6 drops) were added to 50 ml methanol. The clear solution turned yellow after three hours and the reaction was continuously stirred as yellowish solution. The solution was filtered to remove sodium hydrogen carbonate. The solvent and formic acid were removed under reduced pressure to give a yellow solid product with a yield of (80%) and M.p (81 – 83 °C).^{1}H NMR ($CDCl_3$, δ (ppm), *J* (Hz)) : δ 2.25 (s, 3H, *p*-C_6H-$_3$-OH) δ 3.12 (t, 2H, J = 6.4, C<u>H</u>$_2$-C-CNH); δ 3.95 (t, 2H, J = 6.4, CH=N-C<u>H</u>$_2$), δ 6.56 (s, 1H, HN-

C<u>H</u>=C), δ 6.62 (m, 1H, *o*-C_6H-2-OH), δ 6.90 (m, 1H, *m*-C_6H-3-OH), δ 7.14 (d, 1H, J = 8, *m*-C_6H-5-OH) δ 7.87 (s, 1H, N-C<u>H</u>-N); δ 8.13 (s, 1H, C<u>H</u>=N). ^{13}C NMR: ($CDCl_3$): δ 20.48 (CH_3-*p*-C_6H-$_3$-OH), δ 27.90 (im-N-C-CH_2); δ 59.19 (-CH=NCH_2-); δ 117.11 (HN-CH-); δ 118.50; δ 119.89; δ 131.52; δ 132.60; δ 133.69 (CH-C_6H_5); δ 134.15 (im-N-C-); δ 137.02 (-N-CH-N-); δ 161.68 (C_6H_4-OH); δ 165.67 (-CH=N-). ^{15}N ($CDCl_3$): (CH=<u>N</u>) 291.50. FT-IR cm^{-1}: 3464 υ(OH); 3331 υ(NH); 2922 υ(C-H); 2850 υ(O-H---N); 1616 υ(C=N: imine); 1580 υ(C=N imidazole). UV-vis transitions 279nm (imidazole), 325nm (phenol), 415nm (imine). Analytical calculations for $C_{13}H_{15}N_3O$ (%): C, 68.10; H, 6.54; N, 18.33. Found (%): 0.50 CH_3OH, C, 67.22; H, 6.44; N, 17.20. HRMS (ESI): calculated for $[M+H]^+$ 230.1215, found m/z 230.1294.

2.2.2.6 Synthesis of 3-methyl-6-{[2-(1H-imidazol-4-yl)-ethylimino]-methyl}-phenol [L6]

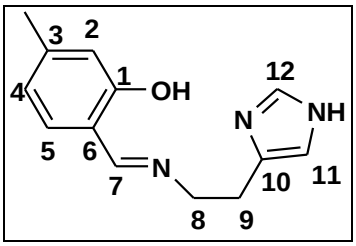

Preparation of **L6** followed the same synthesis procedure as for **L1**. The aldehyde, 2-hydroxy-4-methylbenzaldehyde (1.50 g, 0.01 mol), histamine dihydrochloride (2.00 g, 0.01 mol), sodium hydrogen carbonate (1.83 g, 0.02 mol) and catalytic amount of formic acid (six, 6 drops) were added to 50 ml methanol. The clear solution turned yellow after four hours and the reaction was continuously stirred as yellowish solution. The solution was filtered to remove sodium hydrogen carbonate. The solvent and formic acid were removed under reduced pressure to give a yellow solid product which was dissolved in chloroform and filtered to remove insoluble impurities. The chloroform was removed under reduced pressure to give a solid product with (88%) yield and M.p (105 – 107 °C). The product was crystallised from ethanol. ^{1}H NMR ($CDCl_3$, δ (ppm), *J* (Hz)) : δ 2.28 (s, 3H, *m*-C_6H-$_3$-OH) δ 2.97 (t, 2H, J = 6.4, C<u>H</u>$_2$-C-CNH); δ 3.82 (t, 2H, J = 6.4, CH=N-C<u>H</u>$_2$), δ 6.61 (s, 1H, HN-C<u>H</u>=C), δ 6.79 (m, 1H, *o*-C_6H-2-OH), δ 6.80 (m, 1H, *p*-C_6H-4-

OH), δ 7.05 (d, 1H, J = 8, *m*-C_6H-5-OH) δ 7.61 (s, 1H, N-C<u>H</u>-N); δ 8.16 (s,1H, C<u>H</u>=N). ^{13}C NMR: ($CDCl_3$): δ 22.25 (CH_3- *m*-C_6H-$_3$-OH), δ 28.33 (im-N-C-CH_2); δ 58.06 (-CH=NCH_2-); δ 116.03 (HN-CH-); δ 117.65; δ 117.74; δ 119.58; δ 121.19; δ 131.33; δ 134.44 (CH-C_6H_5); δ 143.75 (im-N-C-); δ 162.26 (-N-CH-N-); δ 165.17 (C_6H_4-OH); δ 165.56 (-CH=N-). ^{15}N ($CDCl_3$): (CH=N) 283.70. FT-IR cm^{-1}: 3512 υ(OH); 3325 υ(NH); 2905 υ(C-H); 2849 υ(O-H---N); 1640 υ(C=N: imine); 1570 υ(C=N imidazole). UV-vis transitions 280nm (imidazole), 320nm (phenol), 406nm (imine). Analytical calculations for $C_{13}H_{15}N_3O$ (%): C, 68.10; H, 6.54; N, 18.33. Found (%): 0.32 CH_3OH, C, 68.55; H, 6.41; N, 19.23. HRMS (ESI): calculated for $[M+H]^+$ 230.1215, found m/z 230.1304.

2.2.2.7 Synthesis of 3-methoxy-6-{[2-(1H-imidazol-4-yl)-ethylimino]-methyl}-phenol [L7]

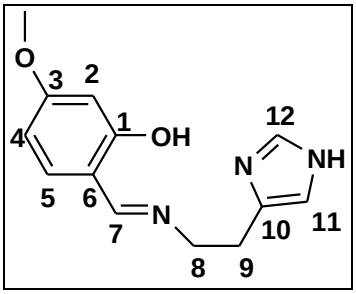

Preparation of **L7** followed the same synthesis procedure as for **L1**. The aldehyde 2-hydroxy-5-methoxybenzaldehyde (2.50 g, 0.02 mol), histamine dihydrochloride (3.00 g, 0.02 mol), sodium hydrogen carbonate (2.74 g, 0.03 mol) and catalytic amount of formic acid (six, 6 drops) were added to 50 ml methanol. The clear solution turned to yellow after thirty minutes, and then turned brown solution after two hours. The solution was filtered to remove sodium hydrogen carbonate. The solution was purified by column chromatography using an eluent of 90% hexane and 10% ethyl acetate. The solvents and formic acid were removed under reduced pressure to give a brown solid product with a yield of 82% and M.p (80 – 83 °C). ^{1}H NMR ($CDCl_3$, δ (ppm) *J* (Hz)): δ 2.96 (t, 2H, J = 6.4, C<u>H</u>$_2$-C-CNH); δ 3.81 (t, 2H, J = 6.4, CH=N-C<u>H</u>$_2$), δ 3.75 (s, 3H, C<u>H</u>$_3$-O) 6.26 (s, 1H, HN-C<u>H</u>=C), δ 6.27 (d, 1H, J = 7.2, *m*-C_6H-2-OH), δ 6.81 (s, 1H, *o*-C_6H-4-OH), δ 6.99 (d, 1H, J = 9.2, *p*-C_6H-5-OH), δ 7.55 (s, 1H, N-C<u>H</u>-N); δ 7.94 (s, 1H, C<u>H</u>=N). ^{13}C

NMR ($CDCl_3$): δ 27.72 (im-N-C-CH_2); δ 54.28 (CH_3O); δ 54.34 (-CH=NCH_2-); δ 100.58 (HN-CH-); δ 105.53; δ 110.43; δ 115.05; δ 115.75 (CH-C_6H_5); δ 132.18, δ 134.22 (im-N-C-); δ 162.64 (-N-CH-N-); δ 163.89 (C_6H_4-OH); δ 168.90 (-CH=N-). ^{15}N ($CDCl_3$): (CH=N) 282.10. FT-IR cm^{-1}: 3416 $_U$(OH); 3325 $_U$(NH); 2942 $_U$(C-H); 2846 $_U$(O-H---N); 1613 $_U$(C=N: imine); 1579 $_U$(C=N imidazole). UV-vis transitions 280nm (imidazole), 319nm (phenol), 390nm (imine). Analytical calculations for $C_{13}H_{16}N_3O$ (%): 0.59 CH_3OH, C, 63.66; H, 6.52; N, 17.13. Found (%): 0.59 CH_3OH, C, 64.77; H, 5.93; N, 16.77. HRMS (ESI): calculated for $[M+H]^+$ 246.1164, found m/z 246.1246.

2.2.2.8 Synthesis of 2-tert-butyl-6-{[2-(1H-imidazol-4-yl)-ethylimino]-methyl}-phenol [L8]

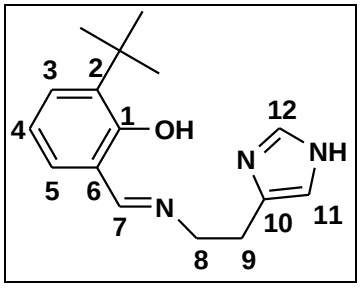

Preparation of **L8** followed the same synthesis procedure as for **L1.** The amount of 3-tert-butyl-2-hydroxy-benzaldehyde (2.91 g, 0.02 mol), histamine dihydrochloride (3.00 g, 0.02 mol), sodium hydrogen carbonate (2.74 g, 0.03 mol) and catalytic amount of formic acid (six, 6 drops) were added to 50 ml methanol solution. The clear solution turned yellow after two hours and the reaction was continuously stirred as yellowish solution. The solution was filtered to remove sodium hydrogen carbonate. The solvent and formic acid were removed under reduced pressure to give a yellow solid product with a yield of 88% and M.p (79 – 82 °C). ^1H NMR ($CDCl_3$, δ (ppm), *J* (Hz)): δ 1.40 (s, 9H, C_6H_2-3-C(CH_3)$_3$); δ 3.10 (t, 2H, J = 6.8, CH_2-C-CNH); δ 3.93 (t, 2H, J = 6.8, CH=N-CH_2); 6.82 (s, 1H, HN-CH=C); δ 7.12 (d, 1H, J = 8.8, *p*-C_6H-4-OH); δ 7.15 (d, 1H, J = 8.8, *m*-C_6H-3-OH) 7.32 (d, 1H, J = 8.8, *m*-C_6H-5-OH); 7.64 (s, 1H, N-CH-N); 8.24 (s, 1H, CH=N). ^{13}C ($CDCl_3$): δ 26.90 (C_6H_2-3-C (CH_3)$_3$); δ 28.41 (C_6H_2-3-C (CH_3)$_3$); δ 28.41 (C_6H_2-5-C (CH_3)$_3$); δ 28.47 (im-N-C-CH_2); δ 57.84 (-CH=NCH_2-); δ 116.51 (HN-CH-); δ 117.10; δ

129,29; δ 133.29; δ 134.61; δ 133.97 (CH-C_6H_5); δ 136.36 (im-N-C-); δ 159.97 (-N-CH-N-); δ 166.91 (C_6H_4-OH); δ 168.37 (-CH=N-). ^{15}N ($CDCl_3$): (CH=N) 291.90. FT-IR cm^{-1}: 3427 υ(OH); 3323 υ(NH); 2995 υ(C-H); 2894 υ(O-H---N); 1613 υ(C=N: imine); 1570 υ(C=N imidazole). UV-vis transitions 277nm (imidazole), 325nm (phenol), 420nm (imine). Analytical calculations for $C_{16}H_{21}N_3O$ (%): C, 70.82; H, 7.74; N, 15.49. Found (%): 0.27 CH_3OH, C, 69.66; H, 8.39; N, 14.37. HRMS (ESI): calculated for $[M+H]^+$ 272.1687, found m/z 272.1765.

2.2.2.9 Synthesis of 2-methyl-6-{[2-(1H-imidazol-4-yl)-ethylimino]-methyl}-phenol [L9]

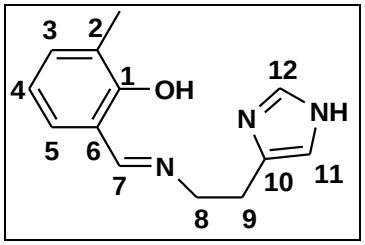

Preparation of **L9** followed the same synthesis procedure as for **L1.** The aldehyde 2-hydroxy-3-methylbenzaldehyde (2.22 g, 0.02 mol), histamine dihydrochloride (3.00 g, 0.02 mol), sodium hydrogen carbonate (2.74 g, 0.03 mol) and catalytic amount of formic acid (six, 6 drops) were added to 50 ml methanol. The clear solution turned yellow after one hour and the reaction was continuously stirred as yellowish solution. The solution was filtered to remove sodium hydrogen carbonate. The solvent and formic acid were removed under reduced pressure to give a yellow solid product with a yield of 90% and M.p (90 – 92 °C). The product was crystallised from ethanol. ^{1}H NMR ($CDCl_3$, δ (ppm), *J* (Hz)): δ 2.27 (s, 3H, *o*-C_6H_3-OH); δ 3.01 (t, 2H, J = 6.4, CH_2-C-CNH); δ 3.88 (t, 2H, J = 6.4, CH=N-CH_2), δ 6.83 (s, 1H, HN-CH=C), δ 6.77 (t, 1H, J = 7.2, *p*-C_6H-3-OH), δ 7.07 (d, 1H, J = 7.2, *m*-C_6H-4-OH), δ 7.19 (d, 1H, J = 8, *m*-C_6H-5-OH); δ 7.58 (s, 1H, N-CH-N); δ 8.23 (s, 1H, CH=N). ^{13}C NMR: ($CDCl_3$): δ 15.58 (CH_3- *o*-C_6H_3-OH), δ 28.76 (im-N-C-CH_2); δ 58.77 (-CH=NCH_2-); δ 116.60 (HN-CH-); δ 117.80; δ 118.01; δ 126.02; δ 129.05 (CH-C_6H_5); δ 133.33 (im-N-C-); δ 134.66 (-N-CH-N-); δ 159.84 (C_6H_4-OH); δ 165.60 (-CH=N-). ^{15}N ($CDCl_3$): (CH=N) 291.90. FT-IR cm^{-1}: 3440 υ(OH); 3273 υ(NH);

2976 υ(C-H); 2883 υ(O-H---N); 1636 υ(C=N: imine); 1580 υ(C=N imidazole). UV-vis transitions 279nm (imidazole), 318nm (phenol), 415nm (imine). Analytical calculations for $C_{13}H_{15}N_3O$ (%): C, 68.10; H, 6.54; N, 18.33. Found (%): 0.31 CH_3OH, C, 67.10; H, 6.73; N, 16.04. HRMS (ESI): calculated for $[M+H]^+$ 230.1215, found m/z 230.1298.

2.2.2.10 Synthesis of 4-tert-butyl-6-{[2-(1H-imidazol-4-yl)-ethylimino]-methyl}-phenol [L10]

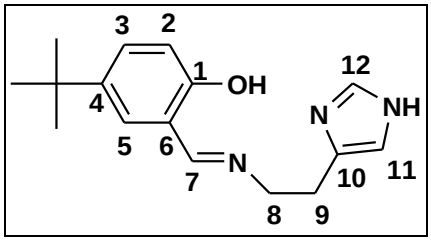

Preparation of **L10** followed the same synthesis procedure as for **L1**. The amount of 2-hydroxy-3-methylbenzaldehyde (0.97 g, 5.43 mmol), histamine dihydrochloride (1.00 g, 5.43 mmol), sodium hydrogen carbonate (0.91 g, 0.01 mol) and catalytic amount of formic acid (six, 6 drops) were added to 50 ml methanol. The clear solution turned brown after four hours and the reaction was continuously stirred as brown solution. The solution was filtered to remove sodium hydrogen carbonate. The solvent and formic acid were removed under reduced pressure to give a brown solid product which was dissolved in diethyl ether and filtered to remove insoluble impurities. The diethyl ether was removed under reduced pressure to give a product with a yield of 80% and M.p (80 – 83 °C). ^{1}H NMR ($CDCl_3$, δ (ppm), *J* (Hz)): δ 1.19 (s, 9H, C_6H_2-5-C($C\underline{H}_3$)$_3$); δ 2.89 (t, 2H, J = 6.8, $C\underline{H}_2$-C-CNH); δ 3.76 (t, 2H, J = 6.8, CH=N-$C\underline{H}_2$); 6.71 (s, 1H, HN-C$\underline{H}$=C); δ 6.76 (d, 1H, J = 2.4, *m*-C_6H-3-OH); δ 7.10 (d, 1H, J = 8.4, *o*-C_6H-2-OH); 7.23 (d, 1H, J = 2.4, *m*-C_6H-5-OH); 7.50 (s, 1H, N-C$\underline{H}$-N); 8.20 (s, 1H, CH=N). ^{13}C ($CDCl_3$): δ 31.42 (C_6H_2-5-C (CH_3)$_3$); 29.72 (C_6H_2-5-C (CH_3)$_3$); δ 28.64 (im-N-C-CH_2); δ 58.71 (-CH=NCH_2-); δ 117.80 (HN-CH-); δ 118.73; δ 120.07; δ 127.78; δ 129.87 (CH-C_6H_5); δ 134.77 (im-N-C-); δ 142.78 (-N-CH-N-); δ 159.33 (C_6H_4-OH); δ 165.73 (-CH=N-). ^{15}N ($CDCl_3$): (C$\underline{H}$=N) 291.90. FT-IR cm^{-1}: 3430 υ(OH); 3310 υ(NH); 2962 υ(C-H); 2868 υ(O-H---N); 1633 υ(C=N: imine); 1570 υ(C=N imidazole). UV-vis transitions 282nm

(imidazole), 320nm (phenol), 415nm (imine). Analytical calculations for $C_{16}H_{21}N_3O$ (%): C, 70.82; H, 7.74; N, 15.49. Found (%): 0.31 CH_3OH, C, 72.22; H, 8.50; N, 14.98. HRMS (ESI): calculated for $[M+H]^+$ 272.1685, found m/z 272.1298.

2.2.3 Synthesis of complexes

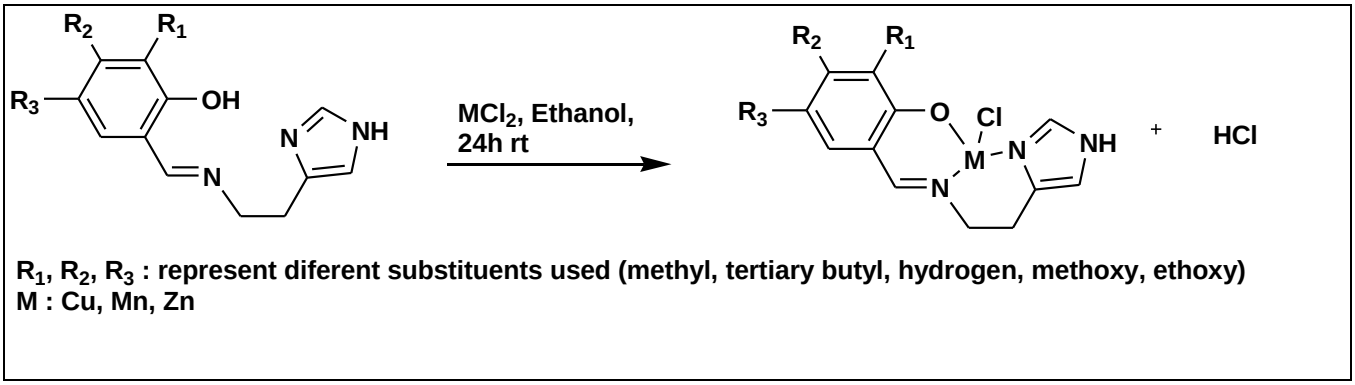

R_1, R_2, R_3 : represent diferent substituents used (methyl, tertiary butyl, hydrogen, methoxy, ethoxy)
M : Cu, Mn, Zn

Scheme 2.2 Generalised reaction scheme for the reaction of Schiff base ligands with metal(II) Chlorides

2.2.3.1 Synthesis of 2, 4-di-tert-butyl-6-{[2-(1H-imidazol-4-yl)-ethylimino]-methyl}-phenol Mn(II) chloride [C1]

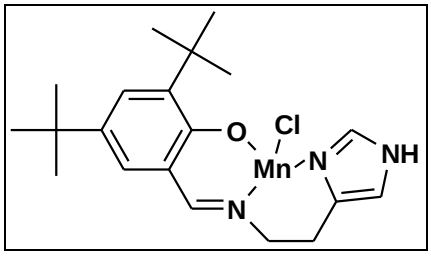

All complexes were prepared by following the method reported by Boltina *et al*. [3]. To a three necked round bottomed flask equipped with stirrer bar under inert condition of high purity nitrogen gas, a solution of 2, 4-di-tert-butyl-6-{[2-(1H-imidazol-4-yl)-ethylimino]-methyl}-phenol (0.50 g, 1.53 mmol) and $MnCl_2$ (0.20 g, 1.53 mmol) were added to 25 ml ethanol. The solution was stirred for twenty four hours at room

temperature (rt), the yellowish solution turned to black colour after three hours. The solvent was removed under a reduced pressure and a black solid powder was obtained washed with hexane and dried in vacuum desiccator over anhydrous calcium chloride to obtain 60% yield; M.p (185 – 188 °C). FT-IR cm^{-1}: 3321 υ(NH); 2950 υ(C-H); 1613 υ(C=N: imine); 1570 υ(C=N imidazole). UV-vis transitions 280nm (imidazole), 400nm (phenol). Analytical analyses calculations for $C_{20}H_{28}N_3OMnCl$ (%): 0.42 CH_3CH_2OH, C, 57.63; H, 6.72; N, 10.08. Found (%): C, 58.22; H, 9.40; N, 9.34. HRMS (ESI) m/z: Calculated 416.1301 and found $[M]^+$ 416.1304.

2.2.3.2 Synthesis of 4-methoxy-6-{[2-(1H-imidazol-4-yl)-ethylimino]-methyl}-phenol Mn(II) chloride [C2]

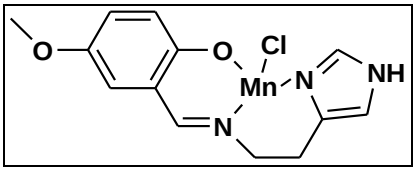

The synthesis of **C2** was similar to procedure followed in **C1** where 4-methoxy-6-{[2-(1H-imidazol-4-yl)-ethylimino]-methyl}-phenol (0.50 g, 2.04 mmol) and $MnCl_2$ (0.27 g, 2.04 mmol) were added to 25 ml ethanol. The brown solution turned green after five hours. The solvent was removed under a reduced pressure and a green solid powder was obtained washed with hexane and dried in vacuum desiccator over anhydrous calcium chloride to obtain 69% yield; M.p (220 – 223 °C). FT-IR cm^{-1}: 3320 υ(NH); 2990 υ(C-H); 1613 υ(C=N: imine); 1578 υ(C=N imidazole). UV-vis transitions 295nm (imidazole), 390nm (phenol). Analytical analyses calculations for $C_{13}H_{15}N_3O_2MnCl$ (%): C, 46.67; H, 4.48; N, 12.56. Found (%): C, 48.52; H, 3.96; N, 11.50. HRMS (ESI) m/z: Calculated 334.0155 and found $[M\text{-}OCH_3Cl]^+$ 268.1067.

2.2.3.3 Synthesis of 2-ethoxy-6-{[2-(1H-imidazol-4-yl)-ethylimino]-methyl}-phenol Mn(II) Chloride [C3]

The synthesis of **C3** was similar to procedure followed in **C1** where 2-ethoxy-6-{[2-(1H-imidazol-4-yl)-ethylimino]-methyl}-phenol (0.50 g, 1.93 mmol) and $MnCl_2$ (0.24 g, 1.93 mmol) were added to 25 ml ethanol.

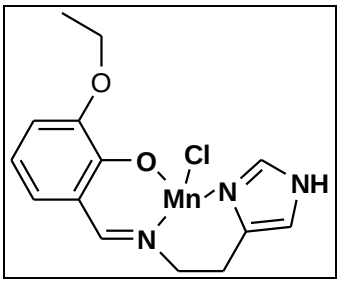

The yellowish solution turned green after three hours. The solvent was removed under a reduced pressure and a green solid powder was washed with hexane dried in vacuum desiccator over anhydrous calcium chloride to obtain 73% yield; M.p (160 – 163 °C). FT-IR cm^{-1}: 3319 υ(NH); 2899 υ(C-H); 1613 υ(C=N: imine); 1580 υ(C=N imidazole). UV-vis transitions 290nm (imidazole), 375nm (phenol). Analytical analyses calculations for $C_{14}H_{16}N_3O_2MnCl$ (%): C, 48.22; H, 4.59; N, 12.05. Found (%): 0.72 CH_3CH_2OH, C, 50.03; H, 4.83; N, 11.07. HRMS (ESI) m/z: Calculated 348.0312 and found $[M-CH_3CH_2]^+$ 232.0526.

2.2.3.4 Synthesis of salicylaldehyde-2-{[2-(1H-imidazol-4-yl)-ethylimino]-methyl}-phenol Mn(II) chloride [C4]

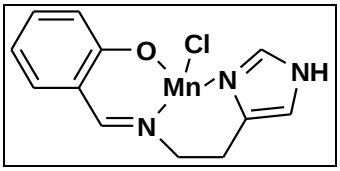

The synthesis of **C4** was similar to procedure followed in **C1** where salicylaldehyde-2-{[2-(1H-imidazol-4-yl)-ethylimino]-methyl}-phenol (0.50 g, 2.32 mmol) and $MnCl_2$ (0.3 g, 2.32 mmol) were added to 25 ml ethanol. The brown solution turned green after seven hours. The solvent was removed under a reduced pressure and a green solid powder was washed with hexane dried in vacuum desiccator over anhydrous calcium chloride to obtain 60% yield; M.p (185 – 188 °C). FT-IR cm^{-1}: 3328 υ(NH); 2902 υ(C-H); 1591 υ(C=N: imine); 1575 υ(C=N imidazole). UV-vis transitions 293nm (imidazole), 380nm

(phenol). Analytical analyses calculations for $C_{14}H_{16}N_3OMnCl$ (%): C, 48.22; H, 4.59; N, 12.05. Found (%): C, 50.03; H, 4.83; N, 11.07. HRMS (ESI) m/z: Calculated 304.0049 and found $[M]^+$ 304.3006

2.2.3.5 Synthesis of 4-methyl-6-{[2-(1H-imidazol-4-yl)-ethylimino]-methyl}-phenol Mn(II) chloride [C5]

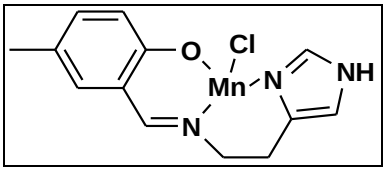

The synthesis of **C5** was similar to procedure followed in **C1** where 4-methyl-6-{[2-(1H-imidazol-4-yl)-ethylimino]-methyl}-phenol (0.50 g, 2.18 mmol) and $MnCl_2$ (0.30 g, 2.18 mmol) were added to 25 ml ethanol. The brown solution turned black after five hours. The solvent was removed under a reduced pressure and the black solid powder was washed with hexane, dried in vacuum desiccator over anhydrous calcium chloride to obtain 63% yield; M.p (125 – 127 °C). FT-IR cm^{-1}: 3331 υ(NH); 2903 υ(C-H); 1610 υ(C=N: imine); 1580 υ(C=N imidazole). UV-vis transitions 290nm (imidazole), 375nm (phenol). Analytical analyses calculations for $C_{13}H_{14}N_3OMnCl$ (%): C, 48.99; H, 3.77; N, 13.19. Found (%): 0.22 CH_3CH_2OH C, 50.36; H, 4.26; N, 12.04. HRMS (ESI) m/z: Calculated 318.0206 and found $[M]^+$ 318.0210

2.2.3.6 Synthesis of 3-methyl-6-{[2-(1H-imidazol-4-yl)-ethylimino]-methyl}-phenol Mn(II) chloride [C6]

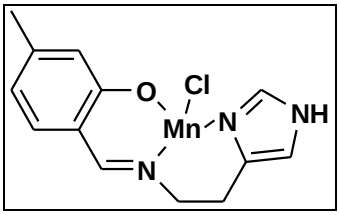

The synthesis of **C6** was similar to procedure followed in **C1** where 3-methyl-6-{[2-(1H-imidazol-4-yl)-ethylimino]-methyl}-phenol (0.50 g, 2.18 mmol) and $MnCl_2$ (0.30 g, 2.18 mmol) were added to 25 ml ethanol. The yellowish solution turned to green colour after

six hours. The solvent was removed under a reduced pressure and the green solid powder was washed with hexane, dried in vacuum desiccator over anhydrous calcium chloride to obtain 75% yield; M.p (200 – 203 °C). FT-IR cm^{-1}: 3230 υ(NH); 2964 υ(C-H); 1610 υ(C=N: imine); 1570 υ(C=N imidazole). UV-vis transitions 290nm (imidazole), 380nm (phenol). Analytical analyses calculations for $C_{13}H_{14}N_3OMnCl$ (%): C, 48.99; H, 3.77; N, 13.19. Found (%): C, 47.23; H, 4.75; N, 13.25. HRMS (ESI) m/z: Calculated 318.0206 and found $[M]^+$ 318.0213.

2.2.3.7 Synthesis of 3-methoxy-6-{[2-(1H-imidazol-4-yl)-ethylimino]-methyl}-phenol Mn(II) chloride [C7]

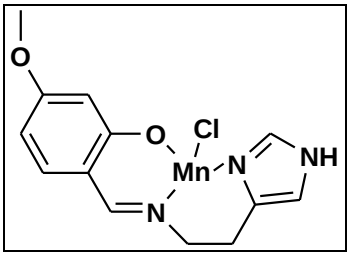

The synthesis of **C7** was similar to procedure followed in **C1** where 3-methoxy-6-{[2-(1H-imidazol-4-yl)-ethylimino]-methyl}-phenol (0.30 g, 1.22 mmol) and $MnCl_2$ (0.15 g, 1.22 mmol) were added to 25 ml ethanol. The brown solution turned to black colour after five hours. The solvent was removed under a reduced pressure and a black solid powder was obtained washed with hexane and dried in vacuum desiccator over anhydrous calcium chloride to obtain 73% yield; M.p (118 – 120 °C). FT-IR cm^{-1}: 3230 υ(NH); 2945 υ(C-H); 1607 υ(C=N: imine); 1579 υ(C=N imidazole). UV-vis transitions 280nm (imidazole), 350nm (phenol). Analytical analyses calculations for $C_{13}H_{15}N_3O_2MnCl$ (%): C, 46.67; H, 4.48; N, 12.56. Found (%): 0.19 CH_3CH_2OH, C, 48.03; H, 5.03; N, 11.04. HRMS (ESI) m/z: Calculated 334.0155 and found $[M]^+$ 334.1391.

2.2.3.8 Synthesis of 2-tert-butyl-6-{[2-(1H-imidazol-4-yl)-ethylimino]-methyl}-phenol Mn(II) chloride [C8]

The synthesis of **C8** was similar to procedure followed in **C1** where 2-di-tert-butyl-6-{[2-(1H-imidazol-4-yl)-ethylimino]-methyl}-phenol (0.30 g, 1.11 mmol) and $MnCl_2$ (0.14 g, 1.11 mmol) were added to 25 ml ethanol.

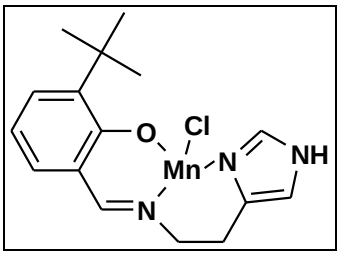

The synthesis of **C8** was similar to procedure followed in **C1** where 2-di-tert-butyl-6-{[2-(1H-imidazol-4-yl)-ethylimino]-methyl}-phenol (0.30 g, 1.11 mmol) and $MnCl_2$ (0.14 g, 1.11 mmol) were added to 25 ml ethanol. The yellowish solution turned to black colour after five hours. The solvent was removed under a reduced pressure and a black solid powder was obtained washed with hexane and dried in vacuum desiccator over anhydrous calcium chloride to obtain 60% yield; M.p (220 – 222 °C). FT-IR cm^{-1}: 3160 υ(NH); 2959 υ(C-H); 1653 υ(C=N: imine); 1570 υ(C=N imidazole). UV-vis transitions 290nm (imidazole), 375nm (phenol). Analytical analyses calculations for $C_{16}H_{20}N_3OMnCl$ (%): C, 53.27; H, 5.44; N, 11.09. Found (%): C, 54.37; H, 5.03; N, 10.12. HRMS (ESI) m/z: Calculated 360.0675 and found $[M]^+$ 360.0680.

2.2.3.9 Synthesis of 2-methyl-6-{[2-(1H-imidazol-4-yl)-ethylimino]-methyl}-phenol Mn(II) chloride [C9]

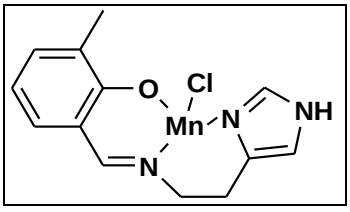

The synthesis of **C9** was similar to procedure followed in **C1** where 3-methyl-6-{[2-(1H-imidazol-4-yl)-ethylimino]-methyl}-phenol (0.30 g, 1.31 mmol) and $MnCl_2$ (0.17 g, 1.31 mmol) were added to 25 ml ethanol. The yellowish solution turned to black colour after

seven hours. The solvent was removed under a reduced pressure and the black solid powder was washed with hexane, dried in vacuum desiccator over anhydrous calcium chloride to obtain 72% yield; M.p (150 – 153 °C). FT-IR cm^{-1}: 3323 υ(NH); 2942 υ(C-H); 1591 υ(C=N: imine); 1580 υ(C=N imidazole). UV-vis transitions 300nm (imidazole), 375nm (phenol). Analytical analyses calculations for $C_{13}H_{14}N_3OMnCl$ (%): C, 48.99; H, 3.77; N, 13.19. Found (%): C, 50.45; H, 4.34; N, 12.11. HRMS (ESI) m/z: Calculated 318.0206 and found $[M]^+$ 318.0214.

2.2.3.10 Synthesis of 2, 4-di-tert-butyl-6-{[2-(1H-imidazol-4-yl)-ethylimino]-methyl}-phenol Cu(II) chloride [C10]

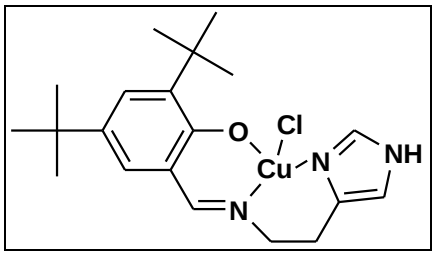

The synthesis of **C10** was similar to procedure followed in **C1** where 2-di-tert-butyl-6-{[2-(1H-imidazol-4-yl)-ethylimino]-methyl}-phenol (0.30 g, 91.60 mmol) and $CuCl_2$ (0.12 g, 91.60 mmol) were added to 25 ml ethanol. The solution was stirred for twenty four hours at room temperature (rt), the yellowish solution turned to brown colour after two hours and turned to green after four hours. The solvent was removed under a reduced pressure and the green solid powder was obtained washed with hexane and dried in vacuum desiccator over anhydrous calcium chloride to obtain 70% yield; M.p (197 – 200 °C). FT-IR cm^{-1}: 3273 υ(NH); 2995 υ(C-H); 1635 υ(C=N: imine); 1570 υ(C=N imidazole). UV-vis transitions 300nm (imidazole), 400nm (phenol). Analytical analyses calculations for $C_{20}H_{28}N_3OCuCl$ (%): C, 56.39; H, 6.57; N, 9.86. Found (%): C, 58.05; H, 5.34; N, 8.23. HRMS (ESI) m/z: Calculated 424.1217 and found $[M\text{-}Cl]^+$ 391.1510.

2.2.3.11 Synthesis of 4-mthoxy-6-{[2-(1H-imidazol-4-yl)-ethylimino]-methyl}-phenol Cu(II) chloride [C11]

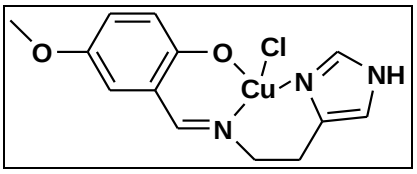

The synthesis of **C11** was similar to procedure followed in **C1** where 4-methoxy-6-{[2-(1H-imidazol-4-yl)-ethylimino]-methyl}-phenol (0.50 g, 2.04 mmol) and $CuCl_2$ (0.27 g, 2.04 mmol) were added to 25 ml ethanol. The brown solution turned to black after four hours. The solvent was removed under a reduced pressure and a black solid powder was obtained washed with hexane and dried in vacuum desiccator over anhydrous calcium chloride to obtain 71% yield; M.p (225 – 227 °C). FT-IR cm^{-1}: 3376 υ(NH); 2922 υ(C-H); 1607 υ(C=N: imine); 1570 υ(C=N imidazole). UV-vis transitions 300nm (imidazole), 400nm (phenol). Analytical analyses calculations for $C_{13}H_{15}N_3O_2CuCl$ (%): C, 45.49; H, 4.37; N, 12.24. Found (%): 0.23 CH_3CH_2OH, C, 47.03; H, 3.28; N, 11.05. HRMS (ESI) m/z: Calculated 342.0071 and found $[M\text{-}Cl]^+$ 307.0385.

2.2.3.12 Synthesis of 2-ethoxy-6-{[2-(1H-imidazol-4-yl)-ethylimino]-methyl}-phenol Cu(II) chloride [C12]

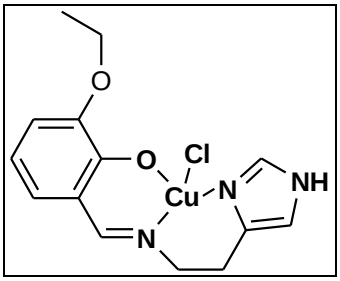

The synthesis of **C12** was similar to procedure followed in **C1** where 2-ethoxy-6-{[2-(1H-imidazol-4-yl)-ethylimino]-methyl}-phenol (0.50 g, 1.93 mmol) and $CuCl_2$ (0.26 g, 1.93 mmol) were added to 25 ml ethanol. The yellowish solution turned to brown colour after one hour and then turned to black after five hours. The solvent was removed under a

reduced pressure and a black solid powder was washed with hexane dried in vacuum desiccator over anhydrous calcium chloride to obtain 75% yield; M.p (160 - 163). FT-IR cm^{-1}: 3399 υ(NH); 2990 υ(C-H); 1626 υ(C=N: imine); 1577 υ(C=N imidazole). UV-vis transitions 280nm (imidazole), 375nm (phenol). Analytical analyses calculations for $C_{14}H_{16}N_3O_2CuCl$ (%): C, 47.06; H, 4.48; N, 11.76. Found (%):0.17 CH_3CH_2OH, C, 48.31; H, 3.90; N, 10.78. HRMS (ESI) m/z: Calculated 356.0121 and found $[M+H]^+$ 357.0133.

2.2.3.13 Synthesis of salicylaldehyde-2-{[2-(1H-imidazol-4-yl)-ethylimino]-methyl}-phenol Cu(II) chloride [C13]

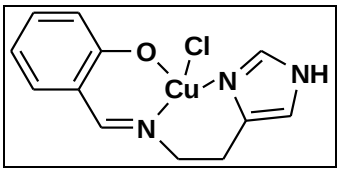

The synthesis of **C13** was similar to procedure followed in **C1** where salicylaldehyde-2-{[2-(1H-imidazol-4-yl)-ethylimino]-methyl}-phenol (0.30 g, 1.39 mmol) and $CuCl_2$ (0.19 g, 1.39 mmol) were added to 25 ml ethanol. The brown solution turned to black after five hours. The solvent was removed under a reduced pressure and a green solid powder was washed with hexane dried in vacuum desiccator over anhydrous calcium chloride to obtain 75% yield; M.p (195 – 197 °C). FT-IR cm^{-1}: 3326 υ(NH); 2899 υ(C-H); 1625 υ(C=N: imine); 1577 υ(C=N imidazole). UV-vis transitions 290nm (imidazole), 390nm (phenol). Analytical analyses calculations for $C_{14}H_{16}N_3OCuCl$ (%): C, 46.01; H, 3.83; N, 13.42. Found (%): 0.15 CH_3CH_2OH, C, 47.81; H, 3.31; N, 12.23. HRMS (ESI) m/z: Calculated 311.9965 and found $[M-Cl]^+$ 277.0282

.

2.2.3.14 Synthesis of 4-methyl-6-{[2-(1H-imidazol-4-yl)-ethylimino]-methyl}-phenol Cu (II) chloride [C14]

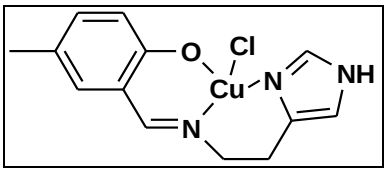

The synthesis of **C14** was similar to procedure followed in **C1** where 4-methyl-6-{[2-(1H-imidazol-4-yl)-ethylimino]-methyl}-phenol (0.30 g, 1.32 mmol) and $CuCl_2$ (0.18 g, 1.32 mmol) were added to 25 ml ethanol. The yellowish solution turned brown after one hour and then turned green after four hours. The solvent was removed under a reduced pressure and the green solid powder was washed with hexane, dried in vacuum desiccator over anhydrous calcium chloride to obtain 69% yield; M.p (200 – 203 °C). FT-IR cm^{-1}: 3331 υ(NH); 2902 υ(C-H); 1624 υ(C=N: imine); 1580 υ(C=N imidazole). UV-vis transitions 290nm (imidazole), 390nm (phenol). Analytical analyses calculations for $C_{13}H_{14}N_3OCuCl$ (%): C, 47.71; H, 3.67; N, 13.42. Found (%): 0.15 CH_3CH_2OH, C, 47.81; H, 3.11; N, 11.66. HRMS (ESI) m/z: Calculated 326.0121 and found $[M\text{-}Cl]^+$ 291.0431.

2.2.3.15 Synthesis of 3-methyl-6-{[2-(1H-imidazol-4-yl)-ethylimino]-methyl}-phenol Cu(II) chloride [C15]

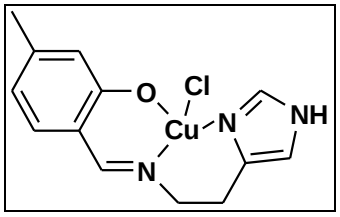

The synthesis of **C15** was similar to procedure followed in **C1** where 3-methyl-6-{[2-(1H-imidazol-4-yl)-ethylimino]-methyl}-phenol (0.30 g, 1.32 mmol) and $CuCl_2$ (0.18 g, 1.32 mmol) were added to 25 ml ethanol. The yellowish solution turned brown after thirty minutes and then turned green after five hours. The solvent was removed under a reduced pressure and the green solid powder was washed with hexane, dried in vacuum desiccator over anhydrous calcium chloride to obtain 75% yield; M.p (198 – 201 °C). FT-IR cm^{-1}: 3325 υ(NH); 2903 υ(C-H); 1633 υ(C=N: imine); 1580 υ(C=N imidazole).

UV-vis transitions 300nm (imidazole), 395nm (phenol). Analytical analyses calculations for $C_{13}H_{14}N_3OCuCl$ (%): C, 47.71; H, 3.67; N, 13.42. Found (%): 0.24 CH_3CH_2OH, C, 50.45; H, 4.15; N, 11.98. HRMS (ESI) m/z: Calculated 326.0121 and found $[M\text{-}Cl]^+$ 291.0432

2.2.3.16 Synthesis of 3-methoxy-6-{[2-(1H-imidazol-4-yl)-ethylimino]-methyl}-phenol Cu(II) chloride [C16]

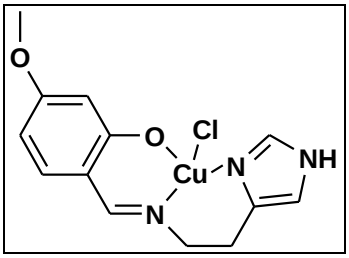

The synthesis of **C16** was similar to procedure followed in **C1** where 3-methoxy-6-{[2-(1H-imidazol-4-yl)-ethylimino]-methyl}-phenol (0.50 g, 2.04 mmol) and $CuCl_2$ (0.27 g, 2.04 mmol) were added to 25 ml ethanol. The brown solution turned green after seven hours. The solvent was removed under a reduced pressure and a green solid powder was obtained washed with hexane and dried in vacuum desiccator over anhydrous calcium chloride to obtain 69% yield; M.p (185 – 187 °C). FT-IR cm^{-1}: 3280 υ(NH); 2930 υ(C-H); 1622 υ(C=N: imine); 1571 υ(C=N imidazole). UV-vis transitions 300nm (imidazole), 400nm (phenol). Analytical analyses calculations for $C_{13}H_{15}N_3O_2CuCl$ (%): C, 45.49; H, 4.37; N, 12.24. Found (%): 0.34 CH_3CH_2OH C, 47;04 H, 3.98; N, 11.76. HRMS (ESI) m/z: Calculated 342.0071 and found $[M\text{-}Cl]^+$ 307.8201.

2.2.3.17 Synthesis of 2-tert-butyl-6-{[2-(1H-imidazol-4-yl)-ethylimino]-methyl}-phenol Cu(II) chloride [C17]

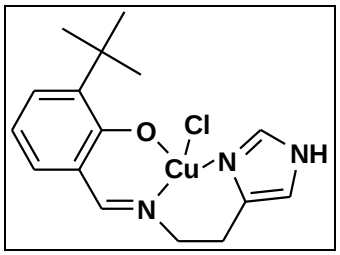

The synthesis of **C17** was similar to procedure followed in **C1** where 2-di-tert-butyl-6-{[2-(1H-imidazol-4-yl)-ethylimino]-methyl}-phenol (0.30 g, 1.22 mmol) and $CuCl_2$ (0.16 g, 1.22 mmol) were added to 25 ml ethanol. The yellowish solution turned to brown colour after two hours and the turned to green after five hours. The solvent was removed under a reduced pressure and a green solid powder was obtained washed with hexane and dried in vacuum desiccator over anhydrous calcium chloride to obtain 74% yield; M.p (180 – 183 °C). FT-IR cm^{-1}: 3207 υ(NH); 2942 υ(C-H); 1623 υ(C=N: imine); 1579 υ(C=N imidazole). UV-vis transitions 300nm (imidazole), 390nm (phenol). Analytical analyses calculations for $C_{16}H_{20}N_3OCuCl$ (%): C, 52.03; H, 5.41; N, 11.38. Found (%): 0.09 CH_3CH_2OH, C, 53.98; H, 4.15; N, 11.58. HRMS (ESI) m/z: Calculated 369.0591 and found $[M]^+$ 369.0491.

2.2.3.18 Synthesis of 2-methyl-6-{[2-(1H-imidazol-4-yl)-ethylimino]-methyl}-phenol Cu(II) chloride [C18]

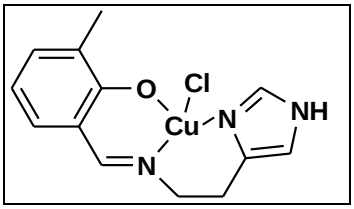

The synthesis of **C18** was similar to procedure followed in **C1** where 2-methyl-6-{[2-(1H-imidazol-4-yl)-ethylimino]-methyl}-phenol (0.30 g, 1.32 mmol) and $CuCl_2$ (0.18 g, 1.32 mmol) were added to 25 ml ethanol. The yellowish solution turned to brown colour after one hour and then turned green after four hours. The solvent was removed under a reduced pressure and the green solid powder was washed with hexane, dried in

vacuum desiccator over anhydrous calcium chloride to obtain 78% yield; M.p (191 - 193 °C). FT-IR cm^{-1}: 3200 υ(NH); 2908 υ(C-H); 1617 υ(C=N: imine); 1570 υ(C=N imidazole). UV-vis transitions 300nm (imidazole), 395nm (phenol). Analytical analyses calculations for $C_{13}H_{14}N_3OCuCl$ (%): C, 47.71; H, 3.67; N, 13.42. Found (%): C, 49.65; H, 2.98; N, 11.07. HRMS (ESI) m/z: Calculated 326.0121 and found $[M\text{-}Cl]^+$ 291.0434.

2.2.3.19 Synthesis of 2-methyl-6-{[2-(1H-imidazol-4-yl)-ethylimino]-methyl}-phenol Zn(II) chloride [C19]

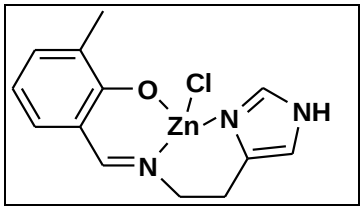

The synthesis of **C19** was similar to procedure followed in **C1** where 2-methyl-6-{[2-(1H-imidazol-4-yl)-ethylimino]-methyl}-phenol (1.00 g, 4.36 mmol) and $ZnCl_2$ (0.59 g, 4.36 mmol) were added in ethanol. The yellowish solution never changed for the entire twenty-four hours; the solvent was removed under a reduced pressure and a yellowish solid powder was obtained with 80% yield and M.p (192 – 194 °C). ^{1}H NMR (CD_3OD, δ (ppm), *J* (Hz)) : δ 2.17 (s, 3H, *o*-C_6H_3-OH) δ 3.02 (t, 2H, J = 6.4, C$\underline{H}_2$-C-CNH); δ 3.83 (t, 2H, J = 6.4, CH=N-C$\underline{H}_2$), δ 6.75 (s, 1H, HN-C$\underline{H}$=C), δ 6.64 (s, 1H, *m*-C_6H-3-OH), δ 7.13 (s, 1H, J = 4.5, *p*-C_6H-4-OH), δ 7.14 (d, 1H, J = 8, *m*-C_6H-5-OH) δ 7.99 (s, 1H, N-C$\underline{H}$-N); δ 8.29 (s, 1H, C$\underline{H}$=N). ^{13}C NMR (CD_3OD): δ 20.43 (CH_3- m-C_6H_3-OH), δ 27.31 (im-N-C-CH_2); δ 54.40 (-CH=NCH_2-); δ 119.85 (HN-CH-); δ 120.14; δ 131.90; δ 134.25; δ 136.55 (CH-C_6H_5); δ 136.77 (im-N-C-); δ 138.19 (-N-CH-N-); δ 169.82 (C_6H_4-OH); δ 169.82 (-CH=N-). HRMS (ESI) m/z: Calculated 327.0117 and found $[M\text{-}Cl]^+$ 293.0427.

2.2.4 Synthesis of quinoxaline derivatives

2.2.4.1 Synthesis of 2-quinoxalinone [Q1]

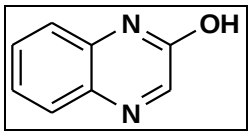

According to the method reported by W. Nxumalo [4], to a round bottomed flask equipped with stirrer bar was added *o*-phenylenediamine (10.01 g, 0.092 mol) dissolved in glacial acetic acid (10.00 ml) and methanol (10.00 ml) and the solution was cooled to -15℃ by ice bath while stirring. Glyoxylic acid (8.50 g, 0.092 mol) in water (20 ml) was added drop-wise over thirty minutes to the solution, maintaining the temperature at -15℃. The solution was allowed to warm up to 0℃ for ninety minutes, filtered, the filtrate washed with water (15 ml), methanol (15 ml) and air dried to give a grey solid. Recrystallization from DMF gave 2-quionoxalinone as tan solid with a yield of 81%. ^{1}H NMR (DMSO, *J* (Hz)): δ 7.28 - 7.32 (m, 2H); δ 7.52 - 7.56 (t, 1H, j = 8.8); δ 7.75 - 7.77 (d, 1H, j = 9.6); δ 8.14 (1H, s). ^{13}C NMR: (DMSO): δ 116.17; δ 123.75; δ 129.22; δ 131.23; δ 132.24; δ 134.47; δ 152.03; δ 155.38. M.p (265 – 267 ℃) and literature report (266 - 267 °C).

2.2.4.2 Synthesis of 2-benzenesulfonyloxyquinoxaline [Q2]

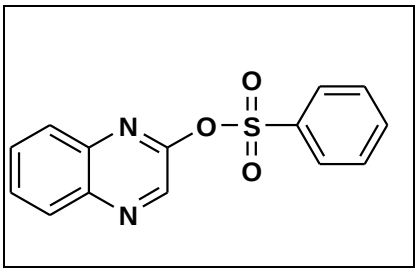

In line with the method reported by W. Nxumalo [4], to a round bottomed flask, 2-quinoxalinone (10.00 g, 68.4 mmol), DMAP (0.84 g, 6.84 mmol) and benzenesulfonyl chloride (17.50 ml, 136.85 mmol) were dissolved in a dry DCM (100 ml), cooled to 0℃ and stirred for five minutes. Et_3N (19.04 ml, 136.85 mmol) was added drop-wise over a period of five minutes. The solution was stirred at room temperature for another hour, and the reaction quenched with saturated $NaHCO_3$ (100 ml). The two layers were separated and the aqueous layer washed with DCM twice (50 ml). The combined organic layers were dried over Na_2SO_4, concentrated and excess ethyl acetate was added for selective solvation of 2-benzenesulfonyloxyquinoxaline. The solution was filtered. The product was recrystallised from hexane to obtain 2-benzenesulfonyloxyquinoxaline a brown solid with a yield 96% [4]. ^1H NMR ($CDCl_3$): δ 7.57 - 7.61 (m, 2H); δ 7.68 - 7.76 (m, 3H); δ 7.86 - 7.88 (m, 1H); δ 8.07 - 8.10 (m, 1H); δ 8.14 - 8.15 (m, 2H); δ 8.65 (s, 1H). ^{13}C NMR: ($CDCl_3$): δ 128.84; δ 129.05; δ 129.18; δ 129.23; δ 129.85; δ 131.23; δ 134.74; δ 136.32; δ 139;09; δ 139.66; δ 141.24; δ 150.88. M.p (88 - 91 °C) and literature report (91 °C).

2.2.4.3 Synthesis and procedure for Sonogashira coupling on 2-benzenesulfonyloxyquinoxaline using ethynyltrimethylsilane [Q3]

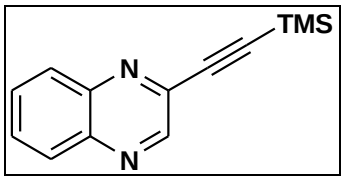

Following method reported by W. Nxumalo [4] and published by She and Aldrich [5], to a Schlenk tube equipped with a stirrer bar under nitrogen gas, 2-benzenesulfonyloxyquinoxaline (0.60 g, 2.10 mmol), $Pd(PPh_3)_4$ (76.00 mg, 0.10 mg, 5mol%), Et_3N (0.4 ml, 4.2 mmol, 2 equivalence) and ethynyltrimethylsilane (0.36 ml, 2.52 mmol, 1.2 equivalence) were dissolved in dry THF (10 ml). The solution was heated to 50℃ for twelve hours, partitioned between EtOAc/water (40ml 3:2), the layers were separated and the aqueous layer washed with EtOAc (30 ml). The combined organic layers were dried over Na_2SO_4, concentrated and purified on flash silica. The solvent was removed using rotary evaporator to obtain an oily brown product with a yield of 70% [4]. ^{1}H NMR ($CDCl_3$): δ 0.33 (s, 9H); δ 7.77 - 7.79 (m, 2H); δ 8.07 - 8.10 (m, 2H); δ 8.90 (s, 1H). ^{13}C NMR: ($CDCl_3$): δ 0.00; δ 86.31; δ 88.60; δ 100.74; δ 102.19; δ 129.90; δ 131.01; δ 131.13; δ 139.62; δ 141.46; δ 142.81; δ 147.81.

2.2.5 Attempted synthesis of organo-bridged Schiff base complexes to 2-ethynyltrimethylsilanequinoxaline

2.2.5.1 The reaction of Schiff base complexes to 2-ethynylrrinethylsilane-quinoxaline

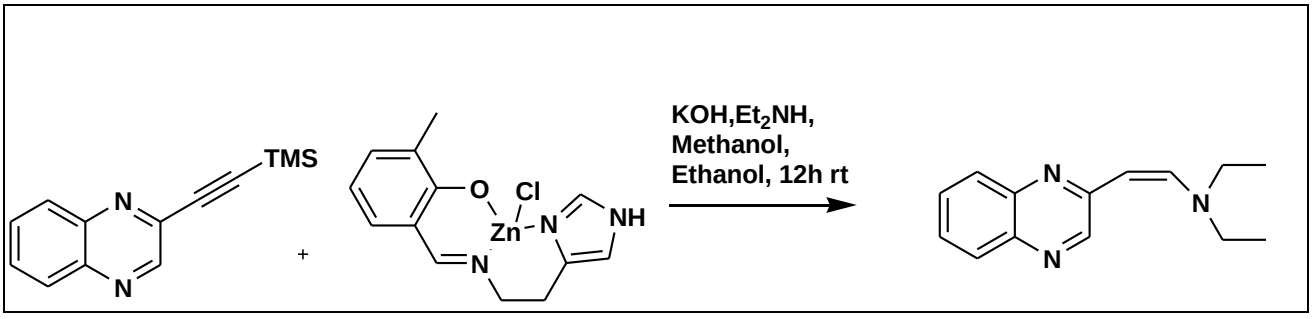

Into a Schlenk tube equipped with a stirrer bar in the presence of nitrogen gas, a solution of 2-methyl-6-{[2-(1H-imidazol-4-yl)-ethylimino]-methyl}-phenol Zn(II) chloride (0.06 g, 0.18 mmol), 2-ethynyltrimethylsilanequinoxaline (0.04 g, 0.18 mmol), Et_2NH (0,01 g, 0.18 mmol) and KOH (0.01 g, 0.18 mmol) in ethanol (15 ml) and (methanol 15 ml) was stirred for twelve hours at rt. The solution was filtered and the solvent was removed. The filtered yellowish paste product with a yield of 60% was characterised by

^{1}H NMR. ^{1}H NMR ($CDCl_3$, δ (ppm), J (Hz)): δ 1.24 (t, 6H, J = 1.6); δ 3.36 - 3.30 (q, 4H, J = 7.2) δ 5.35 - 5.32 (d, 1H, J = 13.2); δ 7.44 - 7.42 (t, 1H, J = 8.0); δ 7.58 - 7.56 (t, 1H, J = 7.2); δ 7.72 - 7.75 (d, 1H, J = 13.6); δ 7.87 - 7.85 (d, 1H, J = 8.0). ^{13}C NMR: ($CDCl_3$): δ 18.42; δ 58.31; δ 91.97; δ 125.65; δ 127.25; δ 128.71; δ 129.62; δ 139.35; δ 142.84; δ 144.74; δ 145.19; δ 154.15. HRMS (ESI): calculated for $[M+H]^+$ 228.1422, found m/z 228.1508.

2.5.2.2 Attempted transmetalation of $ZnCl_2$ to 2-ethynylrrinethylsilanequinoxaline in the presence of Et_2NH

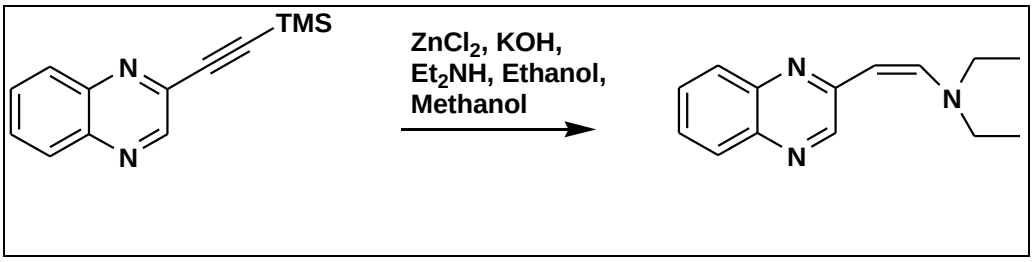

Into a Schlenk tube equipped with a stirrer bar in the presence of nitrogen gas, a solution of $ZnCl_2$ (0.03 g, 0.22 mmol), 2-ethynyltrimethylsilanequinoxaline (0.05 g, 0.18 mmol), Et_2NH (0,02 g, 0.22 mmol) and KOH (0.02 g, 0.22 mmol) in ethanol (15 ml) and (methanol 15 ml) was stirred for twelve hours at rt. The solution was filtered and the solvent was removed to obtain a paste yellowish product (90%). ^{1}H NMR ($CDCl_3$, δ (ppm), J (Hz)): δ 1.24 (t, 6H, J = 1.6); δ 3.36 - 3.30 (q, 4H, J = 7.2) δ 5.35 - 5.32 (d, 1H, J = 13.2); δ 7.44 - 7.42 (t, 1H, J = 8.0); δ 7.58 - 7.56 (t, 1H, J = 7.2); δ 7.72 - 7.75 (d, 1H, J = 13.6); δ 7.87 - 7.85 (d, 1H, J = 8.0). ^{13}C NMR: ($CDCl_3$): δ 18.42; δ 58.31; δ 91.97; δ 125.65; δ 127.25; δ 128.71; δ 129.62; δ 139.35; δ 142.84; δ 144.74; δ 145.19; δ 154.15. HRMS (ESI): calculated for $[M+H]^+$ 228.1422, found m/z 228.1508.

2.3 References

[1] M. Zarei, A. Jarrahpour; Green and efficient synthesis of azo Schiff bases, *Iranian Journal of Science & Technology,* 3 (2011) 235-242.

[2] W. Qin, S. Long, M. Panunzio, S. Biondi; Schiff Bases; A Short Survey on an Evergreen Chemistry Tool, *Molecules,* 18 (2013) 12264-12289.

[3] S. Boltina, M. Yankey, I.A. Guzei, L.C. Spencer, S.O. Ojwacha, J. Darkwa; Novel O-N-N Pyrazolyl-imine and Imidazolyl-imine Pincer Palladium Complexes as Heck Coupling Catalysts*, South African Journal of Chemistry*, 65 (2012) 75-83.

[4] W. Nxumalo, The development of novel pterin chemistry leading to potential dihydrofolate reductase inhibitors with potential antimalarial activity, *PhD thesis, University of Witwatersrand Library*, (2011) 69-74.

[5] C. Shi, C.C. Aldrich, Efficient Pd-Catalyzed Coupling of Tautomerizable Heterocycleswith Terminal Alkynes via C-OH Bond Activation Using PyBrOP, *Organic Letters*, 10 (2010); 2286–2289.

CHAPTER THREE

RESULTS AND DISCUSION OF IMIDAZOLYL-SALICYLALDEMINE SCHIFF BASES AND THEIR COMPLEXES, QUINOXALINE DERIVATIVES AND SCHIFF BASE COMPLEXES COUPLED TO QUINOXALINE DERIVATIVE.

3.1 Synthesis and properties of ligands

The ligands **L1** - **L10** were prepared following the reaction procedure illustrated in **Table 3.1**. All ligands were obtained by the condensation of histamine dihydrochloride salt with the appropriate aldehyde in methanol refluxing at 64.7 °C for twenty four hours under inert condition. Two equivalents of dehydrating agent $NaHCO_3$ was used [1]. The condensation reaction forms the anticipated product in good yield and only few cases where there are little amount of unreacted aldehydes or incomplete reactions. The purification of Schiff base ligands containing heteroatom substituent of methoxy (**L2** and **L7**) was done by column chromatography with 90% hexane and 10% ethyl acetate. For **L3** 90% diethyl ether and 10% ethyl acetate was used. Chloroform dissolved (**L1** and **L6**) and precipitated the impurities. **L10** was re-dissolved in diethyl ether and precipitated impurities were filtered. Ligands containing alkyl group substituents on the phenyl ring were found to be more stable to moisture except **L6** which contains methyl group on position **3** refer **Table 3.1** which decomposes if exposed to moisture. Ligands containing heteroatom substituents such as methoxy and ethoxy on the phenyl ring were also found to be sensitive to moisture. Preparation of ligands in methanol solution was accompanied by a color change within a period of thirty minutes to four hours under reflux. The preparation of ligands **L1**, **L3**, **L5**, **L6**, **L8** and **L9** in methanol solution was accompanied by color change from a clear solution to a yellowish solution. Ligands **L2** and **L10** changed from a clear methanol solution to brown solution. Ligands **L4** and **L7** changed from a clear methanol solution to yellow after thirty minutes then changed to brown after two hours. The melting points range for ligands was within the range of 79 °C to 105 °C. The analytical data from the Elemental analysis showed that the found

and calculated values. The presence of methanol in other ligands was observed from the analytical data. All ligands were solid powders. The ligands **L1**, **L6** and **L9** formed crystals from ethanol solution. Schiff base ligands with different substituents were successfully synthesised and purified with good yields.

Table 3.1: Generalised procedure for preparation of imidazolyl-salicylaldemine Schiff base ligand derivatives

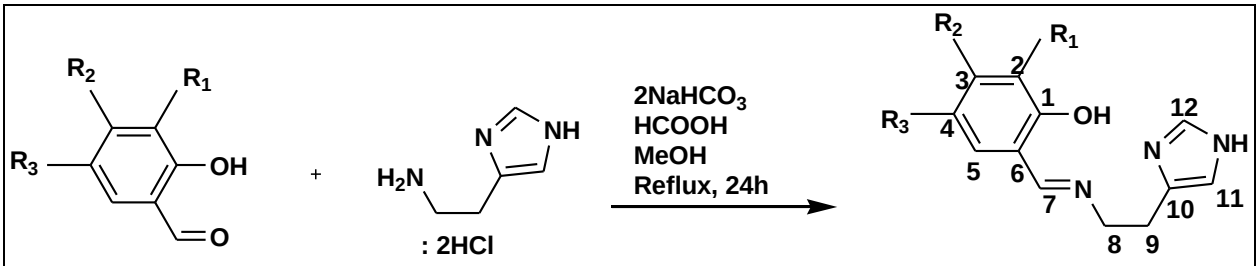

Ligands	R_1	R_2	R_3
L1	Tertiary butyl	Hydrogen	Tertiary butyl
L2	Hydrogen	Hydrogen	Methoxy
L3	Ethoxy	Hydrogen	Hydrogen
L4	Hydrogen	Hydrogen	Hydrogen
L5	Hydrogen	Hydrogen	Methyl
L6	Hydrogen	Methyl	Hydrogen
L7	Hydrogen	Methoxy	Hydrogen
L8	Tertiary butyl	Hydrogen	Hydrogen
L9	Methyl	Hydrogen	Hydrogen
L10	Hydrogen	Hydrogen	Tertiary butyl

3.2 Characterisation of ligands

3.2.1 NMR studies of L1 - L10

Imidazolyl-salicylaldemine Schiff base ligands were characterised by (^{1}H, ^{13}C, DEPT-135 ^{15}N).

The ligands vary from each other by the substituents on the phenyl ring at position **2**, **3** and **4**. The DEPT-135 shows two negative peaks to all ligands and only **L3** has three negative peaks due to ethoxy substituent. The coupling of nitrogen and proton showed by ^{15}N NMR revealed the imine nitrogen and hydrogen N=CH coupling by J^2 and CH_2-CH_2-N by J^3 for all ligands.

(**a**) The NMR characterisation of 2,4-di-tert-butyl-6-{[2-(1H-imidazol-4-yl)-ethylimino]-methyl}-phenol [**L1**] refer to the structure on **Figure 3.1**. On **Figure 3.2** ^{1}H NMR spectrum shows two singlets appearing at 1.29 ppm and 1.44 ppm from tertiary butyl substituents on the phenyl ring each integrating for nine protons, two triplets appearing at 2.98 ppm and 3.88 ppm assigned to protons **9** and **8** respectively from -CH_2-CH_2- linker each integrating for two protons with a coupling constant (J = 6.8 Hz), two singlets from the imidazole ring appearing at 6.81 ppm and 7.57 ppm assigned to protons **11** and **12** respectively each integrating for one proton, two doublets from the phenyl ring appearing at 7.01 ppm and 7.37 ppm assigned to protons **3** and **5** each integrating for one proton with a coupling constant (J = 2.4 Hz) and a singlet appearing at 8.28 ppm assigned to proton **7** integrating for one proton from the imine group. The phenolic OH appears on the most downfield at 13.85 ppm integrating for one proton illustrated on **Figure 3.2**. ^{13}C NMR on **Figure 3.3** shows the imine carbon at 166.53 ppm, phenolic OH carbon at 158.08 ppm, phenyl ring (126.84 ppm - 139.93 ppm); imidazole (117.11 ppm - 125.81 ppm), -CH_2-CH_2- (34.94 ppm and 59.09 ppm) and tertiary butyl carbons (29.65 ppm - 34.04 ppm). The DEPT-135 shows two negative peaks for HC=N-CH_2- (59.09 ppm) and CH_2-C (28.74 ppm) on the upfield, two positive peaks for CH_3 (29.42 ppm and 31.48 ppm) on the upfield and three positive peaks for CH (134.55 ppm, 126.94 ppm, 125.88 ppm) on the downfield at **Figure 3.4**. The ^{15}N

NMR shows the imine proton (8.28 ppm) coupling with the imine nitrogen (293.40 ppm) through J^2 coupling interaction (N=C-H) which are two bonds away from each other. The $-CH_2-$ bonded to the imidazole group interact with the imine nitrogen by J^3 coupling interaction (N-CH_2-CH_2) which are three bonds away from each other at **Figure 3.5.** The expectations were that both $–CH_2-CH_2-$ should couple with the nitrogen from the imine group by J^2 and J^3 because they are two and three bonds away from each other, however only one CH_2 is observed interacting through J^3 coupling interaction. The imine (N=C) and the (N-H) groups from the imidazole ring showed no interaction to its adjacent protons within the ring and the $–CH_2-CH_2-$ linker. The molecular mass calculated was 327.2311 and mass spectrum found from HRMS [M+H] is 328.2383 which is consistent with the prepared compound. **Figure 3.1** shows 2,4-di-tert-butyl-6-{[2-(1H-imidazol-4-yl)-ethylimino]-methyl}-phenol [**L1**] prepared by method reported by Boltina *et al*. [1] and the results were consistent with literature [1].

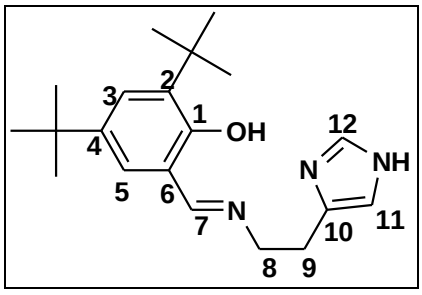

Figure 3.1: The structure of 2,4-di-tert-butyl-6-{[2-(1H-imidazol-4-yl)-ethylimino]-methyl}-phenol [**L1**] [1].

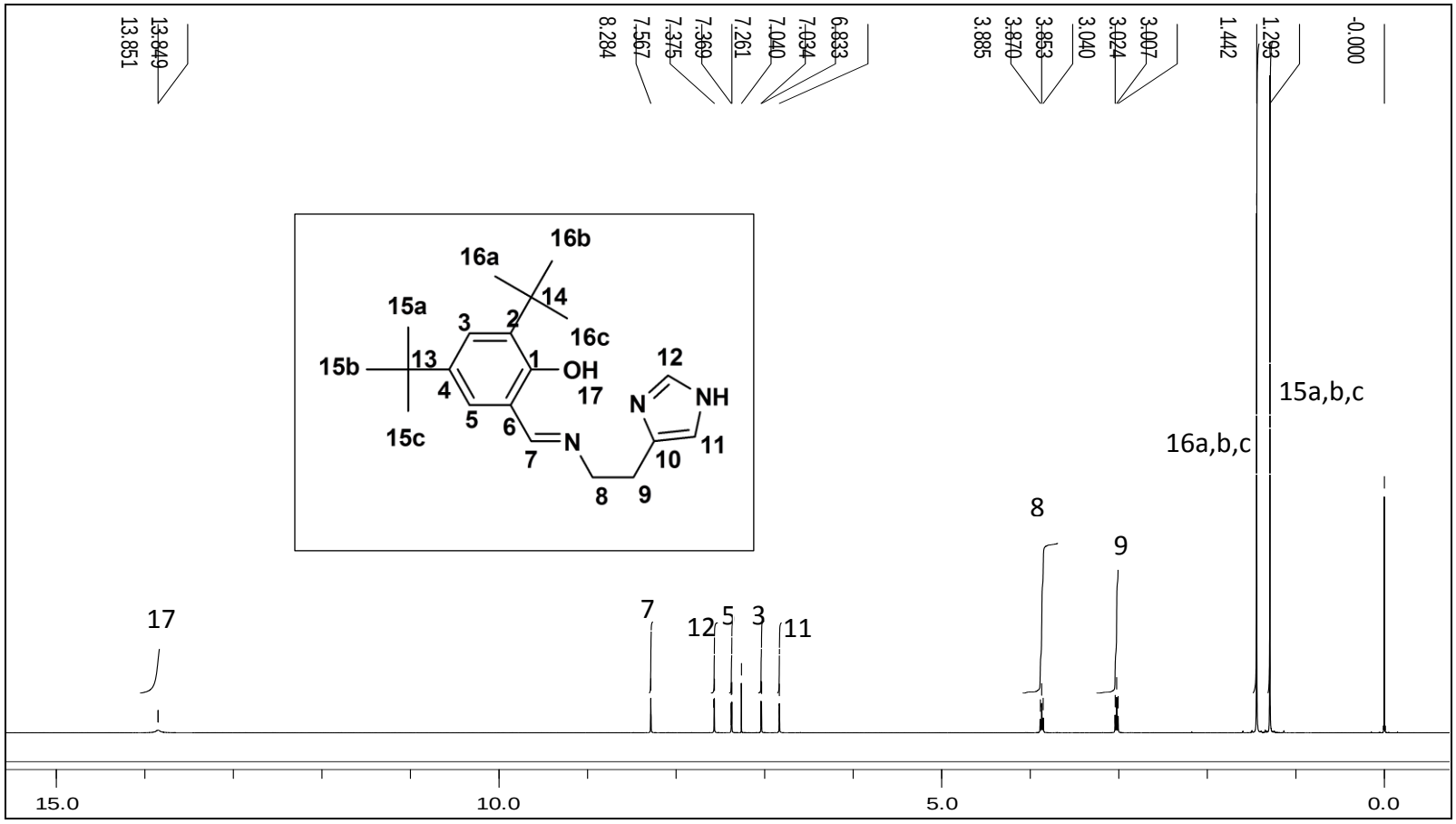

Figure 3.2: ^{1}H NMR of 2, 4-di-tert-butyl-6-{[2-(1H-imidazol-4-yl)-ethylimino]-methyl}-phenol [**L1**]

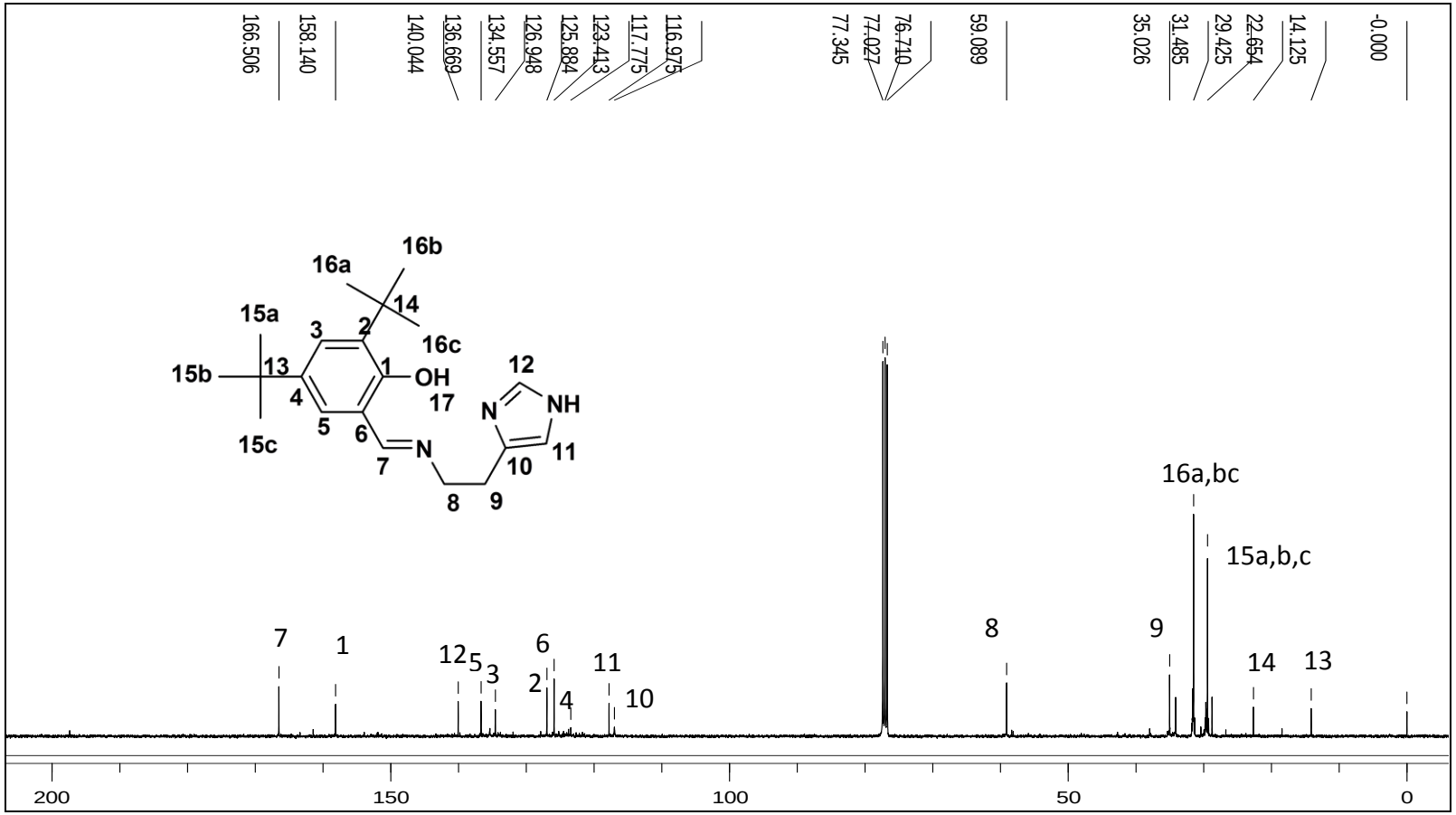

Figure 3.3: ^{13}C NMR of 2, 4-di-tert-butyl-6-{[2-(1H-imidazol-4-yl)-ethylimino]-methyl}-phenol [**L1**]

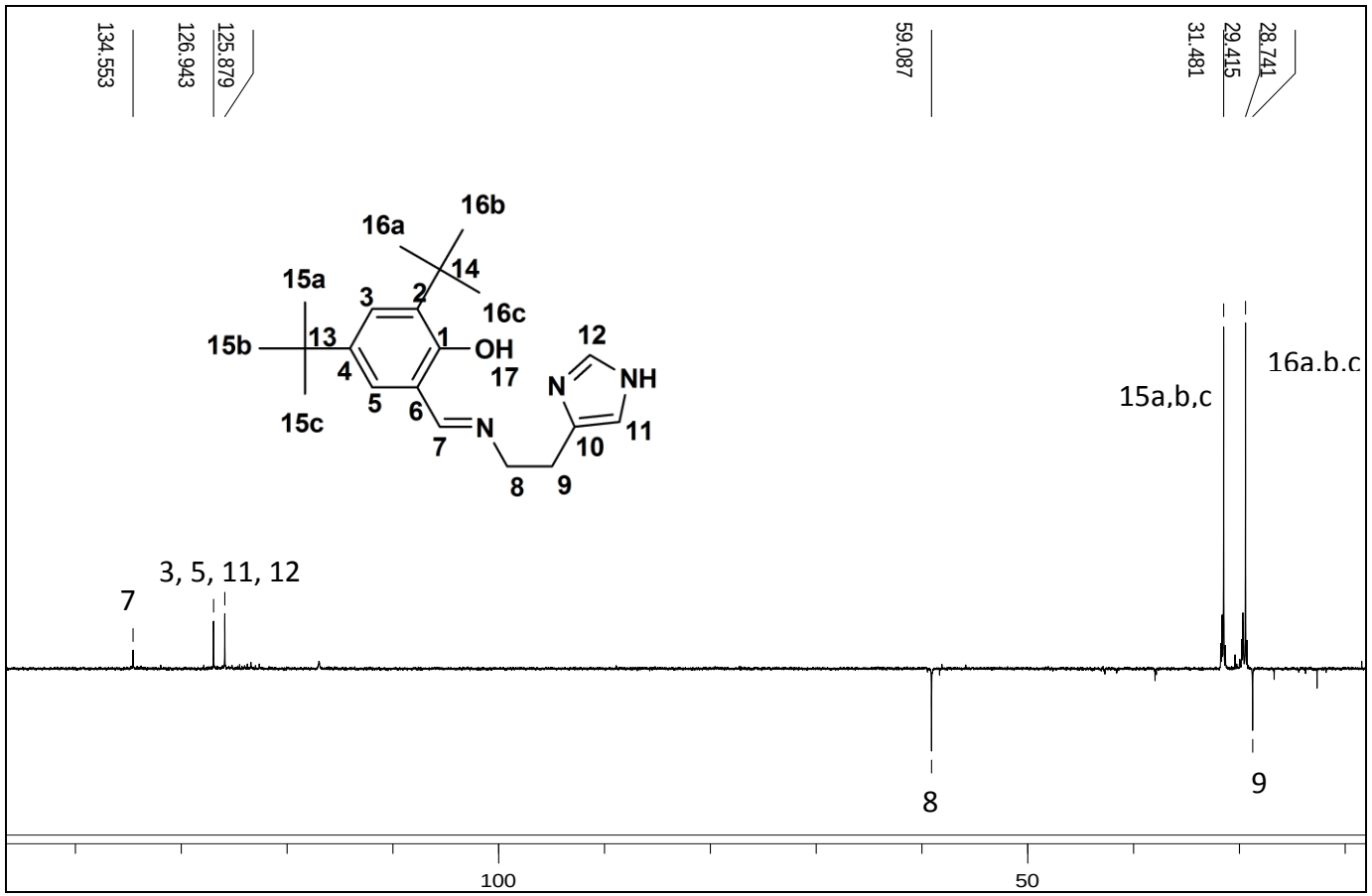

Figure 3.4: DEPT-135 NMR of 2, 4-di-tert-butyl-6-{[2-(1H-imidazol-4-yl)-ethylimino]-methyl}-phenol [**L1**]

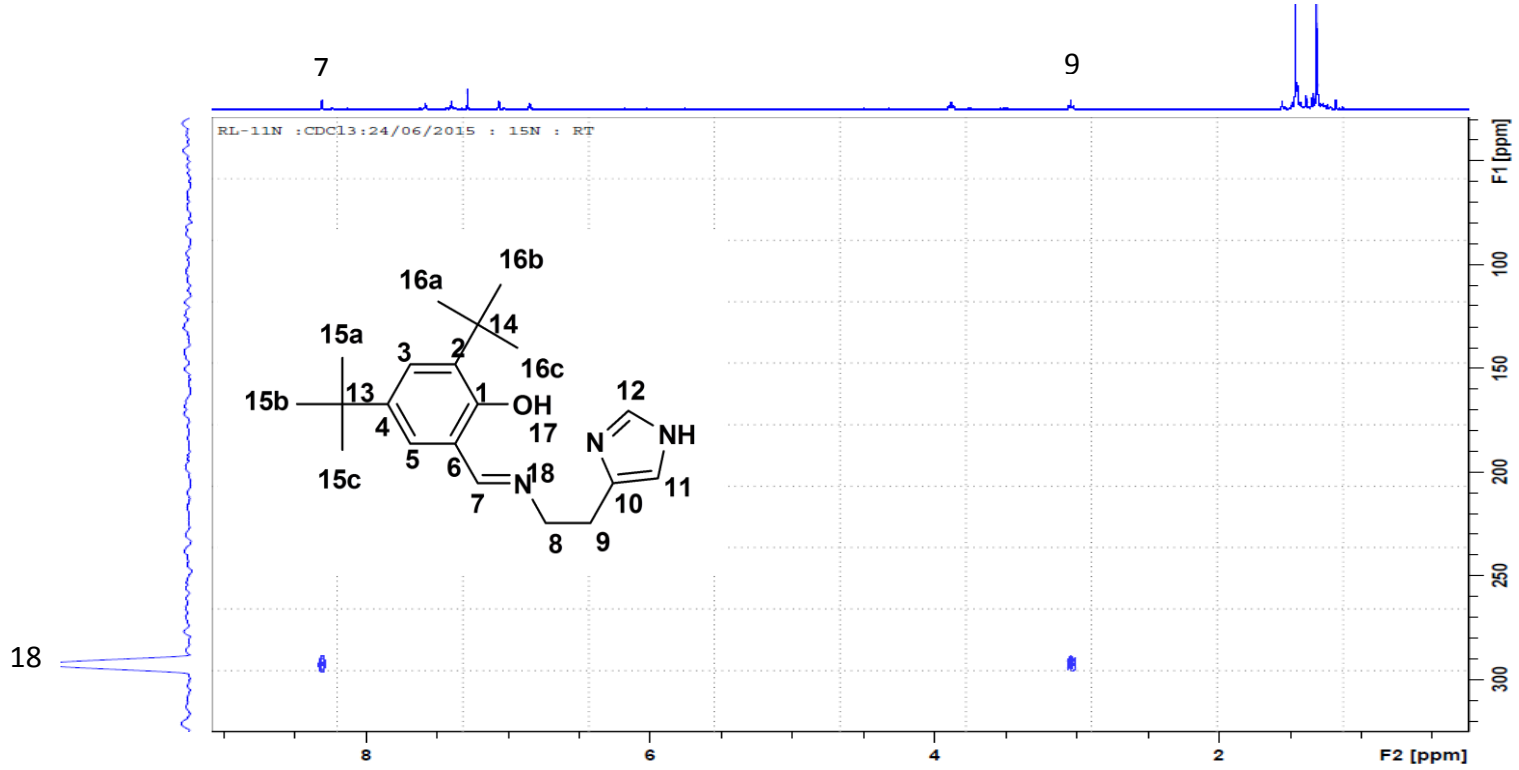

Figure 3.5: ^{15}N NMR of 2, 4-di-tert-butyl-6-{[2-(1H-imidazol-4-yl)-ethylimino]-methyl}-phenol [**L1**]

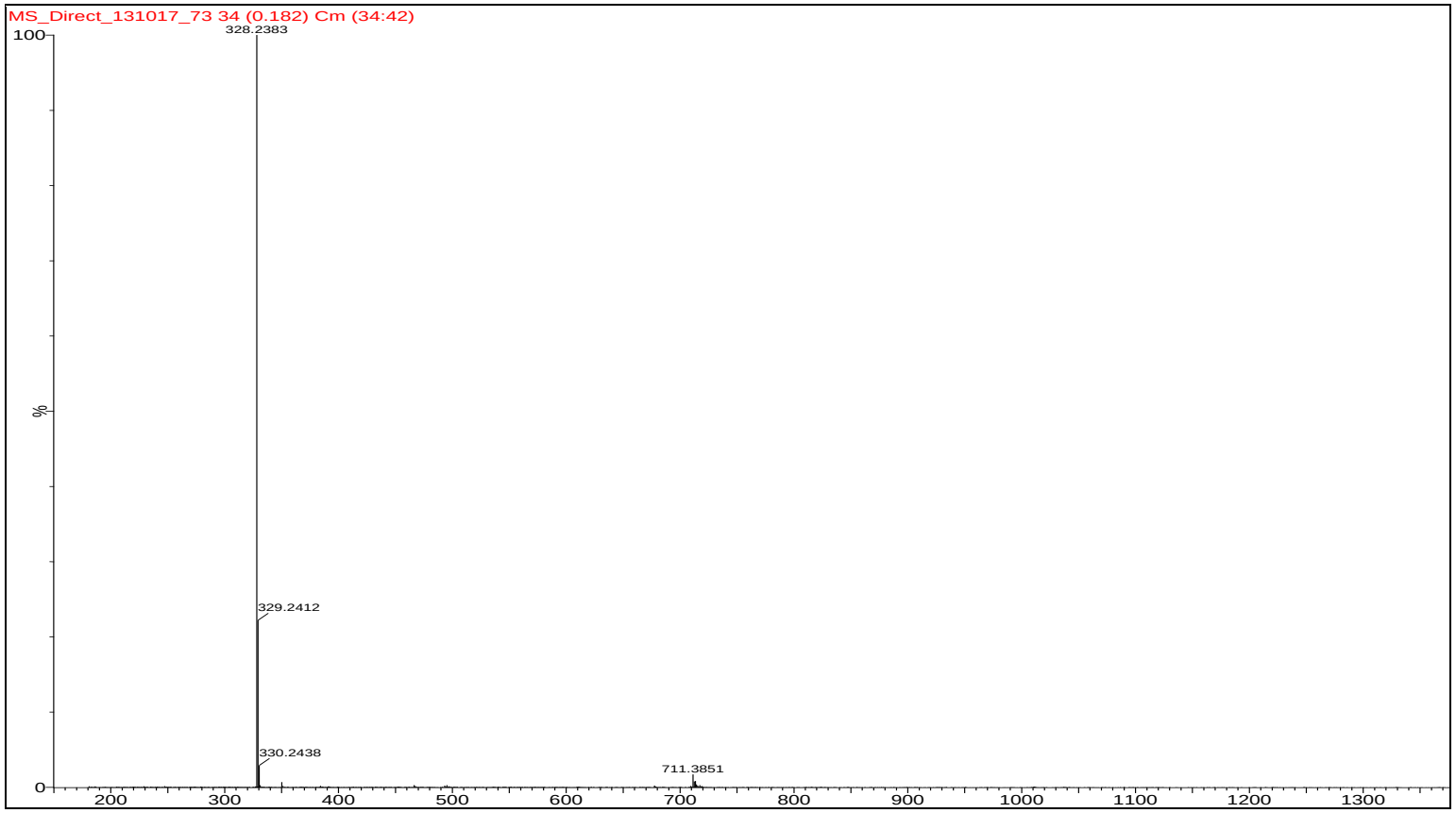

Figure 3.6: Mass spectrum of **L1**

(**b**) The NMR interpretation of 4-methoxy-6-{[2-(1H-imidazol-4-yl)-ethylimino]-methyl}-phenol [**L2**] refer to the structure on **Figure 3.7**. **L2** shows a singlet from the phenyl substituent of methoxy appearing at 3.74 ppm integrating for three protons. Three doublets from the phenyl ring appearing at 6.79 ppm with coupling constant (J = 2.8 Hz), 6.85 ppm with coupling constant (J = 7.2 Hz) and 6.88 ppm with coupling constant (J = 7.2 Hz) assigned to protons **2**, **3** and **5** respectively observed on both ^{1}H NMR and ^{13}C NMR in **Figure 1** and **Figure 9** in the Appendices. The molecular mass calculated was 245.1116 and mass spectrum found from HRMS [M+H] is 246.1246 which is consistent with the prepared compound. **Figure 3.7** shows 4-methoxy-6-{[2-(1H-imidazol-4-yl)-ethylimino]-methyl}-phenol. [**L2**] was prepared following method reported by Boltina *et al*. [1].

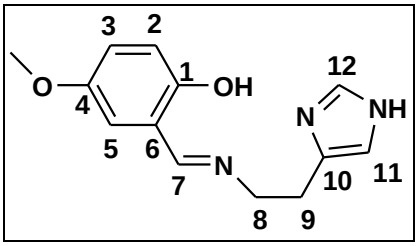

Figure 3.7: Structure of 4-methoxy-6-{[2-(1H-imidazol-4-yl)-ethylimino]-methyl}-phenol [**L2**]

(**c**) The NMR interpretation of 2-ethoxy-6-{[2-(1H-imidazol-4-yl)-ethylimino]-methyl}-phenol [**L3**] refer to the structure on **Figure 3.8**. **L3** shows a triplet from the phenyl substituent of ethoxy appearing at 1.47 ppm integrating for three protons with coupling constant (J = 6.8 Hz), a quartet appearing at 4.09 ppm integrating for two protons with coupling constant (J = 7.2 Hz). Three doublets from the phenyl ring each integrating for one proton appearing at 6.80 ppm with coupling constant of (J = 9.2 Hz), 6.89 ppm with coupling constant (J = 8 Hz) and 6.88 ppm with coupling constant (J = 7.6 Hz) assigned to protons **3**, **4** and **5** respectively which was observed on both ^{1}H NMR and ^{13}C NMR in **Figure 2** and **Figure 10** in the Appendices. The molecular mass calculated was 259.1321 and mass spectrum found from HRMS [M+H] is 260.1398 which is consistent with the prepared compound. **Figure 3.8** shows 2-ethoxy-6-{[2-(1H-

imidazol-4-yl)-ethylimino]-methyl}-phenol [**L3**] which was prepared following method reported by Boltina *et al*. [1].

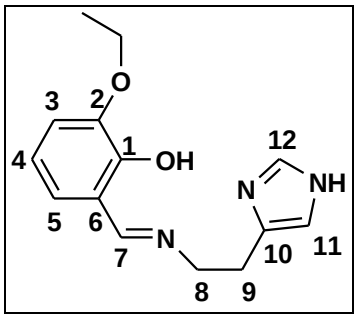

Figure 3.8: Structure of 2-ethoxy-6-{[2-(1H-imidazol-4-yl)-ethylimino]-methyl}-phenol [**L3**]

(**d**) The NMR interpretation of salicylaldehyde-2-{[2-(1H-imidazol-4-yl)-ethylimino]-methyl}-phenol [**L4**] refer to the structure on **Figure 3.9**. The ligand **L4** has protons on position **2**, **3**, **4** and **5** four multiplets from the phenyl ring appearing at 6.80 ppm, 6.85 ppm, 6.89 ppm and 7.14 ppm each integrating for one proton which was observed on both ^{1}H NMR and ^{13}C NMR in **Figure 3** and **Figure 11** in the Appendices. The molecular mass calculated was 215.1059 and mass spectrum found from HRMS [M+H] is 216.1302 which is consistent literature reported. **Figure 3.9** shows salicylaldehyde-2-{[2-(1H-imidazol-4-yl)-ethylimino]-methyl}-phenol [**L4**] which was prepared following method reported by Boltina *et al*. [1].

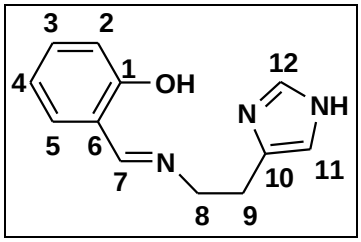

Figure 3.9: structure of salicylaldehyde-2-{[2-(1H-imidazol-4-yl)-ethylimino]-methyl}-phenol [**L4**][1].

(**e**) The NMR interpretation of 4-methyl-6-{[2-(1H-imidazol-4-yl)-ethylimino]-methyl}-phenol [**L5**] refer to the structure on **Figure 3.10**. **L5** shows a singlet appearing at 2.25 ppm integrating for three protons from the methyl substituent on position **4.** One doublet from the phenyl ring appearing at 7.14 ppm assigned to proton **2** integrating for one proton with coupling constant (J = 8.0 Hz), two multiplets appearing at 6.85 ppm and 6.90 ppm assigned to protons **3** and **5** respectively from the phenyl ring each integrating for one proton which was observed on both ^{1}H NMR and ^{13}C NMR in **Figure 4** and **Figure 12** in the Appendices. The molecular mass calculated was 229.1215 and mass spectrum found from HRMS [M+H] is 230.1294 which is consistent with the prepared compound. **Figure 3.10** shows 4-methyl-6-{[2-(1H-imidazol-4-yl)-ethylimino]-methyl}-phenol [**L5**] which was prepared following method reported by Boltina *et al*. [1].

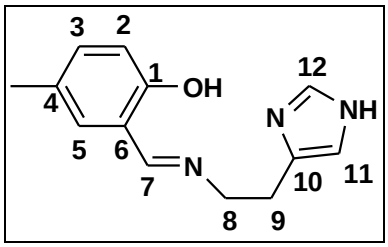

Figure 3.10: Structure of 4-methyl-6-{[2-(1H-imidazol-4-yl)-ethylimino]-methyl}-phenol [**L5**]

(**f**) The NMR interpretation of 3-methyl-6-{[2-(1H-imidazol-4-yl)-ethylimino]-methyl}-phenol [**L6**] refer to the structure on **Figure 3.11**. **L6** shows singlet appearing at 2.28 ppm integrating for three protons from the methyl substituent at position **3.** Two multiplets from the phenyl ring appearing at 6.79 ppm and 6.80 ppm each integrating for one proton, a doublets appearing at 7.05 ppm integrating for three protons with coupling constant of (J = 8.0 Hz) which was observed on both ^{1}H NMR and ^{13}C NMR in **Figure 5** and **Figure 13** in the Appendices. The molecular mass calculated was 229.1215 and mass spectrum found from HRMS [M+H] is 230.1304 which is consistent with literature [1]. **Figure 3.11** shows 3-methyl-6-{[2-(1H-imidazol-4-yl)-ethylimino]-methyl}-phenol [**L6**] which was prepared following method reported by Boltina *et al*. [1].

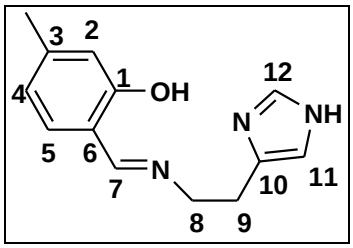

Figure 3.11: Structure of 3-methyl-6-{[2-(1H-imidazol-4-yl)-ethylimino]-methyl}-phenol [**L6**][1].

(**g**) The NMR interpretation of 3-methoxy-6-{[2-(1H-imidazol-4-yl)-ethylimino]-methyl}-phenol [**L7**] refer to the structure on **Figure 3.12**. **L7** has a singlet from the phenyl substituent of methoxy appearing at 3.75 ppm integrating for three protons. Two doublets from the phenyl ring appearing at 6.27 ppm with coupling constant (J = 7.2 Hz) and 6.99 ppm with coupling constant (J = 9.2 Hz) each integrating for one proton assigned to protons **4** and **5** respectively, a singlet appearing at 6.81 ppm assigned to proton **2** integrating for one proton which was observed on both ^{1}H NMR and ^{13}C NMR in **Figure 6** and **Figure 14** in the Appendices. The molecular mass calculated was 245.1164 and mass spectrum found from HRMS [M+H] is 246.1246 which is consistent with the prepared compound. **Figure 3.12** shows 3-methoxy-6-{[2-(1H-imidazol-4-yl)-ethylimino]-methyl}-phenol [**L7**] which was prepared following method reported by Boltina *et al*. [1].

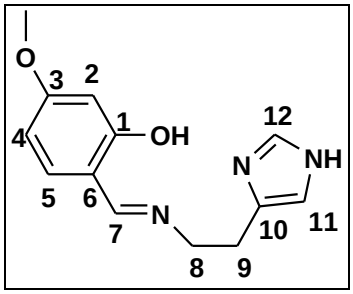

Figure 3.12: Structure of 3-methoxy-6-{[2-(1H-imidazol-4-yl)-ethylimino]-methyl}-phenol [**L7**]

(**h**) The NMR interpretation of 2-tert-butyl-6-{[2-(1H-imidazol-4-yl)-ethylimino]-methyl}-phenol [**L8**] refer to the structure on **Figure 3.12**. **L8** shows a singlet appearing at 1.44 ppm from tertiary butyl substituent on position **2** integrating for nine protons. Three doublets from the phenyl ring appearing at 6.80 ppm, 7.12 ppm and 7.15 ppm assigned to protons **4**, **3** and **5** respectively each integrating for one proton with coupling constant (J = 8.8 Hz) which was observed on both ^{1}H NMR and ^{13}C NMR in **Figure 7** and **Figure 15** in the Appendices. The molecular mass calculated was 271.1685 and mass spectrum found from HRMS [M+H] is 272.1765 which is consistent with the prepared compound. **Figure 3.12** shows 2-tert-butyl-6-{[2-(1H-imidazol-4-yl)-ethylimino]-methyl}-phenol [**L8**] which was prepared following method reported by Boltina *et al*. [1].

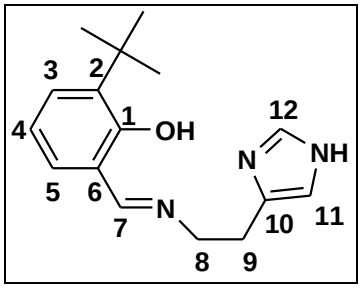

Figure 3.13: Structure of 2-tert-butyl-6-{[2-(1H-imidazol-4-yl)-ethylimino]-methyl}-phenol [**L8**]

(**i**) The NMR interpretation of 2-methyl-6-{[2-(1H-imidazol-4-yl)-ethylimino]-methyl}-phenol [**L9**] refer to the structure on **Figure 4.14**. **L9** shows a singlet appearing at 2.27 ppm integrating for three protons from the methyl substituent on position **2**. Two doublets from the phenyl ring appearing at 7.07 ppm with coupling constant (J = 7.2 Hz) and 7.19 ppm with coupling constant (J = 8 Hz) each integrating for one proton assigned to protons **3** and **5** respectively, a triplet appearing at 6.77 ppm assigned to proton **4** integrating for one proton with coupling constant (J = 7.2 Hz) which was observed on both ^{1}H NMR and ^{13}C NMR in **Figure 8** and **Figure 16** in the Appendices. The molecular mass calculated was 229.1215 and mass spectrum found from HRMS [M+H] is 230.1298 which is consistent with the prepared compound. **Figure 3.14** shows

2-methyl-6-{[2-(1H-imidazol-4-yl)-ethylimino]-methyl}-phenol [**L9**] which was prepared following method reported by Boltina *et al*. [1].

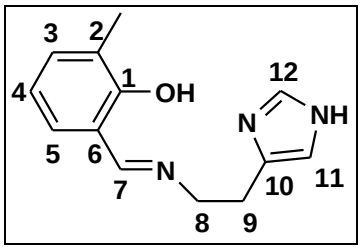

Figure 3.14: Structure of 2-methyl-6-{[2-(1H-imidazol-4-yl)-ethylimino]-methyl}-phenol [**L9**]

(**j**) The NMR interpretation of 4-tert-butyl-6-{[2-(1H-imidazol-4-yl)-ethylimino]-methyl}-phenol [**L10**] refer to the structure on **Figure 3.14** below. **L10** shows a singlet appearing at 1.19 ppm from tertiary butyl substituent on position **4** integrating for nine protons. Three doublets from the phenyl ring appearing at 6.76 ppm, 7.10 ppm and 7.23 ppm assigned to protons **2**, **3** and **5** each integrating for one proton with coupling constant (J = 6.8 Hz), (J = 8.8 Hz) and (J = 8.4 Hz) respectively which was observed on both ^{1}H NMR and ^{13}C NMR in **Figure 9** and **Figure 17** in the Appendices. The molecular mass calculated was 271.1298 and mass spectrum found from HRMS [M+H] is 272.1765 which is consistent with literature [1]. **Figure 3.15** shows 4-tert-butyl-6-{[2-(1H-imidazol-4-yl)-ethylimino]-methyl}-phenol [**L10**][1].

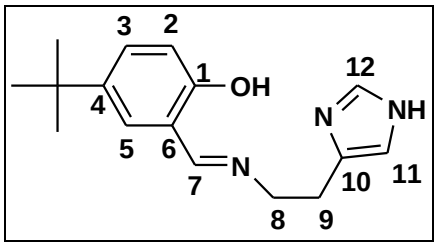

Figure 3.15: Structure of 4-tert-butyl-6-{[2-(1H-imidazol-4-yl)-ethylimino]-methyl}-phenol [**L10**] which was reported by S. Boltina *et al*. [1].

The (^{1}H and ^{13}C NMR) showed all the protons and carbons from respective ligands at different chemical shifts. The DEPT-135 showed two negative peaks for all ligands from $-CH_2-CH_2-$ linker and only **L3** had three negative peaks due to the ethoxy substituent on the phenyl ring. In addition the positive peaks from CH_3 were observed on the upfield and CH peaks were observed from the downfield.

The coupling of nitrogen and proton showed by ^{15}N NMR revealed the imine nitrogen and hydrogen N=CH coupling by J^2 and CH_2-CH_2-N by J^3 for all ligands. Only ligand **L6** showed all three nitrogen signals and it is *meta* to the phenolic (OH). Ligand (**L7**) with methoxy substituent also has same position substituent as **L6** however it showed one nitrogen signal, which suggest that they have different structural arrangement despite having substituents on same position. The ligand (**L8)** all $-CH_2-CH_2-$ were able to couple with the imine group by both J^2 and J^3 this also suggest that the structural arrangement of **L8** is different to other relative ligands with same position substituent. **L9** has substituent on same position as **L8** but they have different structural arrangement based on their ^{15}N coupling.

3.2.2 FT-IR studies

The FT-IR studies were performed to ascertain the formation of the imine (N=C) characteristic bands after condensation reactions during the formation of Schiff bases. The imine N=C for ligands was measured as follows: **L1** (1633 cm^{-1}), **L2** (1591 cm^{-1}), **L3** (1638 cm^{-1}), **L4** (1636 cm^{-1}) **L5** (1616 cm^{-1}), **L6** (1640 cm^{-1}), **L7** (1613 cm^{-1}), **L8** (1613 cm^{-1}), **L9** (1636 cm^{-1}), **L10** (1633 cm^{-1}). The imine group bands ranges from 1591 cm^{-1} to 1640 cm^{-1} for the ligands which are consistent with the reported literature [2; 3]. There is also imine (N=C) bands from the imidazole group which appears next to the newly formed imine group which ranges from 1470 cm^{-1} to 1580 cm^{-1} which is also consistent with the reported literature [4]. There is an intra-molecular hydrogen bond between hydroxyl group and the imine group (OH---N=C) which ranges from 2804 cm^{-1} to 2846 cm^{-1} [3]. The (OH) bands ranged from 3416 cm^{-1} to 3520 cm^{-1}. The (NH) bands observed ranges from 3273 cm^{-1} to 3399 cm^{-1} from the imidazole group which is consistent with the reported literature [3]. The (C-H) bands ranges from 2905 cm^{-1} to 2995 cm^{-1} from the phenol ring and imidazole conjugations. The **Figure 3.16** represents a typical FT-IR spectrum of Schiff base ligand. The observed bands from the FT-IR are in support to the functional groups present on the synthesised ligands shown in Appendices **Figure 41**.

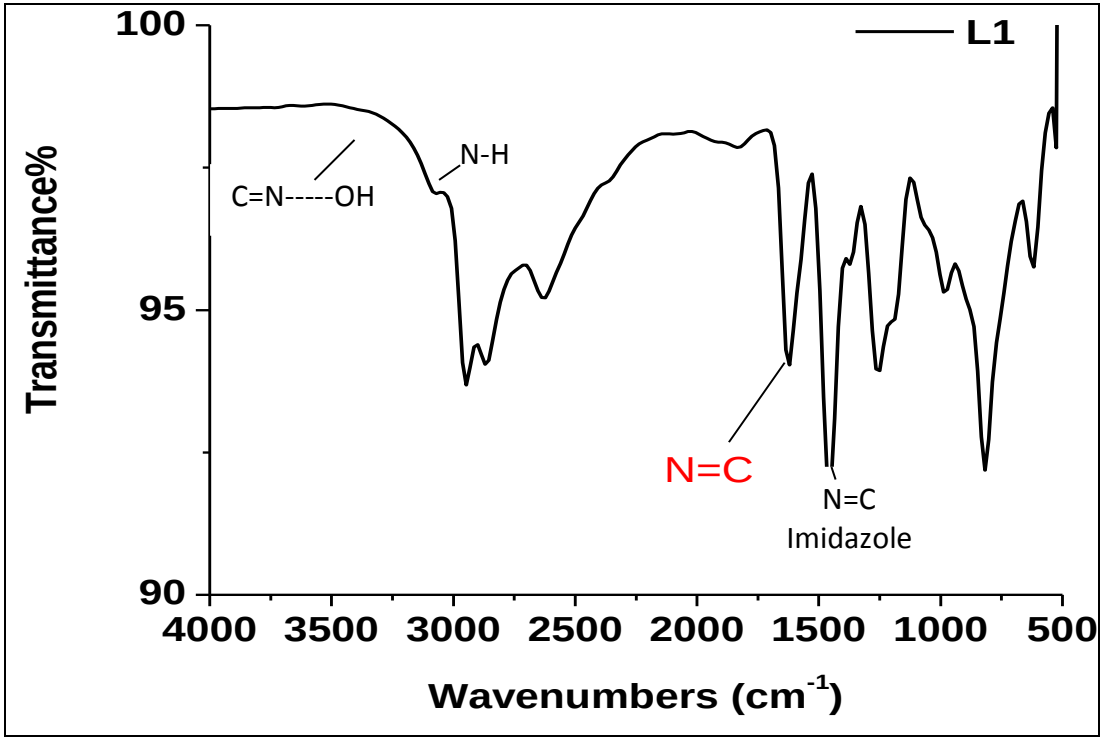

Figure 3.16: FT-IR spectrum of 2, 4-di-tert-butyl-6-{[2-(1H-imidazol-4-yl)-ethylimino]-methyl}-phenol [**L1**]

3.2.3 UV-vis studies

The electronic UV-vis of Schiff bases were performed using different organic solvents such as acetonitrile, dimethyl sulfoxide, ethanol and methanol showing absorption ranging from 190 nm - 1200 nm. The Schiff base ligands comprise of phenyl ring, imine moiety and the imidazole ring. The absorption of Schiff base ligands was found to absorb at three different wavelengths with various absorption maxima. The shoulder absorption between 270 nm - 285 nm is due to the π electrons (π-π^* transitions) of the imidazole ring [5], the absorption between 290 nm - 330 nm is due to the π electrons (π-π^* transitions) on the benzene ring and the absorption between 390 nm - 430 nm is due to the imine (N=C) group non-bonding electrons lone pair (n-π^*) [6, 7]. The longer wavelength for the non-bonding lone pair of electrons is due to the intramolecular hydrogen bonding between the imine nitrogen and the phenolic OH group (N---HO) [8]. These results in decrease of energy and favors the red shift because of increase in wavelength. Different solvents were used to study the solvent effect; same functional group on the ligands showed different behavior in different solvents. The shape, intensity and maximum absorption wavelength of an absorbance band depend on the solvent polarity [9]. Different solvents polarities results in solvatochromic behavior which is the shift of absorption wavelength [9]. The polar protic solvents used were methanol and ethanol almost showed similar shape trend with difference in maximum absorption wavelength. Aprotic polar solvents used were dimethylsulfoxide and acetonitrile showed similar shape trend of absorption with different maximum absorption wavelength. Protic solvents used and aprotic polar solvents used showed difference in shape trends, maximum absorption wavelength and intensity. Methanol as solvent in **Figure 3.17** and **Table 3.2** and ethanol as solvent in **Figure 3.18** and **Table 3.3** both showed three absorption maxima clearly and with good proportional intensity as compared to acetonitrile at **Figure 3.20** and **Table 3.5** and dimethylsulfoxide **Figure 3.19** and **Table 3.4**. The π electrons (π-π^* transitions) on the benzene ring showed the highest absorption maxima as compared to imine and imidazole groups for all solvents used. In acetonitrile the non-bonding lone pair of electrons absorption maxima was small in-terms of intensity relative to the imidazole and the benzene group absorptions as

demonstrated on **Figure 3:20** and **Table 3.5**. The absorption maxima in dimethylsulfoxide solvent showed less intensity for imidazole group and non-bonding lone pair of electrons from the imine group and showed high intensity for benzene **Figure 3.19** and **Table 3.4**. Six ligands out of ten possible ligands were soluble in acetonitrile. Ligands such as **L2**, **L3** and **L7** with heteroatoms substituents on the phenyl ring were not soluble in acetonitrile and **L4** which has no substituent on the phenyl ring was also insoluble. Other solvents such as dichloromethane, acetone, diethyl ether, hexane and tetrahydrofuran were found to only dissolve 40% percent or less of all ligands which was not enough for solvent comparison studies.

Table 3.2 UV-vis absorption band of ligands in methanol

Ligands	Absorption maxima (nm) (π-π^* transition) imidazole ring	Absorption maxima (nm) (π-π^* transition) benzene ring	Absorption maxima (nm) (n-π^* transition) imine (N=C) group
L1	281	327	425
L2	277	300	400
L3	276	300	415
L4	280	319	410
L5	279	325	415
L6	280	320	406
L7	280	319	390
L8	277	325	420
L9	279	318	415
L10	282	320	415

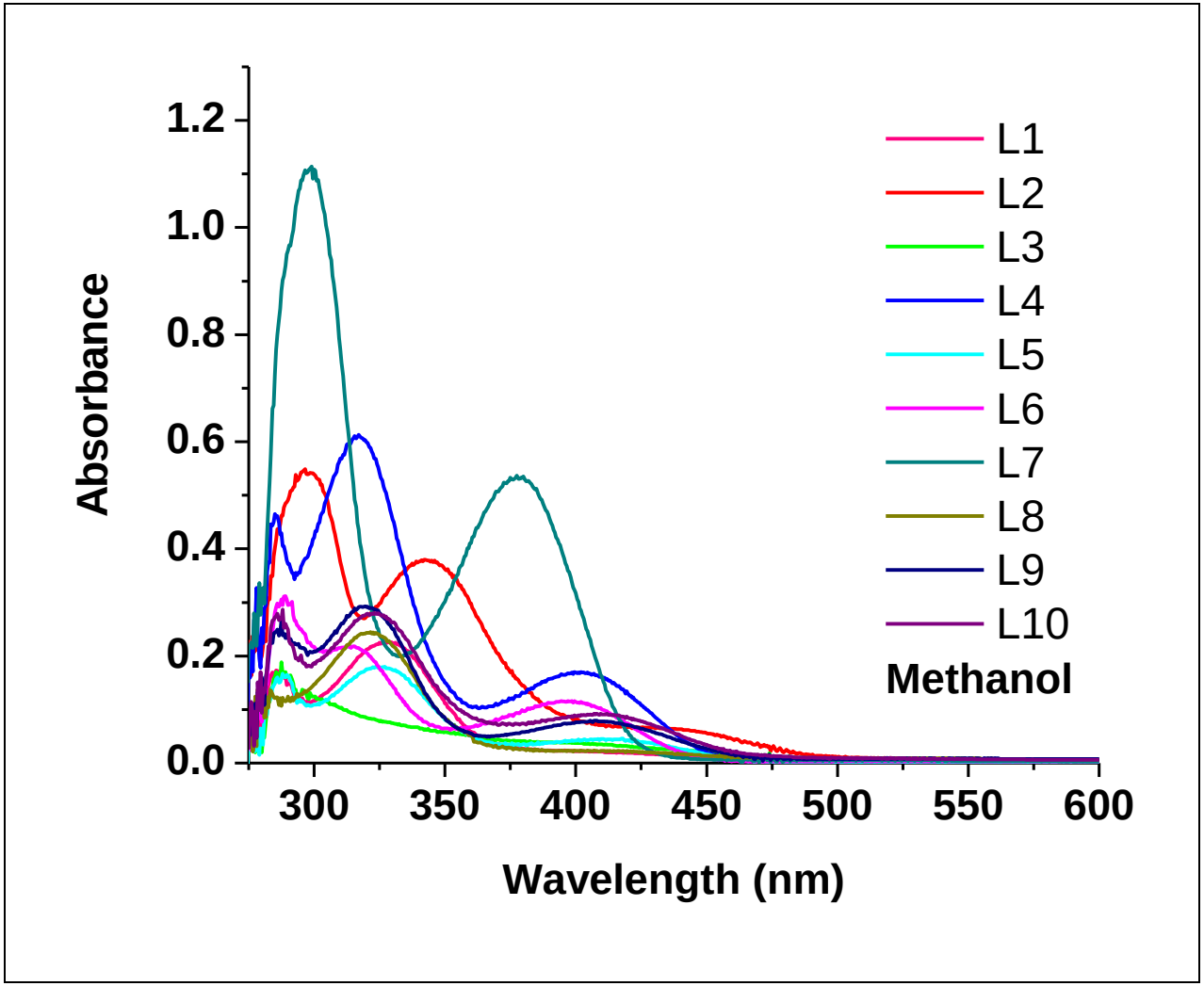

Figure 3.17: Electronic absorption spectra of ligands in methanol

Table 3.3 UV-vis absorption band of ligands in ethanol

Ligands	Absorption maxima (nm) (π-π^* transition) imidazole ring	Absorption maxima (nm) (π-π^* transition) benzene ring	Absorption maxima (nm) (n-π^* transition) imine (N=C) group
L1	280	329	400
L2	285	300	404
L3	284	300	417
L4	285	325	405
L5	285	326	410
L6	285	331	400
L7	277	325	385
L8	283	300	405
L9	284	329	407
L10	281	331	412

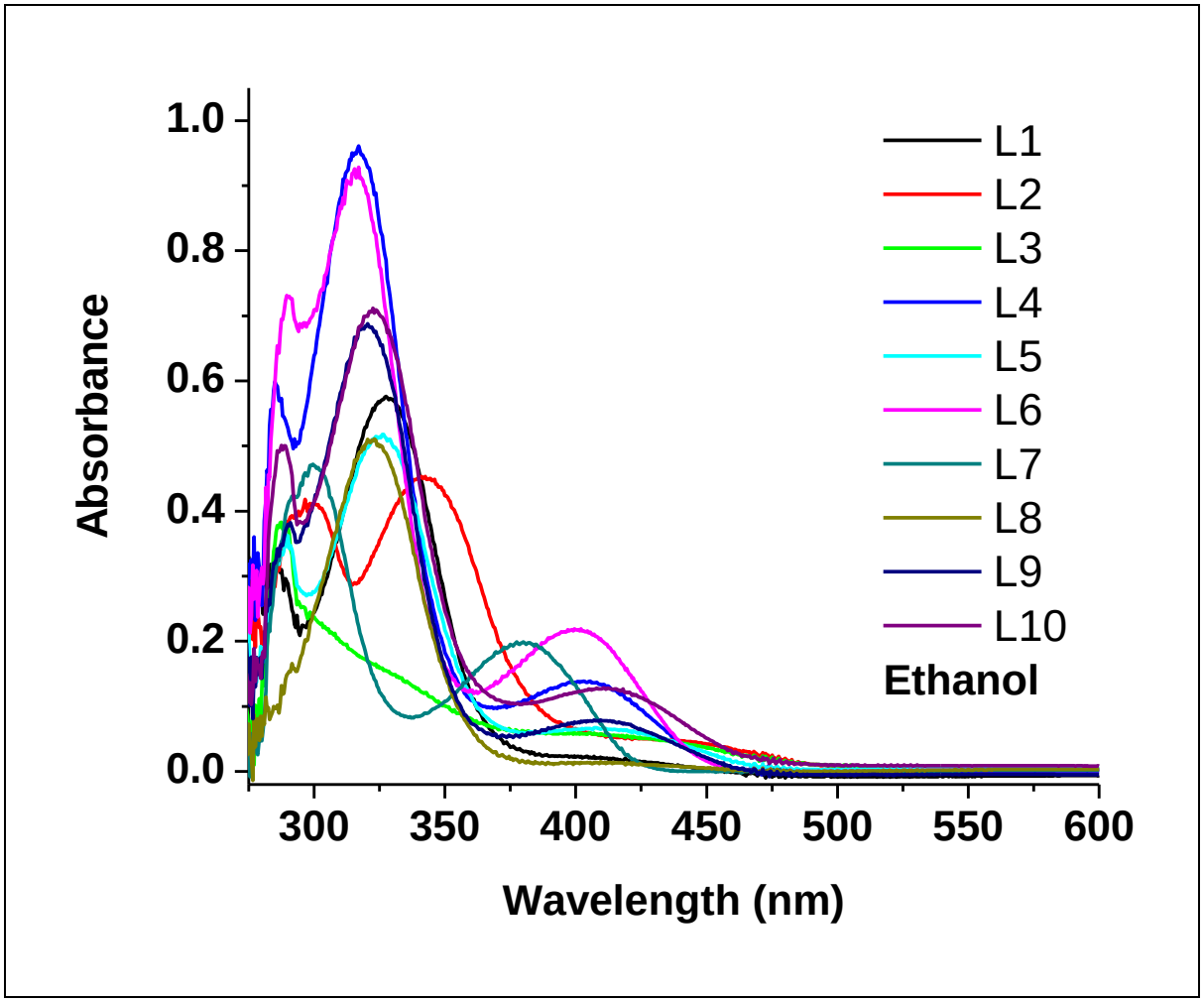

Figure 3.18: Electronic absorption spectra of ligands in ethanol

Table 3.4 UV-vis absorption band of ligands in dimethylsulfoxide

Ligands	Absorption maxima (nm) (π-π^* transition) imidazole ring	Absorption maxima (nm) (π-π^* transition) benzene ring	Absorption maxima (nm) (n-π^* transition) imine (N=C) group
L1	280	315	405
L2	285	310	400
L3	280	305	365
L4	285	313	390
L5	280	317	395
L6	280	311	390
L7	285	302	375
L8	280	312	410
L9	280	316	405
L10	280	315	412

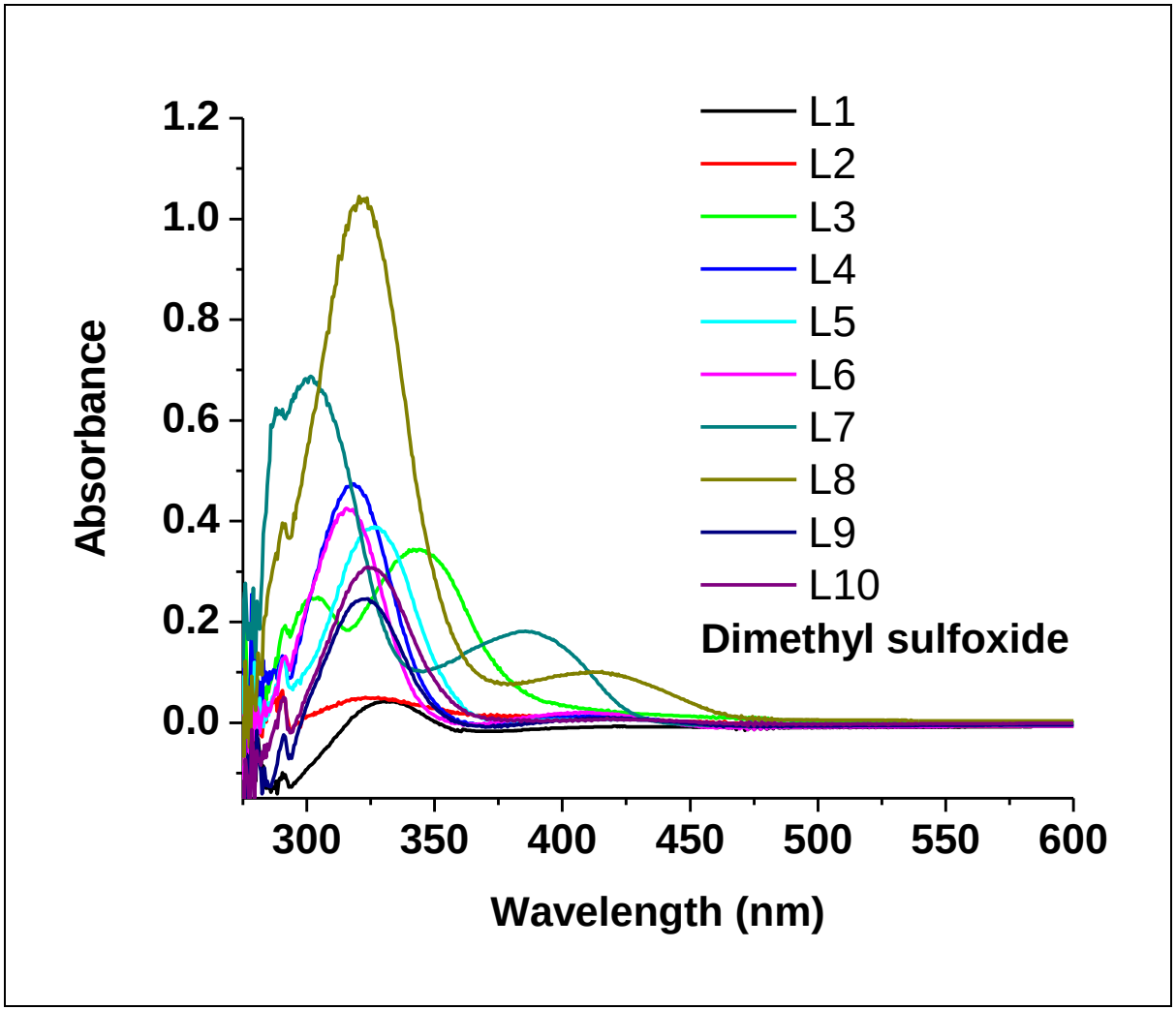

Figure 3.19: Electronic absorption spectra of ligands in dimethylsulfoxide

Table 3.5 UV-vis absorption band of ligands in acetonitrile

Ligands	Absorption maxima (nm) (π-π^* transition) imidazole ring	Absorption maxima (nm) (π-π^* transition) benzene ring	Absorption maxima (nm) (n-π^* transition) imine (N=C) group
L1	285	319	405
L5	285	312	413
L6	280	311	410
L8	285	310	415
L9	281	323	400
L10	284	325	411

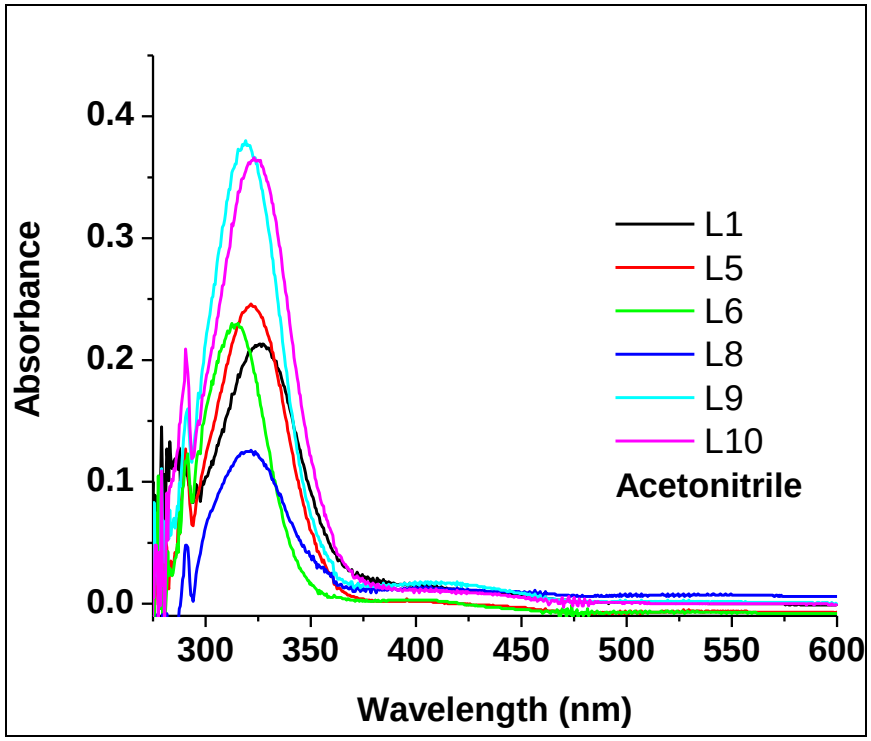

Figure 3.20: Electronic absorption spectra of ligands in acetonitrile

3.3 Synthesis and properties of complexes

Complexes (**C1** - **C19**) were all prepared by the procedure illustrated in **Scheme 2.2** and described in **Table 3.6** with a prepared Schiff base and appropriate metal halides to give Schiff base complexes [1]. All complexes were soluble in ethanol, dimethylsulfoxide and methanol. The complexes **C1, C8, C10** and **C17** were also soluble in dichloromethane. Complexes **C2, C3, C4, C5, C6, C7, C9, C11, C12, C13, C14, C15, C16, C18 and C19** showed precipitation in dichloromethane. The insolubility in dichloromethane was due lack of substituent on the phenyl ring in **C4** and **C13**, complexes containing heteroatoms as substituents on the phenyl ring were also not soluble in dichloromethane **C2**, **C3**, **C7**, **C11**, **C12**, **C16** and complexes containing methyl substituents on the phenyl ring **C5**, **C6**, **C9**, **C14**, **C15**, **C18** and **C19** were not soluble in dichloromethane. The complexes colours were dark as compared to ligands i.e. (**C1** - **C18**) has green and black colours, only **C19** has a bright yellow color. The melting points range for complexes was within the range of 120 °C to 227 °C. All complexes were in solid powder phase. The analytical data from the Elemental analysis showed the found and calculated. The presence of ethanol was observed in other complexes from the analytical data. The complexes did not form crystals. Schiff base complexes with different substituents were successfully synthesised in good yields. During the synthesis as demonstrated in **Table 3.6** there was no strong base to deprotonate the phenolic OH group. The reaction time which was twenty four hours played a key role to complete deprotonation of the acid phenolic OH group without strong bases such as triethylamine, diethylamine, butyl lithium, methyl lithium and sodium or potassium hydride. Complexes (**C1** - **C18**) could not be characterised by (^{1}H, ^{13}C and ^{15}N NMR) because of they are paramagnetic except **C19** which is diamagnetic was characterised by (^{1}H and ^{13}C NMR) and the spectrum showed little of ethanol solvent in **Figure 3.22**. Characterisation techniques such as UV-vis, FT-IR, Mass Spectroscopy and Elemental analysis were therefore used for analysis of complexes.

Table 3.6: Generalised procedure for preparation of imidazolyl-salicylaldemine Schiff base complex derivatives

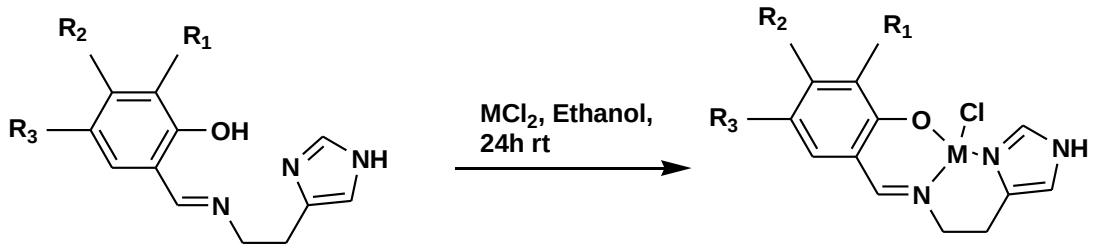

Complexes	Metals	R_1	R_2	R_3
C1	Mn	Tertiary butyl	Hydrogen	Tertiary butyl
C2	Mn	Hydrogen	Hydrogen	Methoxy
C3	Mn	Ethoxy	Hydrogen	Hydrogen
C4	Mn	Hydrogen	Hydrogen	Hydrogen
C5	Mn	Hydrogen	Hydrogen	Methyl
C6	Mn	Hydrogen	Methyl	Hydrogen
C7	Mn	Hydrogen	Methoxy	Hydrogen
C8	Mn	Tertiary butyl	Hydrogen	Hydrogen
C9	Mn	Methyl	Hydrogen	Hydrogen
C10	Cu	Tertiary butyl	Hydrogen	Tertiary butyl
C11	Cu	Hydrogen	Hydrogen	Methoxy
C12	Cu	Ethoxy	Hydrogen	Hydrogen
C13	Cu	Hydrogen	Hydrogen	Hydrogen
C14	Cu	Hydrogen	Hydrogen	Methyl
C15	Cu	Hydrogen	Methyl	Hydrogen
C16	Cu	Hydrogen	Methoxy	Hydrogen
C17	Cu	Tertiary butyl	Hydrogen	Hydrogen
C18	Cu	Methyl	Hydrogen	Hydrogen
C19	Zn	Methyl	Hydrogen	Hydrogen

3.4 Characterisation of complexes

3.4.1 NMR studies

^{1}H NMR spectrum of **C19** in **Figure 3.22** shows a significant chemical shift compared to its corresponding ligand **L9** before coordinating to the zinc metal centre. The -CH_2-CH_2- protons on position **8** closer to the imine nitrogen shifted from 3.88 ppm to 3.83 ppm and the protons on position **9** were not affected. There is also a significant shift on the downfield observed from the imidazolyl proton at position **12** which shifted from 7.58 ppm to 7.99 ppm and the imine proton shifted from 8.25 ppm to 8.29 ppm. These chemical shift results support zinc chloride coordinated to the imine nitrogen and the imidazolyl nitrogen.

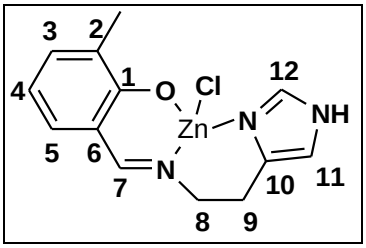

Figure 3.21: 2-methyl-6-{[2-(1H-imidazol-4-yl)-ethylimino]-methyl}-phenol Zn(II) chloride [**C19**]

The ^{1}H NMR spectrum of **C19** in **Figure 3.22** below shows two triplets appearing at 3.02 ppm and 3.83 ppm assigned to protons **9** and **8** respectively from -CH_2-CH_2- linker each integrating for two protons with coupling constant of (J = 6.4 Hz). A singlet from the phenyl substituent of methyl appearing at 2.17 ppm integrating for three protons, two singlets from the imidazole ring appearing at 6.57 ppm and 7.99 ppm assigned to protons **11** and **12** each integrating for one proton, two doublets from the phenyl ring appearing at 7.13 ppm with coupling constant (J = 7.2 Hz) and 7.14 ppm with coupling constant (J = 8.0 Hz) assigned to protons **3** and **5** each integrating for one proton , apparent triplet appearing at 6.72 ppm assigned to proton **4** integrating for one proton with coupling constant (J = 7.2 Hz) and a singlet appearing at 8.29 ppm assigned to

proton **7** integrating for one proton from the imine group. ^{13}C NMR in **Figure 3.23** shows the imine carbon at 169.82 ppm, phenolic OH at 169.82 ppm, phenyl ring (131.90 ppm - 138.19 ppm) imidazole (119.85 ppm - 120.14 ppm), $-CH_2-CH_2-$ (26.95 ppm and 57.22 ppm) and methyl carbon at (13.92 ppm). The molecular mass calculated was 329.12 and the mass spectrum found from HRMS $[M-Cl]^+$ 293.0425 which confirms fragmentation.

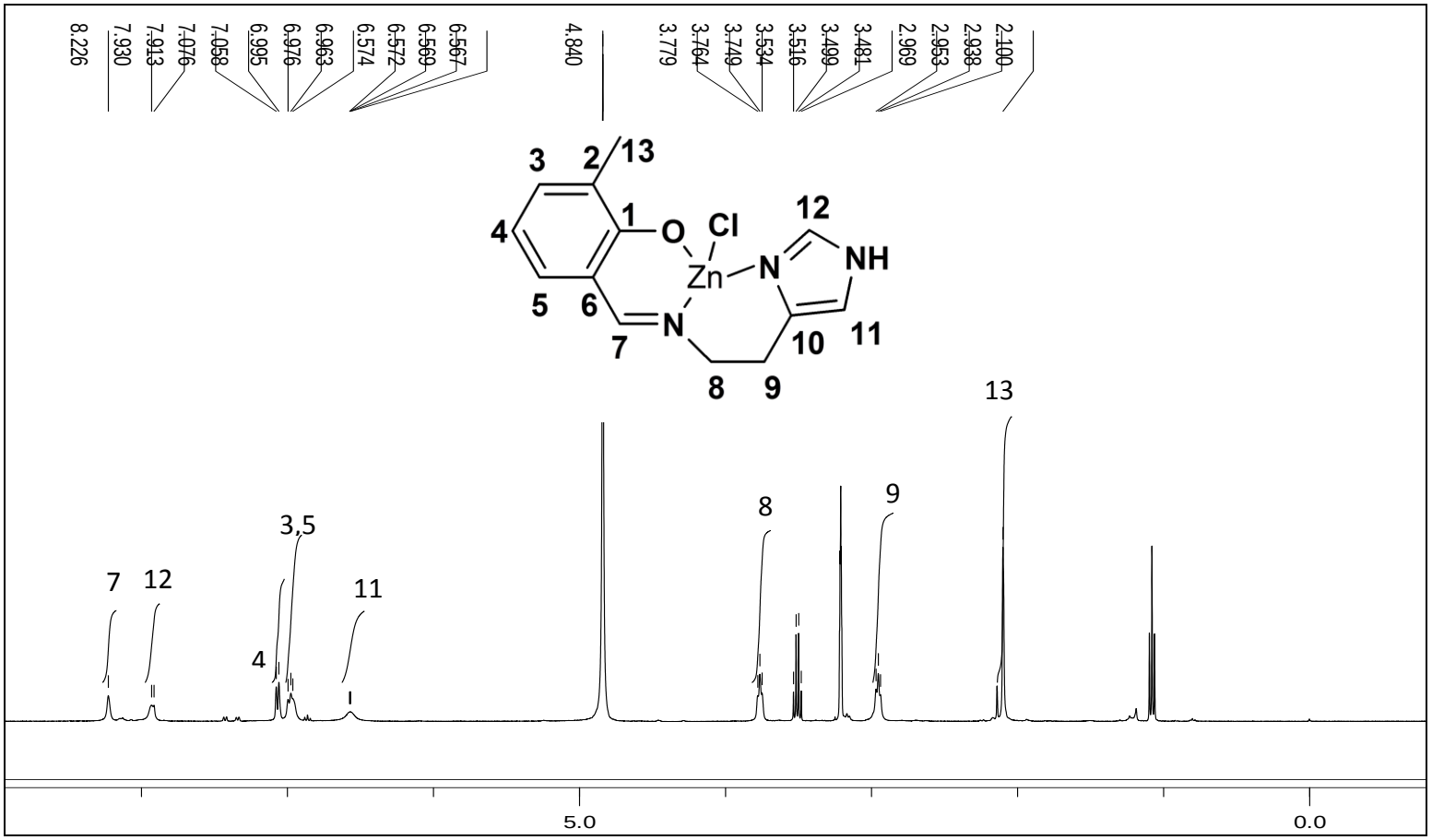

Figure 3.22: ^{1}H NMR of 2-methyl-6-{[2-(1H-imidazol-4-yl)-ethylimino]-methyl}-phenol Zn(II) chloride [**C19**]

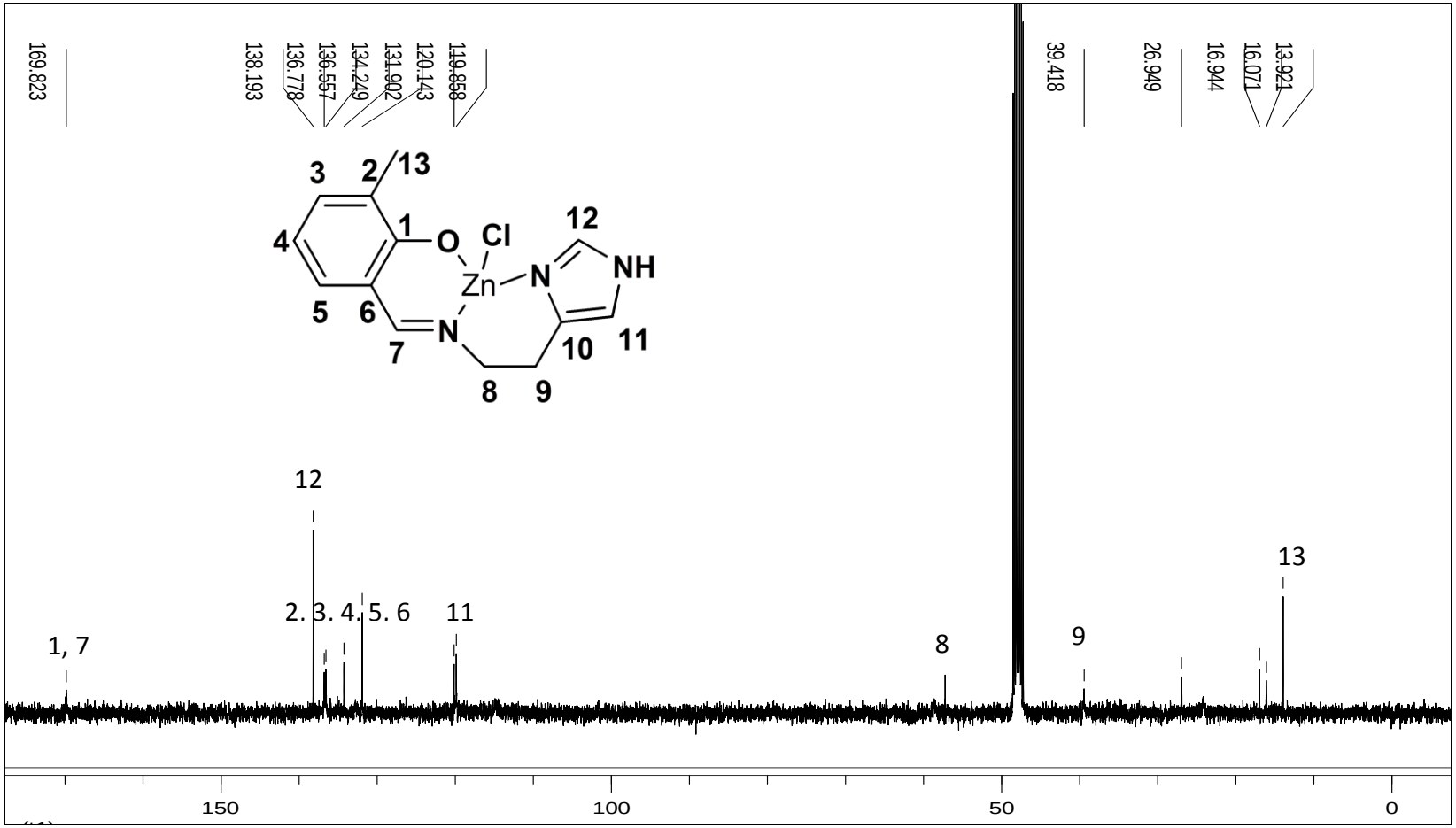

Figure 3.23: ^{13}C NMR of 2-methyl-6-{[2-(1H-imidazol-4-yl)-ethylimino]-methyl}-phenol Zn (II) chloride [**C19**]

The Mass spectroscopy of paramagnetic complexes was recorded to confirm the synthesised complexes. Positive electrospray ionization (ESI) mass spectroscopy data were collected:

The spectra of **C1, C4, C5, C6, C8, C9, C12** and **C17** gave peaks corresponding to the molecular ion of the complexes as shown on **Table 3.7.** Other complexes showed $[M\text{-}Cl]^+$, $[M\text{-}H]^+$, $[M\text{-}OCH_3Cl]^+$ and $[M\text{-}CH_2CH_3]^+$ ion fragments as shown on **Table 3.7**. Manganese complexes mostly showed corresponding peaks for the molecular ion of complexes as compared to copper and zinc complexes which showed mass fragmentation of chlorine loss $[M\text{-}Cl]^+$. Complexes which show a peak with a value that correspond to the molecular ion of the complex shown on **Table 3.7** suggest mono-chelation and tri-dentate coordination by the ligands through two donor nitrogen's, phenolic oxygen and chlorine. The results from mass spectra showing chlorine presence and chlorine loss to the molecular ion of the complexes during fragmentation confirms the presence of chlorine, tri-dentate ligand coordination, mono-chelation and helped in proposing of the complexes structures. The mass spectra of compounds are shown in the Appendices on **Figure 42 - Figure 46.**

Table 3.7: Positive ion mass spectroscopy data of complexes

Compound	Expected Molecular mass	Observed ion	m/z of observed ion
C1	416.84	$[M]^+$	416.1304
C2	334.66	$[M\text{-}OCH_3Cl]^+$	268.1067
C3	348.69	$[M\text{-}CH_2CH_3]^+$	232.0526
C4	304.62	$[M]^+$	304.3006
C5	318.66	$[M]^+$	318.0210
C6	318.66	$[M]^+$	318.0213
C7	334.66	$[M]^+$	334.1291
C8	360.74	$[M]^+$	360.0680
C9	318.66	$[M]^+$	318.0214
C10	425.99	$[M\text{-}Cl]^+$	391.1510
C11	343.27	$[M\text{-}Cl]^+$	307.0385
C12	357.30	$[M]^+$	357.0133
C13	313.99	$[M\text{-}Cl]^+$	277.0282
C14	327.27	$[M\text{-}Cl]^+$	291.0431
C15	327.27	$[M\text{-}Cl]^+$	291.0432
C16	343.27	$[M\text{-}Cl]^+$	307.8201
C17	369.35	$[M]^+$	369.0491
C18	327.27	$[M\text{-}Cl]^+$	291.0434

3.4.2 FT-IR studies

The FT-IR was used to compare the imine (N=C) group stretching frequencies of complexes with their respective ligands. The following were observed: **C1** (1613 cm^{-1}), **C2** (1613 cm^{-1}), **C3** (1613 cm^{-1}), **C4** (1591 cm^{-1}), **C5** (1610 cm^{-1}), **C6** (1610 cm^{-1}),**C7** (1607 cm^{-1}), **C8** (1653 cm^{-1}), **C9** (1591 cm^{-1}) **C10** (1635 cm^{-1}), **C11** (1607cm^{-1}), **C12** (1626 cm^{-1}), **C13** (1625 cm^{-1}), **C14** (1624 cm^{-1}), **C15** (1633 cm^{-1}), **C16** (1622 cm^{-1}), **C17** (1623 cm^{-1}), **C18** (1617cm^{-1}). The ligands to complex frequencies showed a shift difference of 20, 22, 25, 45, 6, 30, 6, 40, 45, 2, 16, 13, 11, 8, 7, 9, 10 and 19 cm^{-1} respectively. The (OH) bands is not appearing due to the coordination of hydroxyl hydrogen to the metal center of the complexes. **Figure**: **3.24** shows representative FT-IR spectrum of Schiff base complexes of **C2**. The complexes are ranging from (1591 cm^{-1} – 1653 cm^{-1}), the imine (N=C) stretching frequency of ligands increases or decreases by a range of (2 cm^{-1} – 45 cm^{-1}) after coordination to the metal center. There is also imine (N=C) bands from the imidazole group which appears imine group which ranges from 1480 cm^{-1} to 1580 cm^{-1} which is also consistent with the reported literature [4]. The (NH) bands observed ranges from 3160 cm^{-1} to 3399 cm^{-1} from the imidazole group which are consistence with the reported literature [3]. The (C-H) bands ranges from 2995 cm^{-1} to 2905 cm^{-1} from the phenol ring and imidazole conjugations. The observed bands from the FT-IR are in support to the functional groups present on the synthesised Schiff base complexes.

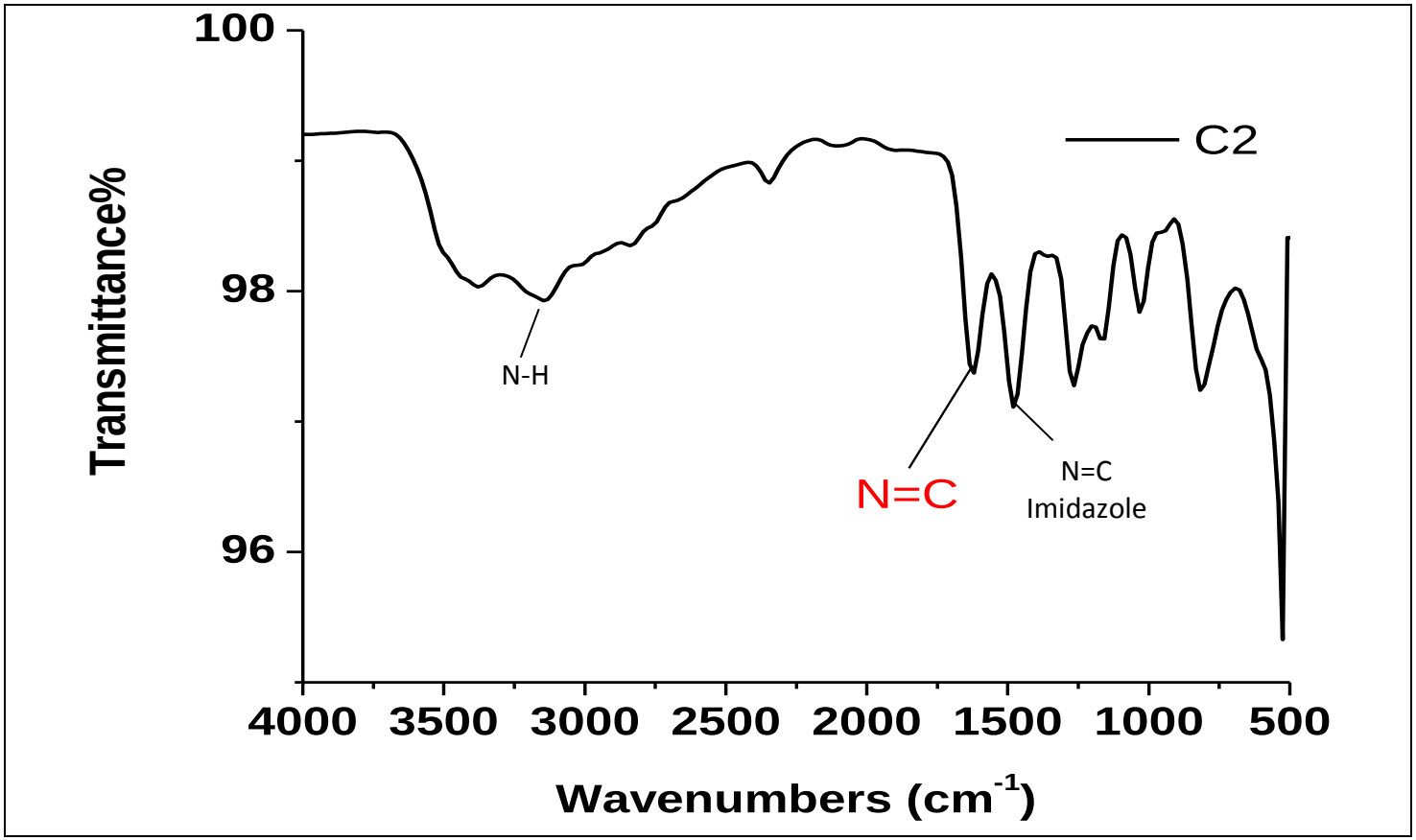

Figure 3.24: FT-IR spectrum of 4-methoxy-6-{[2-(1H-imidazol-4-yl)-ethylimino]-methyl}-phenol Mn(II) chloride [**C2**]

3.4.3 UV-Vis studies

The electronic UV-vis measurement of Schiff base complexes were performed using ethanol and methanol with absorption range of 190 nm - 1200 nm. Other solvents such as dichloromethane, acetonitrile and acetone were only found to partially dissolve complexes while dimethylsulfoxide was not an option because of its possible coordination abilities. Both ethanol and methanol solvents showed two absorption maxima for benzene and the imidazole groups. The imidazole absorption has high intensity compared to the benzene ring. There was significant red shift change observed for complexes compared to the ligands due to metal halide coordination. The disappearance of the non-bonding lone pairs which appeared for all the ligands suggests coordination of metal halides to ligands. The complexes are paramagnetic and are expected to have low spin hence there are no new absorptions excitement from the d electrons and it showed little of red shift for imidazole π-π^* electrons and huge red shift for benzene π-π^* electrons [10]. The absorptions of free ligands were all red-shifted after being coordinated to the metal center with a significant shift from 5 nm - 90 nm refer **Figure 3.29** and **Figure 3.31** [11; 12]. **Table 3.8** and **Figure**: **3.25** show manganese Schiff base complexes in methanol and **Table 3.9** and **Figure**: **3.26** show manganese Schiff base complexes in ethanol. Copper Schiff base complexes are shown in **Table 3.10** and **Figure 3.27** in methanol and **Table 3.11** and **Figure**: **3.28** in ethanol. The imidazole π-π^* electrons and benzene π-π^* electrons transitions of copper Schiff base complexes absorption maxima are relatively broad. The imidazole π-π^* electrons transition absorption maxima are broader compared to benzene π-π^* electrons transitions in manganese Schiff base complexes. Polar protic solvents were used for complexes due to dimethylsulfoxide's ability to coordinate and acetonitrile inability to dissolve the complexes. Methanol and ethanol almost showed similar shape trend with difference in maximum absorption wavelength. Different solvents polarities results in solvatochromic behavior which is the shift of absorption wavelength [9]. The polar protic solvents used were methanol and ethanol almost showed similar shape trend with difference in maximum absorption wavelength which was observed also in ligands.

Table 3.8: UV-vis absorption band of manganese complexes in methanol

Complexes methanol	Absorption maxima (nm) (π-π^* transition) imidazole ring	Absorption maxima (nm) (n-π^* transition) imine (N=C) group	Absorption maxima (nm) (π-π^* transition) benzene ring
C1	280	-	400
C2	295	-	390
C3	290	-	375
C4	293	-	380
C5	290	-	375
C6	290	-	380
C7	280	-	350
C8	290	-	375
C9	300	-	375

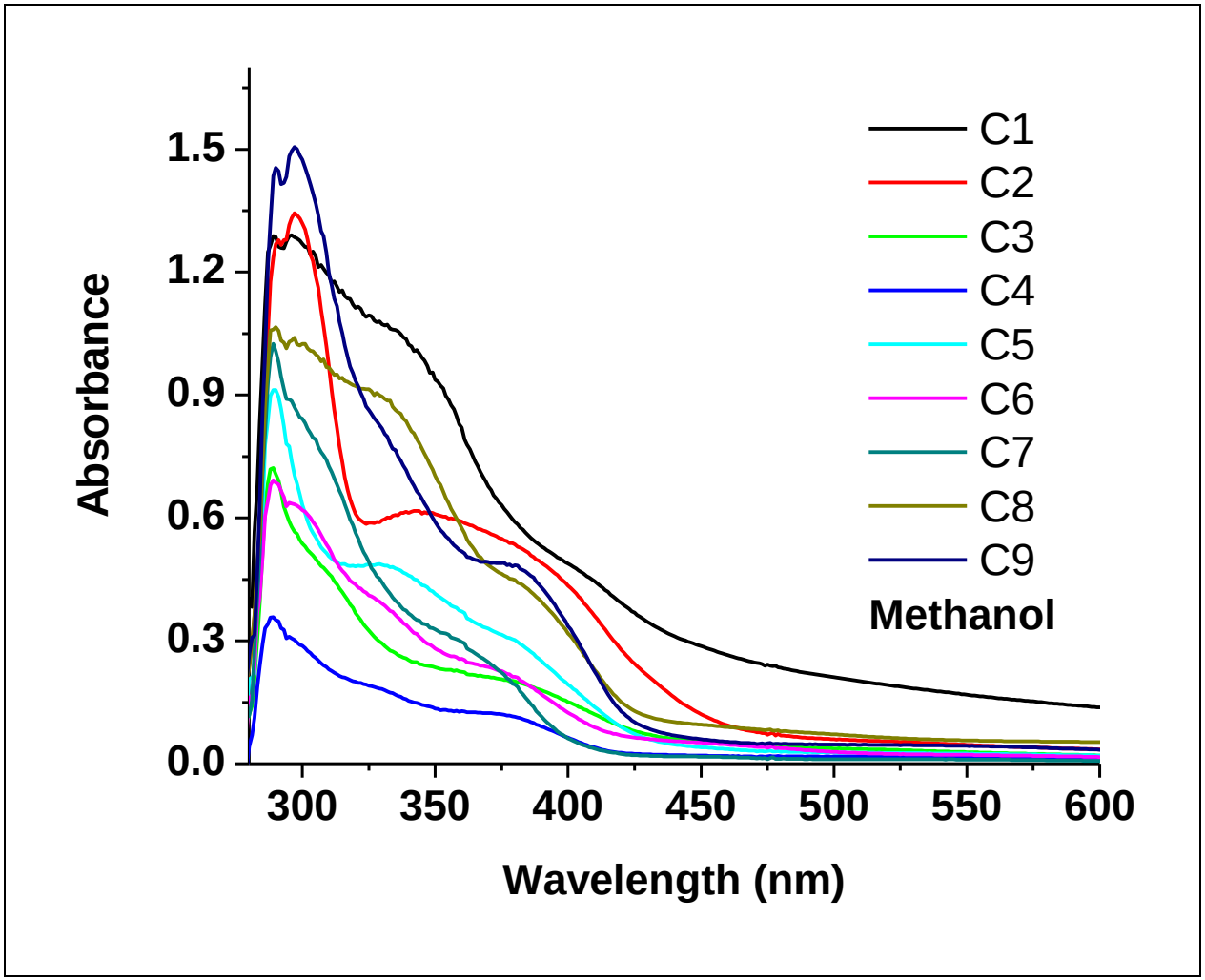

Figure 3.25: Electronic absorption spectra of manganese complexes in methanol

Table 3.9: UV-vis absorption band of manganese complexes in ethanol

Complexes Ethanol	Absorption maxima (nm) (π-π^* transition) imidazole ring	Absorption maxima (nm) (n-π^* transition) imine (N=C) group	Absorption maxima (nm) (π-π^* transition) benzene ring
C1	280	-	400
C2	285	-	395
C3	290	-	390
C4	295	-	385
C5	285	-	395
C6	310	-	385
C7	300	-	375
C8	295	-	395
C9	300	-	390

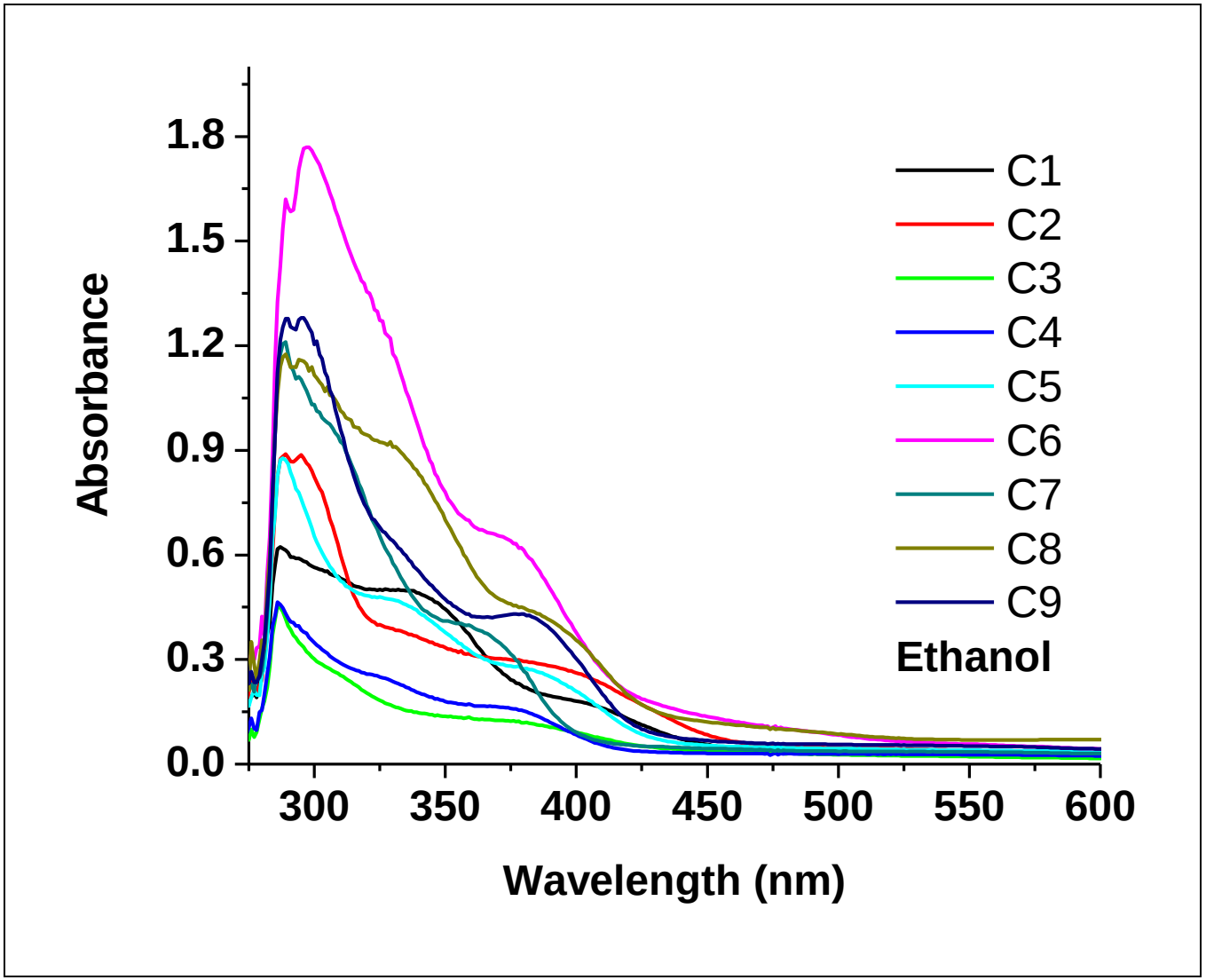

Figure 3.26: Electronic absorption spectra of manganese complexes in ethanol

Table 3.10: UV-vis absorption band of copper complexes in methanol

Complexes Methanol	Absorption maxima (nm) (π-π^* transition) imidazole ring	Absorption maxima (nm) (n-π^* transition) imine (N=C) group	Absorption maxima (nm) (π-π^* transition) benzene ring
C10	300	-	400
C11	300	-	400
C12	280	-	375
C13	290	-	390
C14	290	-	390
C15	300	-	395
C16	300	-	400
C17	300	-	390
C18	300	-	395

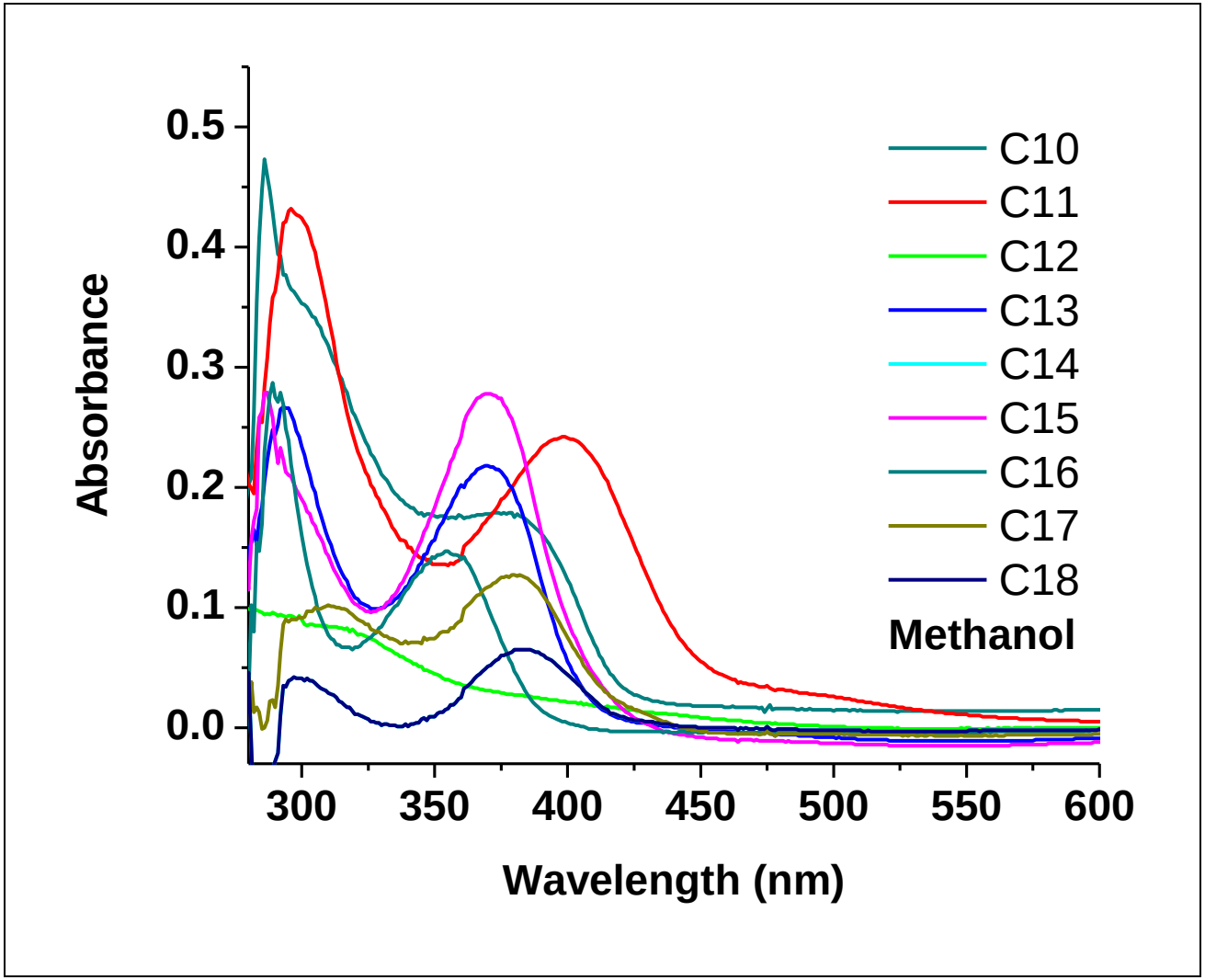

Figure 3.27: Electronic absorption spectra of copper complexes in methanol

Table 3.11: UV-vis absorption band of copper complexes in ethanol

Complexes Ethanol	Absorption maxima (nm) (π-π^* transition) imidazole ring	Absorption maxima (nm) (n-π^* transition) imine (N=C) group	Absorption maxima (nm) (π-π^* transition) benzene ring
C10	279	-	395
C11	300	-	400
C12	290	-	375
C13	295	-	385
C14	290	-	380
C15	305	-	390
C16	300	-	375
C17	280	-	375
C18	305	-	390

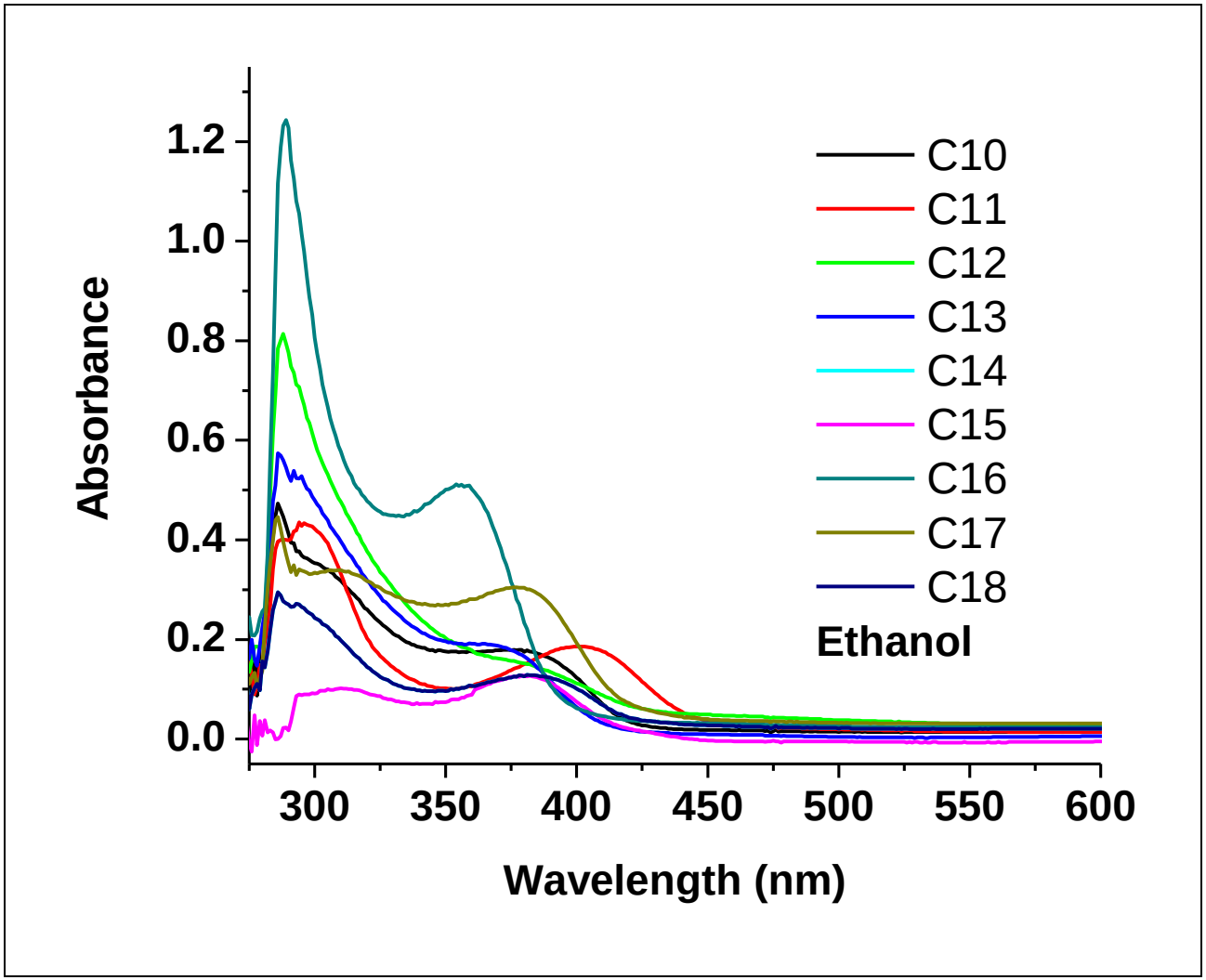

Figure 3.28: Electronic absorption spectra of copper complexes in ethanol

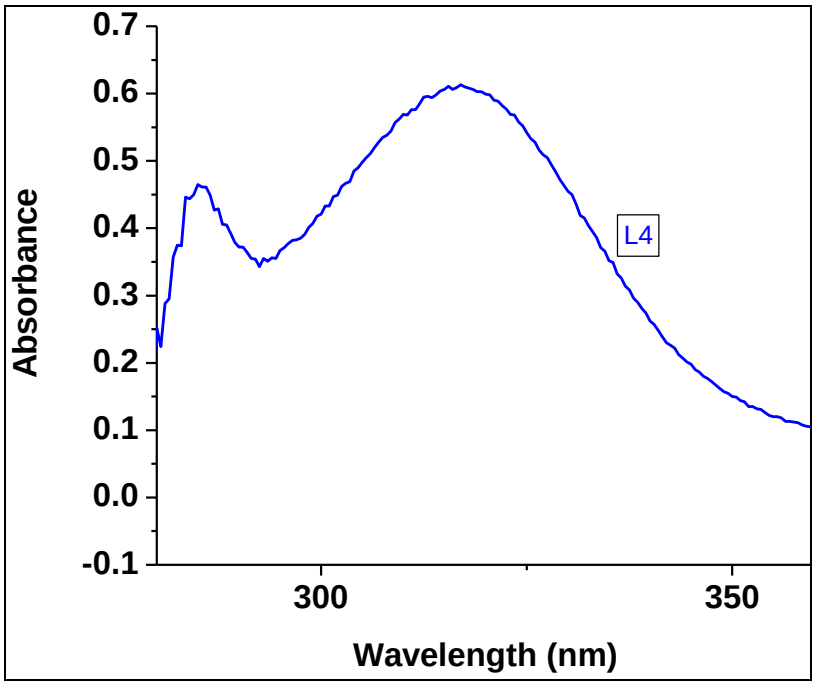

Figure 3.29: Electronic absorption spectra of **L4** showing blue shift in contrast to red shift before ligand coordination as demonstrated in **Figure 3.30**.

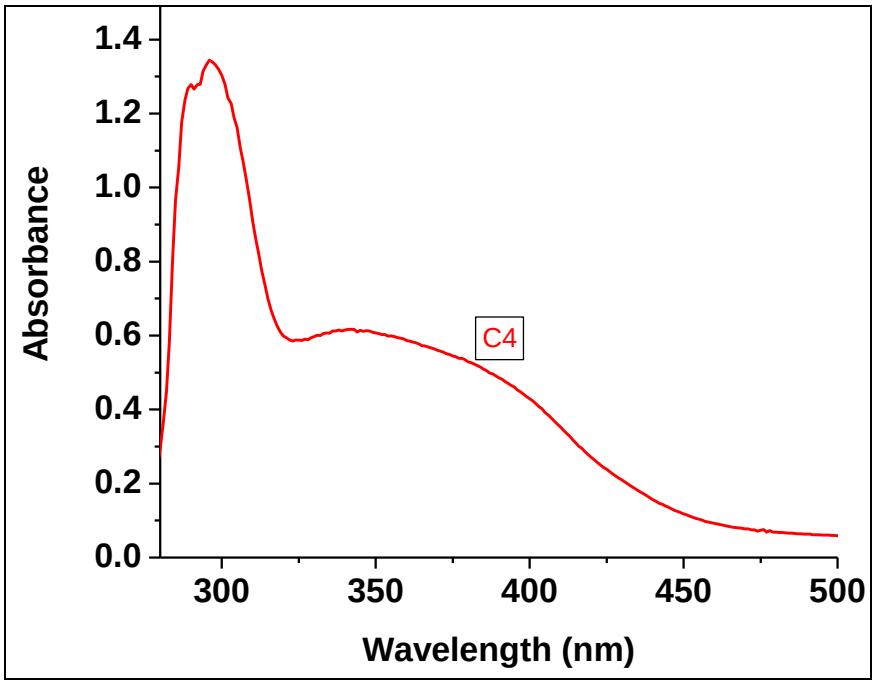

Figure 3.30: Electronic absorption spectra of **C4** showing red shift with respect to **Figure 3.29,** before ligand coordination.

3.5 Preparation of quinoxaline compound

The synthesis of 2-quinoxalinone was achieved by condensation of *o*-phenylenediamine and glyoxylic acid in methanol and glacial acetic acid as demonstrated in **Scheme 3.1**. [13], the reaction was continuously monitored by thin-layer chromatography (TLC) analysis for complete reaction. The reaction mixture was then filtered, washed with water and methanol to obtain a grey solid powder product which was recrystallised from DMF.

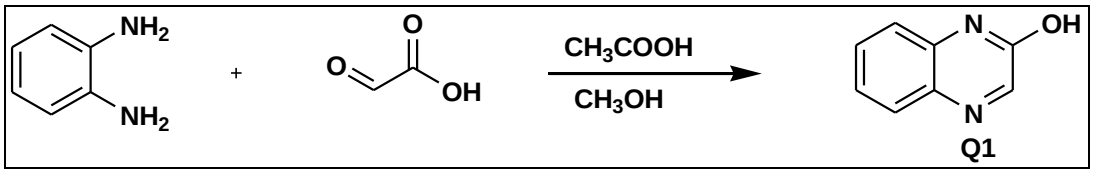

Scheme 3.1: Synthesis of 2-quinoxalinone

The compound 2-quinoxalinone was achieved as a grey solid powder material which was characterised using ^{1}H NMR and ^{13}C NMR in DMSO-d_6. The ^{1}H NMR showed a doublet appearing at 7.79 ppm with coupling constant (J = 8.4 Hz), apparent triplet appearing at 7.51 ppm with coupling constant (J = 7.2 Hz), a doublet appearing at 7.32 ppm with coupling constant (J = 7.6 Hz), a singlet appearing at 7.95 ppm, a singlet appearing at 8.19 ppm and an OH singlet at 12.45 ppm each integrating for one proton. The ^{13}C NMR showed eight peaks around the aromatic region ranging from 116.17 ppm to 155.38 ppm. The melting point was found to be ranging from (265 - 267 °C) and the result was consistence with the reported literature [13]. The percentage yield was found to be 81%.

3.6 Synthesis of 2-benzenesulfonylquinaxaline

The synthesis of 2-benzenesulfonylquinoxaline was prepared in line with the method reported by W. Nxumalo [13]. The synthesised 2-quinoxalinone was treated with benzenesulfonyl chloride in a dried dichloromethane as a solvent in the presence of 4-dimethylaminopyridine and triethylamine to obtain 2-benzensulfonylquinoxaline. The reaction mixture was monitored by TLC analysis for complete reaction. The reaction mixture was then quenched with saturated solution of sodium hydrogen carbonate, filtered and the combined organic layers were dried over Na_2SO_4, concentrated, purified by solvation of product using excess of EtOAc, filtered again and the filtrate was washed and crystallized with hexane to obtain 2-benzenesulfonyloxyquinoxaline a brown solid with a yield 96%. M.p (90 - 92 °C) and reported literature (91 °C).

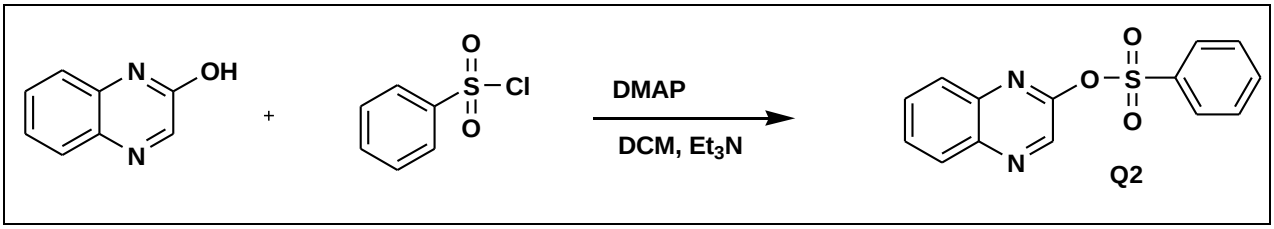

Scheme 3.2: Synthesis of 2-benzenesulfonylquinoxaline

The ^1H NMR analysis of 2-benzenesulfonylquinoxaline was recorded in ($CDCl_3$) chloroform solution, the spectrum showed multiplet of peaks appearing between 7.57 ppm - 7.61 ppm integrating for two protons, 7.68 ppm - 7.76 ppm integrating for three protons, 7.86 ppm - 8.10 ppm integrating for two protons, 8.14 ppm - 8.15 ppm integrating for two protons and the singlet peak appearing at 8.65 ppm from the pyrazine ring N=C-H group integrating for one proton. The ^{13}C NMR spectrum showed twelve carbons instead of expected fourteen carbons on the aromatic region which ranges from 128.84 ppm – 150.88 ppm. This suggests symmetry on the phenyl ring where a possible overlap match of two set of signals are probable.

3.7 Sonogashira cross coupling reaction of 2-benzenesulfonylquinaxalines

The preparation was done in line with method reported by W. Nxumalo [13]. The Sonogashira cross coupling reaction was applied using the following substrates 2-benzenesulfonylquinoxaline and ethynyltrimethylsilane. The incorporated benzenesulfonyl mimic halides normally used in Sonogashira coupling. The preparation involved ethynyltrimethylsilane, 2-benzenesulfonylquinoxaline, tetrakis(triphenylphosphine)palladium(0), triethylamine, copper iodide (I) and a dried tetrahydrofuran as a solvent. The reaction was monitored by TLC analysis for completion of reaction after which the crude material was purified by column chromatography to give a brown oily product as illustrated in **Scheme 3.3**.

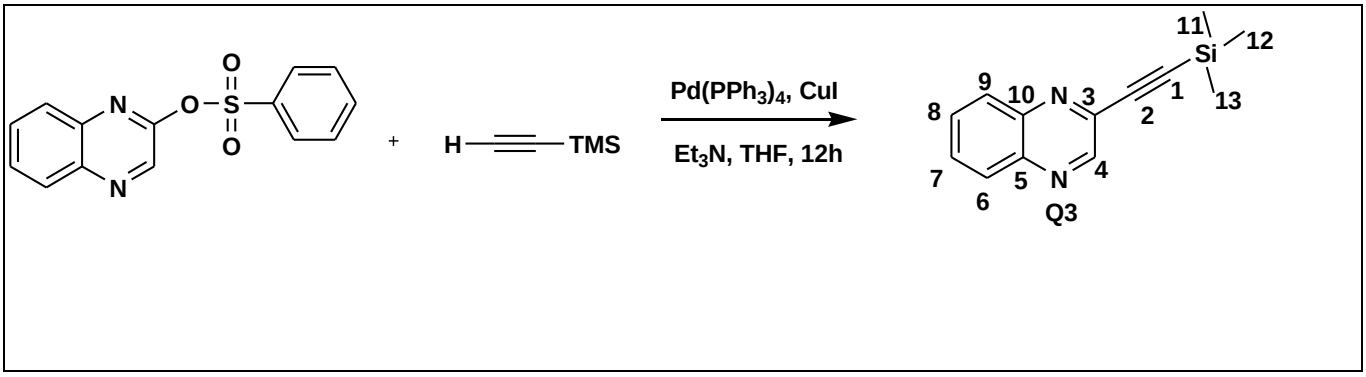

Scheme 3.3: The Sonogashira cross coupling on 2-benzesulfonylquinoxaline

The ^{1}H NMR spectrum showed a characteristic singlet peak appearing at 8.82 ppm integrating for one proton assigned to the pyrazine ring N=C-H, two multiplets appearing at 7.98 ppm - 8.01 ppm integrating for two protons and 7.68 ppm - 7.69 ppm integrating for two protons at the aromatic region. The singlet peak at upfield assigned for trimethylsilane group at 0.25 ppm integrating for nine protons in **Figure 3.31**. ^{13}C NMR showed eleven carbons instead of expected thirteen carbons and this was due to magnetic and chemical equivalences of methyl carbons from the trimethylsilane. The carbons were ranging from 0.00 ppm - 147.81 ppm. The three trimethylsilane carbons were found to be overlapping on **Figure 3.32**.

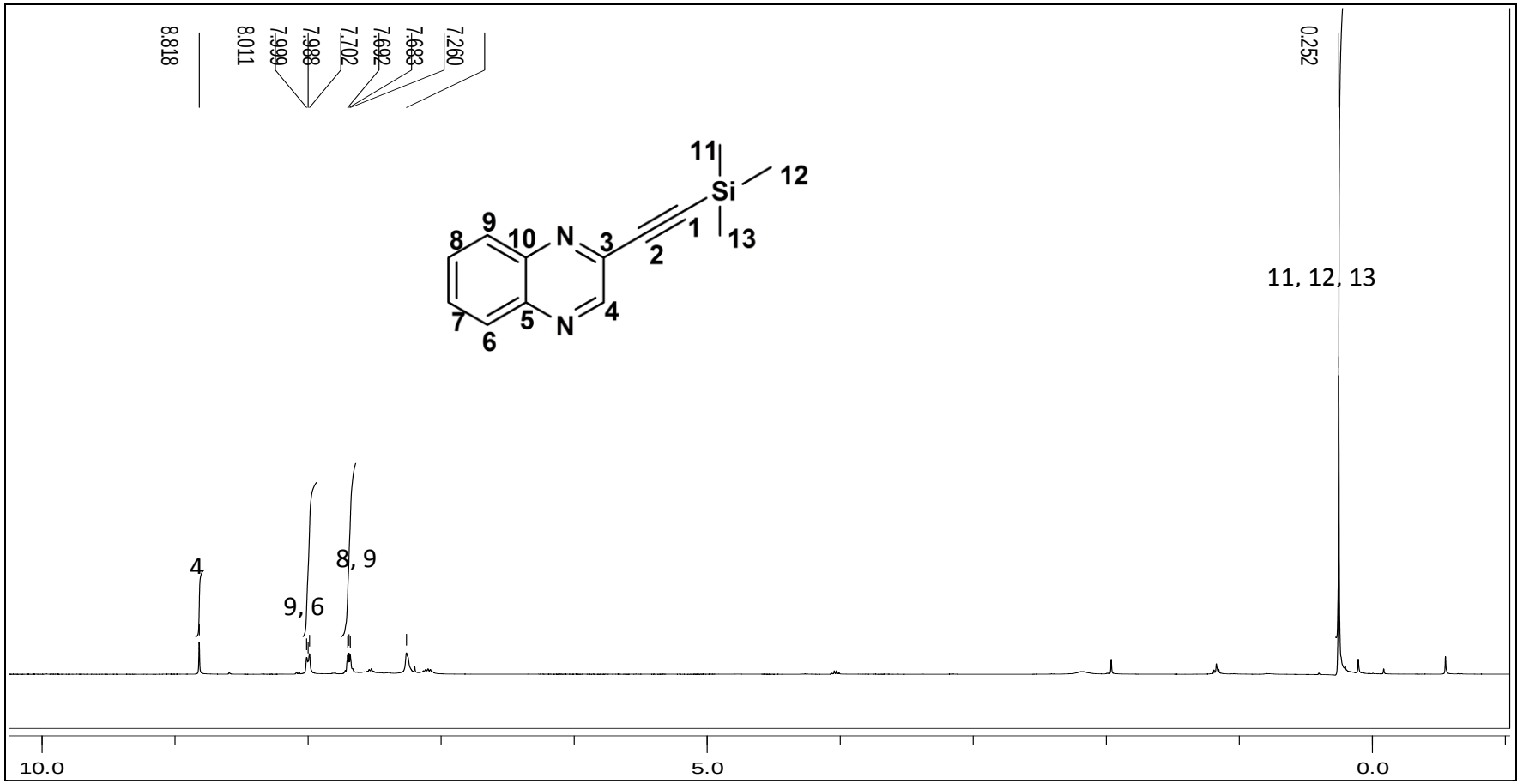

Figure 3.31: ^{1}H NMR of 2-quinoxalineethynyltrimethylsilane [**Q3**]

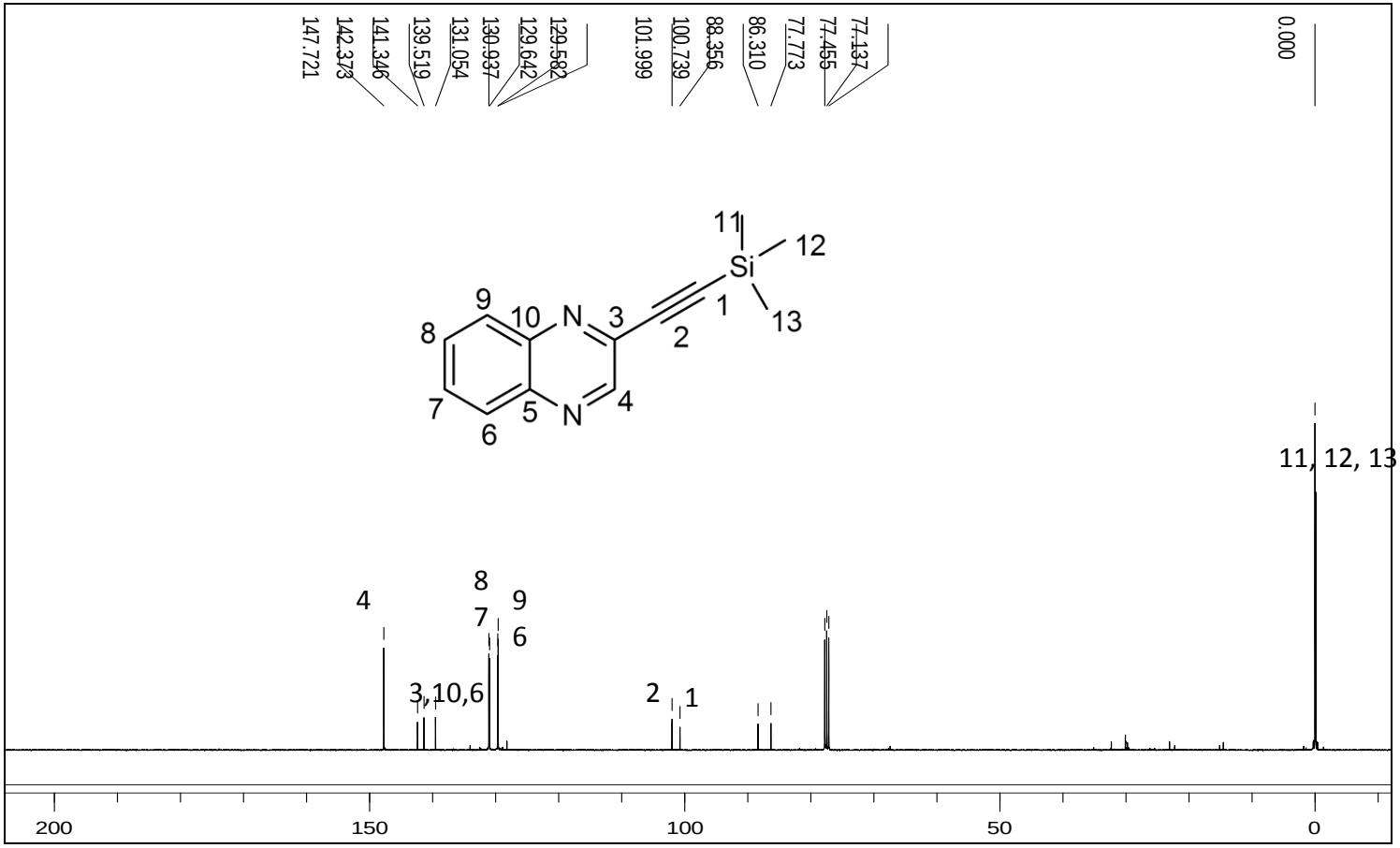

Figure 3.32: ^{13}C NMR of 2-quinoxalineethynyltrimethylsilane [**Q3**]

3.8 The coordination of Schiff base complexes to quinoxaline derivative

One of the objectives of this study was to coordinate Schiff base complexes (**C1 - C19**) with quinoxaline derivative (**Q3**). The synthesised **C19** zinc(II) complex which is diamagnetic and fully characterised by solution NMR and Mass spectroscopy was used for coordination as representative candidate.

(**a**) The first route for coordinating Schiff base complexes to quinoxaline derivative which was attempted included starting materials of **Q3** and **C19.** The analyses of ^{1}H NMR spectrum showed that there was no reaction that took place within twelve hours period at room temperature with potassium iodide base in methanol/ethanol solution ratio of (1:1). The role of potassium iodide was to keep the solution basic, to weaken and cleave the trimethylsilane (TMS). After the removal of TMS, the free anion intermediate from **Q3** which will be negatively charged was expected to be a nucleophilic center and attack the electrophilic metal center which is relatively electron poor as a result of chlorine atom being a good leaving group. The reaction conditions were kept at room temperature, under inert conditions using nitrogen gas and the reaction was monitored by TLC which never showed new spot. The resulting crude product was filtered to remove potassium iodide and the solvent was removed to obtain an oily paste product which was analysed using ^{1}H NMR which showed both starting materials **Q3** and **C19**. The reaction **Scheme 3.4** demonstrates one of the attempts for coordinating which was applied.

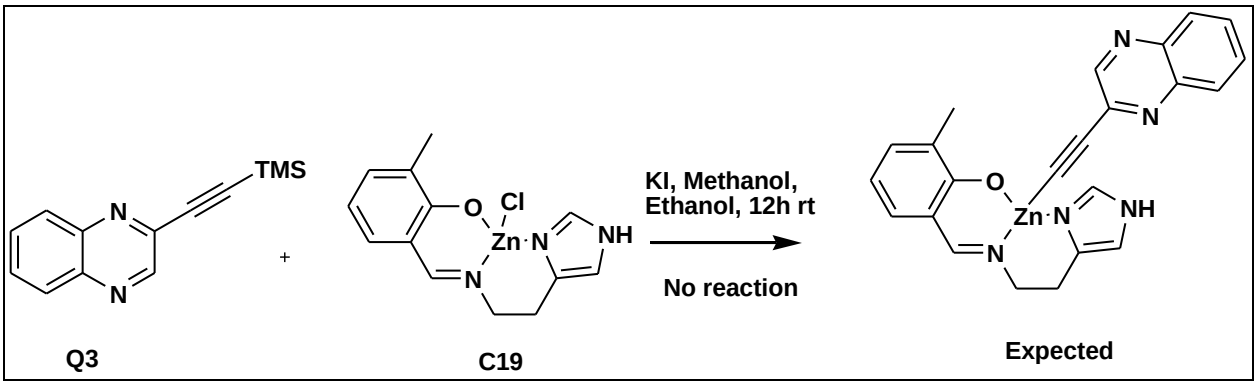

Scheme 3.4: Attempted coordination of Schiff base complexes to quinoxaline derivative

(**b**) The second attempt included **Q3**, **C19** and KOH in methanol/ethanol solution of (1:1) for a period of twelve hours. The resulting crude product was filtered and the solvent was removed to obtain an oily paste product which was analysed using ^{1}H NMR which showed ethanol solvent peaks and two singlets peaks at 6.78 ppm and 6.05 ppm which showed no achievements for coordination.

(**c**) The third attempt included **Q3**, **C19**, diethylamine, potassium hydroxide and both methanol/ethanol mixture with ratio of (1:1) at room temperature for a period of twelve hours. The resultant crude product was filtered and the solvent was removed to obtain a yellowish product which was analysed using ^{1}H NMR. The analysis of ^{1}H NMR spectrum showed the presence of two products. The two products were separated by ethyl acetate selective solvation which dissolved only the yellowish product and precipitates brown product. The outcome showed that there was hydroamination reaction catalysed by zinc complex **C19** [14]. The brown product proved to a decomposed starting material **Q3** and the ^{1}H NMR spectrum of the yellowish product was analysed to give a triplet peak at 1.25 ppm - 1.23 ppm integrating for six protons with coupling constant (J = 7.2 Hz), a quartet at 3.36 ppm - 3.30 ppm integrating for four protons with coupling constant of (J = 7.2 Hz), two doublet 5.35 ppm - 5.32 ppm and 7.72 ppm - 7.75 ppm which each integrating for one proton with coupling constant (J = 13.2 Hz), two triplet at 7.44 ppm - 7.42 ppm and 7.58 ppm - 7.56ppm which each integrating for one proton with coupling constant (J = 8.4 Hz) , two doublets at (7.87

ppm - 7.85 ppm) and (7.71 ppm - 7.40 ppm) each integrating for one proton with coupling constant (J = 8 Hz) and the N=CH peak from the pyrazine at 8.45 ppm integrating for one proton. The ^{13}C NMR showed three quaternary carbons, seven CH carbons, one CH_2 and one CH_3 ranging from 18.42 ppm - 154.15 ppm with 60% percentage yield. Molar mass calculated was 227.30 and mass spectrum found from HRMS [M+H] is 228.1508 in **Figure 3.36**. The reaction **Scheme 3.5** demonstrates the detailed reaction reagents. The reaction confirms hydroamination of alkynes catalysed by zinc complex [14].

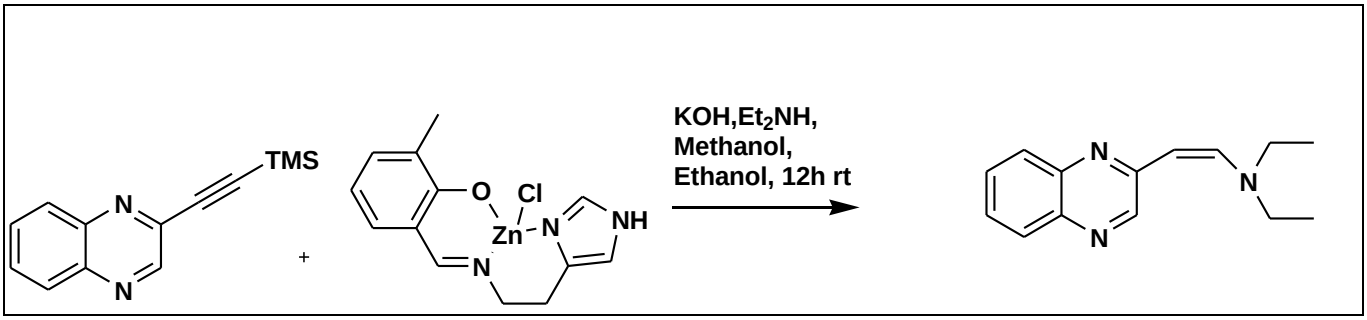

Scheme 3.5: The coordination of Schiff base complexes to quinoxaline derivative

(**d**) The fourth attempt involved the **Q3**, **C19**, potassium hydroxide, triethylamine and ethanol/methanol as solvents ratio of (1:1) for a period of twelve hours. The resultant crude product was filtered and the solvent was removed to obtain a pasty product which was analysed by ^{1}H NMR. The analyses of ^{1}H NMR spectrum showed ethanol solvent peaks, multiplets peaks at 7.74 ppm - 7.40 ppm and multiplets peaks at 7.34 ppm - 7.31 ppm which showed no achievements for coordination.

(**e**) The fifth attempt involved the **Q3**, **C19**, potassium hydroxide, triethylamine, copper iodide and tetrahydrofuran (THF)/methanol as solvent with ratio of (1:1) for a period of twelve hours. The role of potassium hydroxide was to keep the solution basic and to cleave the trimethylsilane (TMS). The role of Copper iodide was to promote transmetalated intermediate after (TMS) removal and facilitate coordination to the metal centre. The resulted crude product was filtered and the solvent was removed to obtain a paste product which was analysed by ^{1}H NMR. The analyses of ^{1}H NMR spectrum

showed ethanol and methanol solvent peaks and a broad peak at 5.21 ppm - 5.13 ppm which showed that the coordination was not achieved.

(**f**)The second route for coordination involved the metal halides coordination to quinoxaline derivative of $ZnCl_2$ to **Q3** followed by the coordination of Schiff base ligand. The first attempt for coordinating using the second route involved **Q3**, zinc chloride, diethylamine, potassium hydroxide and both methanol/ethanol ratio of (1:1) at room temperature for a period of twelve hours. The resulted product shows hydroamination reaction of alkynes catalysed by $ZnCl_2$ [14]. The ^{1}H NMR spectrum is shown in **Figure 3.33**. The ^{13}C NMR spectrum is shown in **Figure 3.35**. The COSY spectrum showed two sets of doublets from the CH=CH interacting with each other, the two triplets from the benzene interacting with each other and with the nearest doublets on the benzene on **Figure 3.34**. The singlet from pyrazine N=CH showed no interaction with any of the protons. The percentage yield was 90%. **Scheme 3.6** shows reaction conditions.

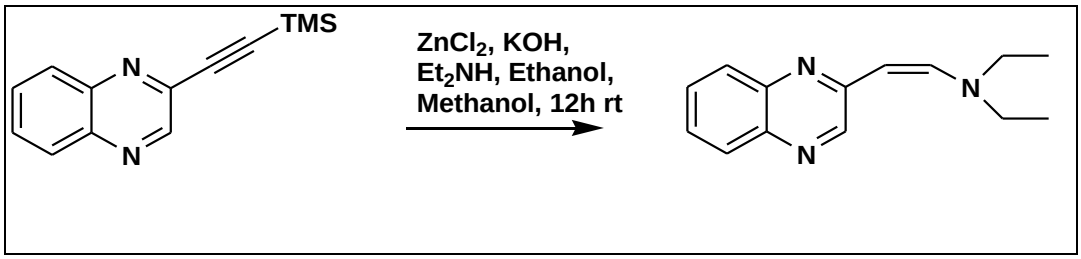

Scheme 3.6: The transmetalation on quinoxaline derivative [**Q3**]

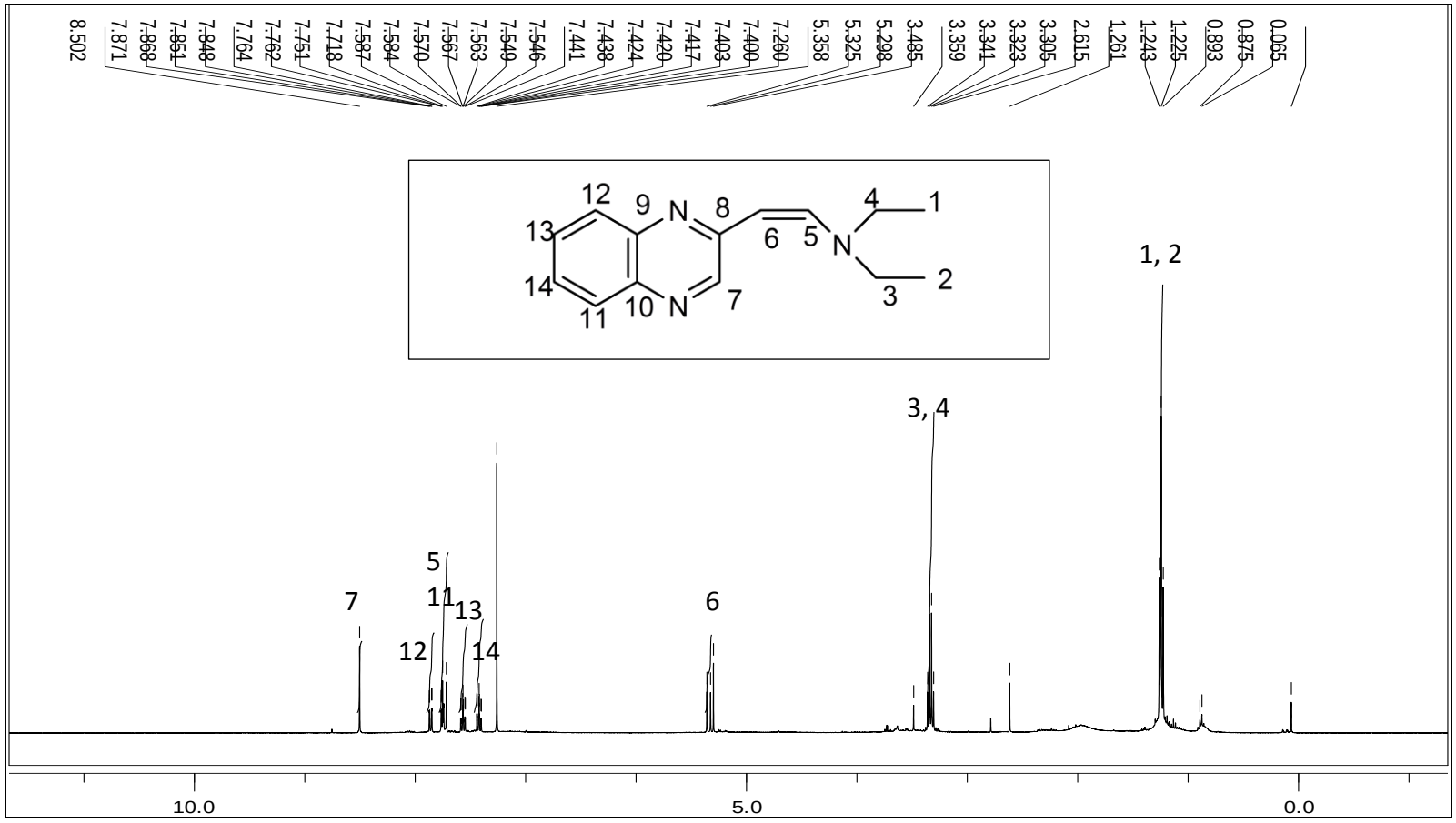

Figure 3.33: ^{1}H NMR for [**QA**]

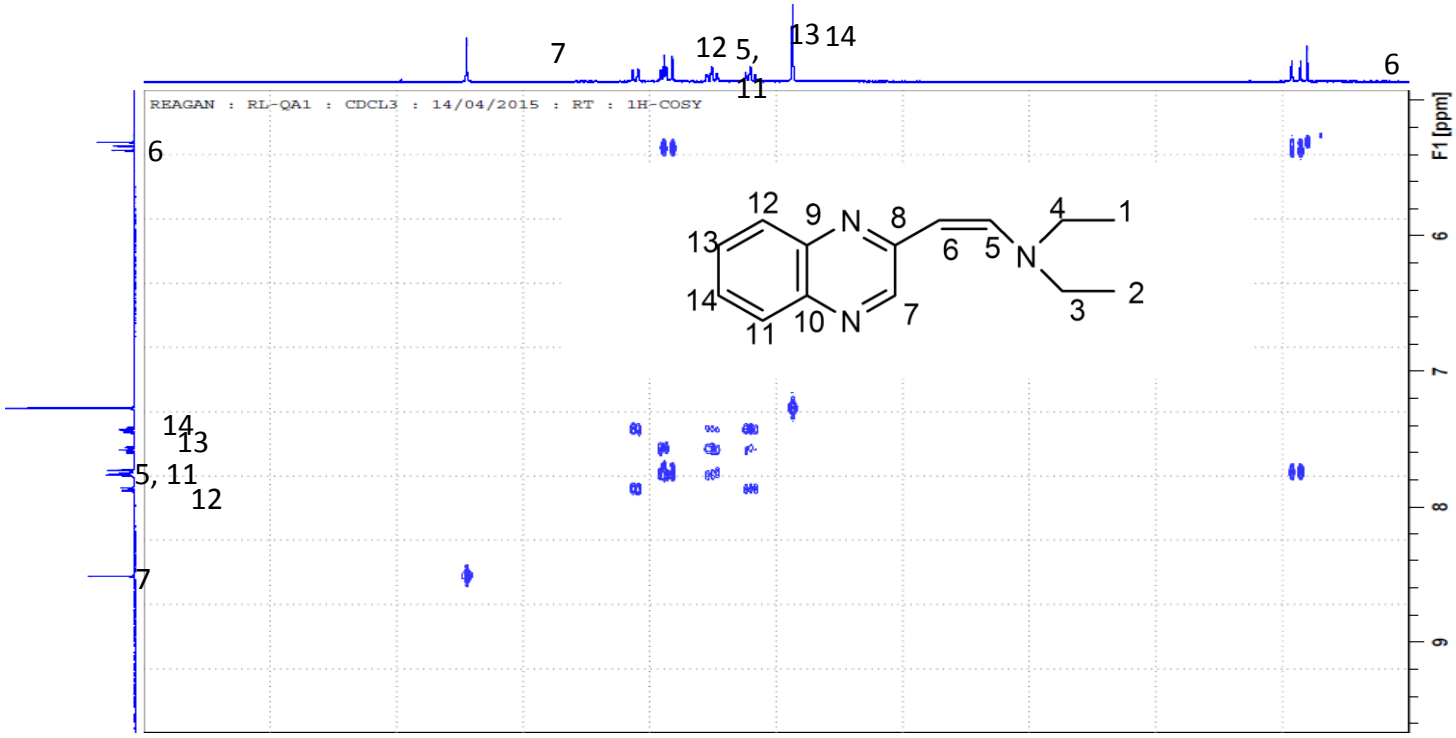

Figure 3.34: COSY NMR for [**QA**]

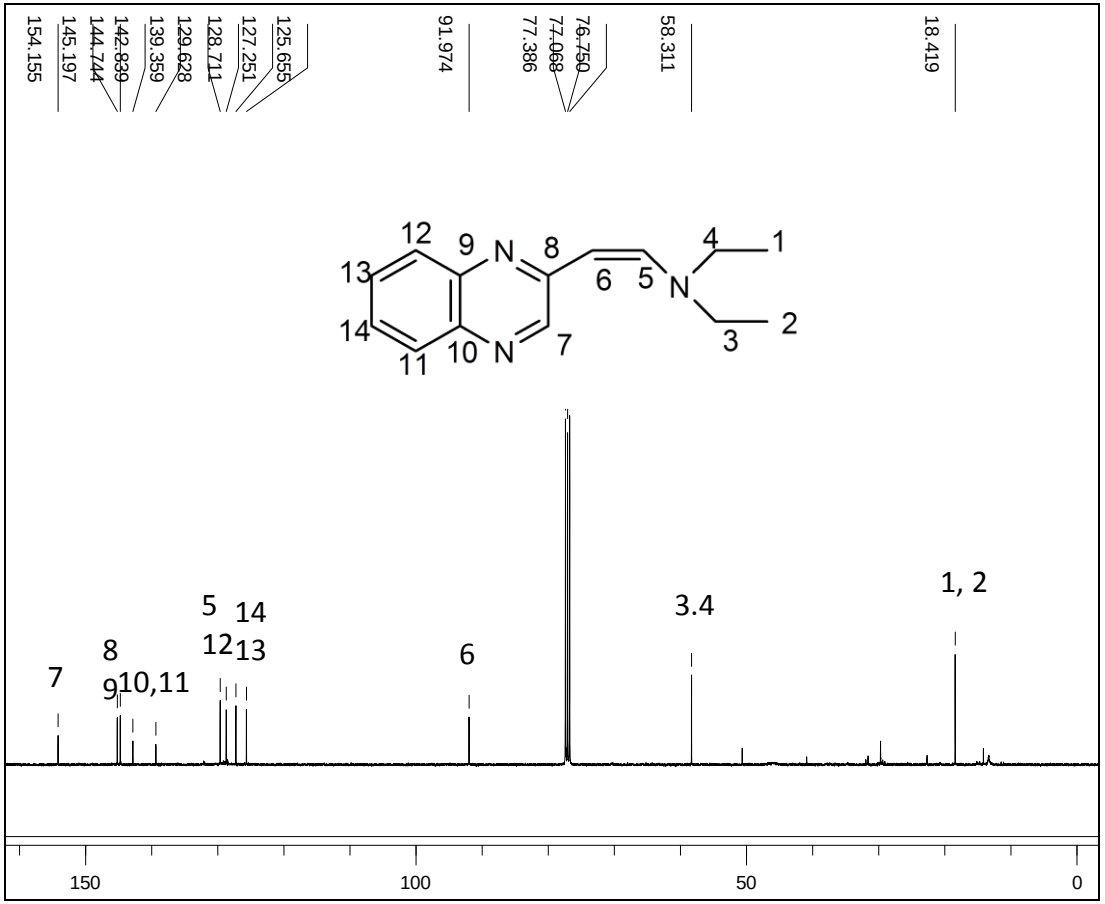

Figure 3.35: ^{13}C NMR for [**QA**]

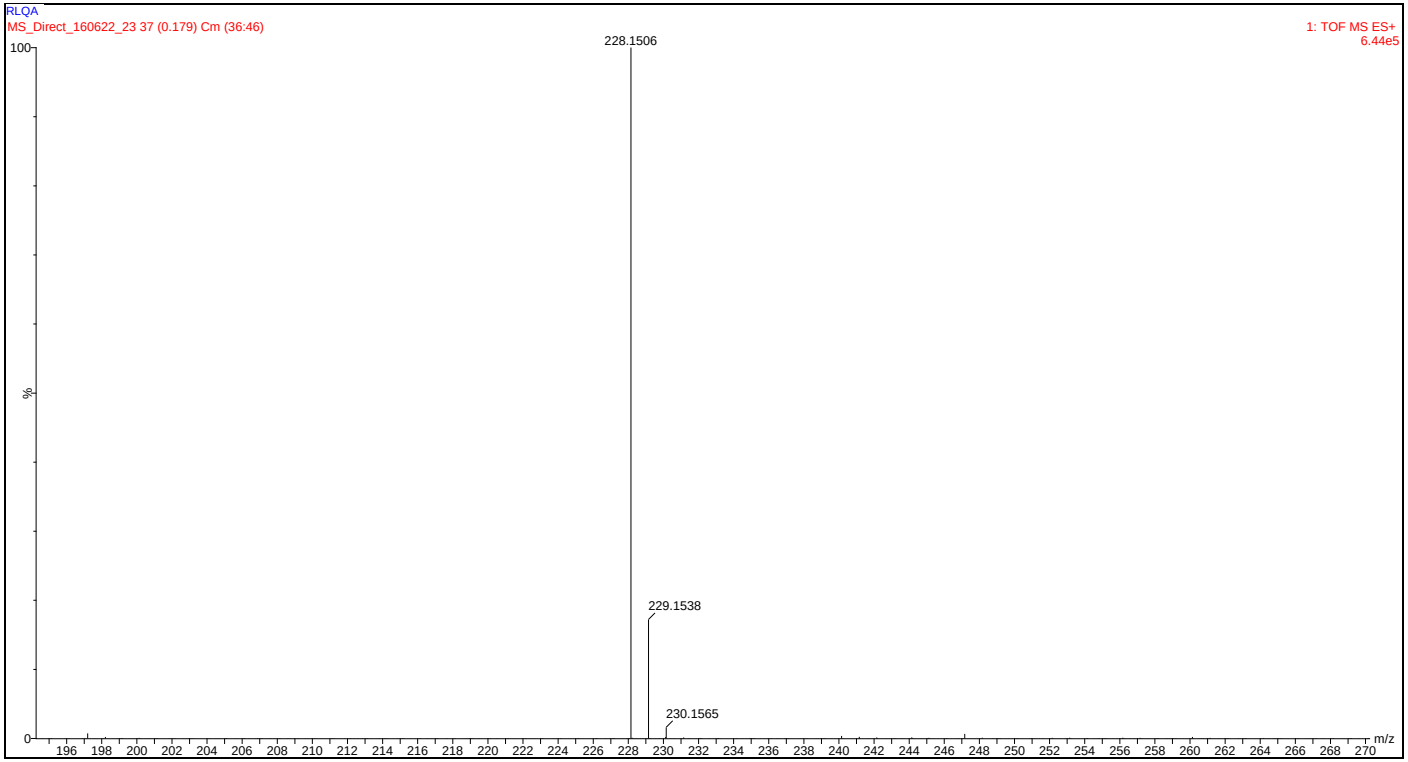

Figure 3.36: Mass spectrum of **QA**

(**g**) The second attempt for metal halides coordination to quinoxaline derivative following a modified second route involved **Q3**, zinc chloride, triethylamine, potassium hydroxide and both methanol/methanol ratio of (1:1) at room temperature for a period of twelve hours. The resultant crude product was filtered and the solvent was removed to obtain a brown product which was analysed but showed no sign of the anticipated product nor the starting material. **Scheme 3.7** shows detailed conditions.

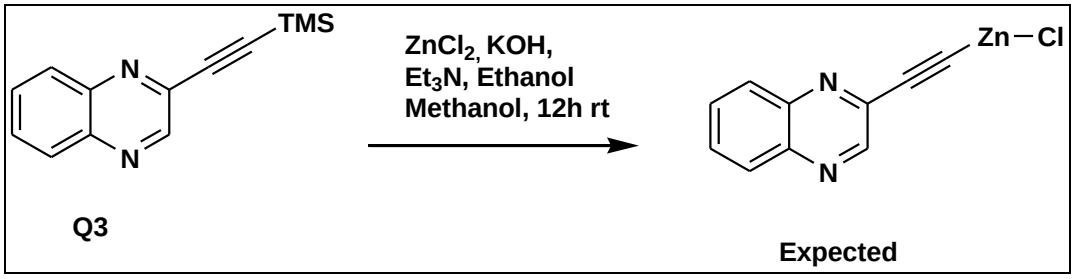

Scheme 3.7: The metal coordination on quinoxaline derivative [**Q3**]

(**h**) The third attempt for metal coordination involved **Q3**, zinc chloride, and both methanol/ethanol solvents ratio of (1:1) at room temperature for a period of twelve hours. The aim was to check if the reaction could continue without KOH with TMS being removed? The reaction conditions were under inert conditions using nitrogen gas and the reaction was monitored by TLC which revealed no new spot. The resultant crude product was filtered to remove the precipitates and the solvents were removed to obtain the starting material **Q3**. The transmetalation was not successful. KOH was observed to be the source to remove TMS.

3.9 Conclusion

Imidazolyl-salicylaldemine Schiff base ligands were successfully synthesised and fully characterised by solution NMR, FT-IR, UV-vis, Mass spectroscopy and Elemental analysis. Complexation of ligand with manganese chloride, copper chloride and zinc chloride yielded tri-dentate Schiff base complexes which were characterised by FT-IR, UV-vis, Mass spectroscopy, Elemental analysis and solution NMR. The complexes decompose if exposed to moisture. The coordination of complexes confirms mono-chelation. Quinoxaline derivatives were synthesised and Sonogashira cross coupling was used to derivatise quinoxaline which was successfully achieved. All quinoxaline compounds were characterised by solution NMR, Mass spectroscopy and Elemental analysis. The coordination of Schiff base complexes to quinoxaline derivative was attempted following different routes. The coordination attempts resulted in hydroamination reaction. The outcome for coordinating yielded quinoxaline derivative (**QA**) compound by hydroamination reaction which was fully characterised by solution NMR spectroscopy where KOH was found to be the source of TMS removal. The Schiff base complex to quinoxaline coordination was not successful after several attempts demonstrated earlier.

3.10 References

[1] S. Boltina, M. Yankey, I.A. Guzei, L.C. Spencer, S.O. Ojwacha, J. Darkwa; Novel O-N-N Pyrazolyl-imine and Imidazolyl-imine Pincer Palladium Complexes as Heck Coupling Catalysts*, South African Journal of Chemistry*, 65 (2012) 75-83.

[2] W. Qin, S. Long, M. Panunzio, S. Biondi; Schiff Bases: A Short Survey on an Evergreen Chemistry Tool, *Molecules,* 18 (2013) 12264-12289.

[3] A. Golcu, M. Tumer, H. Demirell, R.A. Wheatley; Cd(II) and Cu(II) complexes of polydentate Schiff base ligands: synthesis, characterization, properties and biological activity, *Inorganica Chimica Acta*, 358 (2005) 1785-1797.

[4] M.A. Neelakantan, F. Rusalraj, J. Dharmaraja, S. Johnsonraja, T. Jeyakumar, M. Sankaranarayana; Spectral characterization, cyclic voltammetry, morphology, biological activities and DNA cleaving studies of amino acid Schiff base metal(II) complexes, *Spectrochemica Acta*, 71 (2008) 1599–1609.

[5] A. Xavier, N. Srividhya; Synthesis and Study of Schiff base Ligands, *IOSR Journal of Applied Chemistry (IOSR-JAC),* 7 (2014) 06-15.

[6] R.M. Ahmed, E.I. Yousif, M.J. Al-Jeboori; Co(II) and Cd(II) Complexes Derived from Heterocyclic Schiff-Bases: Synthesis, Structural Characterisation, and Biological Activity, *Research Article*, 1 (2013) 1-6.

[7] E. Yousif, A. Majeed, K. Al-Sammarrae, N. Salih, J. Salimon, B. Abdullah; Metal complexes of Schiff base: Preparation, characterization and antibacterial activity, *Arabian Journal of Chemistry*, 10 (2013) 1878-5352.

[8] R.M. Issa, A.M. Khedr, H.F. Rizk; UV–vis, IR and 1H NMR spectroscopic studies of some Schiff bases derivatives of 4-aminoantipyrine, *Spectrochimica Acta Part A*, 62 (2005) 621-629.

[9] M.S. Z akerhamidi, A. Ghanadzadeh, M. Moghadam; Solvent Effects on the UV/ Visible Absorption Spectra of Some Aminoazobenzene Dyes, *Chemical Science Transactions,* 1 (2012) 1-8.

[10] R. Atkins, G. Brewer, E. Kokot, G.M. Mockler, E. Sinn; Copper(I) and Nickel(I) Complexes of Unsymmetrical Tetradentate Schiff Base Ligands, *Inorganic Chemistry* 24 (1985) 127-134.

[11] A. Bottcher, T. Takeuchi, K.I. Hardcastle, T.J. Meade, H.B. Gray, Spectroscopy and Electrochemistry of Cobalt(III) Schiff Base Complexes, *Inorganic Chemistry*, 36 (1997) 2498-2504.

[12] A. Soroceanu , S. Shova, M. Cazacu, I. Balan, N. Gorinchoy, C. Turta; Synthesis and Structural Characterization of the Mononuclear Cobalt(II) Complex: {5,50-Dihydroxy-2,20-[o-phenylenebis(nitrilomethylene)]diphenolato}cobalt(II) Dihydrate, *Journal of chemical crystallography*, 43 (2013) 310-318.

[13] W. Nxumalo; The development of novel pterin chemistry leading to potential dihydrofolate reductase inhibitors with potential antimalarial activity, *PhD thesis, University of Witwatersrand Library*, (2011) 69-74.

[14] F. Pohlki, S. Doye; The catalytic hydroamination of alkynes, *Chemical Society Reviews*, 32 (2003) 104-114.

CHAPTER FOUR

BIOLOGICAL STUDIES: QUANTITATIVE ANTIBACTERIAL ACTIVITY BY ASSAY OF MINIMUM INHIBITION CONCENTRATION (MIC).

4.1 Antibacterial activities

As one of the research objectives, biological studies were done using six selected compounds for testing after the unsuccessful several attempts to cross couple Schiff base complexes with quinoxaline derivative. Bacterial cells which were used as test microorganism were gram negative: *Escherichia coli* and *Pseudomonas aeruginosa*, gram positive: *Staphylococcus aureus* and *Enterococcus faecalis*.

4.1.1 Materials and instruments

The biological studies were done at Biotechnology, Biochemistry and Microbiology department at University of Limpopo, South Africa. All reagents were of analytical grade: acetone, *p*-Iodonitrotetrazolium (INT) and ampicillin was obtained from Sigma Aldrich and analytical nutrient broth No1 was obtained from Fluka.

(**a**) Nutrient broth No 1
(**b**) Ampicillin (positive bacterial control)
(**c**) *p*-Iodonitrotetrazolium (growth indicator)
(**d**) Microtiter plates
(**e**) Incubator shaker (New Brunswick)
(**f**) Auto clave (HICLAVE HVA-110)
(**g**) Acetone (negative bacterial control)

4.1.2 Preparation of inoculation medium and subcultures

Nutrient broth No 1 (25 g): peptone (15g/L), yeast extract (3g/L), sodium chloride (6g/L), D (+)-glucose (1g/l) was dissolved in one (1) litter of distilled water and pH was adjusted to 7.5 to give a gold colored solution. The nutrient broth solution, distilled water and micropipette tips were sterilized by autoclaving at 121 °C for two hours and later cooled to room temperature. The four microorganisms: *Escherichia coli, Enterococcus faecalis*, *Staphylococcus aureus* and *Pseudomonas aeruginosa* were inoculated into four flasks filled with 250 ml of nutrient broth solution using inoculation loop and sealed with cotton and foil. The four inoculated microorganisms in nutrient medium were incubated for twenty four hours at 37 °C to grow subcultures [1].

4.1.3 Testing method prepared in triplicates

Each microtiter plate well was filled with 100 µl of sterilized distilled water. The solutions of : **L9**, **C9**, **C18**, **C19**, **Q3** and **QA** were prepared by dissolving 2 mg in 1 ml (2M) of acetone and 100 µl solutions was loaded to the well of the microtiter plate using micro dilution method. The prepared triplicate microtiter plates were incubated for twenty four hours in 100% relative humidity at 37 °C.

After twenty four hours incubation, a growth indicator was prepared, 40 µl of 0.2 mg/ml of *p*-iodonitrotetrazolium violet (INT) dissolved in distilled water and added to each well of the microtiter plates and incubated for thirty minutes to obtain the results. Acetone was used as a negative control and ampicillin was used as positive control. The lowest concentration of the test solution that led to an inhibition of growth was recorded as the MIC [2; 3].

4.1.4 Results and discussion

The antibiotic resistance of pathogenic microorganisms remains a daily health challenge. The synthesis and screening of novel compounds for antimicrobial activities is vital to explore new effective medicines. In this study, selected and prepared compounds on **Table 4.1** below were evaluated for inhibitory properties on selected pathogenic bacteria such as *Escherichia coli, Enterococcus faecalis*, *Staphylococcus aureus* and *Pseudomonas aeruginosa*. The standardized technique was used to determine the quantitative (micro dilution method) [4]. **Table 4.2** and **Table 4.3** show MIC values and total activities of the compounds respectively. The compounds in **Table 4.1** are representative samples to probe probable biological activity of synthesised compounds.

Table 4.1: Selected and prepared compounds used for MIC tests

Compounds	Code
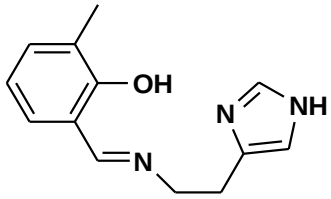	**L9**
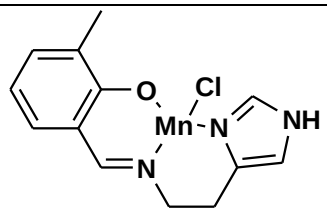	**C19**
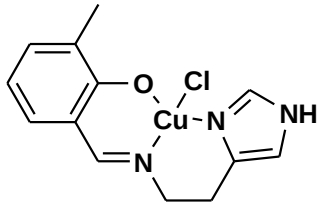	**C18**
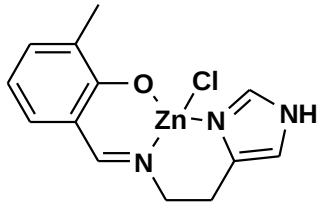	**C19**
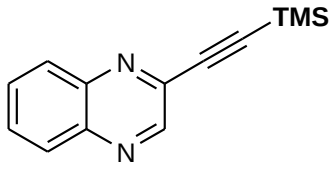	**Q3**
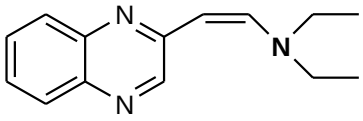	**QA**

Table 4.2: Average minimum Inhibitory Concentration (MIC) of prepared compounds: **L9**, **C9**, **C18**, **C19**, **Q3** and **QA** after twenty four hours and thirty minutes of incubation at 37 ˚C [1-4].

Compounds	**L9**	**C9**	**C18**	**C19**	**Q3**	**QA**			
Mass of compounds	2mg	2mg	2mg	2mg	2mg	2mg			
	MIC values (mg/ml)						**Average**	**Acetone**	**Ampicillin**
E.coli	0,004	0.004	0.004	0.004	0.004	0.004	**0.004**	NI	0.004
P.aeruginosa	0.500	0.250	0.063	0.500	0.500	0.125	**0.323**	NI	0.063
E.faecalis	0,004	0.004	0.004	0.004	0.004	0.004	**0.004**	NI	0.004
S.aureus	0.500	0.500	0.063	0.500	0.250	0.500	**0.386**	NI	0.250
Average	**0.252**	**0.190**	**0.034**	**0.252**	**0.190**	**0.158**			

NI = no inhibition: acetone was used as negative control.

The total activity in mg/ml was calculated by dividing the mass of the compounds 2 mg with the MIC values. The resultant value indicates the volume to which the compound can be diluted and still inhibit the growth of bacteria's. The table below shows total activity of synthesised compounds against four test pathogens. The equation below demonstrates how the total activity was done.

$$\text{Total activity (mg/ml)} = \frac{Amount\ of\ compound\ 2\ mg\ (\frac{mg}{g})}{MIC\ (\frac{mg}{ml})}$$

Table 4.3: Total activity of the compounds in mg/ml

Compounds	**L9**	**C9**	**C18**	**C19**	**Q3**	**QA**	**Average**
E.coli	500	500	500	500	500	500	**500**
P.aeroginosa	4	8	32	4	4	16	**11**
E.faecalis	500	500	500	500	500	500	**500**
S.aureus	4	4	32	4	8	4	**9**
Average	**252**	**253**	**266**	**254**	**253**	**255**	

The MIC values were determined to compare the sensitivity of four microorganisms against synthesised compounds. MIC value is the lowest concentration of the test compound expressed in mg/ml that lead to inhibition of the pathogen growth in test. The MIC values showed similarity for all compounds against *E. coli* and *E. faecalis* with a lowest inhibition of 0.004 mg/ml on **Table 4.1**. The MIC values for *P. aeruginosa* and *S. aureus* had similar lowest inhibition of 0.500 mg/ml for **L9**, 0.063 mg/ml for **C18** and 0.500 mg/ml for **C19** on **Table 4.1**. The MIC values showed significant difference for *P. aeruginosa* and *S. aureus* with lowest inhibition of 0.250 mg/ml and 0.500 mg/ml for **C9** respectively, 0.500 mg/ml and 0.250 mg/ml for **Q3** respectively and 0.125 mg/ml and 0.500 mg/ml for **QA** respectively on **Table 4.1**. *E. coli* and *E. faecalis* were found to be sensitive to antibacterial compounds used for test as compared to *P. aeruginosa* and *S. aureus*. *S. aureus* showed more resistance to inhibition followed by *P. aeruginosa.*

These can be due to insensitivity of the pathogen to the compounds used for inhibition or due to different bacterial walls between gram negative and gram positive bacteria [3; 5]. Gram positive bacteria has thicker peptidoglycan cell wall layer, which causes resistance to uptake antimicrobial agents as compared to their counter parts gram negative with thinner peptidoglycan cell wall layer.

The total activity in mg/ml was calculated by dividing the 2 mg of compounds by MIC values. Total activity indicates the volume to which the bioactive compounds can be diluted and still inhibits growth of bacteria on **Table 4.2**. The complex containing copper **C18** had the highest average total activity compared to other compounds with an average of 266 mg/ml. The MIC value (0.004 mg/ml) which was the same for all compounds for *E.coli* and *E. faecalis* inhibition doesn't conclude the similar activity strength for used compounds. It was the last well of the microtiter plate were compounds were still active to inhibit pathogens.

4.1.5 Conclusion

E. coli and *E. faecalis* had similar MIC values for all compounds and were found to be more sensitive to bioactive compounds compared to *P. aeruginosa* and *S. aureus* which were less sensitive. The copper complex **C18** was found to be more active against all pathogens. Imidazolyl-salicylaldemine Schiff bases and their complexes and quinoxaline derivatives showed antibacterial activities against gram negative: *Escherichia coli* and *Pseudomonas aeruginosa*, gram positive: *Staphylococcus aureus* and *Enterococcus faecalis*

4.1.6 References

[1] P. Mittal, V. Uma; Synthesis, spectroscopic and cytotoxic studies of biologically active new Co (II), Ni (II), Cu (II) and Mn (II) complexes of Schiff base hydrazones, *Pelagia Research Library*, 1 (2010) 124-137.

[2] J.N. Eloff, J.O. Famakin, D.R.P. Katerere; *Combretum woodii* (Combretaceae) leaf extracts have high activity against Gram-negative and Gram-positive bacteria, *African Journal of Biotechnology*, 4 (2005) 1161-1166.

[3] N.P.M. Komape, M. Aderogba, V.P. Bagla, P. Masoko, J.N. Eloff; Anti-bacterial and anti-oxidant activities of leaf extracts of *combretum vendae* (*combretecacea*) and the isolation of an antibacterial compounds, *African Jounal Tradit Complement Alternative Medicines*, 11 (2014) 73-77.

[4] J.N. Eloff; Quantification the bioactivity of plant extracts during screening and bioassay guided fractionation, *Phytomedicine*, 11 (2004) 370-371.

[5] A.M. Balde, L.P ieters, T. Debruyne, S. Geerts, D.V. Berghe, A. Vlietinck; Biological investigations on Harrisonia abyssinica, *Phytomedicine*, 4 (1995) 299-302.

CHAPTER FIVE

CONCLUSIONS AND FUTURE WORK

The aim of this study was to explore the coordination of Schiff base complexes with nitrogen donor atoms to quinoxaline derivative and to test biological activities of prepared compounds against harmful microorganisms such as *Enterococus faecalis*, *Escherichia coli*, *Staphylococcus aureus* and *Pseudonomas aeruginosa*.

Salicylaldehyde-imidazolyl based ligands (**L1** - **L10**) were succesfully perpared and used to prepare Schiff base complexes. The newly synthesised ligands were succesfully coordinated to Cu(II), Mn(II), and Zn(II) metals salts to produces Schiff base complexes. Quinoxaline derivatives were prepared by condensation of di-ketone and primary di-amine. Qunoxaline derivatives and Schiff base complex derivatives were characterised by solution NMR, FT-IR, UV, Elemental analysis and mass spectroscopy. The cross coupling of Schiff base complexes to quinoxaline derivative was not succesful after several attempts.

Selected imidazolyl-salicylaldemine Schiff bases and their complexes, and quinoxaline derivatives were subjected to biological activity tests and showed antibacterial activities against gram negative: *Escherichia coli* and *Pseudomonas aeruginosa*, gram positive: *Staphylococcus aureus* and *Enterococcus faecalis*. Bioactive compounds used for testing were found to be too sensitive to bacterial cells of *E. coli and E. faecalis. P. aeruginosa* and *S. aureus* were found to be less sensitive compared to *E. coli and E. faecalis*.

In future, a broader attention should entail investigation and development of effective methods to link Schiff base complexes to quinoxaline complexes and correlations of Schiff base complexes and quinoxaline derivatives based on their substituents. Diseases such as Tuberculosis, cancer and malaria will be included for evaluation

APPENDICES

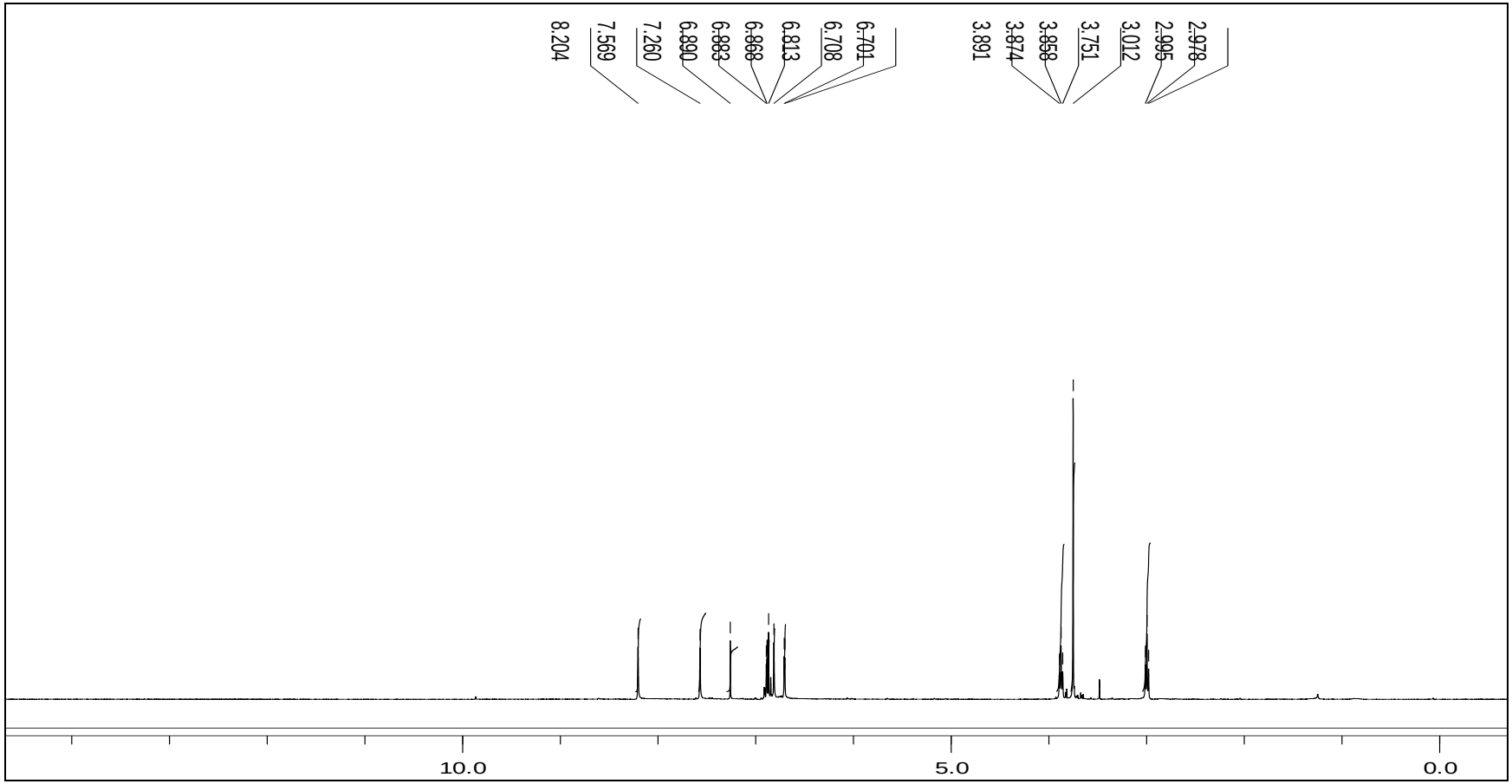

Figure 1: ^{1}H NMR spectrum of 4-methoxy-6-{[2-(1H-imidazol-4-yl)-ethylimino]-methyl}-phenol [**L2**]

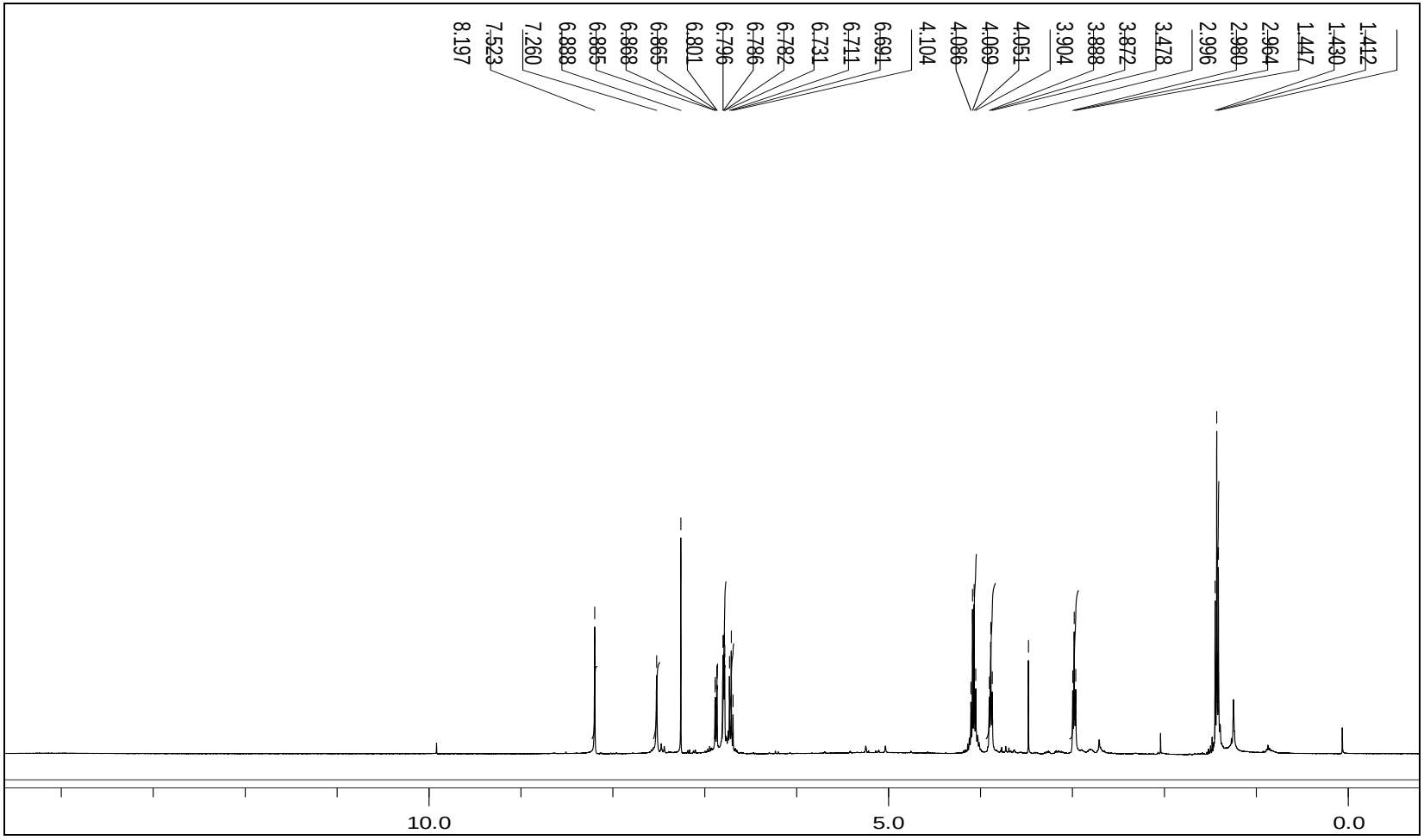

Figure 2: ^{1}H NMR spectrum of 2-ethoxy-6-{[2-(1H-imidazol-4-yl)-ethylimino]-methyl}-phenol [**L3**]

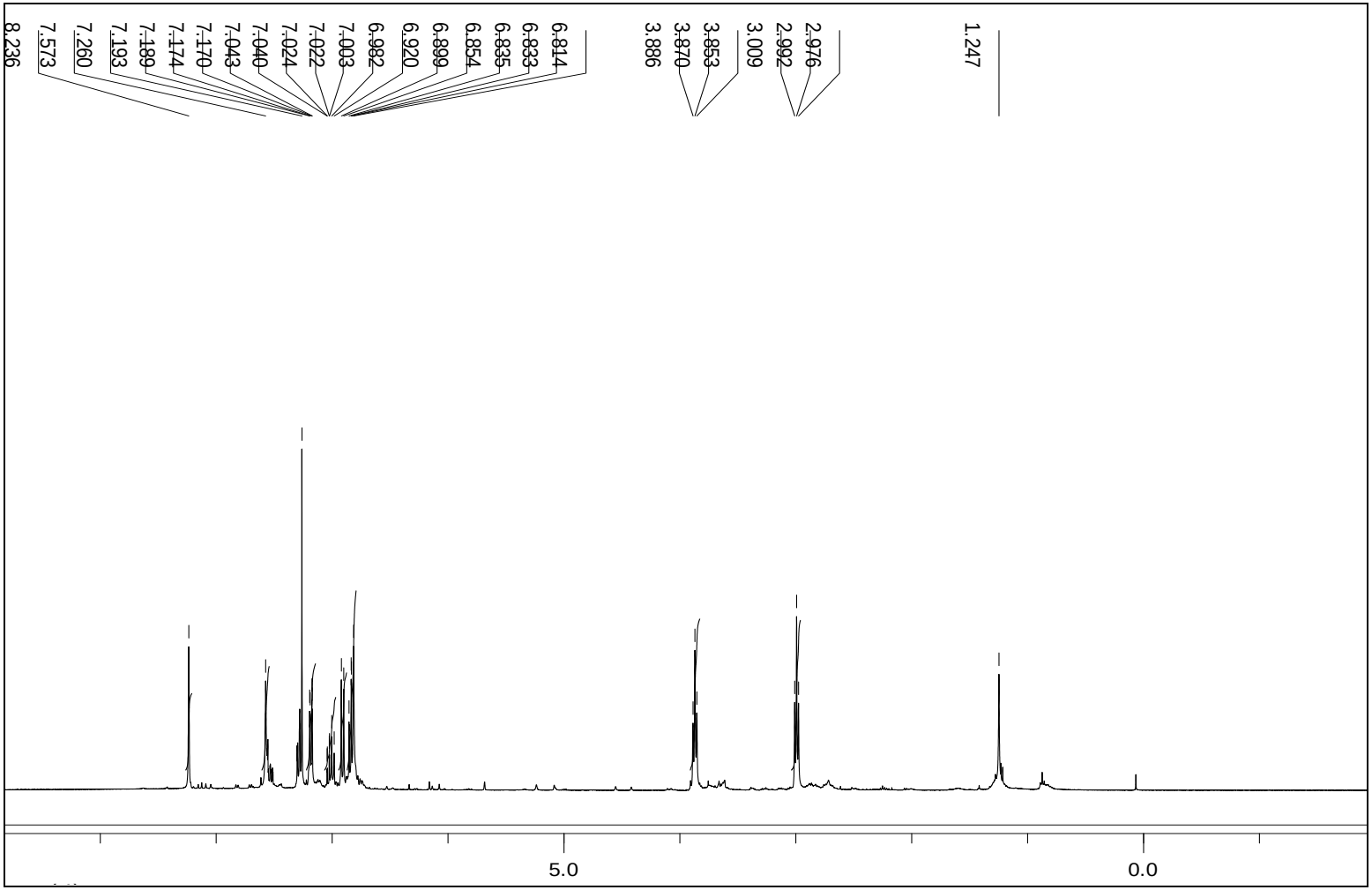

Figure 3: ^{1}H NMR spectrum of salicylaldehyde-2-{[2-(1H-imidazol-4-yl)-ethylimino]-methyl}-phenol [**L4**]

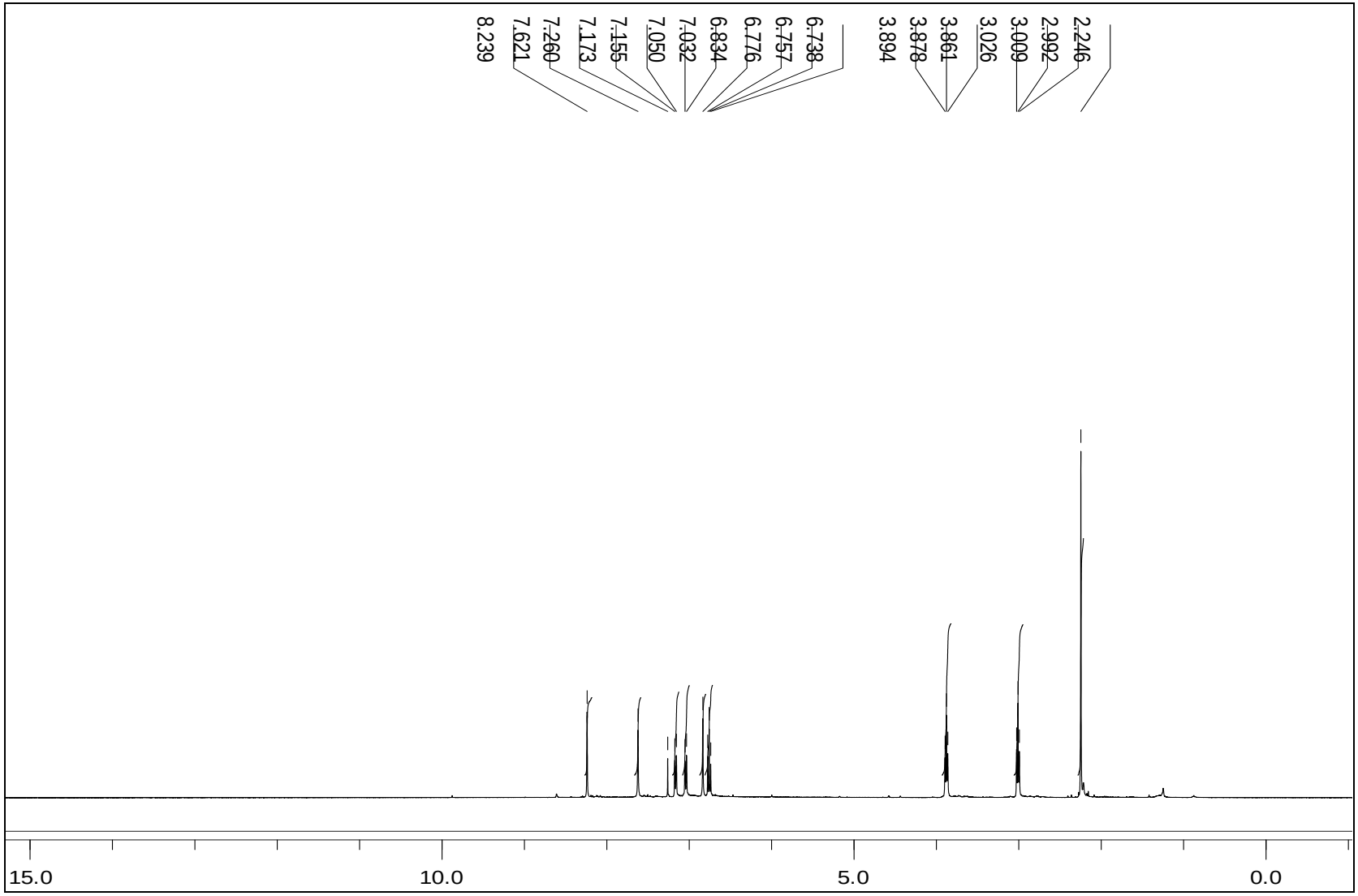

Figure 4: ^{1}H NMR spectrum of 4-methyl-6-{[2-(1H-imidazol-4-yl)-ethylimino]-methyl}-phenol [**L5**]

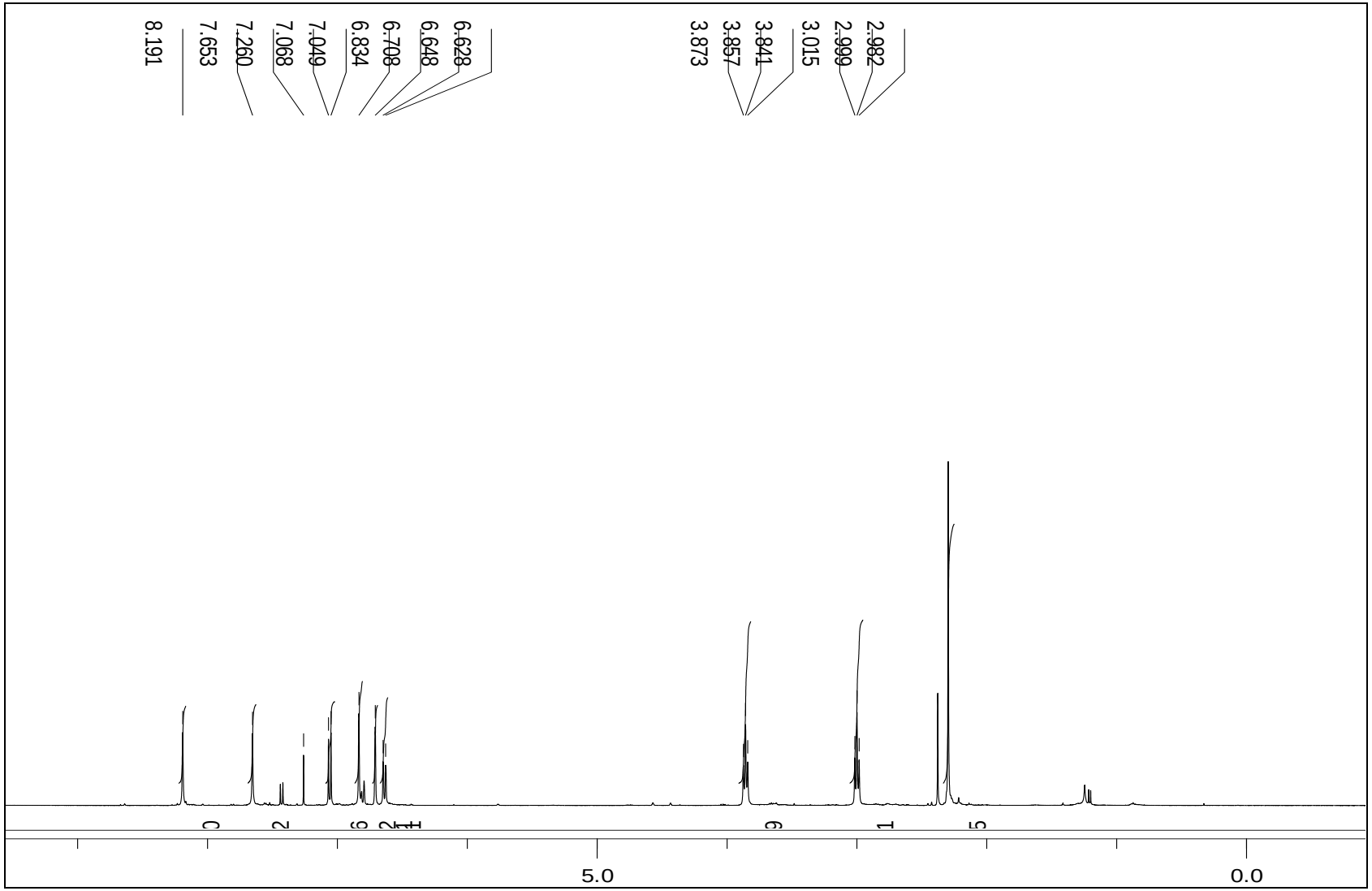

Figure 5: ^{1}H NMR spectrum of 3-methyl-6-{[2-(1H-imidazol-4-yl)-ethylimino]-methyl}-phenol [**L6**]

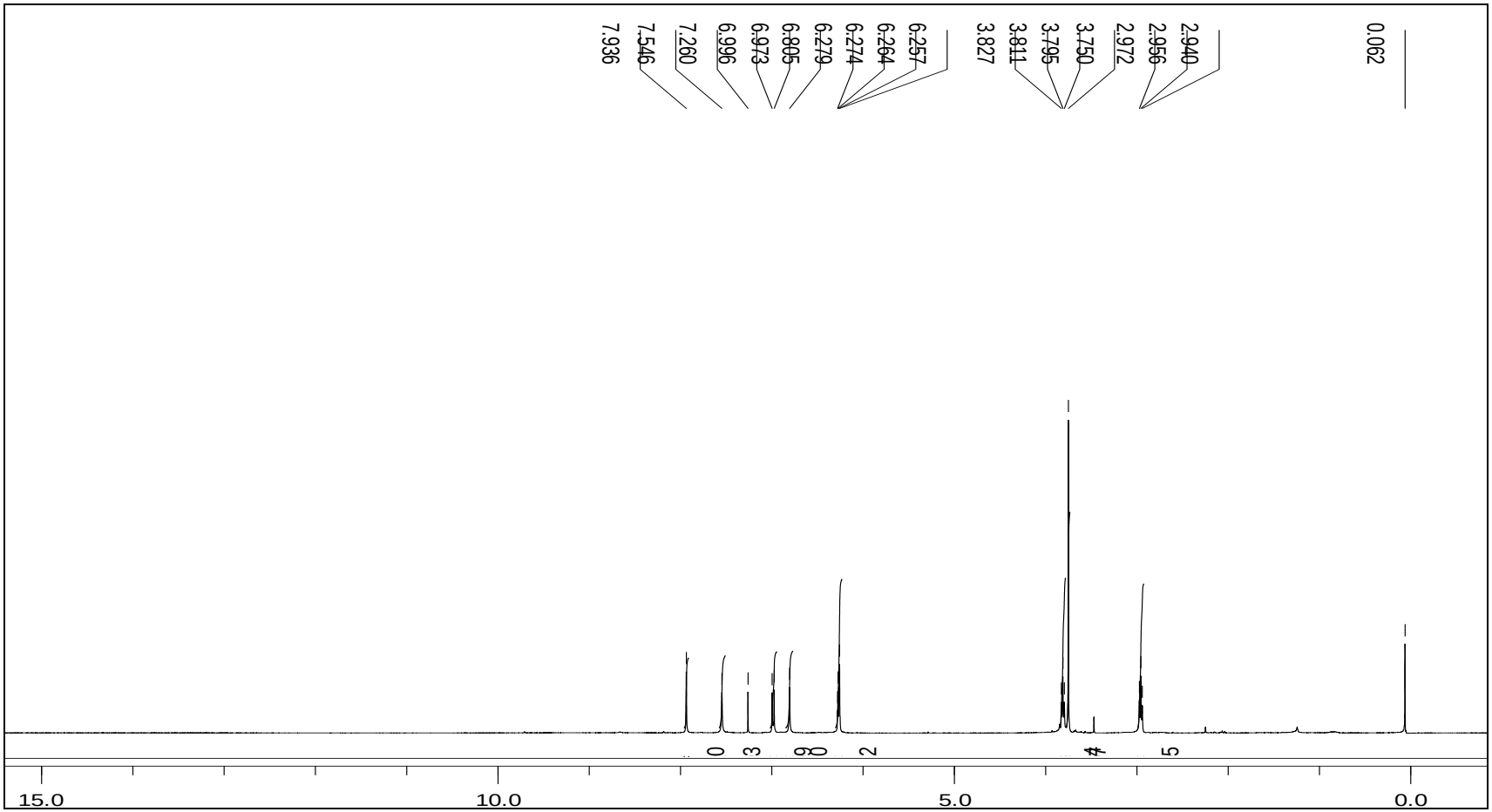

Figure 6: ^{1}H NMR spectrum of 3-methoxy-6-{[2-(1H-imidazol-4-yl)-ethylimino]-methyl}-phenol [**L7**]

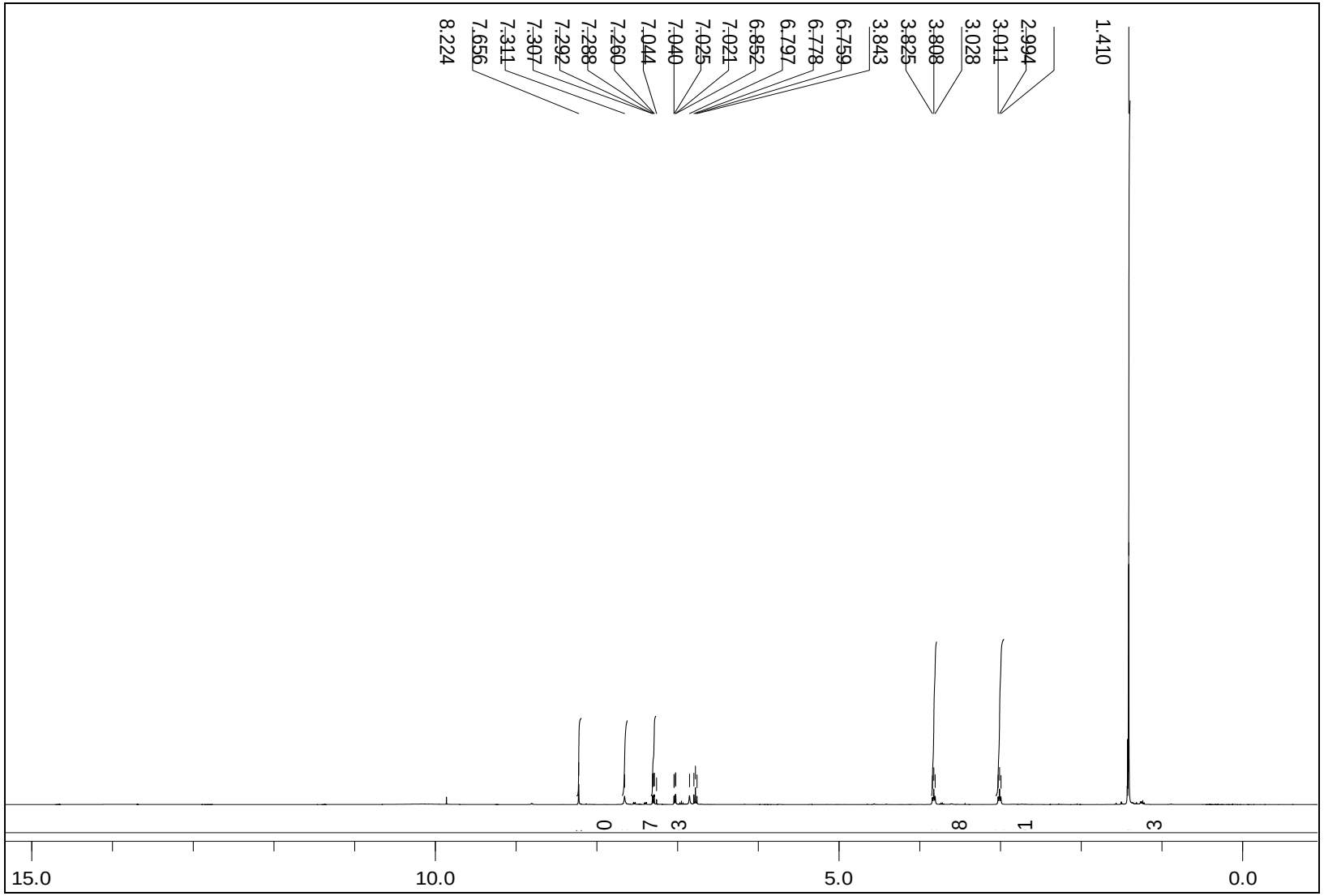

Figure 7: ^{1}H NMR spectrum of 2-tert-butyl-6-{[2-(1H-imidazol-4-yl)-ethylimino]-methyl}-phenol [**L8**]

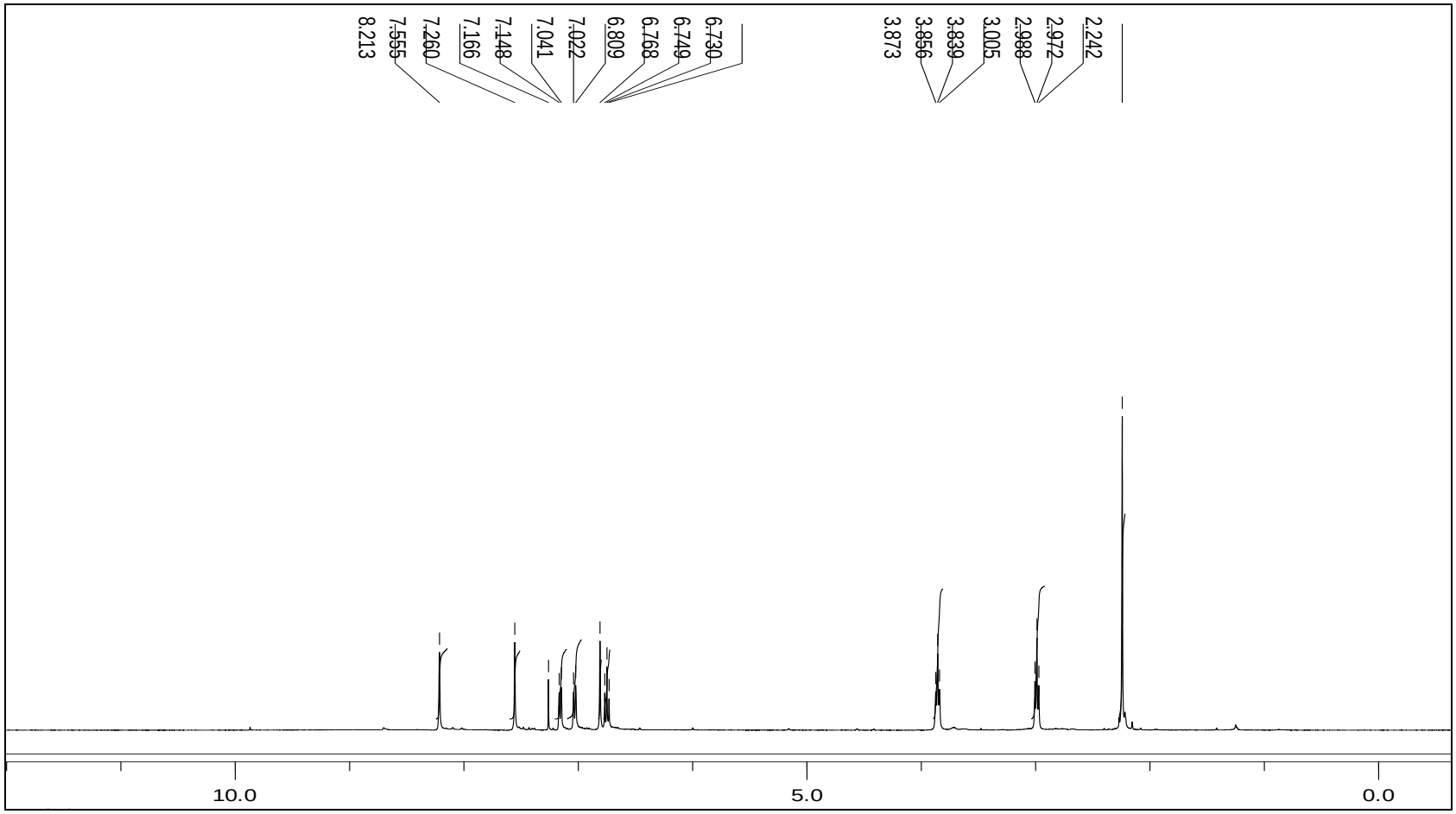

Figure 8: ^{1}H NMR spectrum of 2-methyl-6-{[2-(1H-imidazol-4-yl)-ethylimino]-methyl}-phenol [**L9**]

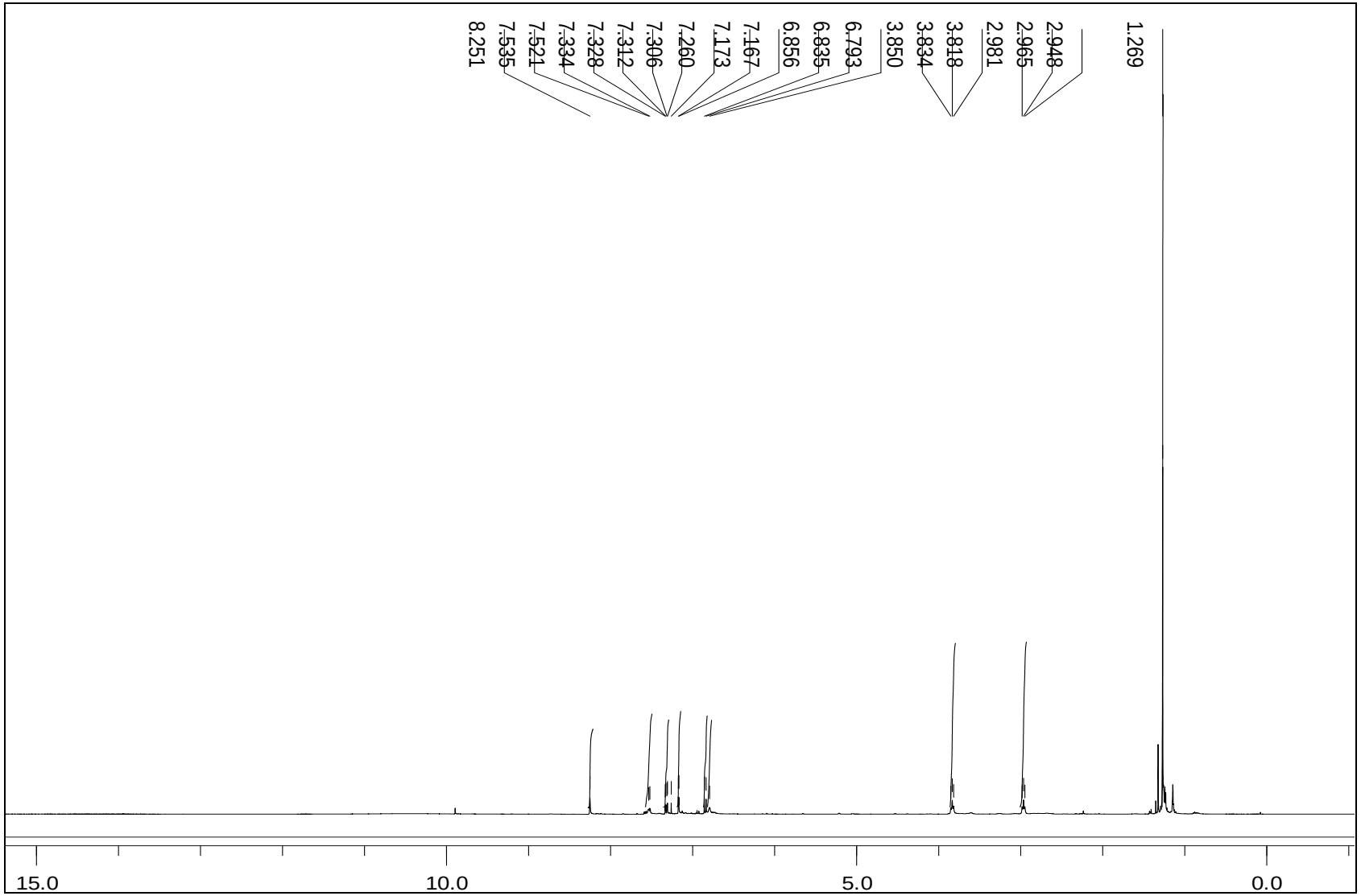

Figure 9: ^{1}H NMR spectrum of 4-tert-butyl-6-{[2-(1H-imidazol-4-yl)-ethylimino]-methyl}-phenol [**L10**]

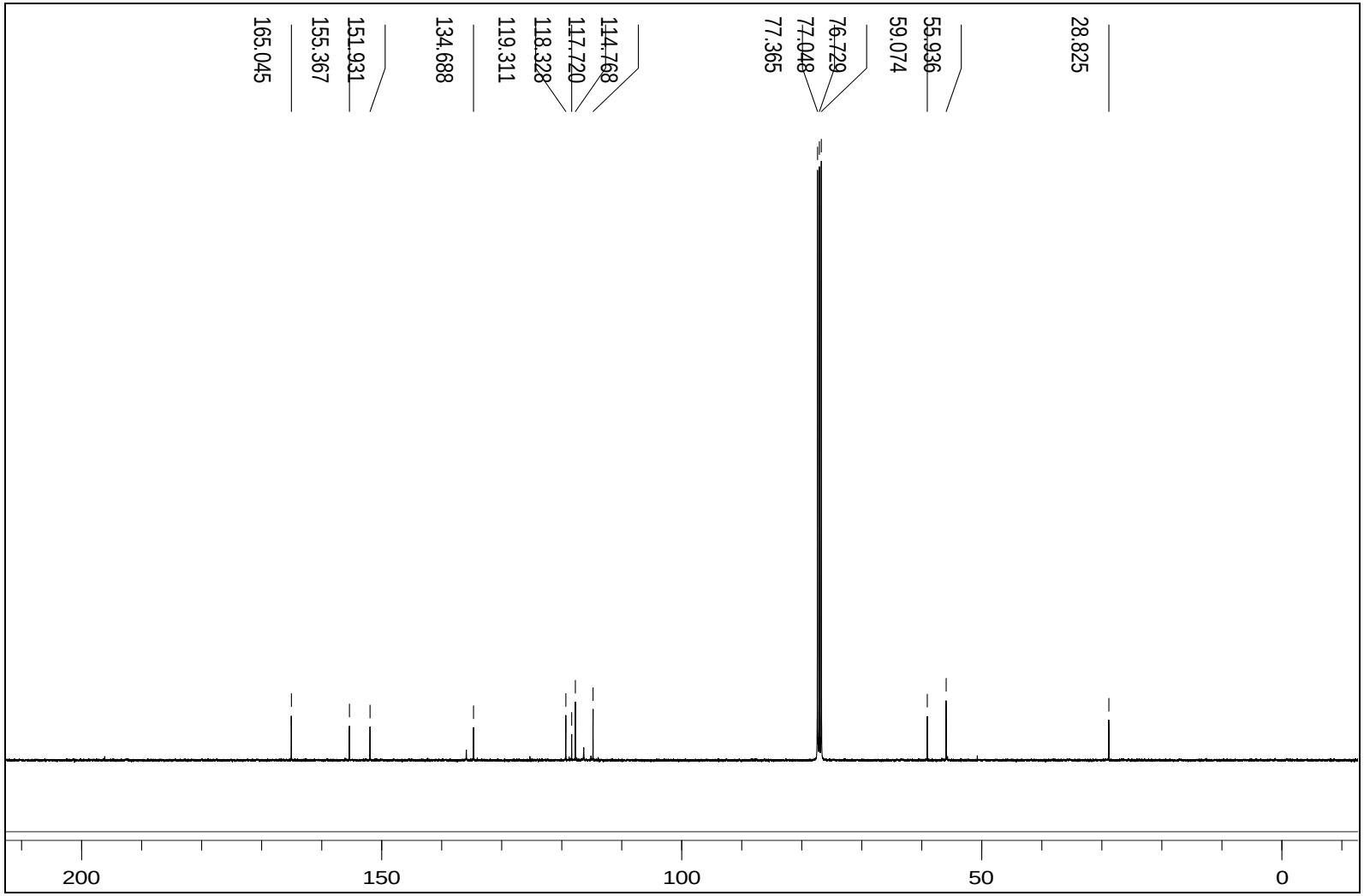

Figure 10: ^{13}C NMR spectrum of 4-methoxy-6-{[2-(1H-imidazol-4-yl)-ethylimino]-methyl}-phenol [**L2**]

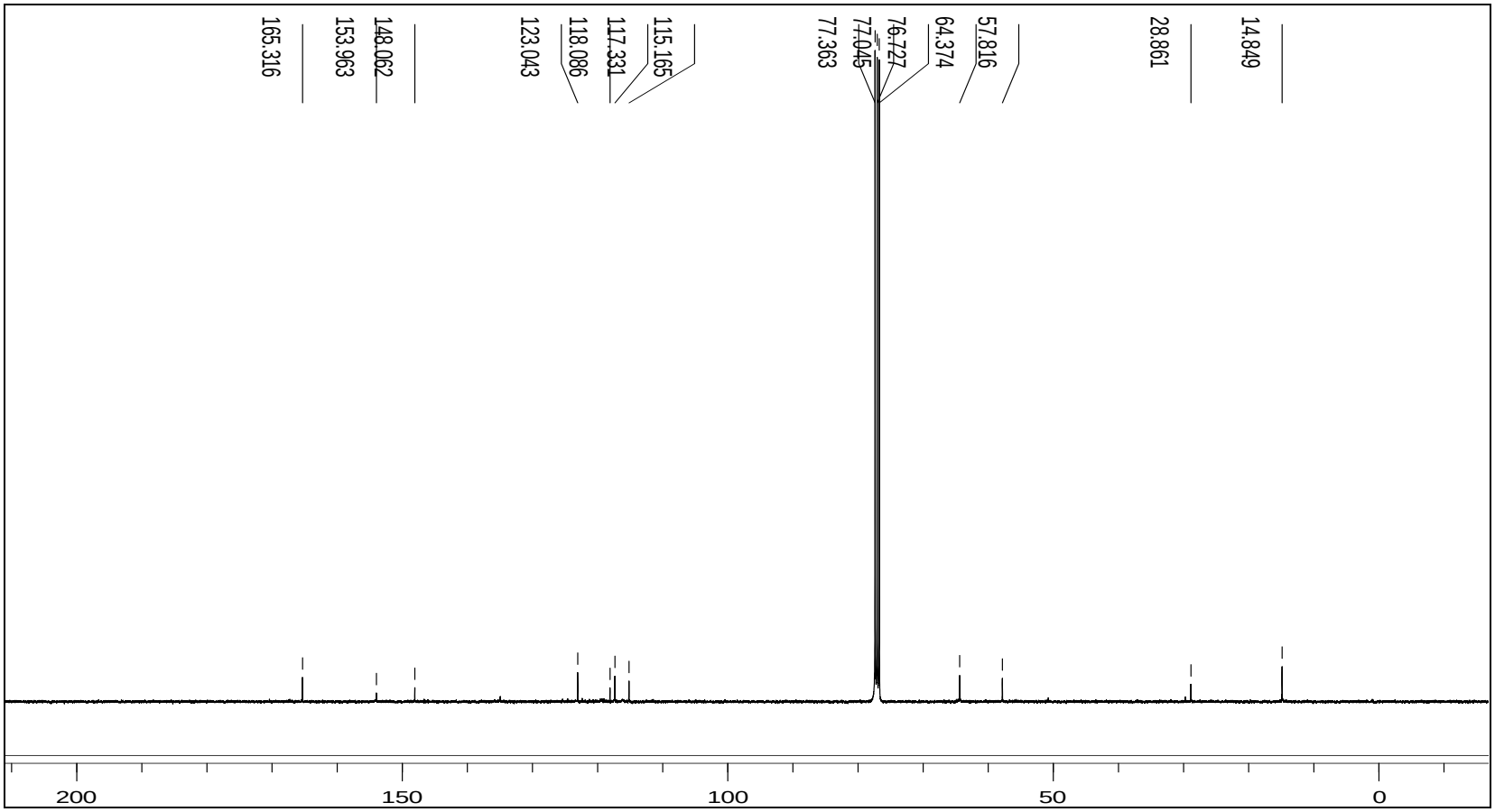

Figure 11: ^{13}C NMR spectrum of 2-ethoxy-6-{[2-(1H-imidazol-4-yl)-ethylimino]-methyl}-phenol [**L3**]

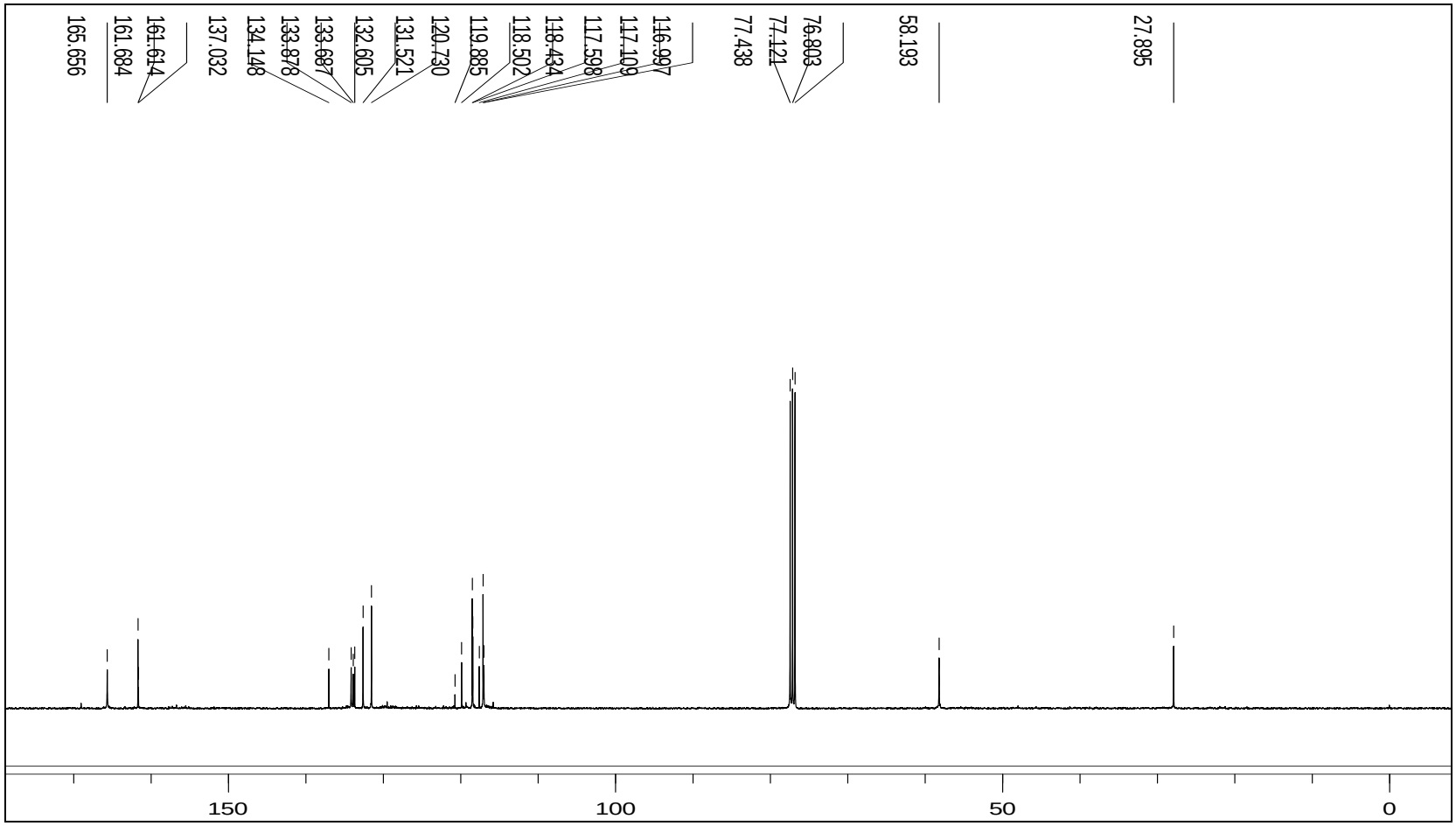

Figure 12: ^{13}C NMR spectrum of salicylaldehyde-2-{[2-(1H-imidazol-4-yl)-ethylimino]-methyl}-phenol [**L4**]

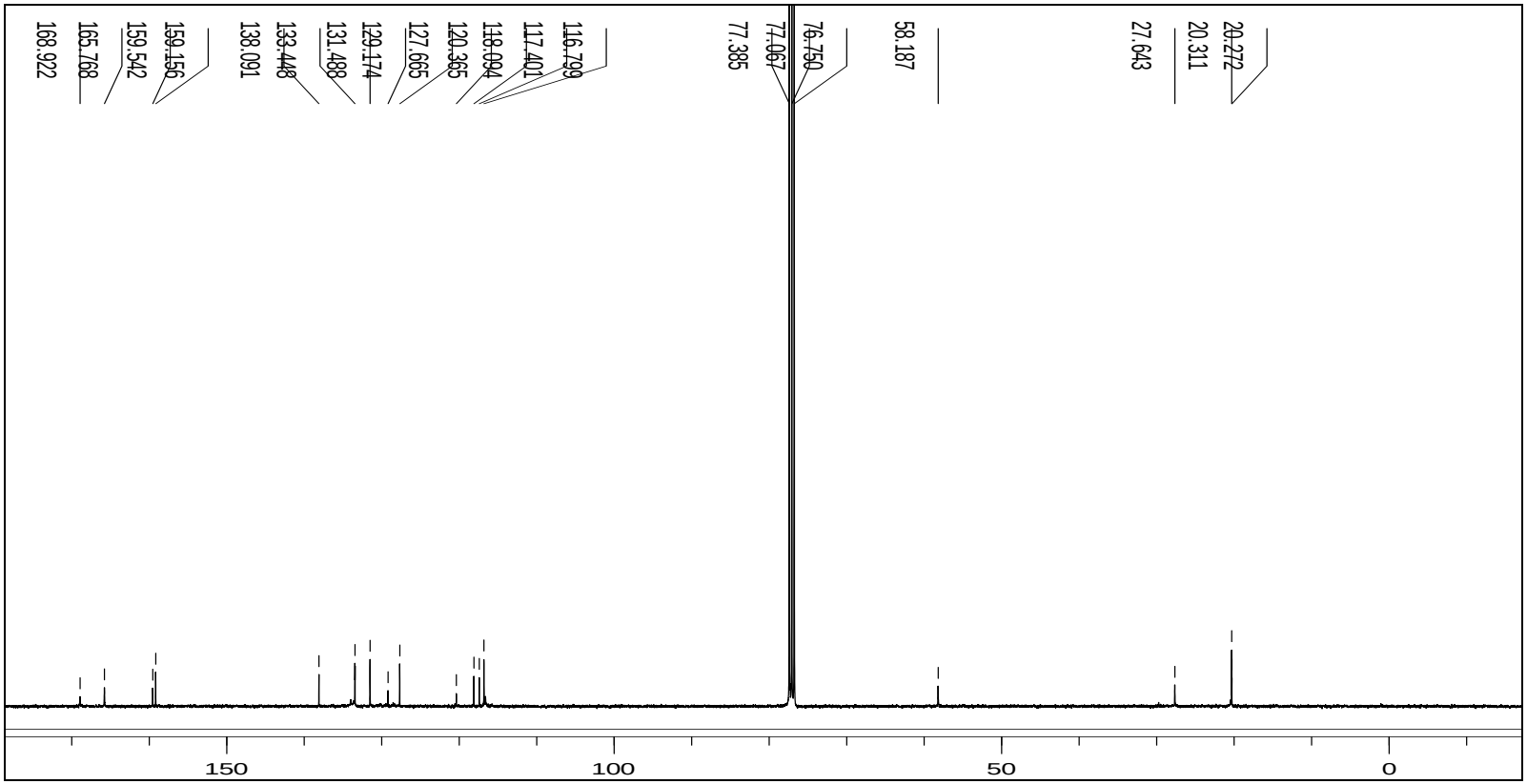

Figure 13: ^{13}C NMR spectrum of 4-methyl-6-{[2-(1H-imidazol-4-yl)-ethylimino]-methyl}-phenol [**L5**]

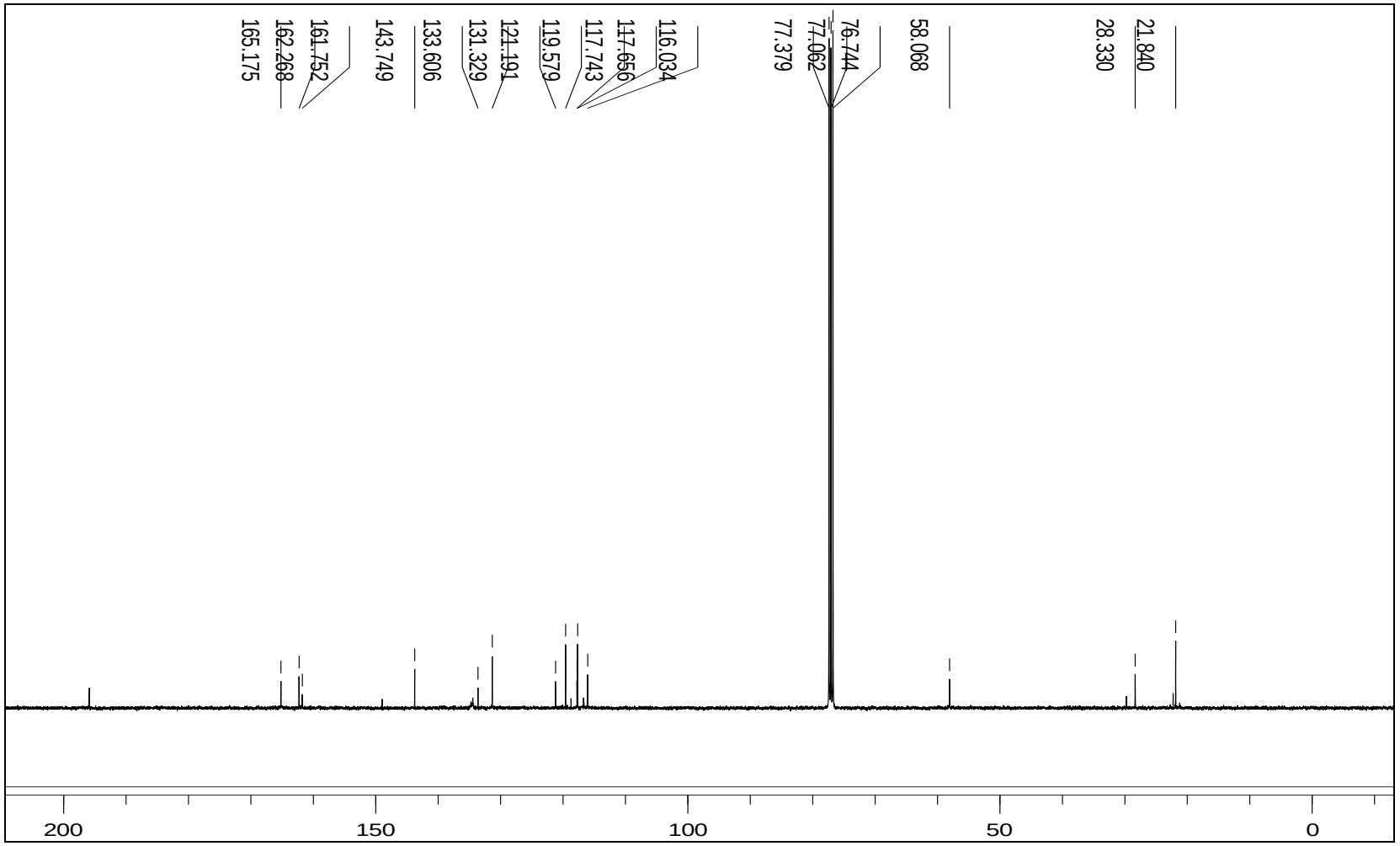

Figure 14: ^{13}C NMR spectrum of 3-methyl-6-{[2-(1H-imidazol-4-yl)-ethylimino]-methyl}-phenol [**L6**]

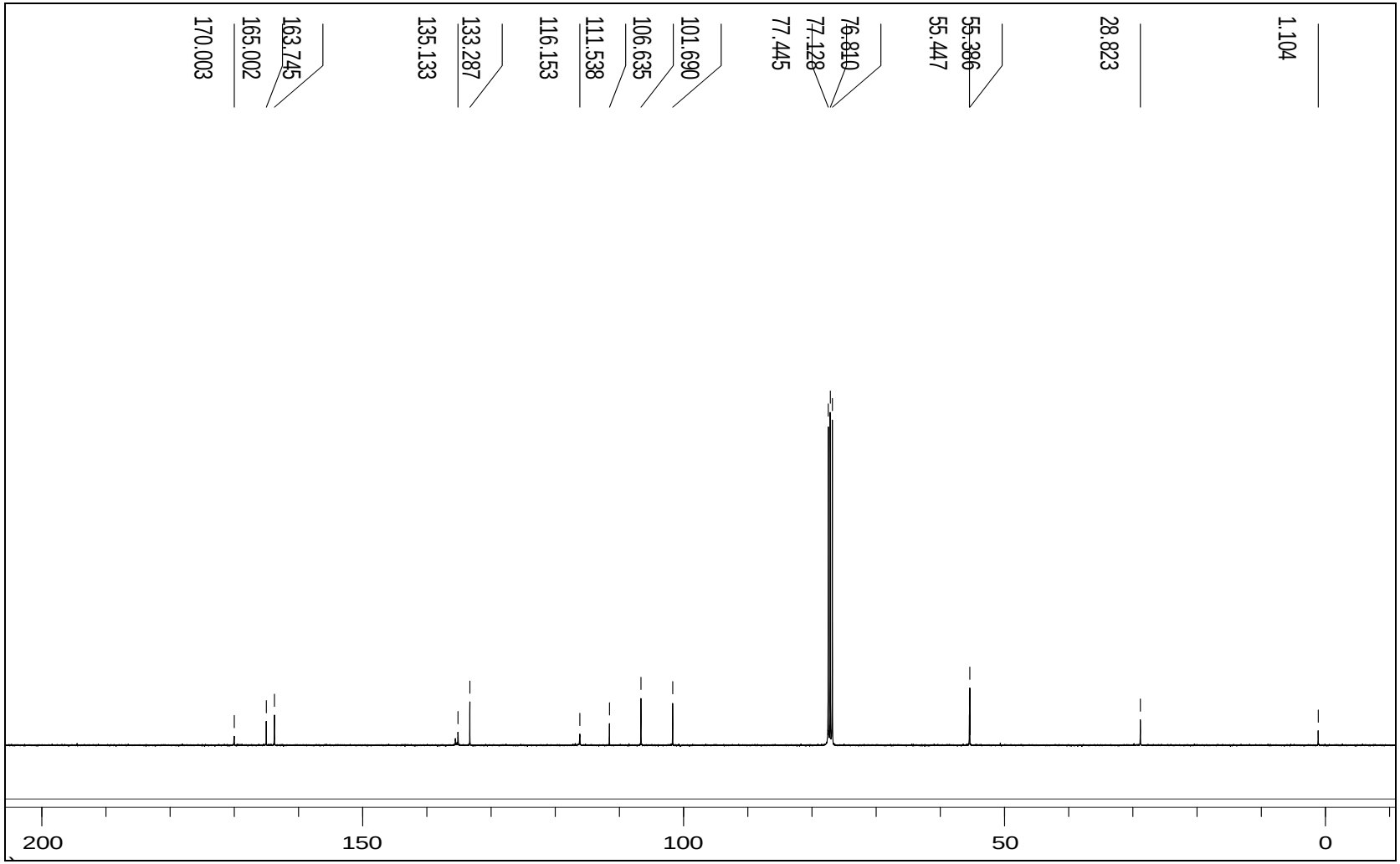

Figure 15: ^{13}C NMR spectrum of 3-methoxy-6-{[2-(1H-imidazol-4-yl)-ethylimino]-methyl}-phenol [**L7**]

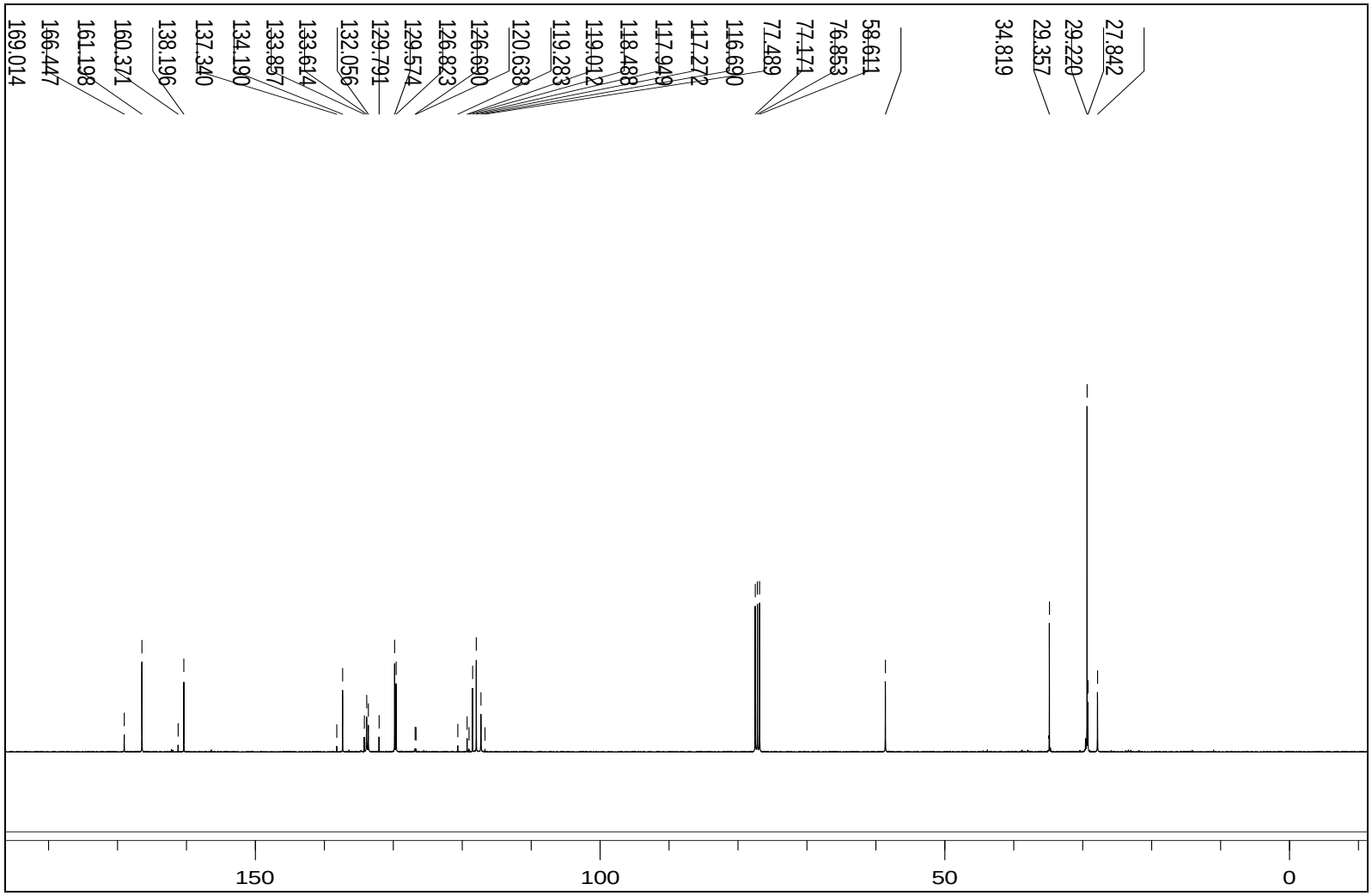

Figure 16: ^{13}C NMR spectrum of 2-tert-butyl-6-{[2-(1H-imidazol-4-yl)-ethylimino]-methyl}-phenol [**L8**]

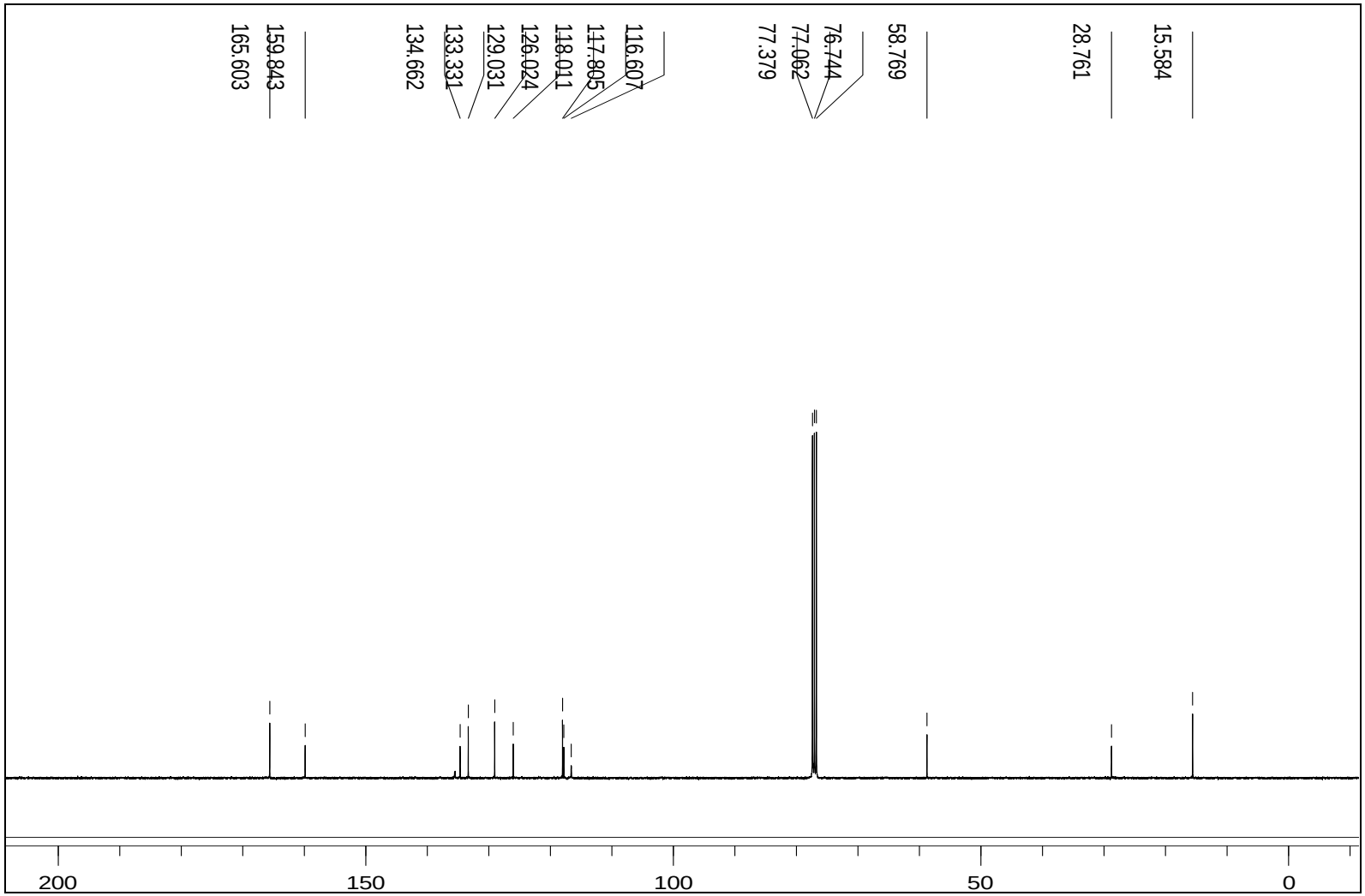

Figure 17: ^{13}C NMR spectrum of 2-methyl-6-{[2-(1H-imidazol-4-yl)-ethylimino]-methyl}-phenol [**L9**]

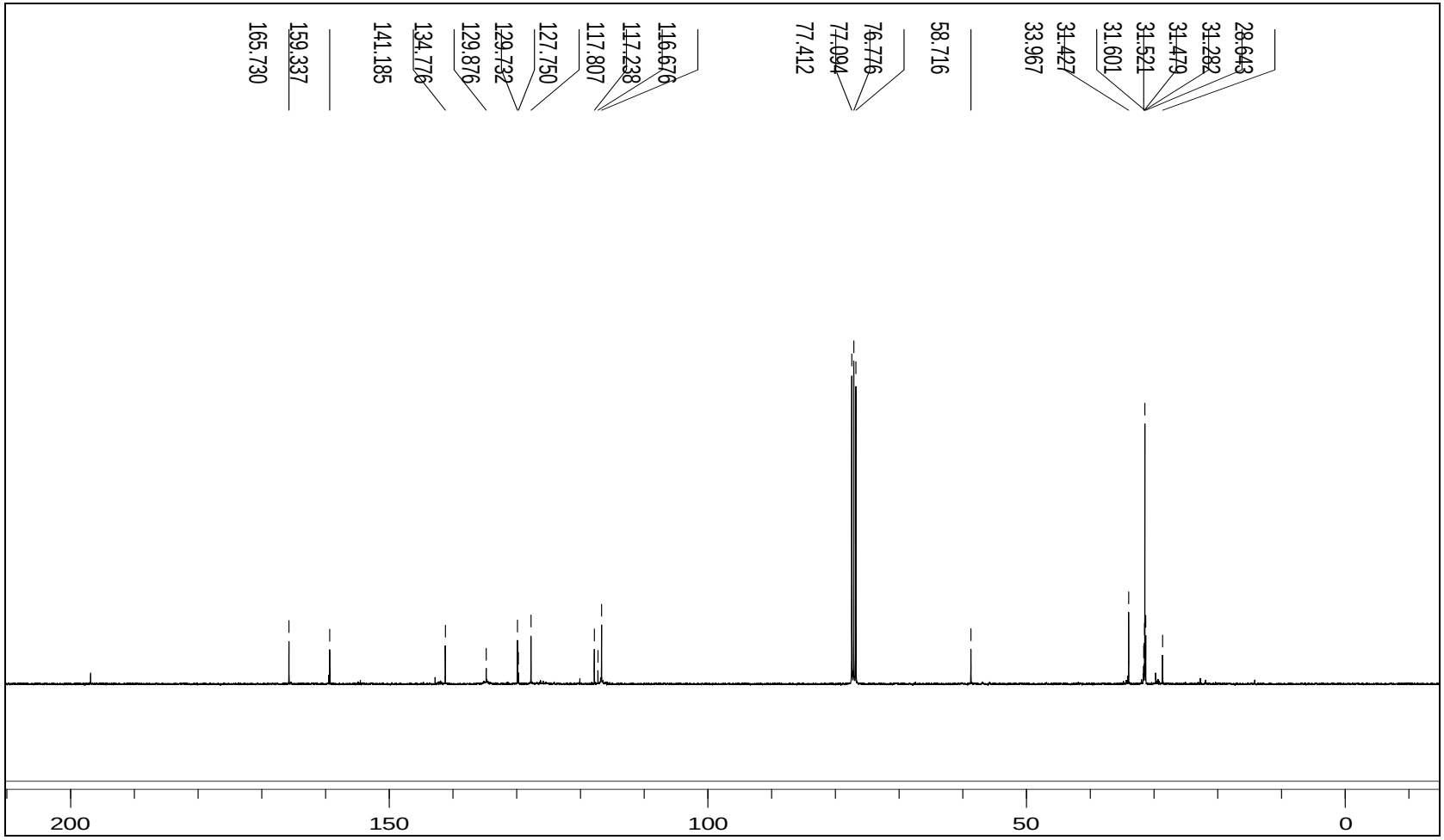

Figure 18: ^{13}C NMR spectrum of 4-tert-butyl-6-{[2-(1H-imidazol-4-yl)-ethylimino]-methyl}-phenol [**L10**]

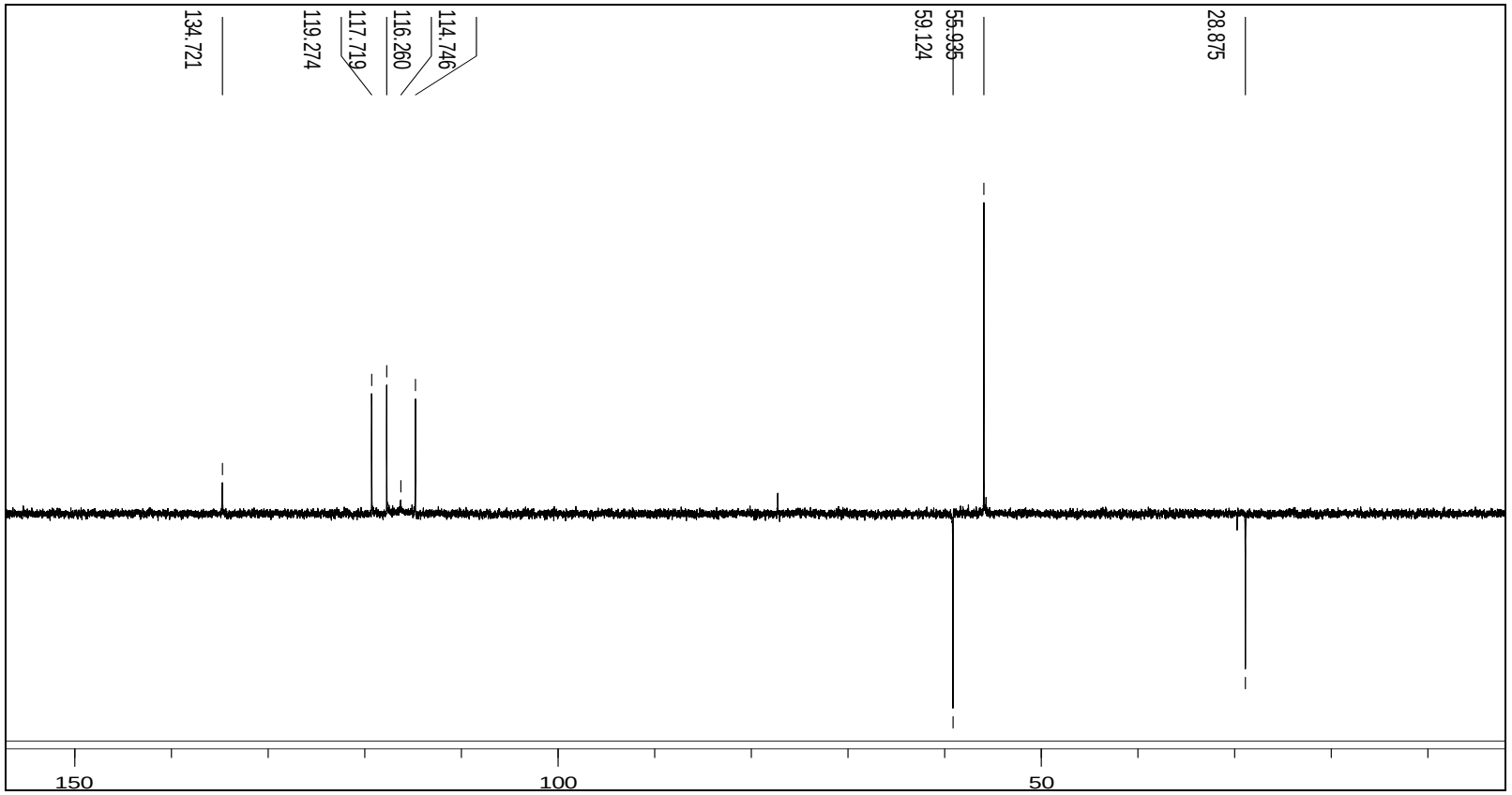

Figure 19: 135 DEPT spectrum of 4-methoxy-6-{[2-(1H-imidazol-4-yl)-ethylimino]-methyl}-phenol [**L2**]

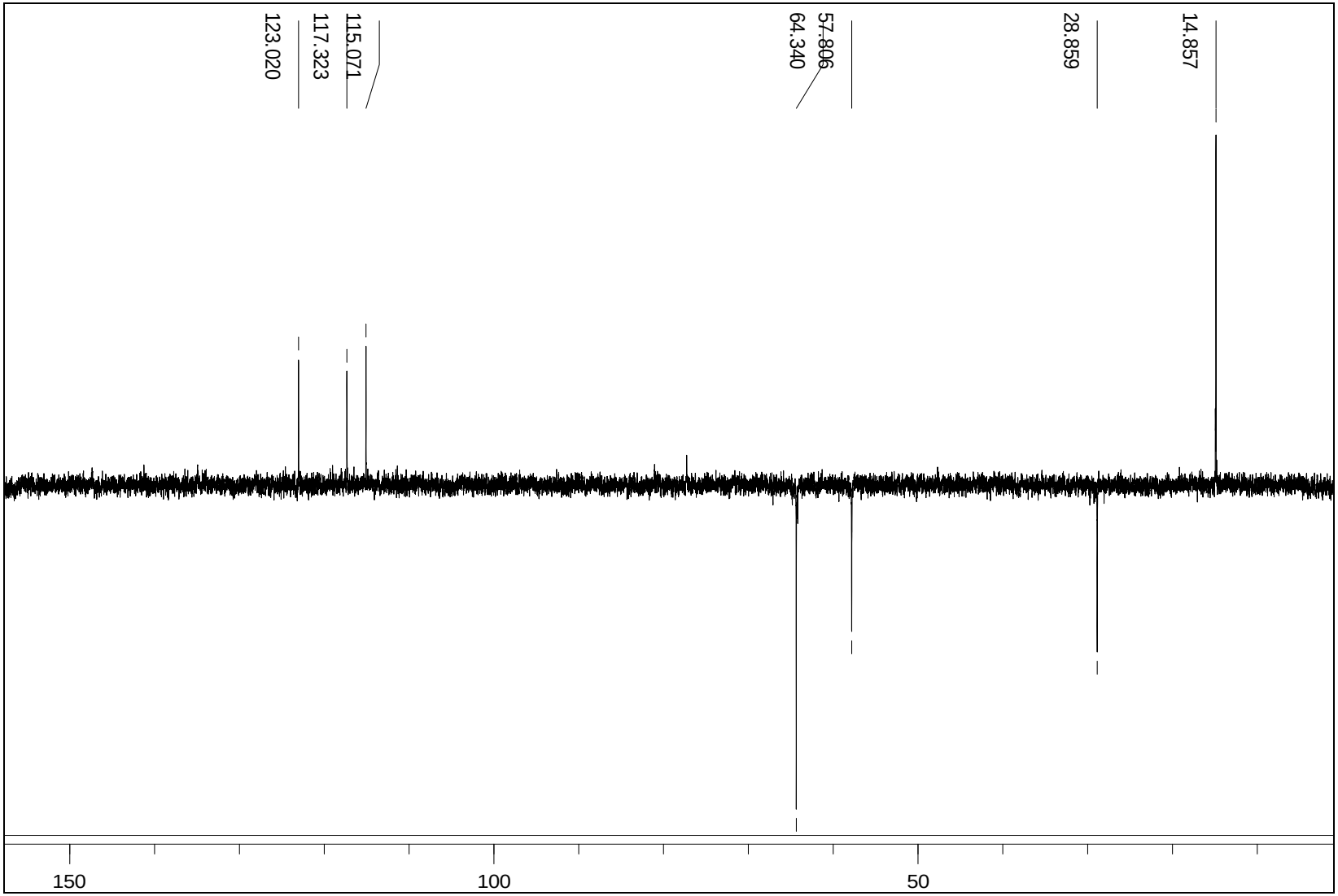

Figure 20: 135 DEPT spectrum of 2-ethoxy-6-{[2-(1H-imidazol-4-yl)-ethylimino]-methyl}-phenol [**L3**]

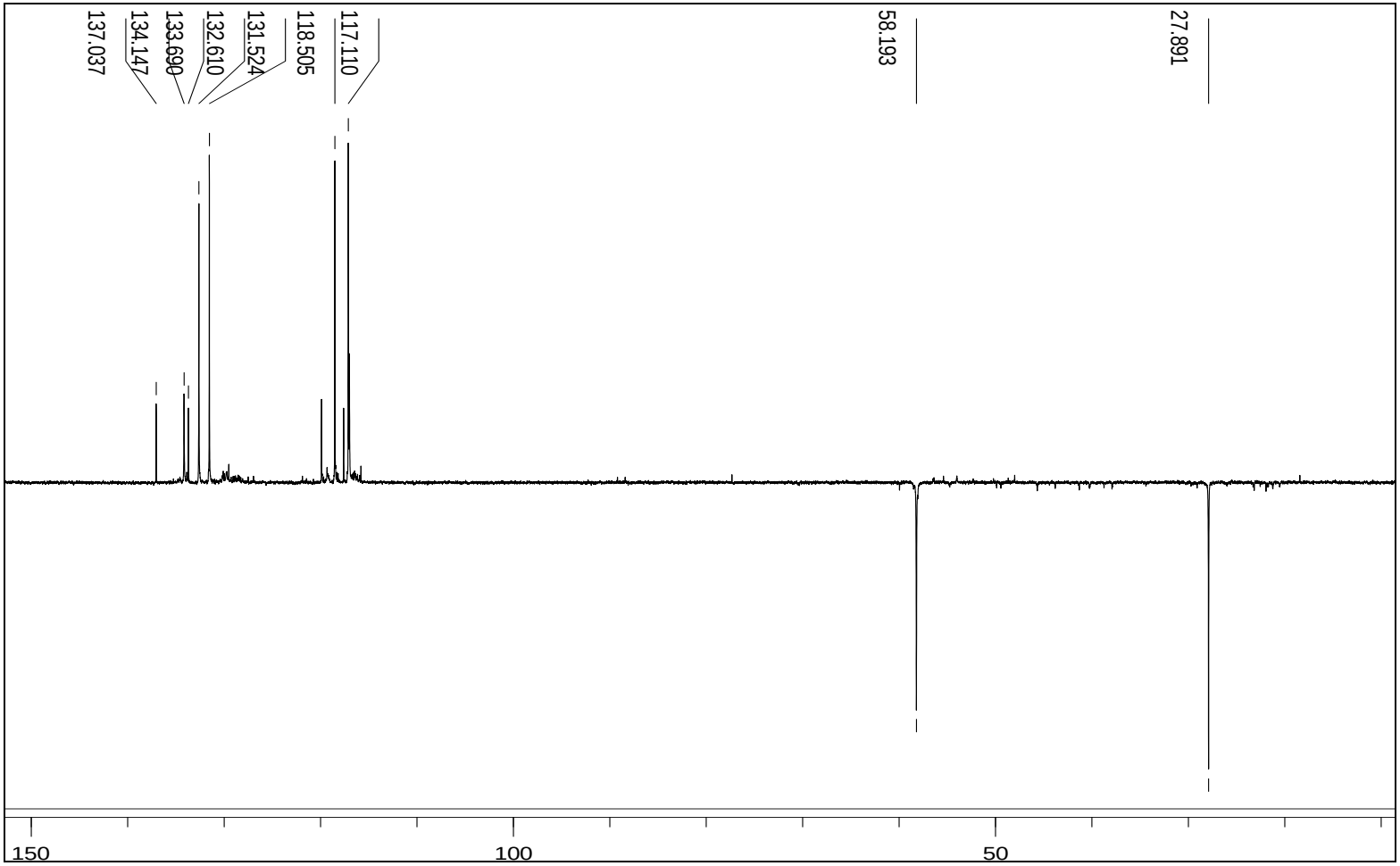

Figure 21: 135 DEPT spectrum of salicylaldehyde-2-{[2-(1H-imidazol-4-yl)-ethylimino]-methyl}-phenol [**L4**]

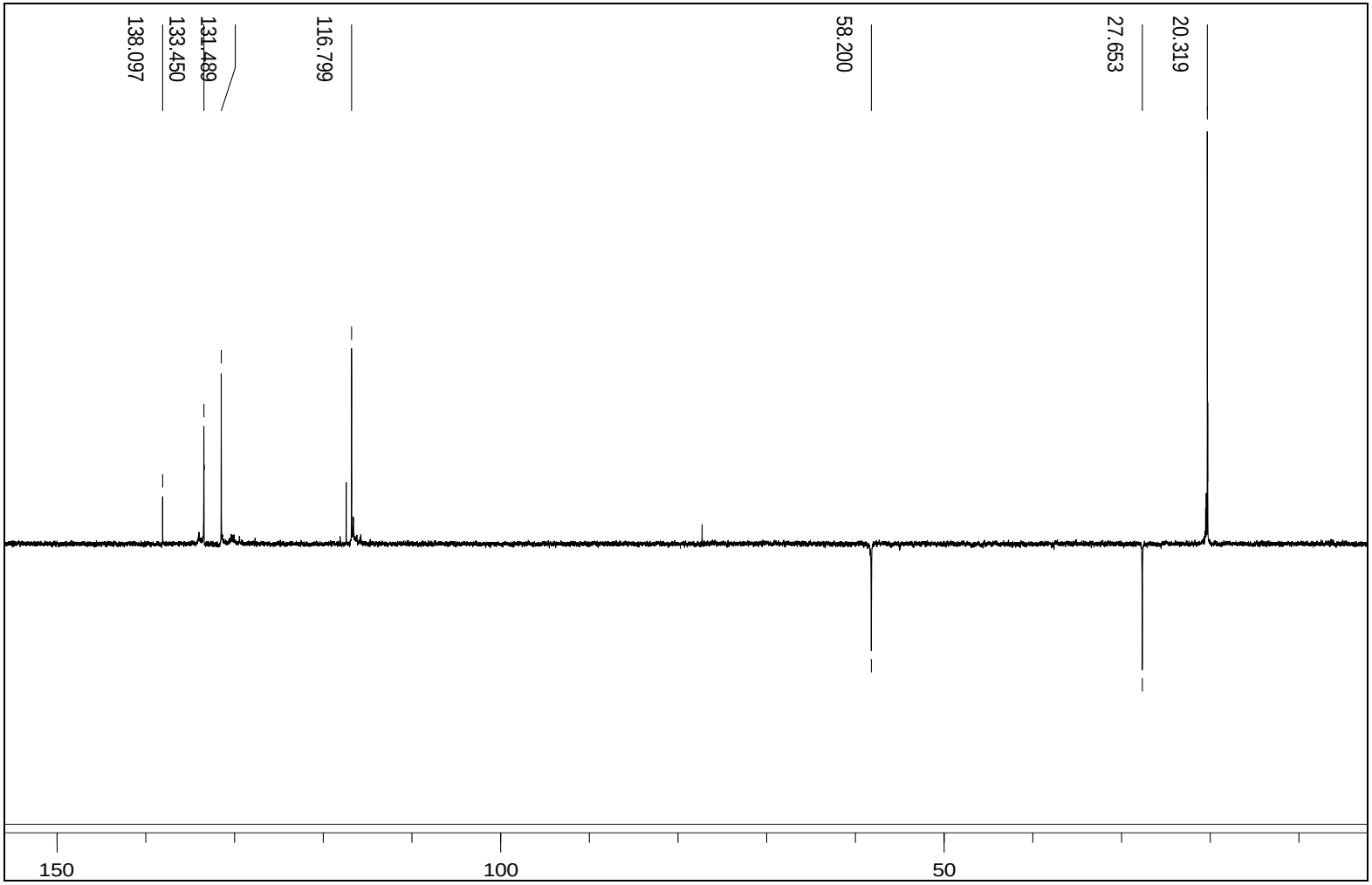

Figure 22: 135 DEPT spectrum of 4-methyl-6-{[2-(1H-imidazol-4-yl)-ethylimino]-methyl}-phenol [**L5**]

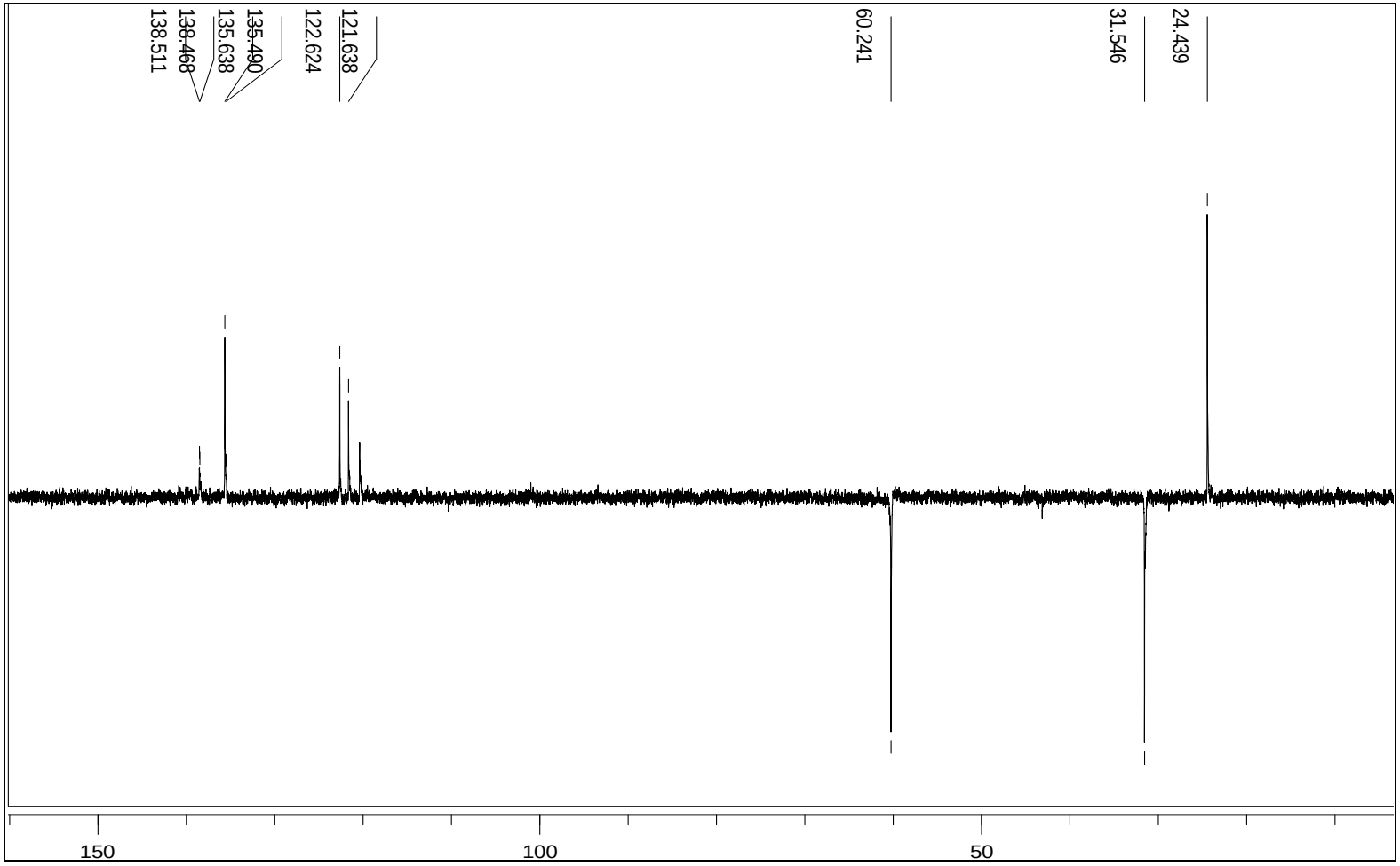

Figure 23: 135 DEPT spectrum of 3-methyl-6-{[2-(1H-imidazol-4-yl)-ethylimino]-methyl}-phenol [**L6**]

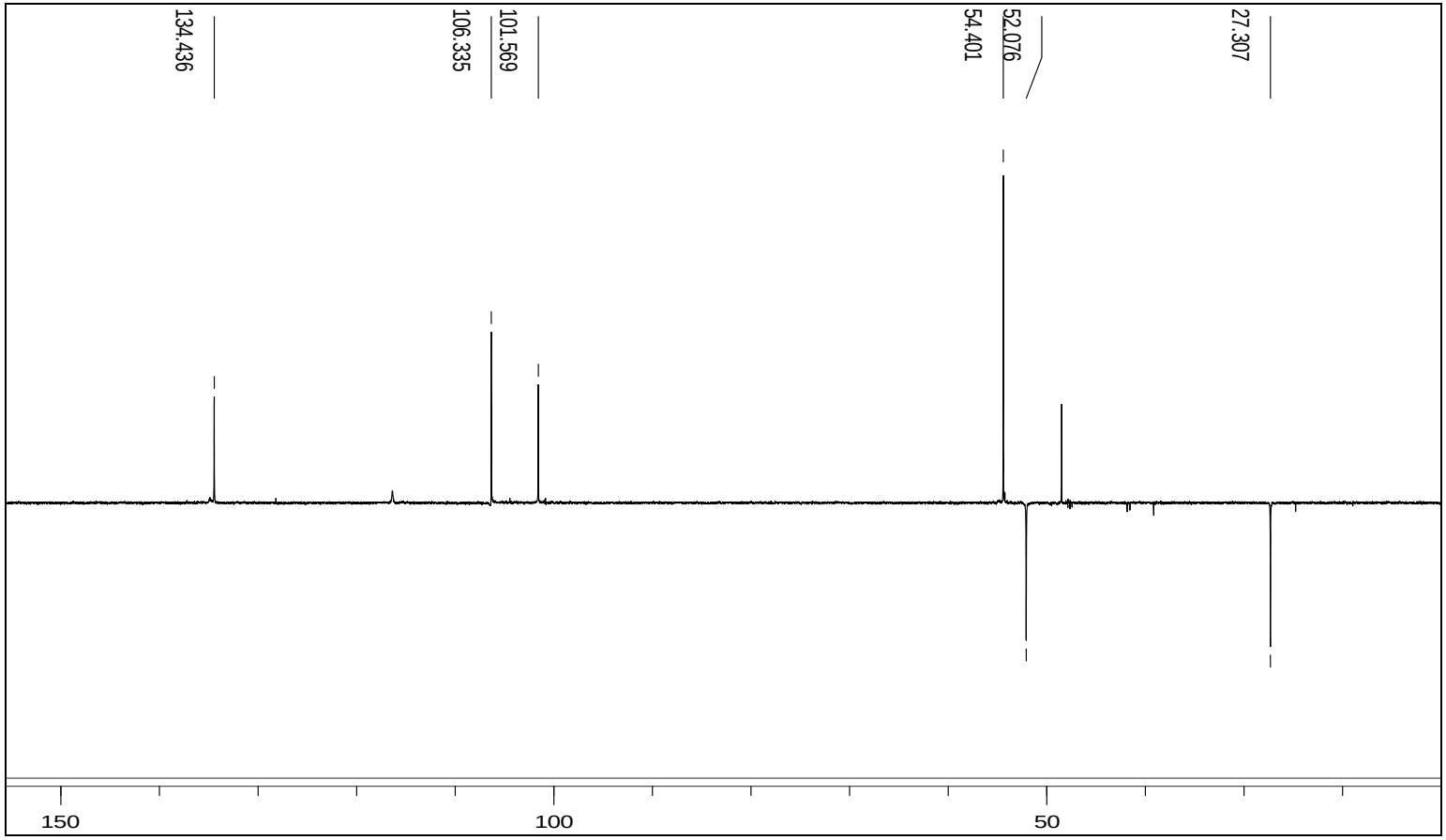

Figure 24: 135 DEPT spectrum of 3-methoxy-6-{[2-(1H-imidazol-4-yl)-ethylimino]-methyl}-phenol [**L7**]

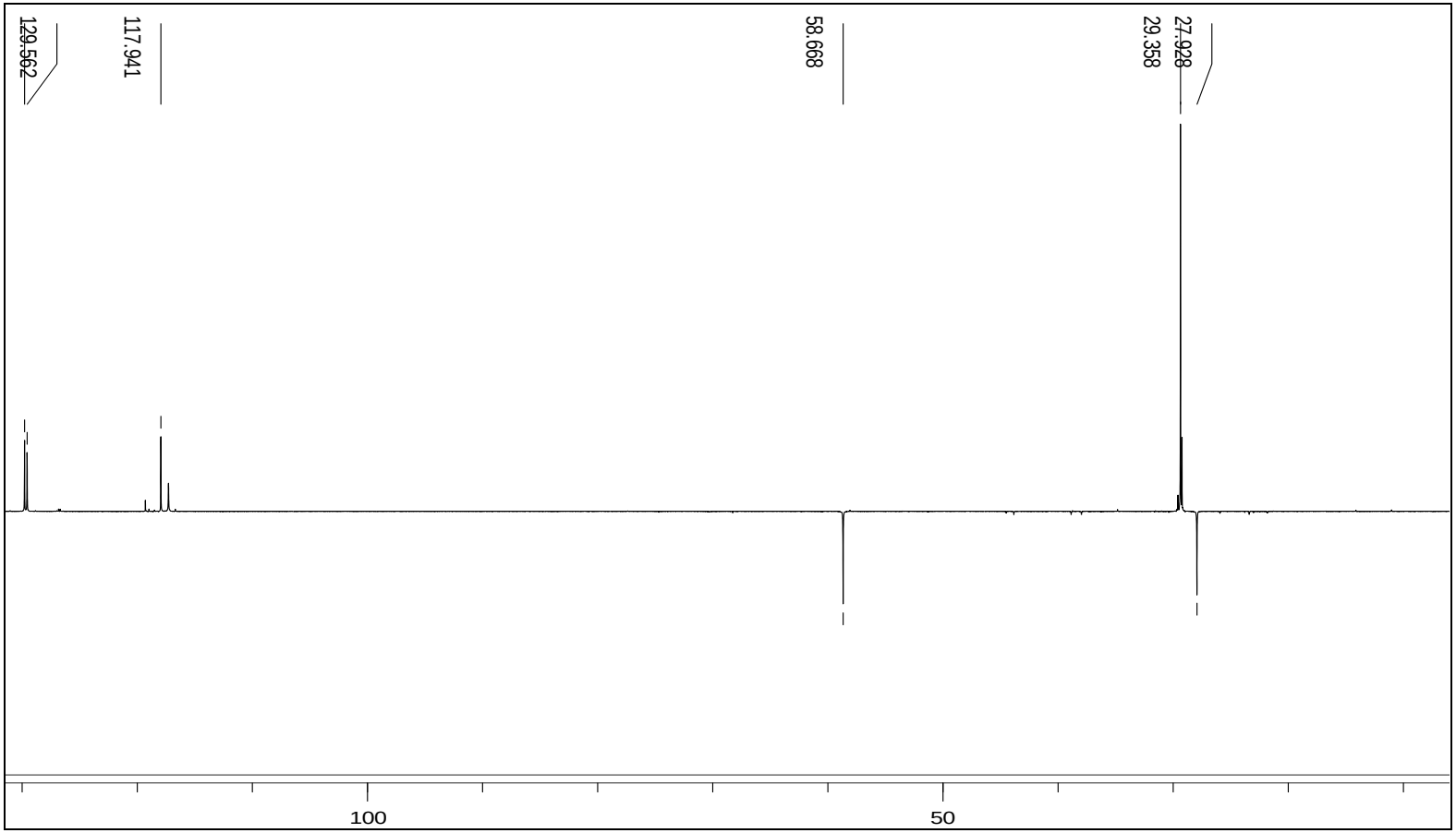

Figure 25: 135 DEPT spectrum of 2-tert-butyl-6-{[2-(1H-imidazol-4-yl)-ethylimino]-methyl}-phenol [**L8**]

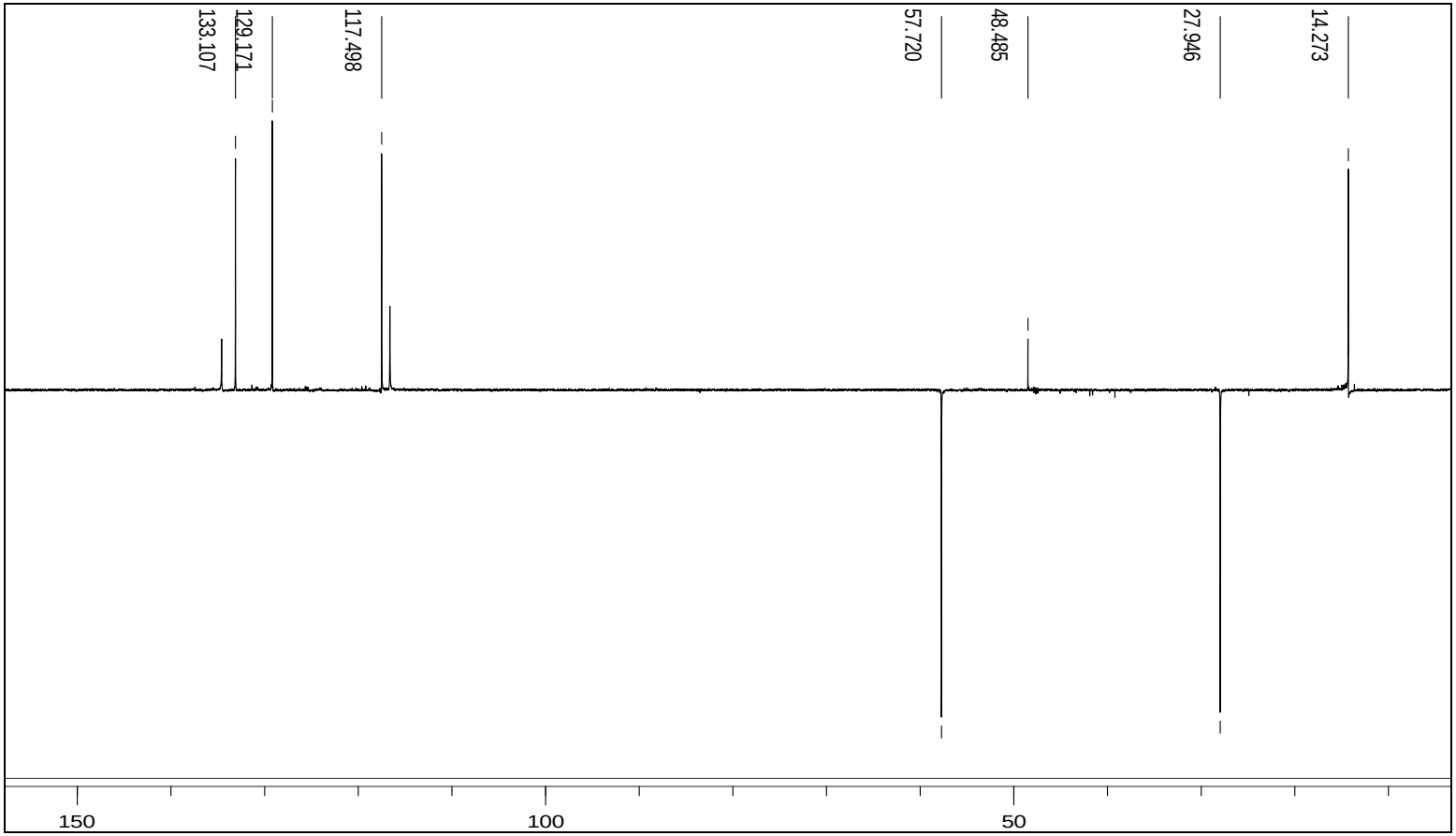

Figure 26: 135 DEPT spectrum of 2-methyl-6-{[2-(1H-imidazol-4-yl)-ethylimino]-methyl}-phenol [**L9**]

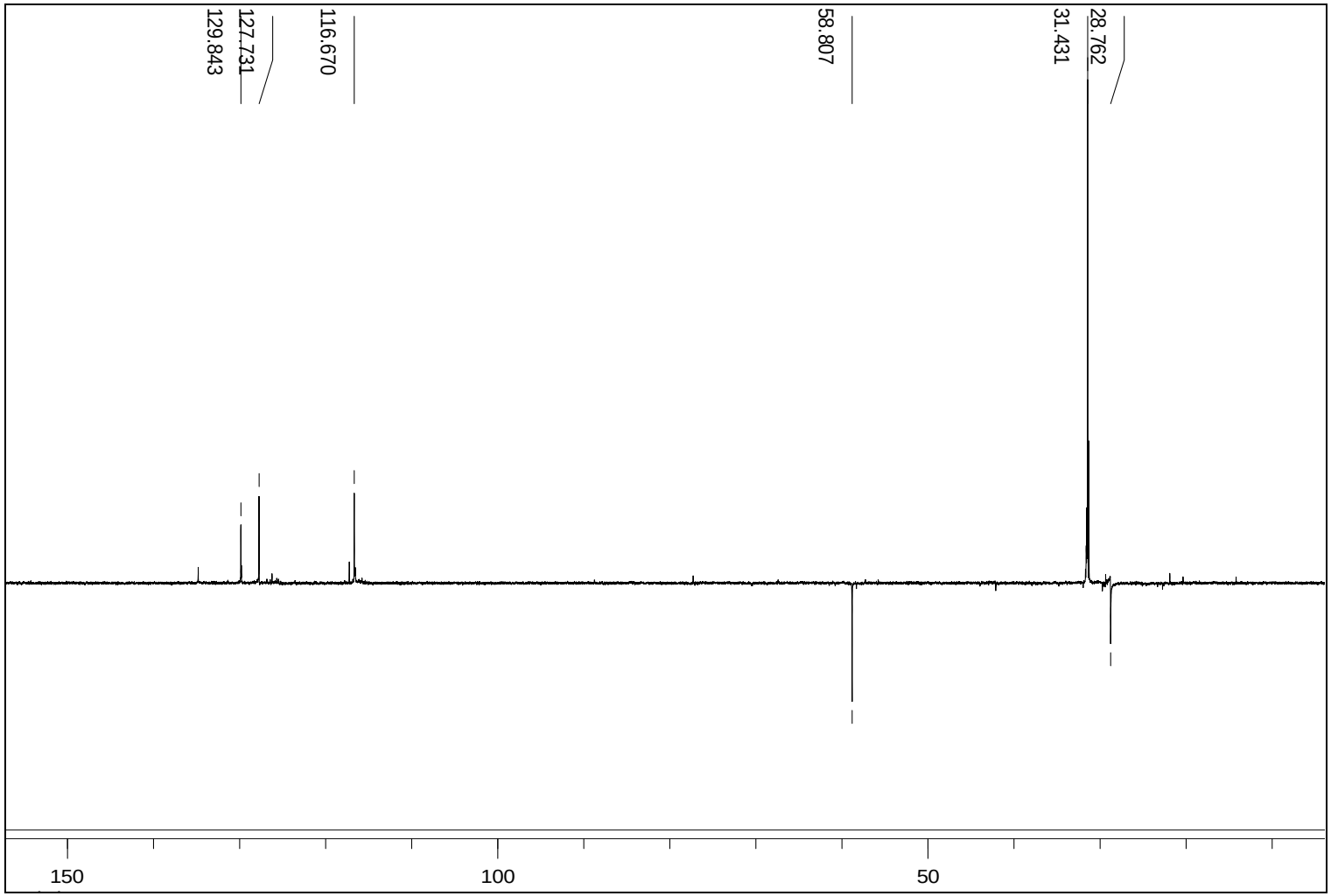

Figure 27: 135 DEPT spectrum of 4-tert-butyl-6-{[2-(1H-imidazol-4-yl)-ethylimino]-methyl}-phenol [**L10**]

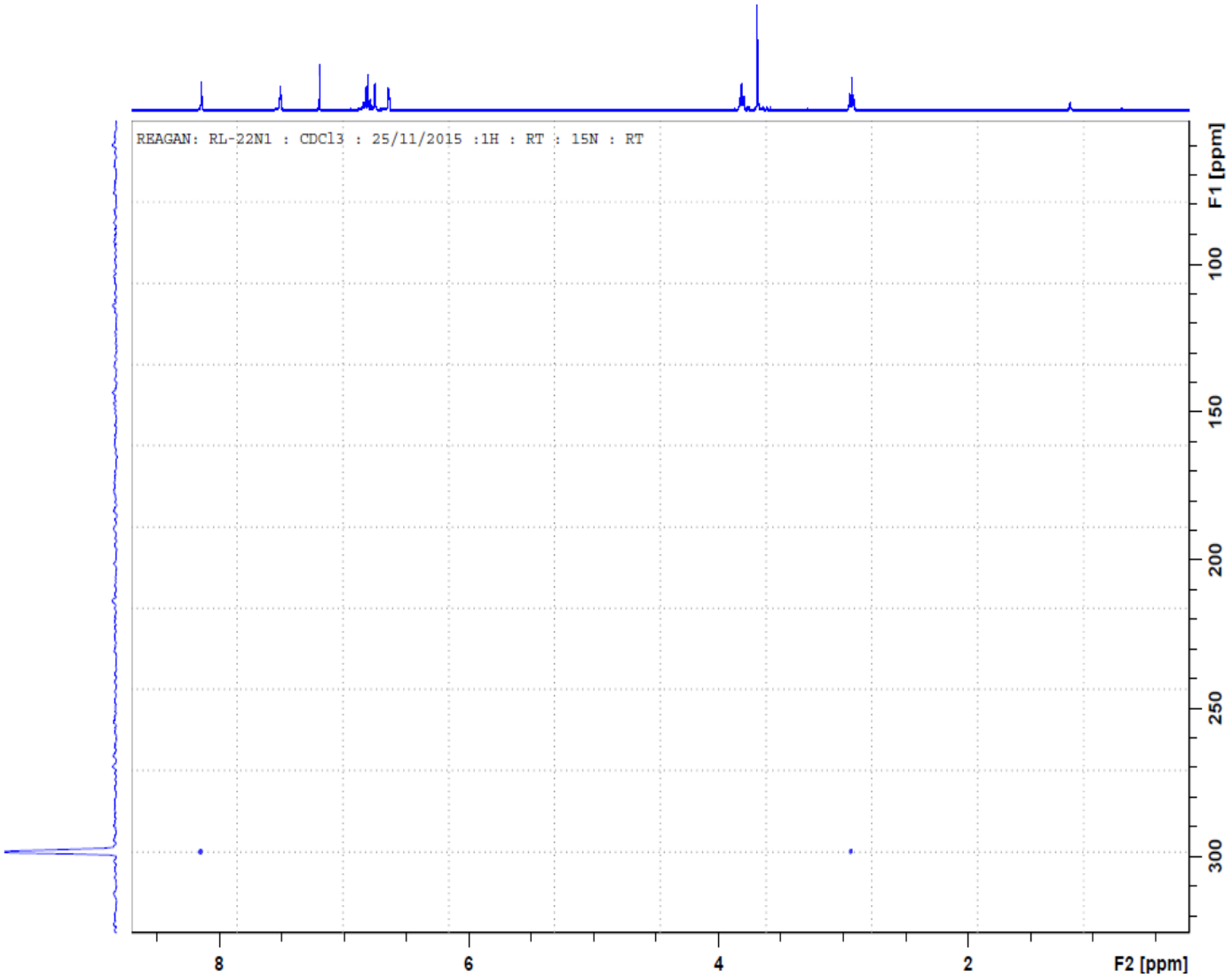

Figure 28: ^{15}N NMR spectrum of 4-methoxy-6-{[2-(1H-imidazol-4-yl)-ethylimino]-methyl}-phenol [**L2**]

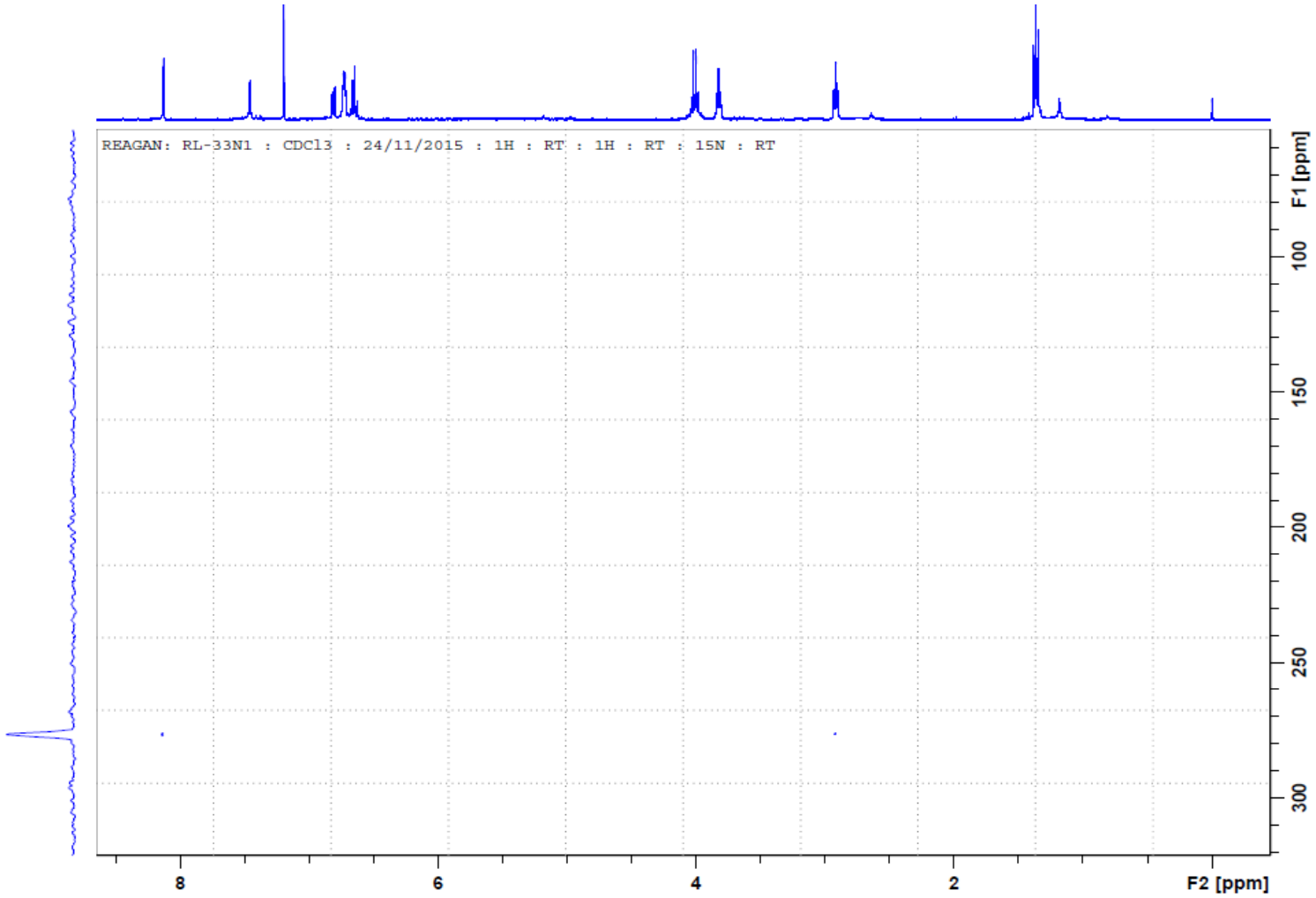

Figure 29: ^{15}N NMR spectrum of 2-ethoxy-6-{[2-(1H-imidazol-4-yl)-ethylimino]-methyl}-phenol [**L3**]

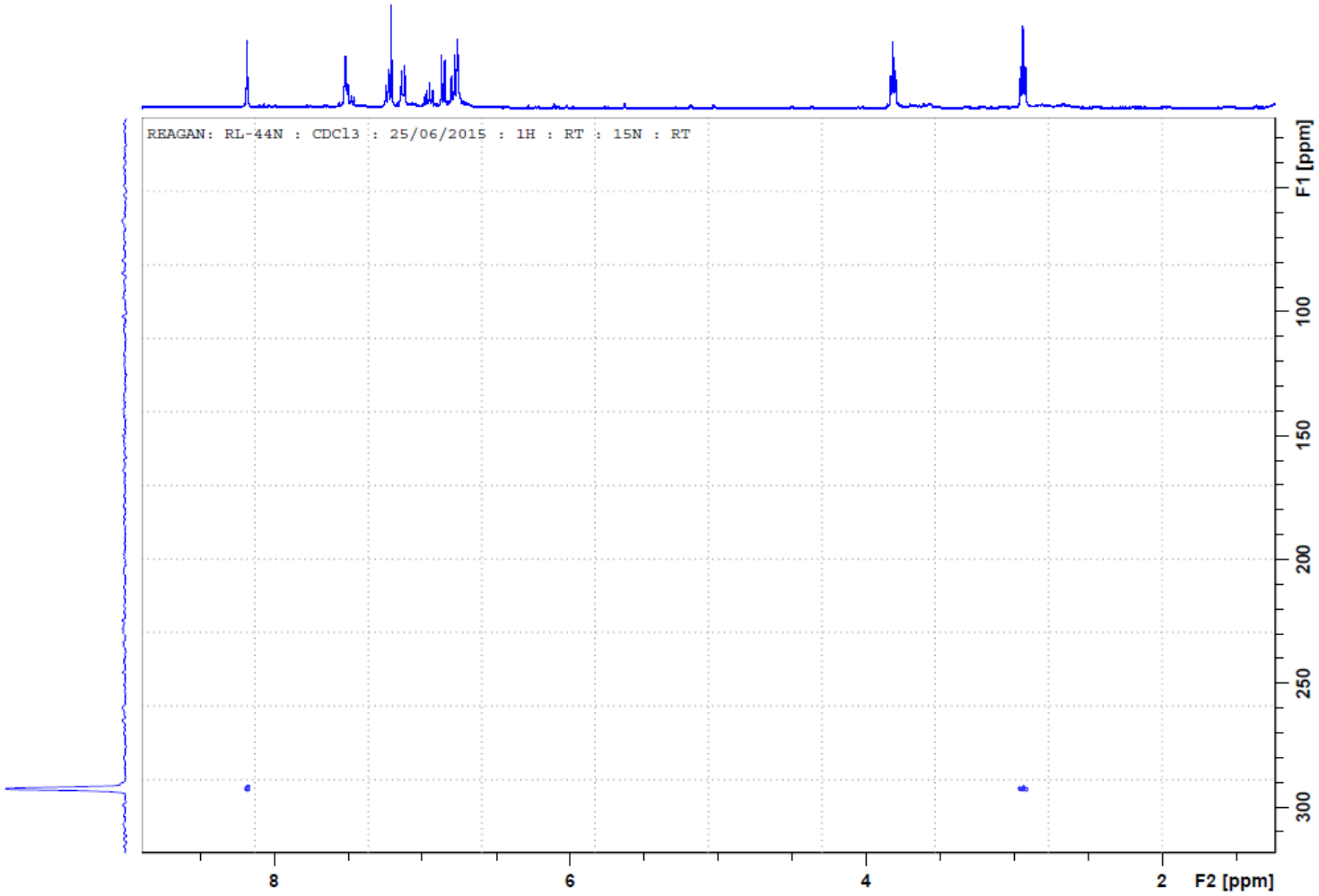

Figure 30: ^{15}N NMR spectrum of salicylaldehyde-2-{[2-(1H-imidazol-4-yl)-ethylimino]-methyl}-phenol [**L4**]

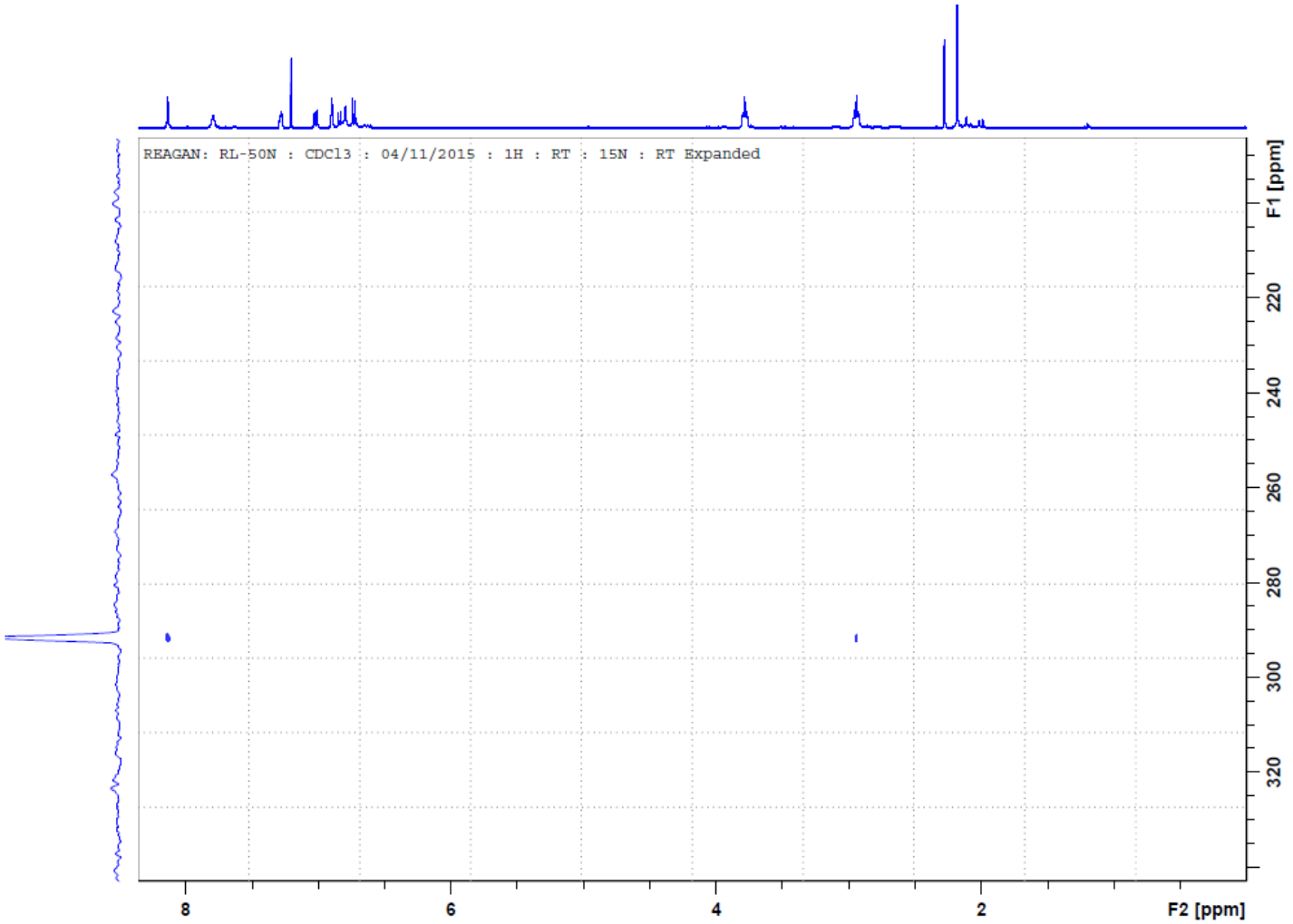

Figure 31: ^{15}N NMR spectrum of 4-methyl-6-{[2-(1H-imidazol-4-yl)-ethylimino]-methyl}-phenol [**L5**]

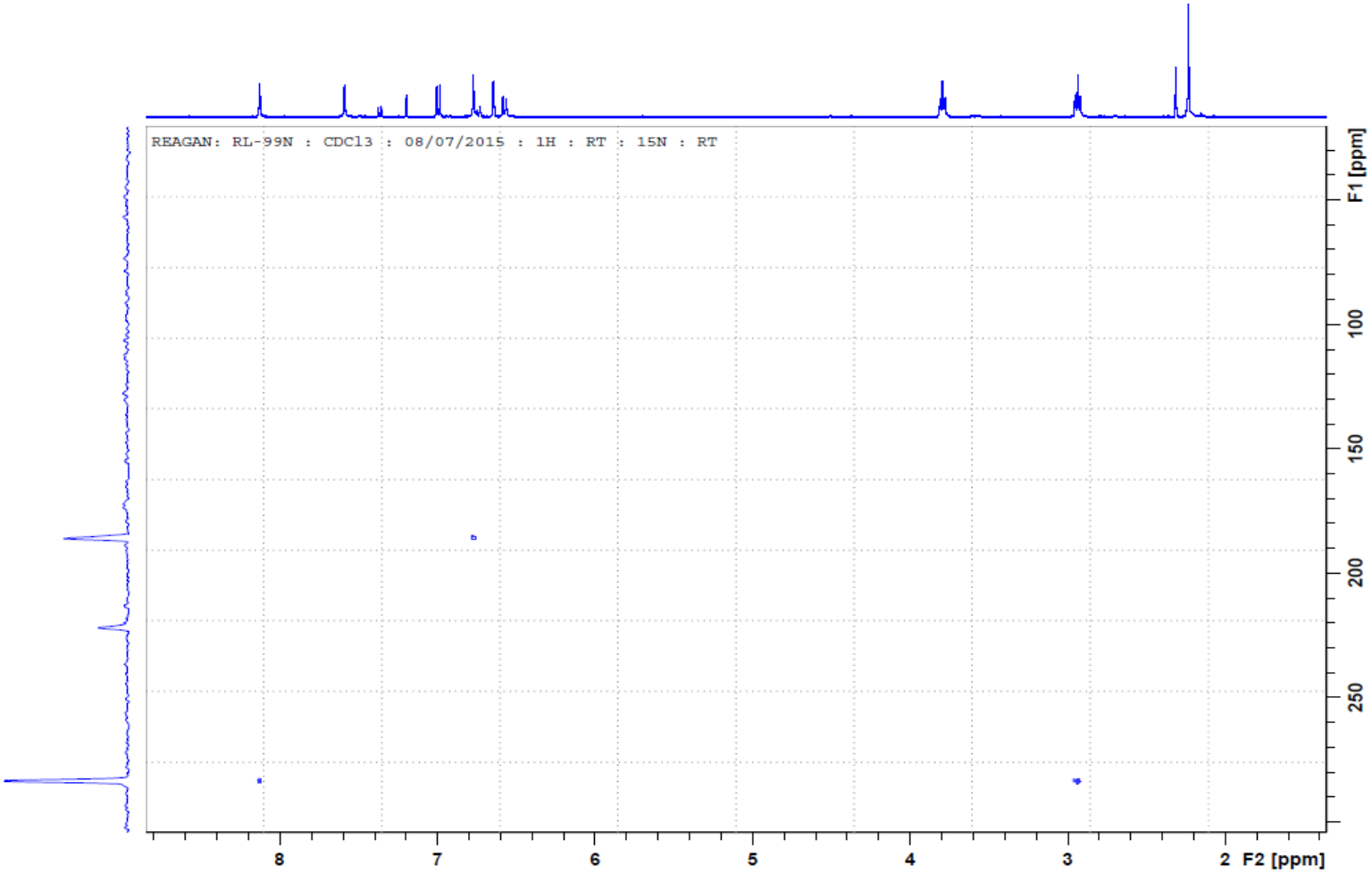

Figure 32: ^{15}N NMR spectrum of 3-methyl-6-{[2-(1H-imidazol-4-yl)-ethylimino]-methyl}-phenol [**L6**]

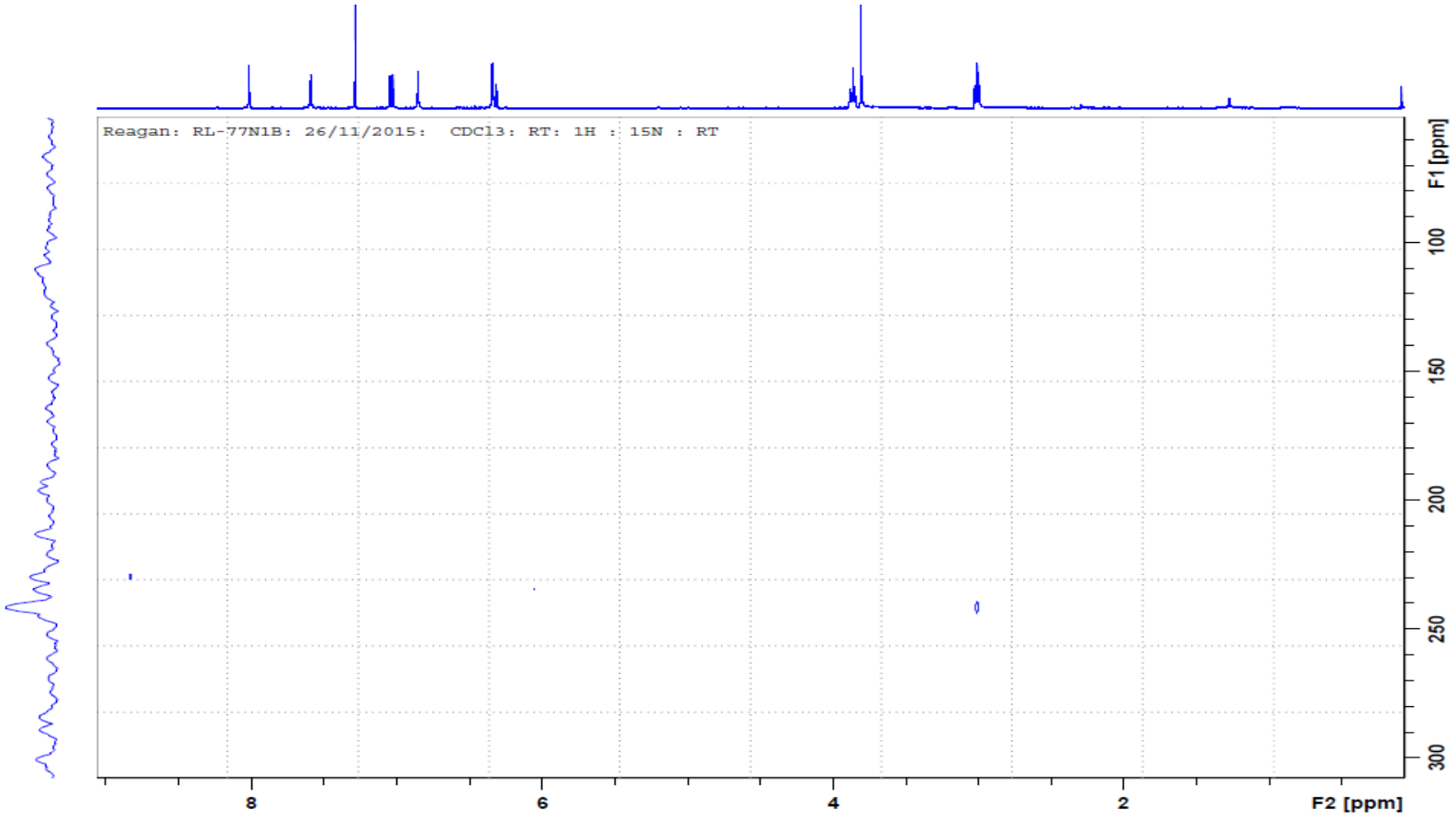

Figure 33: ^{15}N NMR spectrum of 3-methoxy-6-{[2-(1H-imidazol-4-yl)-ethylimino]-methyl}-phenol [**L7**]

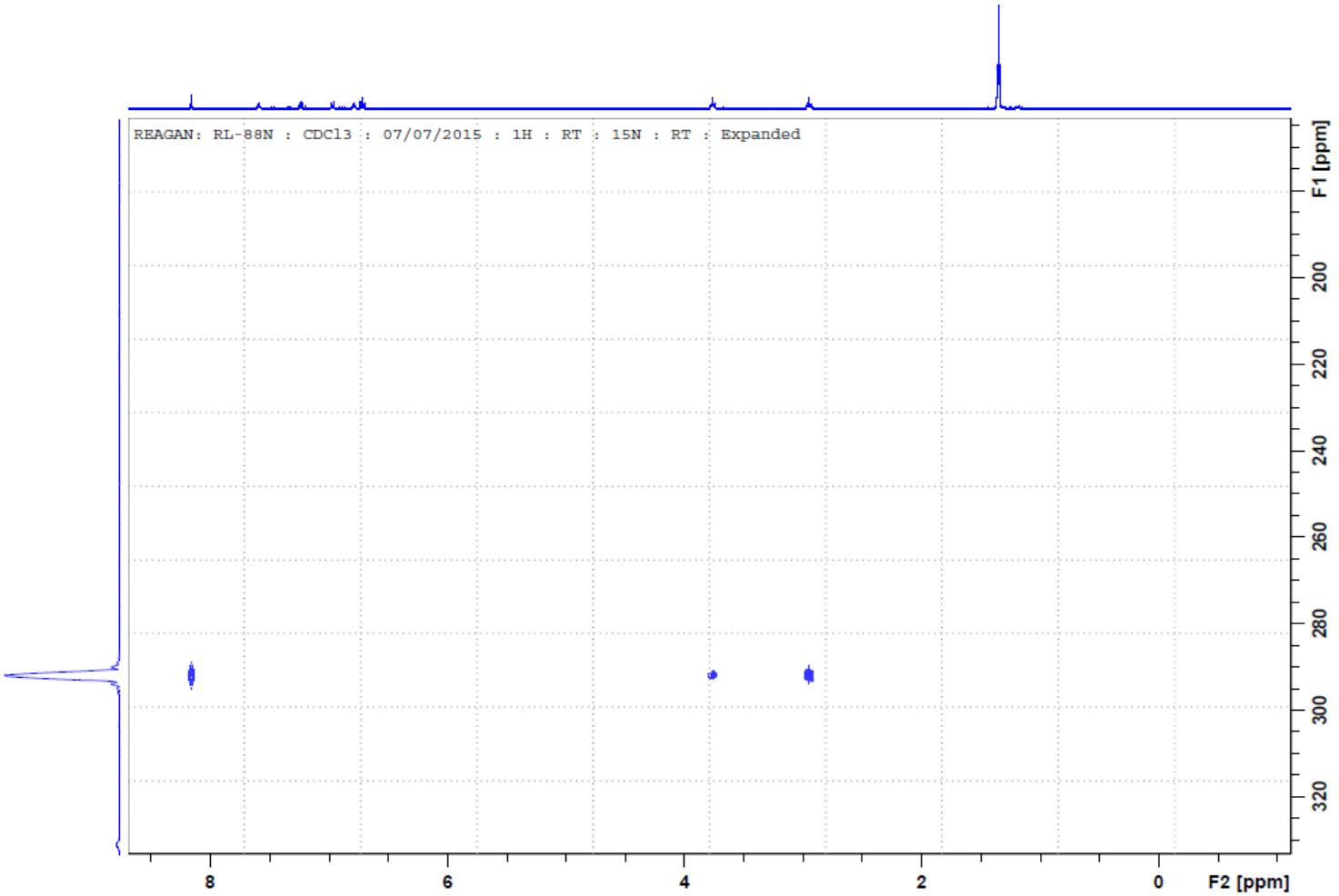

Figure 34: ^{15}N NMR spectrum of 2-tert-butyl-6-{[2-(1H-imidazol-4-yl)-ethylimino]-methyl}-phenol [**L8**]

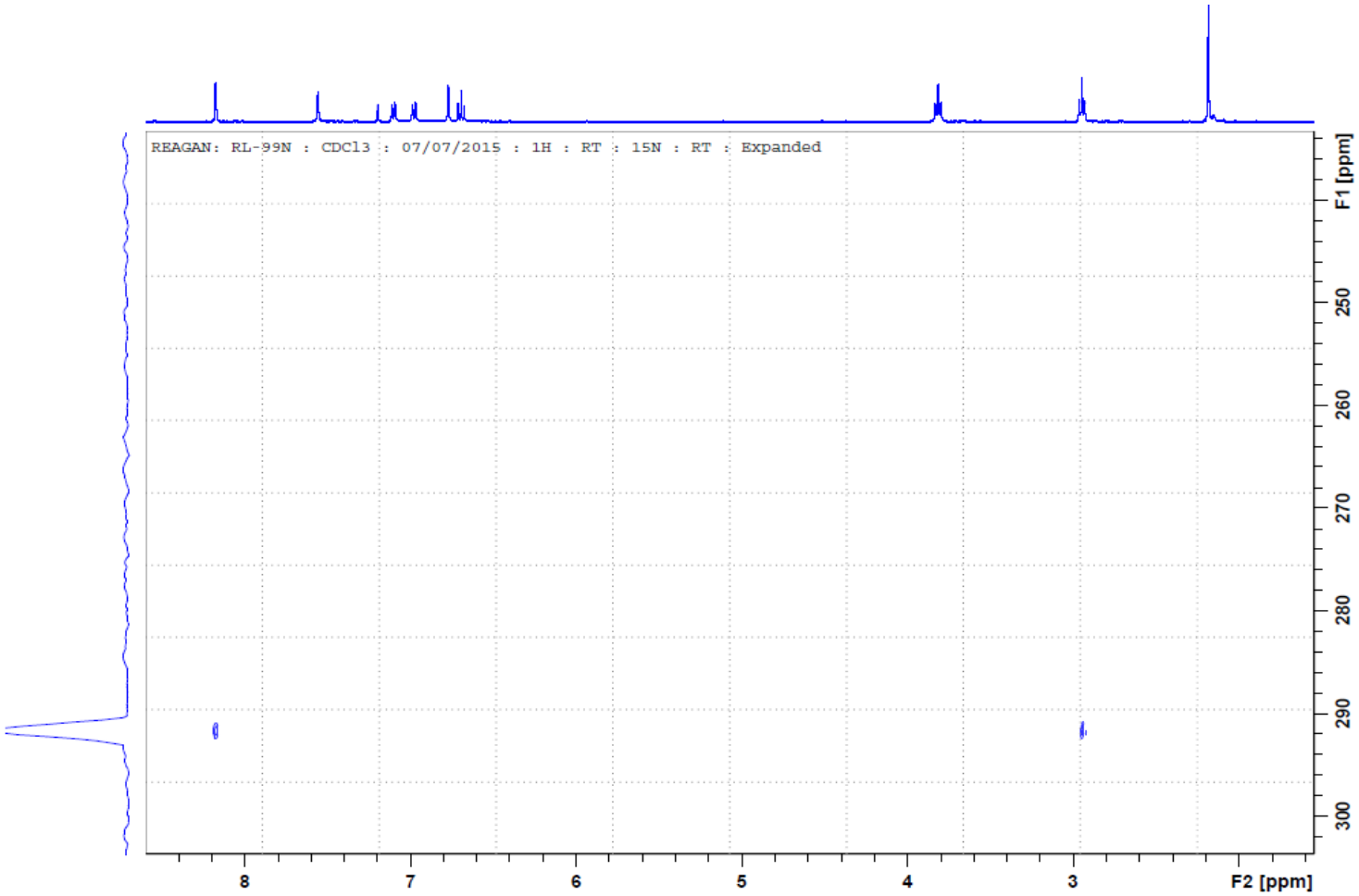

Figure 35: ^{15}N NMR spectrum of 2-methyl-6-{[2-(1H-imidazol-4-yl)-ethylimino]-methyl}-phenol [**L9**]

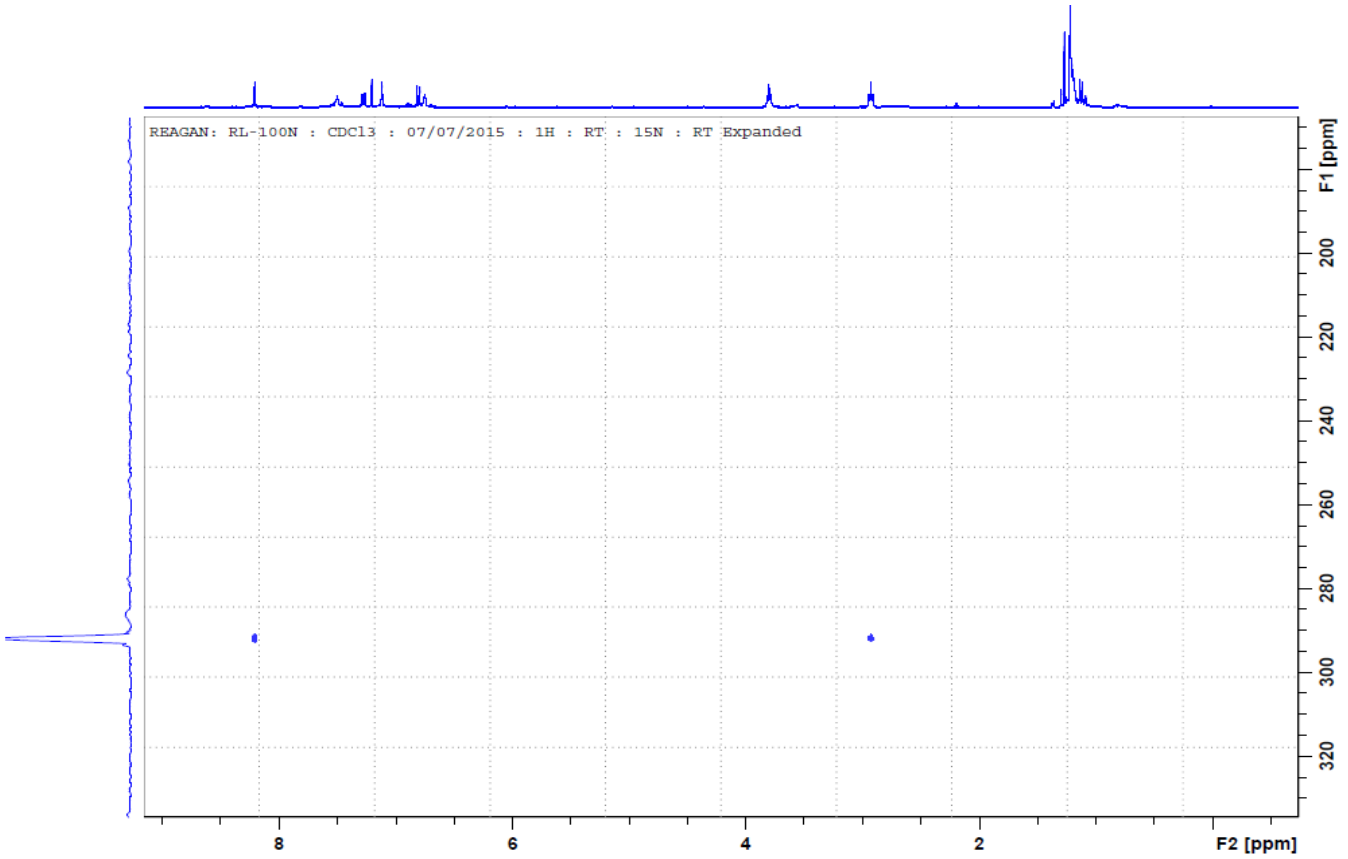

Figure 36: ^{15}N NMR spectrum of 4-tert-butyl-6-{[2-(1H-imidazol-4-yl)-ethylimino]-methyl}-phenol [**L10**]

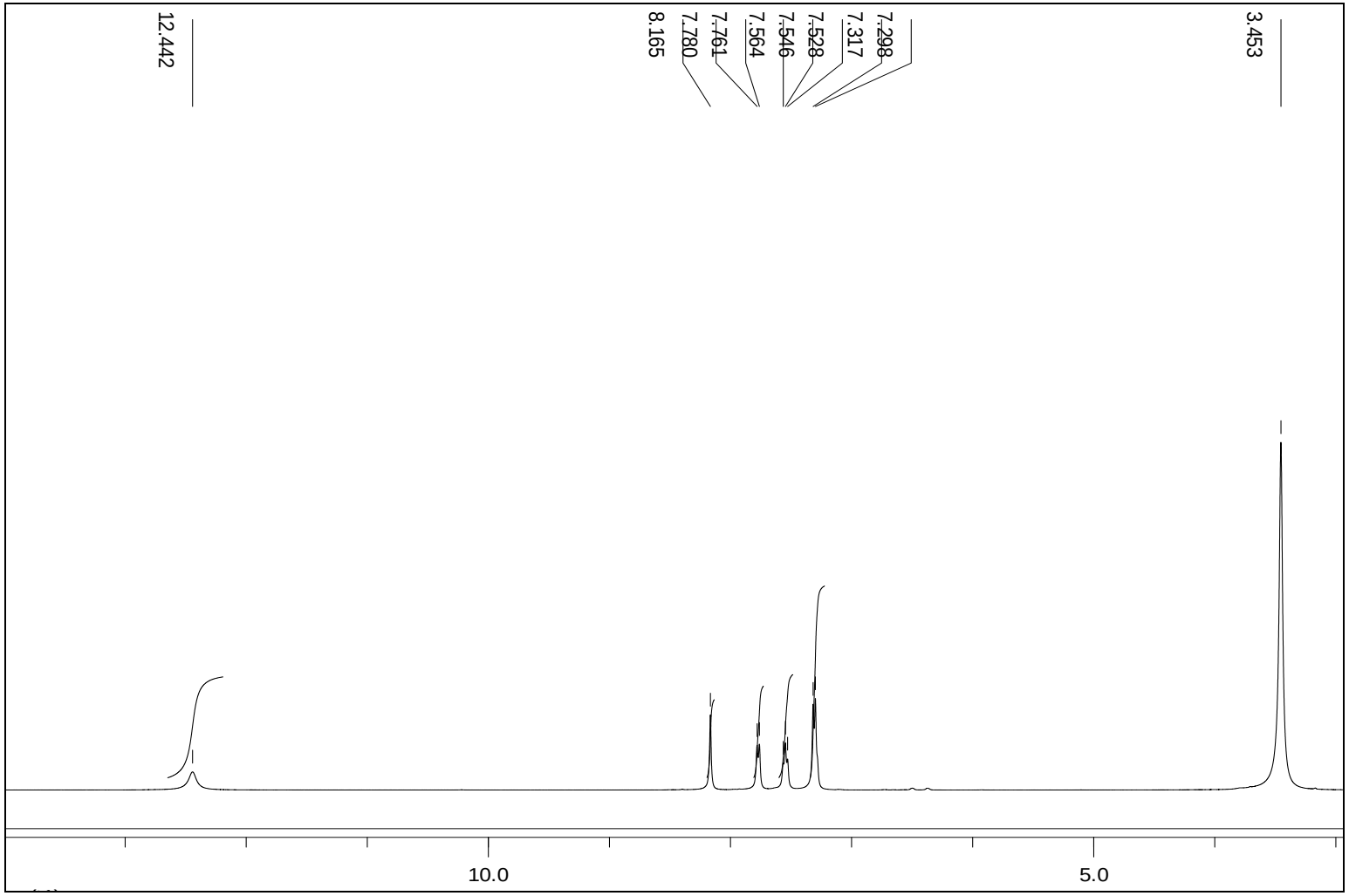

Figure 37: ^{1}H NMR spectrum of 2-quinoxalinone [**Q1**]

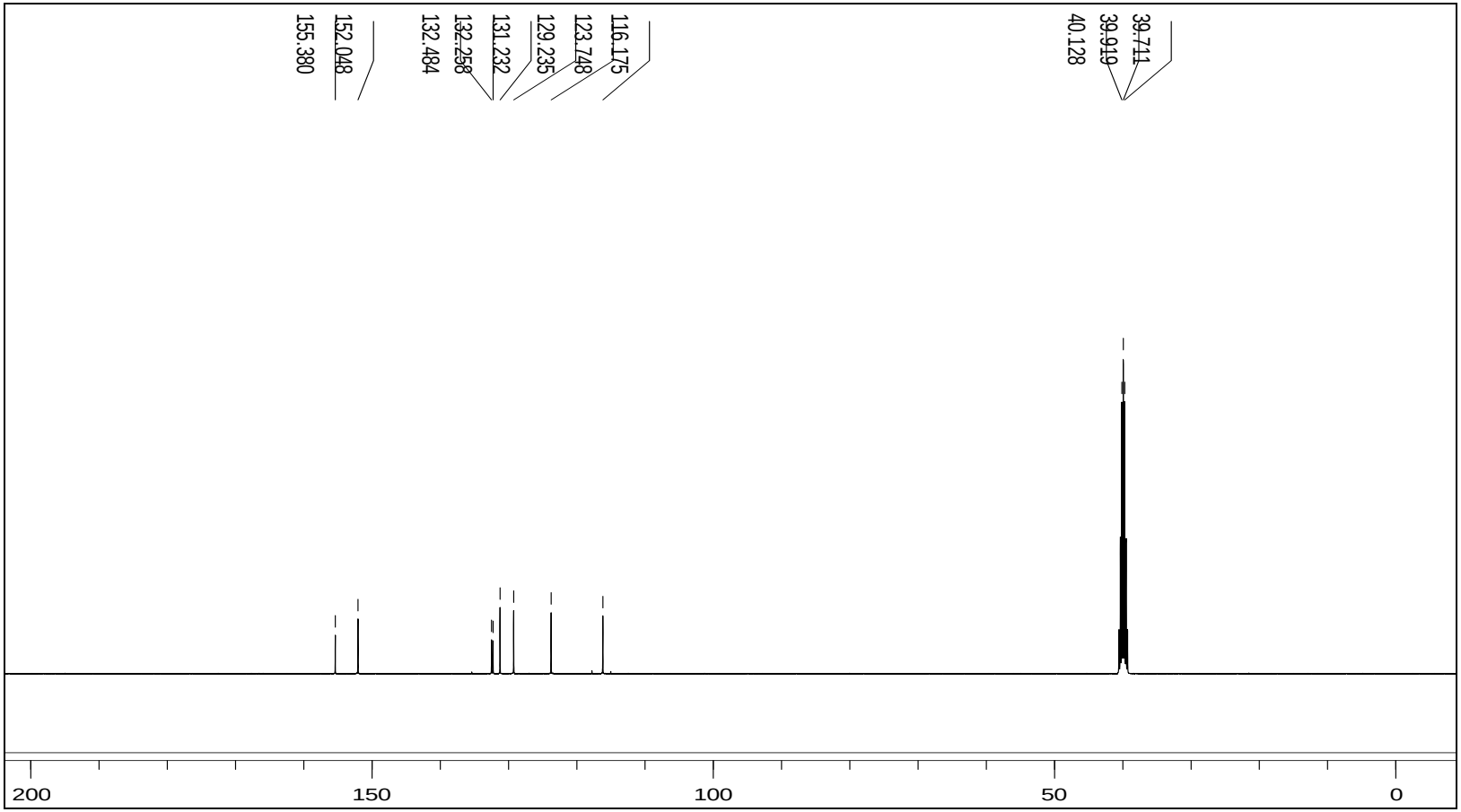

Figure 38: ^{13}C NMR spectrum of 2-quinoxalinone [**Q1**]

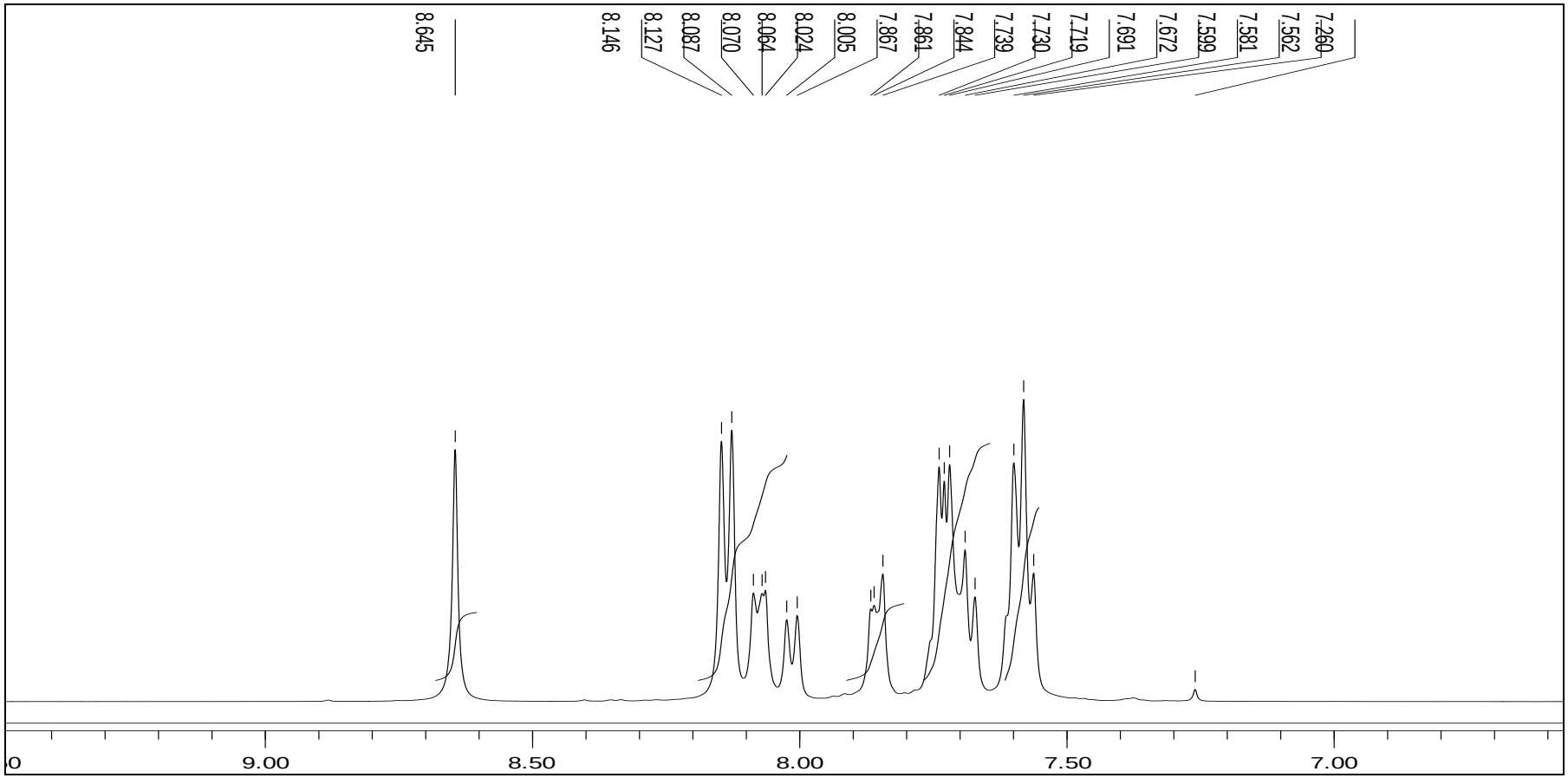

Figure 39: ^{1}H NMR spectrum of 2-benzenesulfonyloxyquinoxaline [**Q2**]

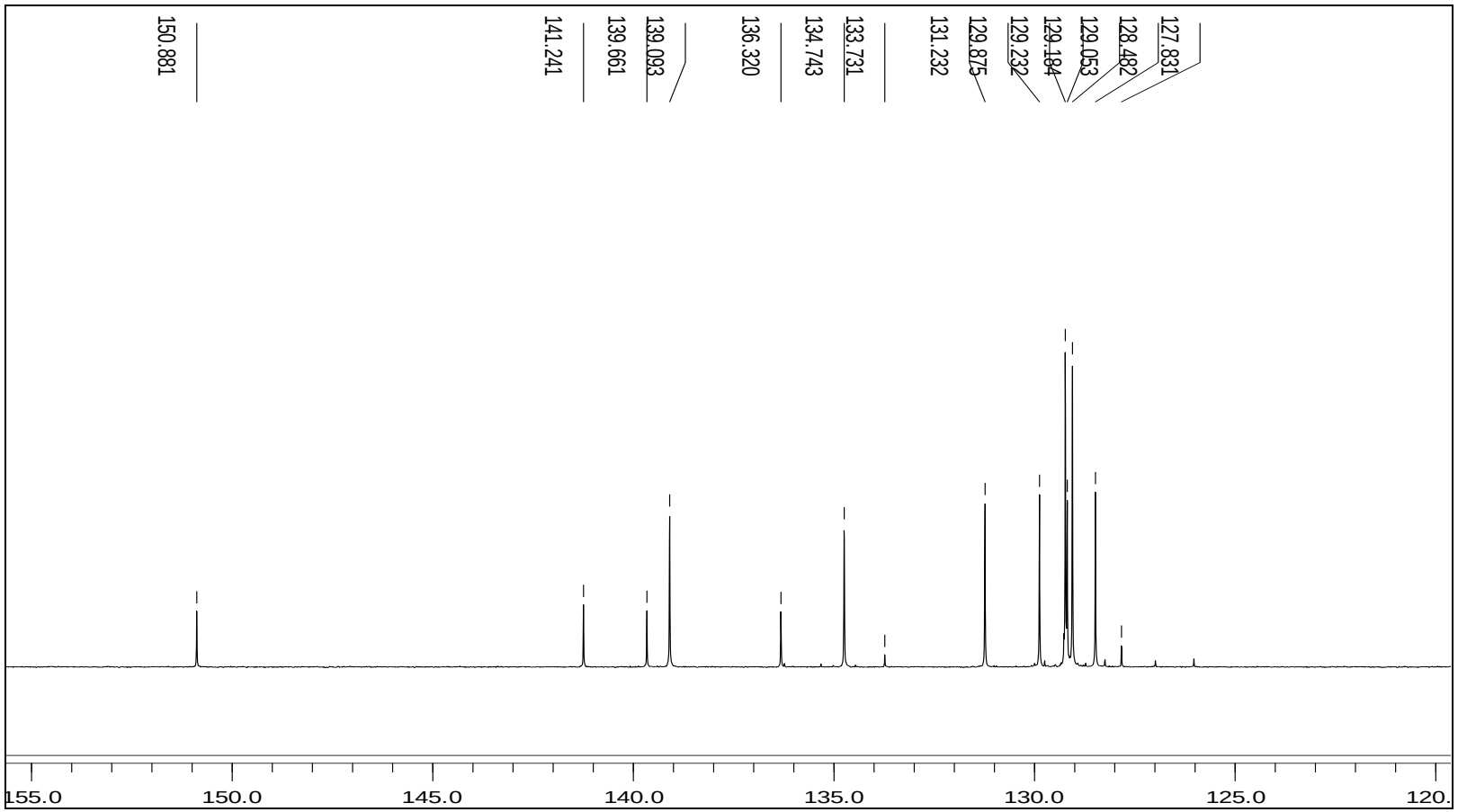

Figure 40: ^{13}C NMR spectrum of 2-benzenesulfonyloxyqunoxline [**Q2**]

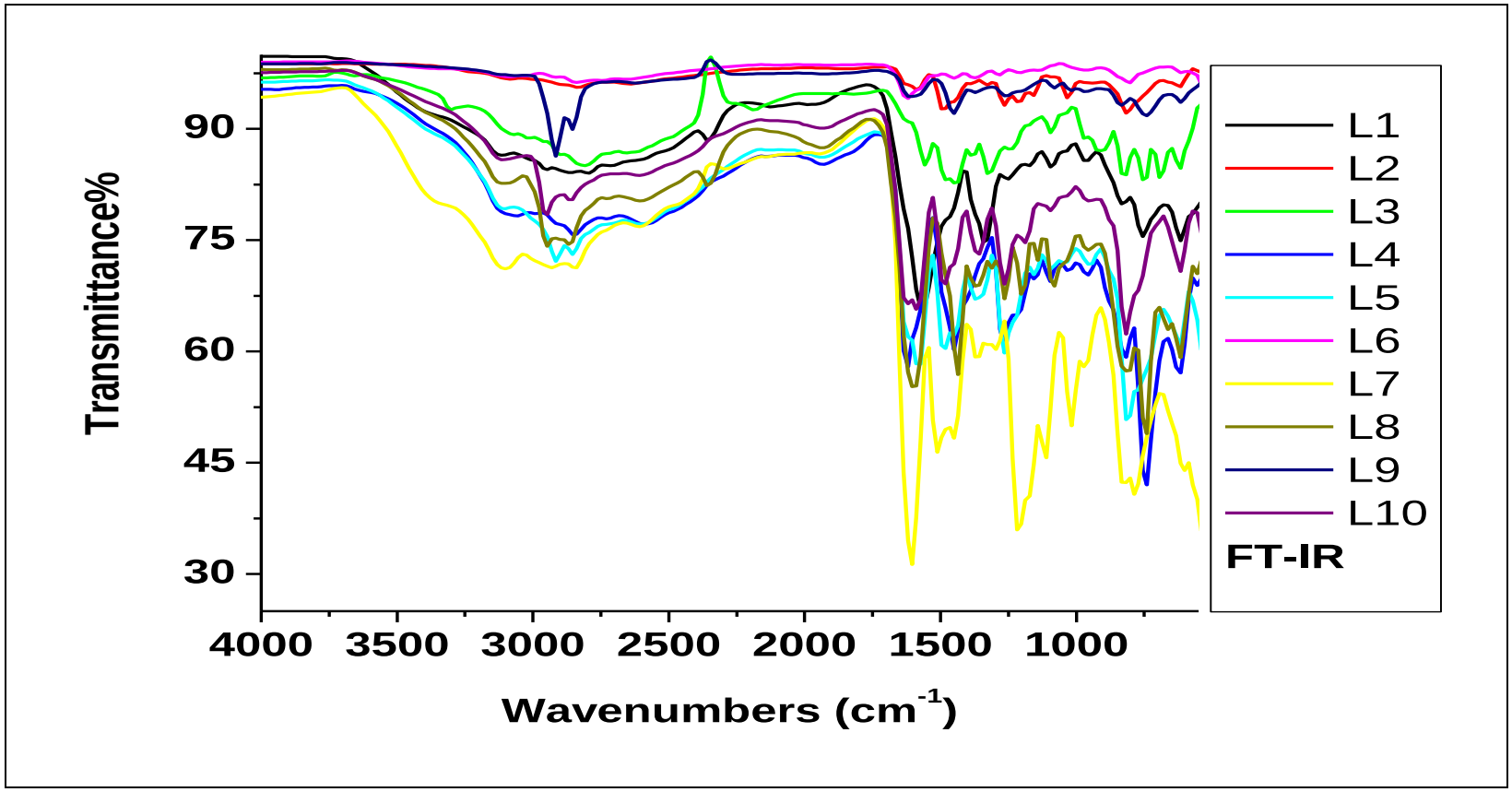

Figure 41: FT-IR spectra of **L1 – L10**

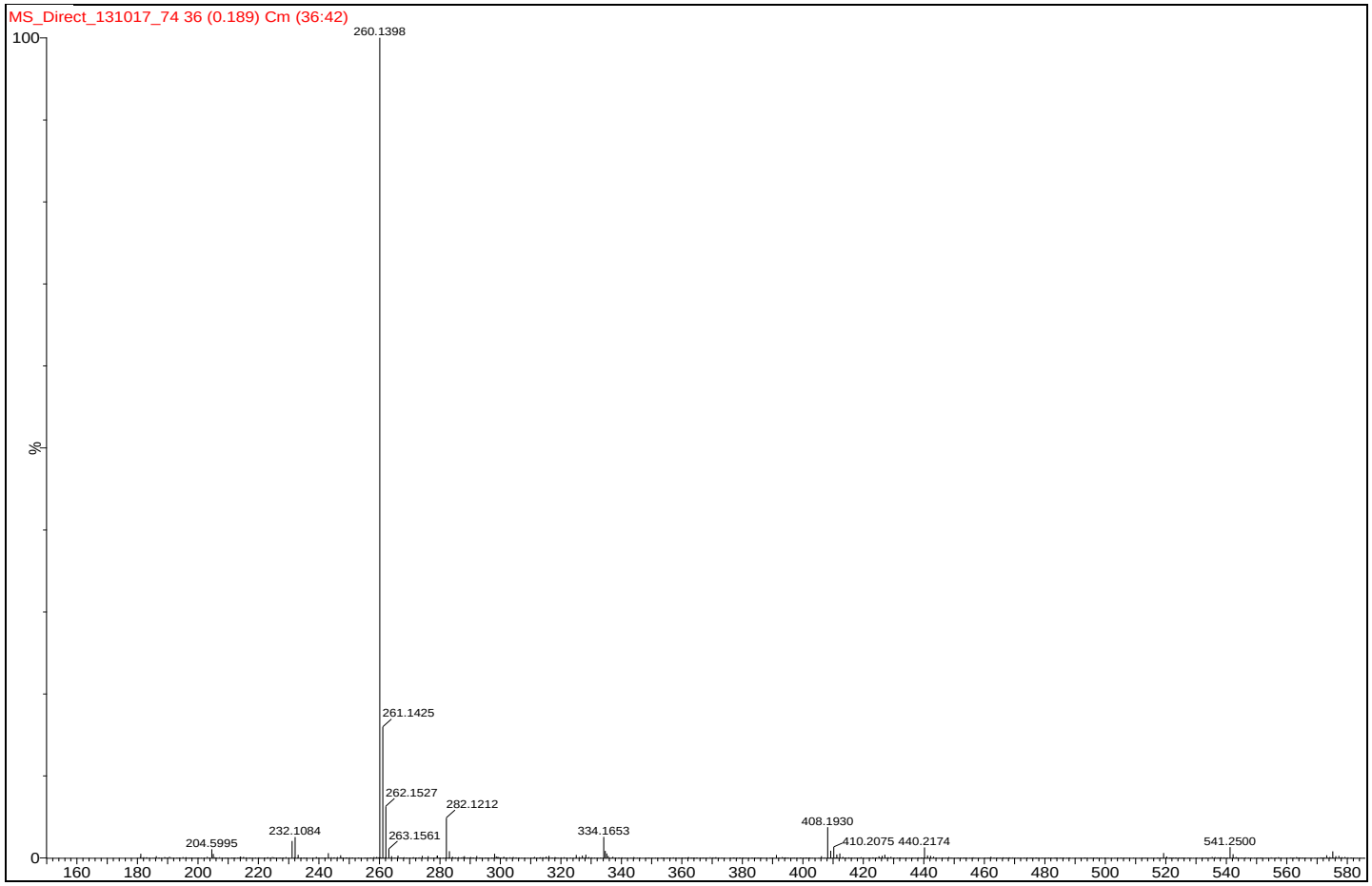

Figure 42: Mass spectrum of **L3**

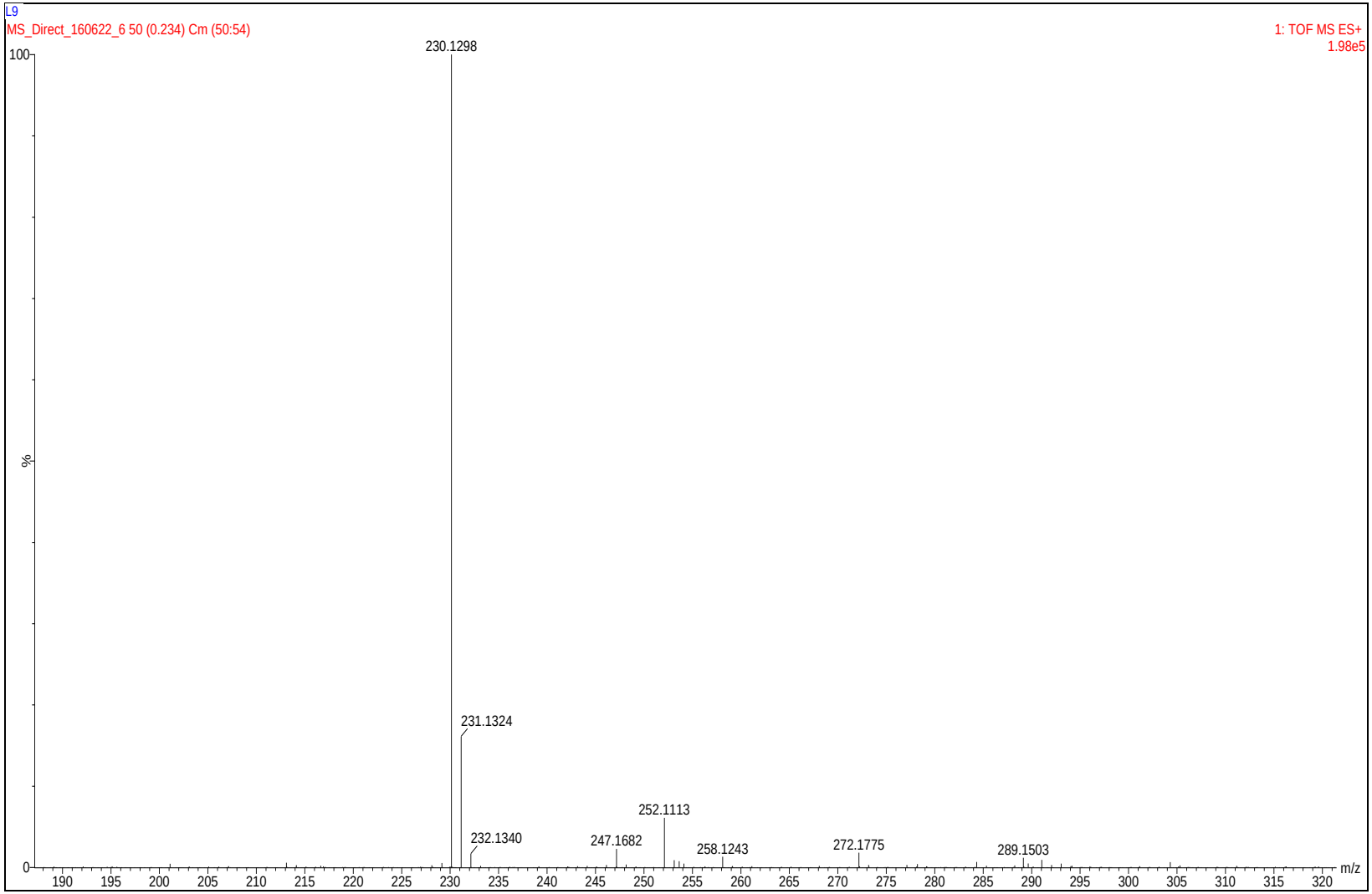

Figure 43: Mass spectrum of **L9**

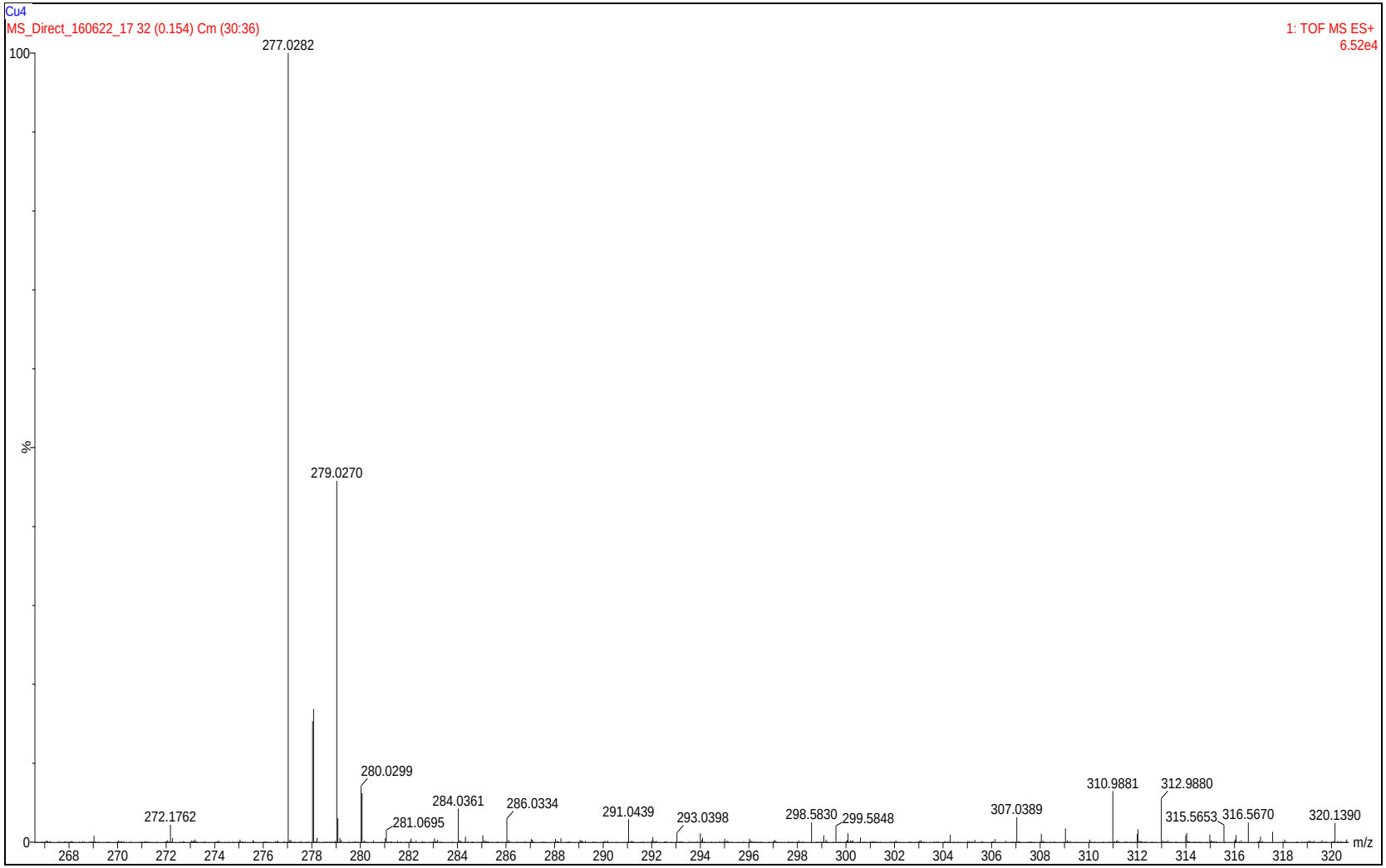

Figure 44: Mass spectrum of **C13**

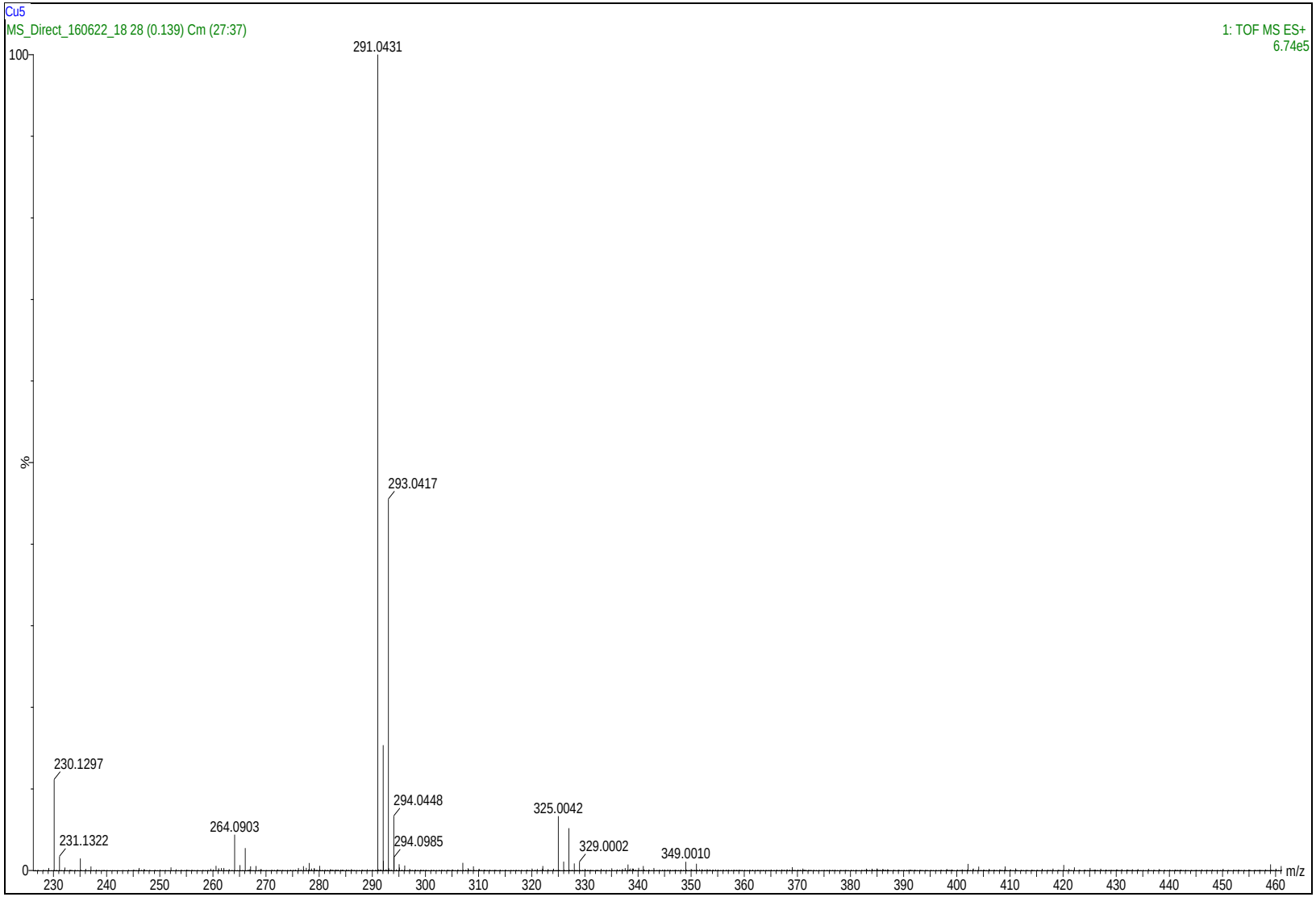

Figure 45: Mass spectrum of **C14**

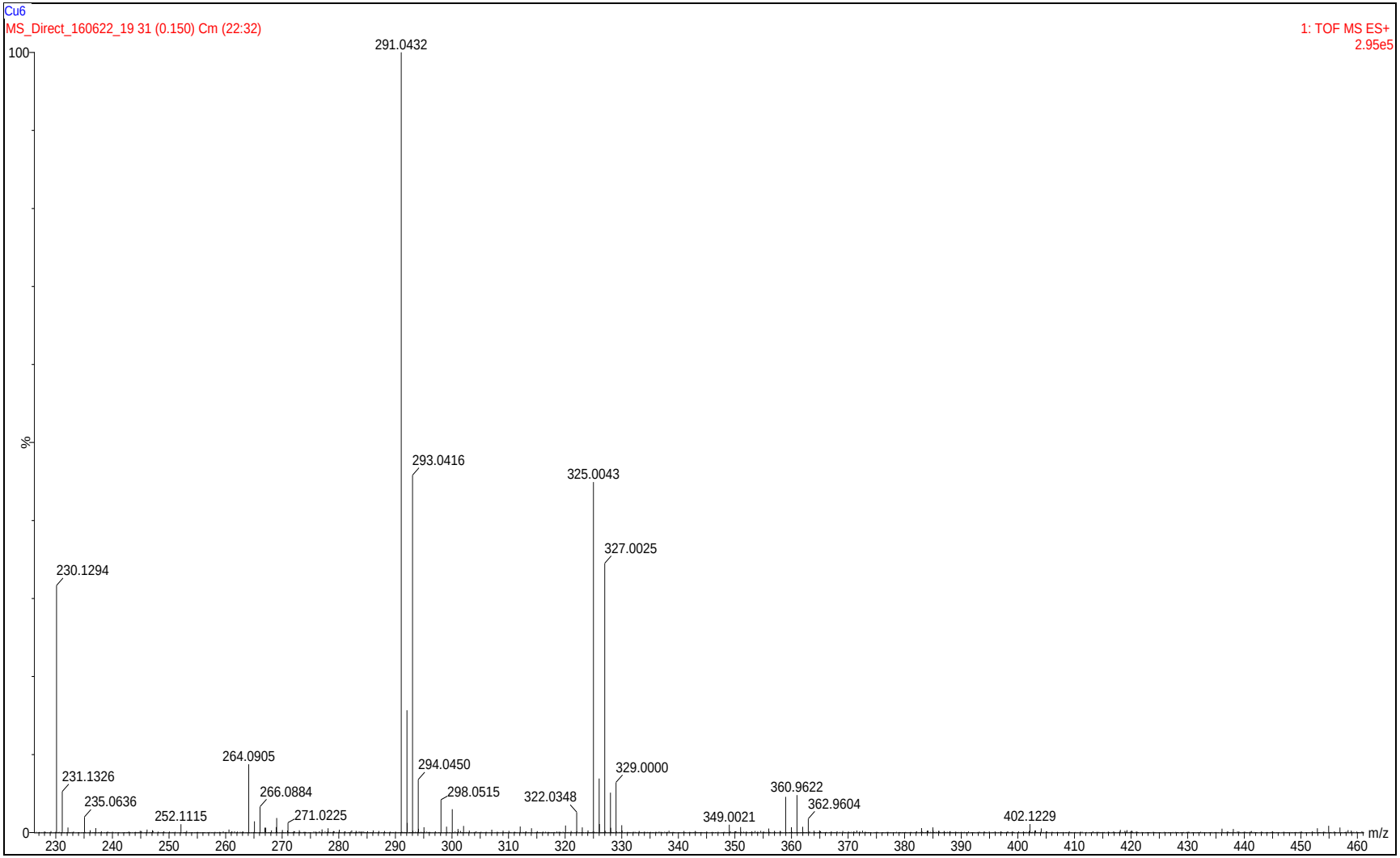

Figure 46: Mass spectrum of **C15**